ABSTRACT

With the exponential growth in the number of automobiles in Malaysia in recent years, the problem generated by waste tyres has also increased. Therefore, incorporating waste tyres as an additive in road pavement might be an option to overcome the increase in the number of waste tyres as well as address some of the pavement problems, such as rutting deformation.

Crumb rubber modified binder is acknowledged to provide better rutting resistance. Many research works have been implemented on the effects of chemical additives to further increase the performance of crumb rubber modified binders. Recent studies have shown that the properties of crumb rubber modified binders can be improved by adding crosslinking agents, such as trans-polyoctenamer (TOR) for which the main function is to activate the rubber-bitumen interaction and improve crosslinking.

This study was conducted to determine a method to improve the rutting resistance of SMA 20 bituminous mixtures. Accordingly, different percentages of crumb rubber were added to bitumen using different blending methods (continuous blend and terminal blend) in order to produce different concentrations of crumb rubber modified binder. In addition, a crosslinking agent, namely, trans-polyoctenamer (TOR), was introduced in the crumb rubber modified binder with the intention of further improving the binder properties and minimizing the rutting problem.

In order to analyse the performance of the binders and mixtures as well as to evaluate the relationship of the rutting characteristics between them, a series of binder tests and bituminous mixture tests were performed. In the final analysis, the author found that the binder tests were not adequate to evaluate the rutting characteristics of bituminous mixtures. For instance, in the case of the crumb rubber modified binder prepared using

the terminal blend method, most of the binder tests show that the terminal blend binder displays the best performance; however, in respect of the bituminous mixtures it became worse.

To further study the creep behaviour (rutting characteristics) of bituminous mixtures, the dynamic creep test was performed using the universal testing machine (UTM) at different temperatures and stress levels. Finally, the creep behaviour of the specimens was estimated using the Zhou three-stage creep model. The results show that crumb rubber and TOR significantly affected the rutting parameters, especially at high stress levels and temperatures. Moreover, based on the Zhou model, it was concluded that resistance to permanent deformation (rutting resistance) was improved by the application of crumb rubber and TOR.

In addition, multiple linear regression (stepwise method) was used for statistical analysis for which the main objective was to develop an equation (regression model) that could be used for predicting the rutting of the mixtures for all factors engaged. A secondary purpose was to use regression analysis as a means of explaining the causal relationship among the factors (significant level).

ABSTRAK

Dengan pertumbuhan yang pesat dalam bilangan kenderaan di Malaysia pada tahun-tahun kebelakangan ini, masalah yang dihasilkan oleh tayar sisa juga telah meningkat. Oleh itu, dengan tayar terpakai sebagai bahan tambahan dalam turapan jalan raya mungkin menjadi satu pilihan untuk mengatasi peningkatan dalam jumlah tayar sisa serta menyelesaikan masalah jalan raya, seperti aluran ubah bentuk.

Crumb getah diubahsuai pengikat diakui untuk menyediakan rintangan aluran yang lebih baik. Banyak kerja-kerja penyelidikan telah dilaksanakan pada kesan bahan tambahan kimia untuk meningkatkan lagi prestasi remah getah pengikat diubah suai. Kajian terbaru menunjukkan bahawa sifat-sifat remah getah diubahsuai pengikat boleh diperbaiki dengan menambah ejen silang, seperti trans-polyoctenamer (TOR) yang mana fungsi utama adalah untuk mengaktifkan interaksi getah - bitumen dan meningkatkan silang.

Kajian ini dijalankan untuk menentukan kaedah untuk memperbaiki rintangan aluran SMA 20 campuran bitumen. Oleh itu, peratusan yang berbeza getah remah telah ditambah kepada bitumen menggunakan kaedah pengadunan yang berbeza (gabungan berterusan dan gabungan terminal) untuk menghasilkan kepekatan yang berbeza remah getah pengikat diubah suai. Di samping itu, ejen silang, iaitu trans-polyoctenamer (TOR), telah diperkenalkan pada remah getah pengikat diubah suai dengan niat untuk meningkatkan lagi sifat-sifat pengikat dan meminimumkan masalah aluran.

Dalam usaha untuk menganalisis prestasi pengikat dan campuran dan juga untuk menilai hubungan ciri-ciri aluran antara mereka, satu siri ujian pengikat dan ujian aggregate campuran bitumen telah dijalankan. Dalam analisis terakhir, penulis mendapati bahawa ujian pengikat tidak mencukupi untuk menilai ciri-ciri aluran

campuran bitumen. Sebagai contoh, dalam kes getah remah pengikat diubahsuai disediakan dengan menggunakan kaedah gabungan terminal, kebanyakan ujian pengikat menunjukkan bahawa gabungan pengikat terminal memaparkan prestasi yang terbaik; walau bagaimanapun, berkenaan dengan campuran bitumen ia menjadi lebih teruk.

Mengkaji lagi kelakuan rayapan (aluran ciri-ciri) campuran bitumen, ujian rayapan dinamik dilakukan dengan menggunakan mesin ujian universal (UTM) pada suhu yang berbeza dan tahap tekanan berbeza. Akhir sekali, tingkah laku rayapan daripada spesimen dianggarkan menggunakan Zhou tiga peringkat model rayapan. Hasil kajian menunjukkan bahawa serbuk getah dan TOR ketara dipengaruhi parameter aluran, terutama pada tahap tekanan dan suhu yang tinggi. Selain itu, berdasarkan model Zhou, ia telah membuat kesimpulan bahawa rintangan kepada ubah bentuk kekal (rintangan aluran) telah bertambah baik dengan penggunaan getah remah dan TOR.

Di samping itu, regresi linear (kaedah langkah demi langkah) telah digunakan untuk analisis statistik yang mana objektif utama adalah untuk membangunkan (model regresi) persamaan yang boleh digunakan untuk meramalkan aluran daripada campuran untuk semua faktor-faktor yang terlibat. Analisis regresi juga digunakan sebagai satu cara untuk menjelaskan hubungan sebab akibat antara faktor (tahap penting).

ACKNOWLEDGEMENTS

First I would like to thank my supervisor, Prof. Ir. Dr. Mohamed Rehan bin Karim for giving me the opportunity to work under their supervision, valuable advices, supporting assistance and continues guidance during this research.

My thanks also go to the staff of Civil Engineering Department, University of Malaya, highway laboratory technician, Mr. Muhairizam bin Manan, and former highway laboratory technician, Mr. Khairul Anwar bin Abu and Mr. Khairul Azri bin Ngadan for their help and technical guidance during the laboratory sessions. My laboratory-mates, Mr. Mehrtash Soltani, Mrs. Suhana binti Koting, Mr. Sina Mirzapour Mounes, Mrs. Nuha Salim Mashaan, Mr. Mohammad Hadi Almasi, and Mr. Mohammad Saeed Pourtahmasb who have been helping and supporting me throughout the laboratory experiments and thesis writing.

My appreciation also goes to the Universiti Tenaga Nasional (UNITEN) for supporting my study by giving me full study leave. To the Vice Chancellor of UNITEN, Dato' Prof. Ir. Dr. Kamal Nasharuddin bin Mustapha, my head of department, Ir. Zakaria bin Che Muda and to all staffs of Civil Engineering Department, UNITEN, thank you very much for your support and kindness.

Not to forget, my deepest appreciations to my beloved husband for his precious assistance, guidance and encouragement especially during the stressful moment of my study. Lastly, I offer my regards to my parents and parents in law for their endless support, love and prayers.

DEDICATION

This thesis is especially dedicated to:

My husband, Mohd Rasdan bin Ibrahim

My parents, Hj. Katman bin Madikon and Hjh. Buninah binti Kusor

My parents in law, Hj. Ibrahim bin Haron and Hjh Fathilah binti Othman

TABLE OF CONTENTS **PAGE**

LIST OF TABLES

LIST OF FIGURES

LIST OF ABBREVIATIONS AND NOTATIONS

APA	Asphalt Pavement Analyzer
AS	Australian Standard
ASTM	American Society for Testing and Materials
CR	Crumb Rubber
CRMB	Crumb Rubber Modified Binder
CRMB-TOR	Crumb Rubber Modified Binder Reinforced with TOR
CRMM	Crumb Rubber Modified Mixture
CRMM-TOR	Crumb Rubber Modified Mixture Reinforced with TOR
ELT	End of life tyres
ETRMA	European Tyre and Rubber Manufacturers' Association
FHWA	The Federal Highway Administration
HMA	Hot Mix Asphalt
ID	Identification name
ITSM	Indirect Tensile Stiffness Modulus
JATMA	Japan Automobile Tyre Manufacturers Association
J_{nr}	Non-Recoverable Compliance
JKR	Jabatan Kerja Raya (Public Works Department)
MPa	Mega Pascal
MQ	Marshall Quotient
N/A	Not Applicable
OBC	Optimum Binder Content
OPC	Ordinary Portland cement
PWD	Public Works Department
%R	% Recovery
R^2	Reliability value

REAM	Road Engineering Association of Malaysia
RPM	Revolutions per Minute
RMA	Rubber Manufacturers Association
s	Second
SBR	Styrene Butadiene Rubber
SMA	Stone Mastic Asphalt
SMA 20	Stone Mastic Asphalt with aggregate nominal size 20mm
SPSS	Statistical Package for the Social Sciences
TOR	Trans-polyoctenamer
TRL	Transport Research Laboratory
UMATTA	Universal Material Testing Apparatus
VFB	Voids Filled with Bitumen
VIM	Voids in Mix
VMA	Voids in Mineral Aggregate
WBCSD	World Business Council for Sustainable Development

CHAPTER 1: INTRODUCTION

1.1 Overview

Many research works have been devoted to rutting parameters in order to formulate a method that can improve rutting resistance. Incorporating waste tyres in bituminous mixtures has been proven by many researchers to not only improve the engineering properties of bituminous mixtures but also to contribute significantly to environmental conservation by reducing the stockpiling of waste tyres and landfilling.

According to reports from the largest associations of tyre and rubber product manufacturers, the annual global production of tyres is some 1.4 billion units, which corresponds to an estimated 17 million tonnes of used tyres each year (RMA, 2009; JATMA, 2010; ETRMA, 2011; WBCSD, 2010). In Malaysia, the number of waste tyres generated annually was estimated to be 8.2 million or approximately 57,000 tonnes, of which 60% are disposed via unknown routes (Kumar, 2006). For this reason, the construction of road pavement with waste tyres appears to be a significant engineering contribution to encourage sustainability. Therefore, studies should be conducted on the many factors that may influence the performance of pavement reinforced with waste tyres before construction can be started. For this reason, it is important to consider the environmental conditions (temperatures and stress levels) together with using local materials in the study.

Many research studies found that incorporating crumb rubber (processed product from waste tyres) in the bituminous mixture improves the mixture performance including rutting resistance (De et al., 2012; Mo et al., 2012, Nuha et al., 2014., Xiao et al., 2014., Xie, Z., & Shen, J.,2016). However, researchers are always looking for better ways to improve the rutting resistance of bituminous mixtures. Due to the benefits offered by

crumb rubber, attempts have been carried out by researchers on the implementation of chemical additives. For instance, chemical stabilizers, activation agents and polymers were incorporated in order to activate the chemical reaction between crumb rubber and bitumen. It is hoped that the attempts at modification would improve the pavement performance including reducing the risk of rutting at high temperatures. In addition, the methods used to blend the crumb rubber with bitumen also affect the properties of crumb rubber modified bitumen (CRMB). From the literature, crumb rubber can be blended with the bitumen using different blending methods, such as continuous blend and terminal blend. Different blending methods would produce a different rheology of CRMB, and, thus, affect the rutting resistance of bituminous mixtures.

The Federal Highway Administration (FHWA) defined rutting as a longitudinal surface depression in the wheel paths of roadways. Rutting, by definition, is a load-related pavement distress, and, typically, occurs in the upper range of pavement service temperatures rather than at low temperatures. The main rutting mechanisms are densification and plastic deformation. Densification, also known as the first stage of rutting, occurs in pavements with insufficient level of compaction. Plastic deformation, known as the second stage of rutting, is considered to be the main mechanism that occurs in the life time of pavements. In this stage, deformation in the wheel path is equal to deformation of the upheaval zone, i.e. no volume change in the bituminous mixture. In general, the pavement authority will implement a rehabilitation process when the pavement reaches the secondary stage of rutting; therefore, the rutting mechanism of the pavement would stop at the second stage.

In the laboratory, bituminous mixtures develop a rutting mechanism similar to pavement. In addition to the first and second stages, the rutting mechanism in bituminous mixtures can be assessed up to the final stage (third stage). In this stage,

rutting reaches a critical value after which the mix cracks. Waller (1993) mentioned that the rutting process in the third stage is more due to crack propagation in addition to the excessive deformation that has developed in the mix. Rutting mechanisms can be evaluated in the laboratory by many test categories, such as fundamental diametral tests, fundamental uniaxial tests, fundamental triaxial tests, fundamental shear tests, empirical tests and simulative tests.

In this study, the rutting mechanism of a bituminous mixture prepared with crumb rubber modified bitumen (CRMB) and crumb rubber modified bitumen reinforced with Trans-polyoctenamer (CRMB-TOR) as crosslinking agent was evaluated using the dynamic creep test. The test is classified as a fundamental uniaxial test. In the dynamic creep test, the rutting value can be characterized by the amount of strain at the respective load cycle. Since rutting is highly affected by various traffic loads and environmental conditions, a dynamic creep test was performed with different stress levels and temperatures in order to reflect the effectiveness of the CRMB and CRMB-TOR on the rutting resistance of the mixtures. Moreover, effects of binder blending methods on the rutting resistance of the mixtures were also studied. Details of the tests used in this study will be discussed further in Chapter 2.

In addition to the laboratory tests, many researchers are interested in developing the performance models to characterize the permanent deformation and further estimate the future service of the pavements. As reported by Zhou et al. (2004), various mathematical models – power-law model, VESYS model, Ohio State model, Superpave, and AASHTO 2002 – have been developed for fitting the creep curve and estimating the flow number (FN) parameter in bituminous mixtures. However, these models are limited to describing only the primary stage. West et al. (2004) also developed a three-stage model, but their model could not estimate the boundary points of the curve stages.

Therefore, a new three-stage model, termed the Zhou model (2004), which is comparable to the field performance, was used in this study to further analyse the performance of the crumb rubber modified mixtures (CRMM) and crumb rubber modified mixtures reinforced with Trans-polyoctenamer (CRMM-TOR).

1.2 Problem Statement

Rutting caused by repeated loads at high temperatures is one of the major distresses in bituminous pavements. It is observed as the main distress mechanism, and, typically, occurs in countries with high pavement in-service temperatures like Malaysia. Malaysia essentially experiences tropical weather with a mean annual air temperature of 28°C, maximum air temperature of 45°C and the maximum average air temperature during the hottest 7-day period (over the pavement design life) being 38°C (ATJ 5/85). However, the road pavement temperature in Malaysia ranges from 20°C in the early hours of the day to as high as 60°C at midday on a hot day.

In addition, overloaded vehicles are very common users of Malaysian roads. In 2008, 27% or 270,000 out of the one million registered commercial vehicles on the roads in the country were commonly overloaded (Karim, et al., 2014). It was also reported recently that overloaded trucks could still be rampant on Malaysian roads resulting in damage to many of the roads, including newly completed roads (Yu, 2015). Overloading together with the high environmental temperatures observed in Malaysia could cause great damage to pavements, and, therefore, deteriorate pavement performance faster than planned.

In considering the increase in traffic together with the fact that Malaysia experiences tropical weather that contributes to the acceleration of rutting deformation, it is important to accurately evaluate the rutting resistance of bituminous mixtures in the

design process of the pavement material. Hence, many researchers in Malaysia seek the use of a modified binder for greater stability at the expense of a lower price.

The aforementioned situation compelled the author to perform a study concerning the effects of crumb rubber on the rutting resistance of the most used aggregate gradation in Malaysia, i.e. SMA 20 (Stone Mastic Asphalt with 20 mm aggregate nominal size). In this study, the crumb rubber was blended with bitumen using two different methods – continuous blend and terminal blend. Moreover, the interaction of the crumb rubber with the binder was further improved by the application of a crosslinking agent namely Trans-polyoctenamer.

1.3 Research Objectives

This research has the following objectives:

1. To investigate the effects of crumb rubber (CR), Trans-polyoctenamer (TOR) and binder blending methods on the physical and rheological properties of bitumen binders.
2. To investigate the effects of crumb rubber (CR), Trans-polyoctenamer (TOR) and binder blending methods to the stability, flow and stiffness characteristics of SMA 20 mixtures.
3. To evaluate the influence of crumb rubber (CR), Trans-polyoctenamer (TOR), binder blending methods, stress levels and temperatures on the rutting parameters of SMA 20 mixtures using the dynamic creep test. Next, the empirical relationship model was developed based on multiple linear regression analysis (Stepwise method).
4. To develop the creep model based on the Zhou three-stage model. Moreover, the creep parameters obtained by the dynamic creep test results (dynamic creep

curve and ultimate strain) were compared with the Zhou three-stage model (slope at secondary stage and flow number).

5. To develop a relationship between the binder rheology (CRMB and CRMB-TOR) and rutting resistance of SMA 20 mixtures.

1.4 Research Questions

This thesis aims to answer the following research questions:

1. What is the effect of the crumb rubber (CR), Trans-polyoctenamer (TOR) and binder blending method on the physical and rheological behaviour of bitumen binder?
2. What is the effect of the crumb rubber (CR), Trans-polyoctenamer (TOR) and binder blending method on the stability, flow and stiffness of the most commonly used aggregate gradation in Malaysia (SMA 20: SMA gradation with nominal size 20mm)?
3. How significant are the crumb rubber (CR), Trans-polyoctenamer (TOR), binder blending method, stress level and temperature in terms of the rutting resistance of the SMA 20? Moreover, what empirical relationship model can be used?
4. What creep model can be used to predict the rutting parameter of crumb rubber modified mixtures (CRMM) and crumb rubber modified mixtures reinforced with Trans-polyoctenamer (CRMM-TOR)? If the Zhou Three-Stage Model was selected, what is the relationship?
5. What is the relationship of the binder rheology with the rutting resistance of the crumb rubber modified mixtures (CRMM) and crumb rubber modified mixtures reinforced with Trans-polyoctenamer (CRMM-TOR)?

1.5 Scope of Work

The scope of work adopted to meet the objectives of this study involves a review of the literature and a laboratory investigation. The literature review is conducted to identify important factors that influence the permanent deformation response of mixtures and the available testing methods that are used to characterize permanent deformation parameters for the binder and mixtures. The available permanent deformation models and suitable statistical analysis are also reviewed.

Laboratory investigations were carried out to develop the relationship between the physical and rheology of the binders with the rutting parameter of the mixtures. In this study, the properties of the binders modified with different percentages of crumb rubber and TOR were performed using conventional test methods (penetration test, ring and ball softening point test and Brookfield viscosity test) and dynamic shear rheometer (DSR). The binder properties obtained were verified by the mix performance. The density test, indirect tensile modulus (ITSM) test, Marshall stability and flow of asphalt concrete test and dynamic creep test were used for this purpose. The dynamic creep test results were used both for evaluation of the effect of various factors (crumb rubber, Trans-polyoctenamer, binder blending method, stress level and temperature) on the rutting parameter and for modelling purposes. The scope of the laboratory works will be discussed further in Chapter 3.

The Zhou three-stage model was utilized for a better understanding of the creep behaviour. Moreover, multiple linear regression analysis (Stepwise method) was used to determine the factors that significantly affect the rutting parameters as well as to develop a model that correlates with the engaged factors.

1.6 Significance of the Study

Many road pavements in Malaysia experience permanent deformation, especially rutting. This is because Malaysia is a tropical country in which 60°C has been observed as the highest pavement temperature. High temperatures lead to increased rutting problems. In addition, an increase in traffic including overloaded vehicles seems to further increase the road damage.

This study was conducted with the intention to improve the rutting resistance of the commonly used aggregate gradation in Malaysia, i.e. SMA 20 (Stone Mastic Asphalt with 20 mm nominal aggregate size). The processed product from waste tyres, namely, crumb rubber, was selected as the modifier. Previous studies mentioned that crumb rubber offers better performance at high temperature, therefore, it might be suitable to resist rutting for Malaysian roads. In addition, a crosslinking agent was utilised in the hope that it would further improve the rutting resistance of the SMA 20 mixture.

1.7 Outline of the Thesis

This thesis consists of five (5) main chapters: Introduction, Literature Review, Methodology, Results and Discussion, and Conclusions and Recommendations. The following chapters describe the work carried out to achieve the research objectives:

Chapter One – Introduction

Chapter One discusses the background and the scope of work carried out to achieve the research objectives. The objectives of this research are also explained in this chapter.

Chapter Two – Literature Review

The background and literature review on the permanent deformation of bituminous mixtures are explained in this chapter. This chapter also entails a brief discussion on the waste tyres, crumb rubber, TOR and SMA mixtures. The available creep models are also carefully reviewed.

Chapter 3 – Methodology

Chapter Three explains the material characterization, which includes the properties of the aggregate, crumb rubber, TOR and 80/100 penetration bitumen. Laboratory tests together with data collections are discussed in this chapter. The tests were performed in accordance with international standards – American Society for Testing and Materials (ASTM), British Standard Institute (BSI), Malaysia Public Works Department (JKR) and Road Engineering Association of Malaysia (REAM).

Chapter 4 – Results and Discussion

The results and data collections obtained from the laboratory works are discussed in this chapter. The results are then presented in the form of a table, graphical method and statistical method. A discussion on the creep model (Zhou three-stage model) for all mixtures is available in this chapter. Moreover, this chapter outlines the relationships and comparisons among the different variables.

Chapter 5 – Conclusion and Recommendations

The final chapter concludes the findings of the research work that has been undertaken. The author's recommendation for future works is also available in this chapter.

CHAPTER 2: LITERATURE REVIEW

2.0 Introduction

This chapter describes the literature that is relevant to the research study. The literature that explains the rutting, creep models, materials and methods that lead to identifying the objectives of the study are critically reviewed. Moreover, recent publications that are relevant to the research are quoted.

2.1 Mechanisms of Rutting

Hot mix asphalt (HMA) pavements have always been affected by the susceptibility for permanent deformation, also called rutting. Rutting is recognized as an accumulation of the permanent deformation of the road pavement, which occurs under applied loading and is highly sensitive to variations in the temperature and traffic volume (Metcalf, 1996). According to İskender, E. (2013), the potential for rutting has recently increased in the highways due to higher traffic volumes and the increased usage of radial tyres that typically exhibit higher inflation pressures.

The main rutting mechanisms can be divided into three stages. The first stage is called the post compaction (densification) stage. During this stage, the void content of HMA is reduced because of densification. Rutting due to densification is usually fairly wide and uniform in the longitudinal direction with heaving on the surface remaining rare. The degree of densification greatly depends on the compaction specification during construction. After the initial stage, rutting enters the second stage in which further rutting is caused by the plastic flow of the bituminous mixture. Plastic flow occurs when the shear stresses imposed by traffic exceed the inherent strength of the pavement layers (Paterson, 1987). Plastic flow essentially involves no volume change, and gives rise to shear displacement in which both depression and heave are usually manifested.

Plastic flow is controlled through the structural and material design specifications, which are normally based on a measure of the shear strength of the materials used. Subsequently, rutting enters the third stage. Rutting increases rapidly in this stage and the pavement is not safe to traffic users anymore. In general, pavements are rehabilitated before they enter the third stage. Among all the stages, the second stage of rutting is considered to be the main mechanism that occurs over most of the lifetime of the pavement.

Moreover, pavement rutting can be divided into two parts based on its occurrence: rutting of the bituminous paving mixtures layers and rutting of the unbound layers. Researchers (Brown et al., 1989; Sousa et al., 1994; Chen et al. 2003) have reported that many ruts occur in the bituminous paving mixtures layers alone. Most of the rutting is attributed to the top 50.8mm of the bituminous paving mixtures layer (Zhou et al., 2007). Coleri et al. (2008) found that 85 to 95% of rutting accumulates in the bituminous paving mixtures layer because pavements are designed to not allow water to pass to the unbound layers. Moreover, the results of surveys conducted by other researchers (Brown et al., 1989; Sousa et al., 1994; Chen et al., 2002) clearly showed that most of the total surface rutting comes from the bituminous paving mixtures layer(s). However, the rutting phenomenon takes place mainly in the unbound layers when the soil bearing capacity is not sufficient to withstand the pavement structure (Perez et al., 2006).

2.2 Permanent Deformation Criteria

In general, rutting can be classified into four levels of severity, as below (Federal Highway Administration, 1979):

1. Hydroplaning, from 5 to 6 mm
2. Low, from 6 to 12.5 mm,
3. Medium, from 12.5 to 25 mm, and
4. High, over 25 mm

A rut depth of 12.5 mm is typically accepted as the maximum acceptable level of rutting in the field (Kandhal and Cooley, 2003; Kim, 2008). Moreover, it is used to differentiate between good and bad performing mixes with respect to rutting (Mohammad, L. N. 2006). Some researchers have suggested limiting the value of the mixture stiffness to limit rutting in bituminous paving mixtures layers to acceptable levels. As quoted by Sousa et al. (1991), such values are obtained from the laboratory creep test at a specific time of loading and a specific temperature (see Table 2.1). However, the criteria for this type must be associated with specific traffic and environmental conditions, and should not be adopted without careful evaluation.

Table 2.1: Limiting Mixture Stiffness (Sousa et al., 1991)

Reference	Temperature, °C	Test Duration, minutes	Applied Stress, MPa	Mix stiffness, MPa
Viljoen et al., (1981)	40	100	0.2	≥ 80
Kronfuss et al., (1984)	40	60	0.1	≥ 50 - 65
Finn et al., (1983)	40	60	0.2	≥ 135

2.3 Factors Influencing Rutting

The resistance of pavement structures to rutting can be influenced by many factors, such as the applied loads (traffic type and traffic volume), the environment (temperature, rainfall), the pavement structure (materials used and their composition), the construction process, or a combination of the above. It was reported by the AASHTO (1988) Joint Task Force on Rutting that the main factors that contribute to rutting are traffic and environmental.

2.3.1 Effect of Traffic Loading on Rutting Potential

In recent years, increased traffic levels, larger and heavier trucks with new axle designs and high tyre pressures, appear to have contributed to the severe demands in terms of the load and the environment on the pavement. Moreover, similar to other countries, Malaysia is suffering from an increase in overloaded vehicles, which accelerates the damage to the pavement (Karim et al., 2014).

The traffic loading is a combination of the magnitude and volume of the loads. Traffic induces stresses within the pavement structure that have to be withstood. It is important to note that a few excessive loads or tyre pressures for which the pavement was not designed may cause stresses that exceed the shear strength of the material. For example, increasing the tyre pressure from 524 to 965.3 kPa is equivalent to an 8.9 kN axle load increase (Bonaquist et al., 1988). Moreover, Gillespie (1993) explained that increased pressure produces deeper rutting because of the higher plastic deformation when the load is concentrated in a smaller area. Furthermore, many research studies conducted in the laboratory show that permanent deformation of bituminous mixtures increases faster at higher stress levels (Xu and Sun., 2013; Moghaddam et al., 2014).

With the passage of time, the repetition of traffic loading with different axle designs applied on the pavement layers, as well as the increase in tyre pressure and amount of axle load, causes an accumulation of unrecoverable strain (rutting). In general, rutting is greatest below the wheel and near the loaded surface. As shown in Figure 2.1, Eisenmann and Hilmer (1987) illustrated the effects of the number of wheel passes on the surface profile of a wheel-track test slab. This figure enables the measurement of the average rut depth as well as the volume of displaced material below the tyres and in the adjacent upheaval zones. In the initial stage of traffic, traffic compaction causes an increase in the irreversible deformation below the tyres. In this stage, the volume of rut depth is distinctly greater than the increase in the upheaval zones. After the initial stage, the volume of decrement beneath the tyres is approximately equal to the volume increment in the adjacent upheaval zones.

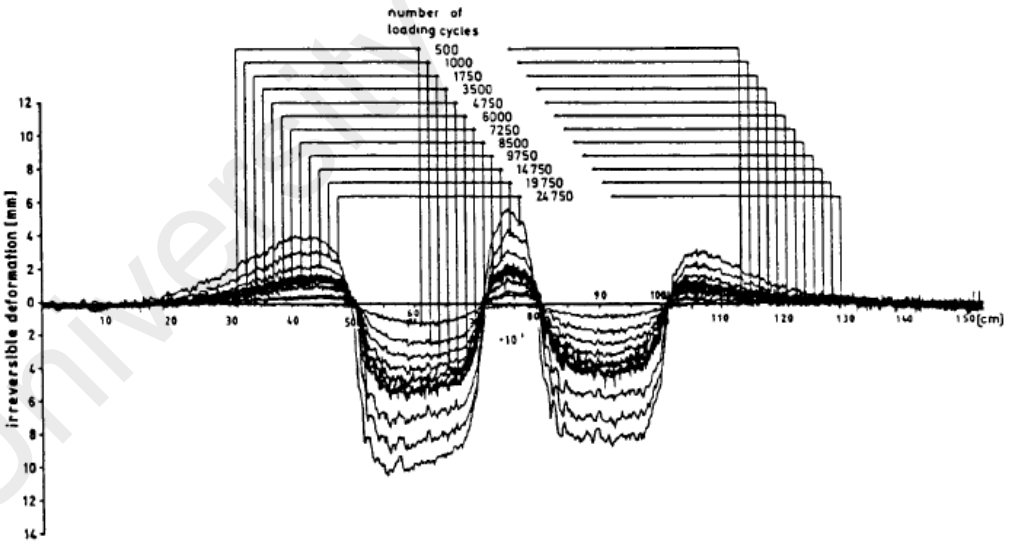

Figure 2.1 Effect of Number of Passes on Transverse Surface Profile (Eisenmann and Hilmer, 1987)

2.3.2 Effect of Temperature on Rutting Potential

The dependence of the flow properties of bituminous mixtures on temperature is due to changes in the rheological properties of the binder. The binder is a temperature susceptible material because of its viscoelastic material characteristics. Therefore, the stiffness of the bitumen can vary with respect to the change of temperature. The change in bitumen stiffness results in a stiffness change of the bituminous mixture. Previous studies showed that the resistance to deformation of bituminous materials decreases rapidly as temperature increases, especially if the ambient temperature approaches or exceeds the softening points of the binders used in such mixes (Van Thanh, D., and Feng, C. P., 2013).

Previous studies indicated that the temperature of the pavement is greatly influenced by the air temperature (De Zhang Huang, 2012; Zhang Min et al., 2012; Song Xiaoyan and Du Yuezong, 2004; Han Zidong, 2001). For instance, when the air temperature is below 35°C, the temperature of bituminous pavement is generally less than 55°C. At this range of temperature, the deformation of the pavement is insignificant. If the air temperature is about 38°C, the temperature of the bituminous pavement reaches 60°C. At this temperature, the deformation of the bituminous pavement under loading is remarkable. The deformation of the pavement becomes a serious problem when the air temperature rises above 38°C. Sometimes, an abnormally high pavement temperature is observed, such as when the air temperature reaches a maximum of about 45°C, which causes the pavement temperature to rise to 70°C.

In Malaysia, the influence of temperature on bituminous pavement performance is considered to be very significant. According to the Malaysian Public Works Department (PWD), Malaysia observes a maximum air temperature of 45°C (ATJ 5/85). The PWD also indicated that the maximum average air temperature during the hottest 7-day period

(over the pavement design life) is 38^{o}C. The corresponding air temperature is proportional to a road pavement temperature of 60°C. A high pavement temperature, as above, would cause the bituminous pavement mixture to rapidly deform under traffic loading.

Rutting has been observed to be the main distress mechanism that typically occurs in countries with high pavement in-service temperatures. With this in mind, researchers have recognized the need to conduct laboratory tests on the rutting potential at high-temperature ranges similar to those encountered in the field. For instance, Hamzah et al. (2009) conducted a dynamic creep test on the wearing course of bituminous concrete (styrene-butadiene-styrene (SBS) modified mixtures) at 40°C and 60°C. They found that a 20°C increase in temperature significantly reduces the creep stiffness of SBS-modified mixtures by as much as 51.8%. The results obtained from the test-truck conducted by Hofstra and Klomo (1972) recorded that rutting increased by a factor of 250 to 350 with a temperature increase from 20°C to 60°C. Similarly, Mahboub and Little (1988), and Bonnot (1986) conservatively selected the hottest pavement profile (60°C) to represent critical conditions.

Moreover, the effects of temperature on permanent deformation have been studied by many researchers at the laboratory scale. Khodaii et al. (2014), and Ahari et al. (2014) investigated the effects of temperature on SBS modified bituminous mixtures. They found that temperature is an influential factor on the creep curves and the accumulated permanent strains of bituminous mixtures modified with SBS polymer modifier.

Since the temperature has been found to have a significant effect on the rutting, the author selected test temperatures of 40°C, 50°C and 60°C for the dynamic creep test. These temperatures were chosen to be relatively high to reproduce the most unfavourable conditions in Malaysia.

2.3.3 Other Factors Affecting Rutting

In addition to traffic loading and temperature, rutting is also affected by the characteristics of the bituminous mixture and test conditions. Table 2.2 summarizes the factors affecting the rutting of bituminous concrete mixtures.

Table 2.2 Factors Affecting the Rutting of Bituminous Concrete Mixtures (Sousa et al., 1991)

Parameter	Factor	Change in Factor	Effect of Change in Factor on Rutting Resistance
Aggregate	Surface texture	Smooth to rough	Increase
	Gradation	Gap to continuous	Increase
	Shape	Rounded to angular	Increase
	Size	Increase in maximum size	Increase
Binder	Stiffness [a]	Increase	Increase
Mixture	Binder content	Increase	Decrease
	Air void content [b]	Increase	Decrease
	VMA	Increase	Decrease
	Method of compaction	[d]	[d]
Test field conditions	Temperature	Increase	Decrease
	State of stress / strain	Increase in tire contact pressure	Decrease
	Load repetitions	Increase	Decrease
	Water	Dry to wet	Decrease if mix is water sensitive

[a]Refers to stiffness at temperature at which rutting propensity is being determined. Modifiers may be utilized to increase stiffness at critical temperatures, thereby reducing rutting potential.

[b]When air void contents are less than about 3 percent, the rutting potential of mixes increases

[c]It is argued that very low VMA's (e.g., less than 10 percent) should be avoided.

[d]The method of compaction, either laboratory or field, may influence the structure of the system and therefore the propensity for rutting.

2.4 Laboratory Tests to Evaluate Rutting Properties

Generally, several testing methods have been developed to evaluate the susceptibility and/or resistance of bituminous mixtures against the rutting phenomenon. Mohammad, L. N. (2006) summarised the tests considered for rutting in the book entitled

Performance Tests for Hot Mix Asphalt (HMA) Including Fundamental and Empirical Procedures. The tests, including the advantages and disadvantages, are shown in Table 2.3.

The main concern of the developed method is the ability of the test to effectively simulate the in-situ pavement conditions. Many of the test methods cannot simulate the stress conditions encountered in the real pavement. Moreover, some of the tests cannot distinguish the pavement deformation behaviour of different types of bituminous mixture (unmodified and modified mixtures). Furthermore, the complexity in equipment requirements and test procedures, and expensive equipment may limit application of the laboratory tests to evaluation of the rutting phenomenon of the mixtures.

Table 2.3 Comparative Assessment of Test Methods (Mohammad, L. N., 2006)

Classification	Test Method	Advantages	Disadvantages
Fundamental Diametral Tests	Diametral Static (creep)	- Easy to perform the test - Easy to fabricate the specimen	- Stress is nonuniform and strongly depended on the shape of the specimen - Inappropriate for estimating permanent deformation - High temperature (load) changes in the specimen shape affect the state of stress and the test measurement significantly. - Overestimate rutting - For the dynamic test, the equipment is complex
	Diametral Repeated Load	- Easy to perform the test - Easy to fabricate the specimen	
	Diametral Dynamic Modulus	- Easy to fabricate the specimen - Non-destructive test	
	Diametral Strength Test	- Easy to perform the test - Equipment is generally available in most labs - Easy to fabricate the specimen - Minimum test time	
Fundamental Uniaxial Test	Uniaxial Static (Creep)	- East to perform - Test equipment is simple and generally available - Wide spread, well known - More technical information	- Ability to predict performance is questionable - Restricted test temperature and load levels does not simulate field dynamic phenomena - Difficult to obtain 2:1 ratio specimens in lab
	Uniaxial repeated Load	- Better simulate traffic conditions	- Equipment is more complex - Restricted test temperature and load levels does not simulate field conditions - Difficult to obtain 2:1 ratio specimens in lab
	Uniaxial Dynamic Modulus	- Non-destructive test	- Equipment is more complex - Difficult to obtain 2:1 ratio specimens in lab
	Uniaxial Strength Test	- Easy to perform - Test equipment is simple and generally available - Minimum test time	- Questionable ability to predict permanent deformation

Table 2.3, continued

Classification	Test Method	Advantages	Disadvantages
Fundamental Triaxial Test	Triaxial Static (creep confined)	- Relatively simple test and equipment - Test temperature and load levels better simulate field conditions than unconfined - Potentially inexpensive	- Requires a triaxial chamber - Confinement increases complexity of the test
	Triaxial Repeated Load	- Test temperature and load levels better simulate field conditions than unconfined - Better expresses traffic conditions - Can accommodate varied specimen sizes - Criteria available	- Equipment is relatively complex and expensive - Required a triaxial chamber
	Triaxial Dynamic Modulus	- Provides necessary input for structural analysis - Non-destructive test	- At high temperature it is a complex test systems - Some possible number problem due to LVDT arrangement - Equipment is more complex and expensive - Requires a triaxial chamber
	Triaxial Strength	- Relative simple test and equipment - Minimum test time	- Ability to predict permanent deformation is questionable - Requires a triaxial chamber
Fundamental Shear Test	SST Frequency Sweep Test – Shear Dynamic Modulus	- The applied shear strain simulate the effect of road traffic - AASHTO standard procedure available - Specimen is prepared with SGC samples - Master curve could be drawn from different temperatures and frequencies - Non-destructive test	- Equipment is extremely expensive and rarely available - Test is complex and difficult to run, usually need special training - SGC samples need to be cut and glued before testing
	SST Repeated Shear at Constant Height	- The applied shear strains simulate the effect of road traffic - AASHTO procedure available - Specimen available from SGC samples	- Equipment is extremely expensive and rarely available - Test is complex and difficult to run, usually need special training - SGC samples need to be cut and glued before testing - High COV of test results - More than three replicates are needed
	Triaxial Shear Strength Test	- Short test time	- Much less used - Confined specimen requirements add complexity

Table 2.3, continued

Classification	Test Method	Advantages	Disadvantages
Empirical Tests	Marshall Test	- Wide spread, well known, standardized for mix design - Test procedure standardized - Easiest to implement and short test time - Equipment available in all labs	- Not able to correctly rank mixes for permanent deformation - Little data to indicate it is related to performance
	Hveem Test	- Developed with a good basic philosophy - Short test time - Triaxial load applied	- Not used as widely as Marshall in the past - California kneading compacter needed - Not able to correctly rank mixes for permanent deformation
	GTM	- Simulate the action of rollers during construction - Parameters are generated during compaction - Criteria available	- Equipment not widely available - Not able to correctly rank mixes for permanent deformation
	Lateral Pressure Indicator	- Test during compaction	- Problems to interpret test results - Not much data available

Table 2.3, continued

Classification	Test Method	Advantages	Disadvantages
Simulative Tests	Asphalt Pavement Analyser	- Simulates field traffic and temperature conditions - Modified and improved from GLWT - Simple to perform - 3-6 samples can be tested at the same time - Most widely used LWT in the US - Guidelines (criteria) are available - Cylindrical specimens use SGC	- Relatively expensive except for new table top version.
	Hamburg Wheel-Tracking Device	- Widely used in Germany - Capable of evaluating moisture-induced damage - 2 samples tested at same time	- Less potential to be accepted widely in the United States (U.S)
	French rutting Tester	- Successfully used in France - Two HMA slabs can be tested at one time	- Not widely available in U.S
	PURWbeel	- Specimen can be from filed as well as lab-prepared	- Linear compactor needed - Not widely available
	Model Mobile Load Simulator	- Specimen is scaled to full-scaled load simulator	- Extra materials needed - Not suitable for routine use - Standard for lab specimen fabrication needs to be developed
	RLWT	- Use SGC sample - Some relationship with APA rut depth	- Not widely used in the United States - Very little data available
	Wessex Device	- Two specimens could be tested at one time - Use SGC samples	- Not widely used or well known - Very little data available

2.4.1 Dynamic Creep Test

The dynamic creep tests, also known as uniaxial repeated load, simulate the actual field situations more realistically than other testing methods (Zhou et al., 2003; Mehrera and Khodaii, 2010 and Li and Xiao, 2014). The test, which is performed under repeated loading and shows the accumulated permanent deformation of the mixture, is probably the most suitable laboratory test for performance-based specifications.

The dynamic creep test method was developed by Monismith et al. in 1975, which is based on the concept of axial compression. The testing parameters were standardized in accordance with the British Standard DD 226, with loading stress, pulse width, rest period, loading cycle, and preload for 600 s as follows: 100 kPa, 1000 ms, 10 ms, 1800 counts and 10 kPa, respectively. Recently, the Australian Standard (AS 2891.12.1), which is in agreement with the European, British and US Standards, has been used by many researchers (Mirzahosseini et al., 2011).

The dynamic creep test, which is performed using well recognized apparatus like the Universal testing Machine (UTM), seems to be the most popular option to evaluate the permanent deformation of bituminous mixtures. This device is equipped with a compressed air loading system and can impose any type of load, such as rectangular and sinusoidal. In the dynamic creep test, a cylindrical test specimen (sample diameter 100 mm with 50mm height) is subjected to repeated dynamic loads in the axial direction.

The test parameter used to evaluate the dynamic creep results is the permanent strain, which is accumulated at each loading cycle. Moreover other parameters can be determined, such as the dynamic creep modulus, which is the applied stress divided by the permanent strain. This indicates that the test provides multiple output data with a reasonable test time and less material consumption. To match the real environmental

conditions, the influence of different temperature and loading conditions (e.g. frequency, duration, load cycle, stress level) on the permanent deformation can be evaluated and incorporated using the UTM.

Previous research reported that the dynamic creep test has a very good correlation with the measured rut depth of the bituminous layers, and shows high capability for estimating the rutting potential of bituminous layers for both modified and unmodified bituminous mixtures. Zhou et al. (2003); Mehrera and Khodaii (2010), and Li and Xiao (2014) reported that the results from the repeated load permanent deformation test matched the field performance closely and that the total permanent strain was also found to be a reasonable indicator of the field rutting performance. Hence, the dynamic creep test has been used extensively to simulate the actual field situations realistically.

Moreover, Tayebali (1990) and Tanco (1992) reported that the dynamic creep test was more responsive to the presence of modified binders in bituminous mixtures than the static creep test. A similar judgement was reported by Kaloush and Witczak (2002) who found that the dynamic creep test is an appropriate laboratory method to investigate the permanent deformation of modified and unmodified bituminous mixtures. Accordingly, many researchers have used the dynamic creep test to analyse the permanent deformation for modified and unmodified bituminous mixtures (Baghaee et al., 2014; Khodaii et al., 2014; Dehnad et al., 2013; Ameri et al., 2013; et al., 2012; Arabani and Azarhoosh, 2012; Alataş et al., 2012; Mirzahosseini et al., 2011; Mehrara and Khodaii, 2011; Kalyoncuoglu and Tigdemir, 2011).

2.5 Permanent Deformation Prediction Models

In addition to the laboratory tests, many researchers are interested in developing the performance models to characterizing the permanent deformation and further estimate

the future service of the pavements (Meena, S., & Biligiri, K. P. , 2016; Zhu, T., Ma, T., Huang, X., & Wang, S. (2016). Moreover, with increases in the axle load, load repetition and tyre pressure on different types of wearing course (bituminous mixtures), a need has developed for a methodology to predict the rut depths in advance of construction to mitigate potential safety problems. Consequently, many prediction models have been developed to predict the permanent deformation response of bituminous mixtures to temperature, number of load applications or time of loading, mixture properties, state of stress and other influential parameters.

Figure 2.2 shows a schematic explaining the relationship between the accumulated permanent deformations and the loading cycles in the dynamic creep tests. As seen from the figure, the accumulated permanent strain curve is divided into three main stages: primary, secondary and tertiary. The derived curves are used to compare the resistance of different bituminous mixtures against permanent deformations and rutting distress. For this purpose, it is necessary to use a prediction model that not only fits the curve but that is also able to identify the location of the boundary points connecting the primary to the secondary stages, and the secondary to the tertiary stages. Moreover, the prediction model should realistically characterize the different bituminous mixtures.

Many models have been proposed to characterize the permanent deformation behaviour of bituminous mixtures under repeated load tests in the past four decades. A summary of the permanent deformation models is tabulated in Table 2.4. Most of the models have limitations, such as they cannot represent all three stages of creep curve and find it difficult to locate the onsets of the secondary and tertiary stages. A recent model developed by Kalyoncuoglu and Tigdemir (2011), and Arash et al. (2014) proposed a logarithmic function for fitting the creep curve of the bituminous mixtures derived from

the dynamic creep tests. However, these models are also limited to describing the primary and secondary stages only.

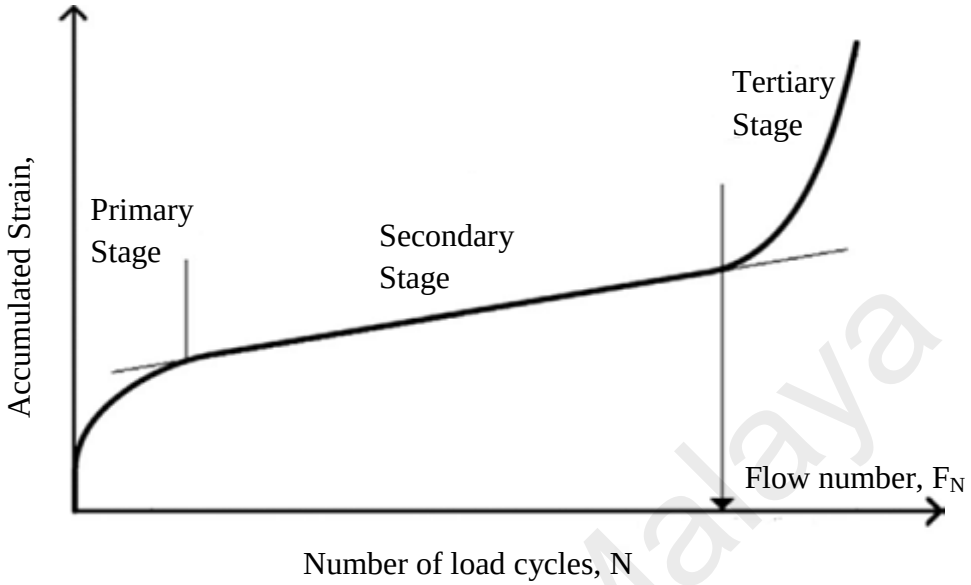

Figure 2.2 Relationship Between the Accumulated Permanent Deformations and the Loading Cycles in the Dynamic Creep Tests (Zhou et al., 2004).

Due to the above limitations, a three-stage model to characterise the three regions of the creep curve from the dynamic creep test were developed by Zhou et al. (2004). Among all the developed models in this field, the proposed three-stage model is the most accurate model to fit to the creep curves (all three stages) and to identify the locations of the two boundary points on the creep curves. Details of the Zhou model are explained in the following section.

Table 2.4 Brief Summary of Permanent Deformation Models

Model	Model Form	Variables
Semi-log model (Barksdale 1972)	$\varepsilon_p = a_1 + b_1 \log N$ $\varepsilon_{pn} = \frac{b_1}{N}\ (N > 1)$	ε_p = accumulated permanent strain ε_{pn} = permanent strain due to a single load application, i.e. at the *N*th application N = number of load cycles 'a_1, b_1 = regression coefficients
Power law model	$\varepsilon_p = aN^b$	N = number of load cycles a, b = regression coefficients
VESYS model (1977)	$\varepsilon_{pn} = \mu\varepsilon_r N^{-\alpha}$	ε_{pn} = permanent strain due to a single load application, i.e. at the *N*th application μ = permanent deformation parameter ε_r = resilient strain, generally assumed to be independent of the number of load repetitions (*N*) α = coefficient
Monismith et al. (1975)	$\varepsilon_p = \delta(T)N^{\alpha}\ \sigma^{n-1}\left[\sigma_z - 0.5^*(\sigma_x + \sigma_y)\right]$	δ(T) = temperature function α = coefficient N = number of load cycles T = load time σ = equivalent stress defined as a function of principle stress
Brown and Bell (1977)	$\varepsilon_p = \left({}^{q}/_{a}\right)^{b} N$	'ε_p = permanent shear strain 'q= deviatoric stress 'a, b = coefficient N = number of load cycles
Francken (1977)	$\varepsilon_p = AN^B + C\ (e^{DN} - 1)$	*A, B, C,* and *D* = coefficients N = number of load cycles
Ohio State Univ. (1986)	${}^{\varepsilon_p}/_{N} = A_a N^{-m}$	A_a= material property, function of resilient modulus and applied stress 'm = material parameter
Tseng and Lytton (1989)	$\varepsilon_p = \varepsilon_0\ \exp(-\left({}^{\rho}/_{N}\right)^{b})$ $\varepsilon_{pn} = \varepsilon_0 \beta \rho^{\beta} \frac{\sqrt[N\beta]{A}}{N^{\beta+1}}$	ε_0, *ρ, b* = regression coefficients N = number of load cycles ε_{pn} = permanent strain due to a single load application, i.e. at the *N*th application β, ρ = regression constant A=$1/e^{\rho^{\beta}}$ is a constant and less than 1
Wilshire and Evans (1994)	$\varepsilon_p = \theta_1\left(1 - e^{\theta_2 N}\right) + \theta_3\left(e^{-\theta_4 N} - 1\right)$	ε_p = creep strain 'ϑ_1,ϑ_3 = primary and tertiary

		strain 'ϑ_2,ϑ_4 = rate parameters quantifying the curvature of the primary and tertiary stages
MEPDG (2002)	$\frac{\varepsilon_p}{\varepsilon_r} = 10^{k_1} T^{k_2} N^{k_3}$	ε_p= resilient strain N = number of load cycles T = temperature 'k_1, k_2, k_3 = regression coefficients
AASHTO 2002	$log\frac{\varepsilon_p}{\varepsilon_r} = \log C + 0.4262\ logN$	ε_p= accumulated permanent strain ε_r= resilient strain N = number of load repetitions $C = T^{2.02755}/5615.391$= function of temperature (*T, °F*)
Zhou et al. (2004)	Primary stage: $\varepsilon_p = aN^b \ , \ \ N < N_{PS}$ Secondary stage: $\varepsilon_p = \varepsilon_{PS} + c\ (N - N_{PS}),$ and $\varepsilon_{PS} = a\ N_{PS}^b,\ N_{PS} \le N \le N_{ST}$ Tertiary stage: $\varepsilon_p = \varepsilon_{ST} + d\ (e^{f(N - N_{ST})} - 1),$ $and\ \varepsilon_{ST} = \varepsilon_{PS} + c(N_{ST} - N_{PS}),\ N \ge N_{ST}$	ε_p= Accumulated permanent strain N = Number of load repittaions N_{ps} = Number of load repetitions corresponding to the starting point of the secondary region N_{ST}= Number of load repetitions corresponding to the starting point of the tertiary region ε_{ps}= Plastic strain at the starting point of the secondary region ε_{ST}= Plastic strain at the starting point of the tertiary region a, b, c, d, f = Regression constants
Mirzahosseini (2011)	$Log(F_n) = \frac{C/S}{(2C/S - 5)(-2VMA - 5)} + \frac{M/F}{(2C/S - 4)(BP - VMA)} + Exp\left(\frac{C/S - VMA + 1}{M/F - VMA - 4}\right)$	C/S = Coarse aggregate to fine aggregate ratio BP(%) = Percentage of bitumen VMA(%) = Percentage of voids in mineral aggregate M/F = Marshall stability to flow ratio (Marshall quotient)

2.5.1 Zhou three-stage model

The Zhou three-stage model could fit the creep curve (primary, secondary and tertiary stage) and estimate its boundary point. The power law, a linear function and an exponential model were used to characterise the primary secondary and tertiary stage, respectively. Corresponding to the primary, secondary and tertiary stages, there were three physical damage processes: strain hardening, microcracking initiation and propagation, and macrocracking initiation and propagation (Zhou and Scullion., 2002).

Many current research studies have used the Zhou model to evaluate the permanent deformation of unmodified and modified bituminous mixtures (Khodaii and Mehrara, 2009; Mehrara, A., and Khodaii, A. 2011; Baghaee Moghaddam et al., 2013). It seems that the Zhou-model outweighs the other models as it can develop mathematical functions to characterize the three-stage permanent deformation behaviour of bituminous mixtures. Moreover, the Zhou model can also be used to identify the transition point between stages, especially the new indicator of bituminous mixtures: flow number, FN (Kaloush et al., 2002, Li et al., 2014, Zhang et al., 2013). Therefore, a new-three stage model comparable to the field performance termed the Zhou three-stage model is proposed under this study. Figure 2.3 shows the model for each stage of the creep curve.

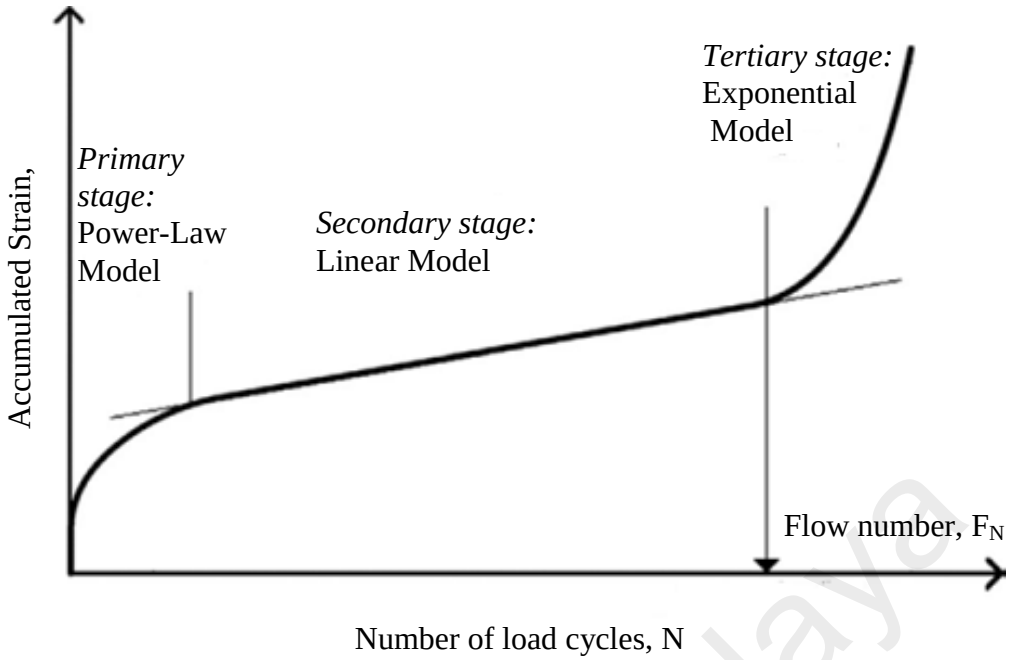

Figure 2.3 Model for Each Stage in Accordance with Zhou's Three-Stage Model (Zhou et al., 2004)

Primary stage: The permanent deformation accumulates rapidly in this stage. The main mechanism that occurs is densification and a reduction in volume. The power law model is selected to describe the primary stage of the permanent deformation curve. It is the most commonly used permanent deformation equation. As reported by Zhou et al. (2004), the model has been widely used in many pavement performance prediction software packages, such as *VESYS*, Ohio State, Superpave and AASHTO 2002. The power law model:

$$\varepsilon_p = aN^b \ , \quad N < N_{PS} \qquad (2.1)$$

where a and b = material constant; and N_{ps}=number of load repetitions corresponding to the initiation of the secondary stage.

Secondary stage: In the secondary stage, the permanent strain is accumulated linearly. Therefore, the simple linear model is utilised to characterize the secondary stage:

$$\varepsilon_p = \varepsilon_{PS} + c\,(N - N_{PS}), \quad \text{and} \quad \varepsilon_{PS} = a\,N_{PS}^{b}, \; N_{PS} \leq N \leq N_{ST} \qquad (2.2)$$

where c=material constant; N_{ST} (or flow number) is the number of load repetitions corresponding to the initiation of the tertiary stage; and ε_{PS} is the permanent strain corresponding to the initiation of the secondary stage.

Tertiary stage: Under the tertiary stage, the permanent strain per cycle increases rapidly and the bituminous mixtures gradually break. The cycle number in which the tertiary zone begins is referred to as the 'Flow Number' of the material, which represents the rutting performance of the mixture. The following equation is used to characterize the tertiary stage:

$$\varepsilon_p = \varepsilon_{ST} + d\left(e^{f(N - N_{ST})} - 1\right), \; and \; \varepsilon_{ST} = \varepsilon_{PS} + c(N_{ST} - N_{PS}), \quad N \geq N_{ST} \quad (2.3)$$

where d and f=material constants; and ε_{ST}=permanent strain corresponding to the initiation of the tertiary stage.

Many research studies found that the Zhou three-stage model perfectly presents all stages of the creep curve (Baghaee Moghaddam et al., 2013; Katman et al., 2015; Khodaii and Mehrara, 2009; Khodaii and Mehrara, 2011). However, under pavement structures, it is unnecessary to expand the rutting model to characterize the secondary and tertiary rutting. Zhou and Scullion (2002) reported that rut depths measured in more than 50 pavement structures under the accelerated pavement test (APT) were limited to the primary stage, even though the accumulated rut depths of the bituminous layer were deeper than 20mm. From the APT results, it is shown that the rutting development follows the power law model. Thus, of the existing rutting models, the well-known

power law model is recommended to predict the rut depth of bituminous mixtures, even though none of the existing rutting models can characterize the secondary and tertiary stages.

2.6 Bitumen Modifiers and Additives

Rutting can be reduced by using materials that intensify mixtures, thus resulting in better permanent deformation resistance. Therefore, many researchers have tried to improve rutting performance by introducing modifiers intended to increase the viscosity of the bituminous binder at high temperatures (O. Xu, et al., 2016; Bai, F., Yang, X., & Zeng, G. ,2016; Podolsky, 2016). There are a number of different bitumen modifiers available on the market, which can either be introduced directly into the bitumen, or added into the mixture containing the aggregate. In order to achieve the improvement of the bitumen properties, any selected modifier should be able to create a secondary network or establish a new balance system within the bitumen through molecular interactions or by reacting chemically with the binder. The reactions between modifiers and base bitumen will change the characteristics of the bitumen and concurrently improve the performance of the bituminous mixture when used as a binder.

There are many types of modifier that provide different benefits. Table 2.5 shows the different groups of additive or modifier, as classified by Read and Whiteoak (2003).

Table 2.5 Types of physical modifier and additive used in the material (Read and Whiteoak, 2003)

Type of modifier	Type of additive
(1) Thermoplastic Elastomers	- Styrene – butadiene – styrene (SBS) - Styrene – butadiene – rubber (SBR) - Styrene – isoprene – styrene (SIS) - Styrene – ethylene – butadiene – styrene (SEBS) - Ethylene – propylene – diene terpolymer (EPDM) - Isobutene – isoprene copolymer (IIR) - Natural rubber - Crumb tyre rubber - Polybutadine (PBD) - Polyisoprene
(2) Thermoplastic Polymer	- Ethylene vinyl acetate (EVA) - Ethylene methyl acrylate (EMA) - Ethylene butyl acrylate (EBA) - Atactic polypropylene (APP) - Polyethylene (PE) - Polypropylene (PP) - Polyvinyl Chloride (PVC) - Polystyrene (PS)
(3) Thermosetting Polymers	- Epoxy Resin - Polyurethane Resin - Acrylic Resin - Phenolic resin

2.7 Crumb Rubber Tyre

The use of crumb rubber in the modification of the binder has continued to evolve since its introduction in the early 1960s. The utilization of crumb rubber in bituminous pavement has been proven to enhance the pavement performance as well as reduce the waste tyre scenario faced around the globe.

2.7.1 Waste Tyre Scenario

The increasing number of vehicles on the roads generates millions of used tyres every year. According to reports from the largest associations of tyre and rubber product manufacturers, the annual global production of tyres is some 1.4 billion units, which corresponds to an estimated 17 million tonnes of used tyres each year (RMA, 2009;

JATMA, 2010; ETRMA, 2011; WBCSD, 2010). In Malaysia, the waste tyres generated annually were estimated to number sum 8.2 million or approximately 57,391 tonnes, of which 60% are disposed of via unknown routes (Kumar 2006). The dynamic growth in the number of used tyres creates problems in terms of landfills, health and environmental risks from the stockpiling of tyres.

Many new technologies for manufacturing rubber products have been created for scrap tyres including material recycling. As illustrated in Figure 2.4, the major method for the recovery of waste tyres in 2010 was material recycling (40%). According to the European Tyre and Rubber Manufacturers' Association (ETRMA, 2011a), the main recovery route within material recycling was reprocessing the waste tyres as tyre rubber granulates and powder in various applications (80%). This was followed by the use in civil engineering applications and public works (18%). Figure 2.5 shows the recovery and recycling of tyres (End-of-life tyres, ELTs) in Europe for 2010.

2.7.2 Waste Tyre Management in Malaysia

Kumar (2006) reported that about 60% of waste tyres generated annually in Malaysia are unknown to what extent they are disposed. As a result, the National Solid Waste Management Department under the Ministry of Housing and Local Government conducted a study on scrap tyres management for Peninsular Malaysia. The report was published in year 2011 which the main objective is to provide the Malaysian Government with sufficient background and recommendations for a decision to establish a collection and treatment system for scrap tyres for Peninsular Malaysia.

Systematic systems in scrap tyre management including the collection method are crucial for sustainable supplies of scrap tyres. A holistic approach in management of waste tyres is challenging since it involves many stakeholders: governmental agencies,

tyre manufacturers, tyre industry associations, tyre businesses, scrap tyres collectors and traders, and scrap tyre treatment and disposal companies. Scrap tyres collectors and traders are responsible to collect and transport the scrap tyres from the tyre shops to retreaders, recycling facilities or to the nearest landfill sites. Collectors charge a service fee to collect the scrap tyres together with the transportation fee if there is undefined coverage of collection. The collected scrap tyres are sorted according to treatment and disposal types. The sorted scrap tyres are then sell to the tyre retreaders or transported to the recycling centres and landfill sites.

There are three groups of scrap tyre collectors/traders available in Malaysia (KPKT, 2011):

1. Collectors that provide disposal service to the tyre shops (paid service). Mainly unwanted tyres that need to be disposed to the nearest landfill.

2. Collectors that buy scrap tyres from the tyre shops. Mainly retreadable and reusable tyre (second hand tyres).

3. Collectors that voluntarily collect the unwanted used tyres from tyre shops without any charges (free disposal service). The frequency of this collection is usually not fixed (Once or twice a week collection).

In Malaysia, the crumb rubber was produced from scrap tyres by the reclaimed rubber production companies. Rubplast Sdn. Bhd., located in Taiping, Perak, Jeng Yuan Reclaimed Rubber Sdn. Bhd. and Yong Fong Rubber Industries Sdn. Bhd., both located in Klang are the companies that actively recycles the scrap tyres and processes the rubber crumbs. Moreover, there are additional six treatment facilities in peninsular Malaysia who involves in processing of scrap tyres.

The existing systematic collecting system provided by the collectors and effective production of crumb rubber by the production companies makes the feasibility of using the crumb rubber in Malaysian roads achievable. Moreover, continuous supports from the government authorities (federal government and state government) seem to further encourage the usage of crumb rubber in road construction.

The increase in the number of registered vehicles was determined as a main contributor to the scrap tyres. A 5% annual growth rate of registered vehicles (KPKT, 2011) contributes to significant increase in scrap tyres. A study conducted by National Solid Waste Management Department, Ministry of Housing and Local Government revealed that the number of scrap tyres in Malaysia increases gradually, i.e 256138, 268945, 282392, 296512 and 311337 tonnes for year 2011, 2012, 2013, 2014 and 2015 respectively (KPKT, 2011). Estimated production of crumb rubber in 2015 approximately between 93401 to 124535 tonnes based on the production of 3-4kg of crumb rubber per truck tyre.

Scrap tyres shredding and granulation industry appears to be a commercial and environmental sustainable facility in the local market. Industry in tyres shredding and granulation took about three years for payback period with the ratio of capital invested to annual profit is RM 15 million to RM 4.9 million per year (RM 15 million divide by RM 4.9 million (KPKT, 2011). The calculation was based on a price of RM 800 per tonne of crumb rubber. It requires a minimum supply of 800,000 tyres per year for a shredding and granulation plant to be economically viable and the sources of tyre supply must be within 250km distance from the facility.

Considering the rapid return period in tyres shredding and granulation industry, this technology offers attractive investment to tyre recycling players. Moreover, tax incentive by the Malaysian government to encourage green technology together with

attractive loan scheme offered by Malaysian financial agencies inspire this industry to a higher level. With the gradual increase in number of scrap tyres in Malaysia and the constant supply of crumb rubber by the tyre recycling industry; the prospect of using crumb rubber in Malaysian road should be given a proper attention. Moreover, many research studies show the benefits offered by crumb rubber in increasing the properties of the mixtures; consequently results in better pavement performance.

2.7.3 History of Crumb Rubber in Road Bituminous Mixture

One of the main markets in the material recycling of waste tyres is by grinding them to produce rubber crumbs for use in a wide variety of consumer and civil engineering applications. Several processes can be used to produce ground rubber crumbs, namely ambient grinding, cryogenic grinding, wet-grinding and hydro jet size reduction, and pyrolysis. Ambient grinding is the most commonly used to increase pavement performance (Shatanawi et al., 2012) and probably the most cost effective method of processing end of life tyres.

According to the Transportation Research Record (1992), the use of recycled tyre rubber in bituminous pavements started in the 1840s, with an experiment involving natural rubber with bitumen. In the 1960s, the use of scrap tyres as secondary materials in the pavement industry started. Charles McDonald, a material engineer from the city of Phoenix in Arizona (USA), was the first to find technology to incorporate crumb rubber with bitumen through the wet mixing process. By 1975, crumb rubber was successfully incorporated into bituminous mixtures, and, in 1988, a definition for rubberized bitumen was included in the American Society for Testing and Materials (ASTM) D8, and later specified in ASTM D6114-97.

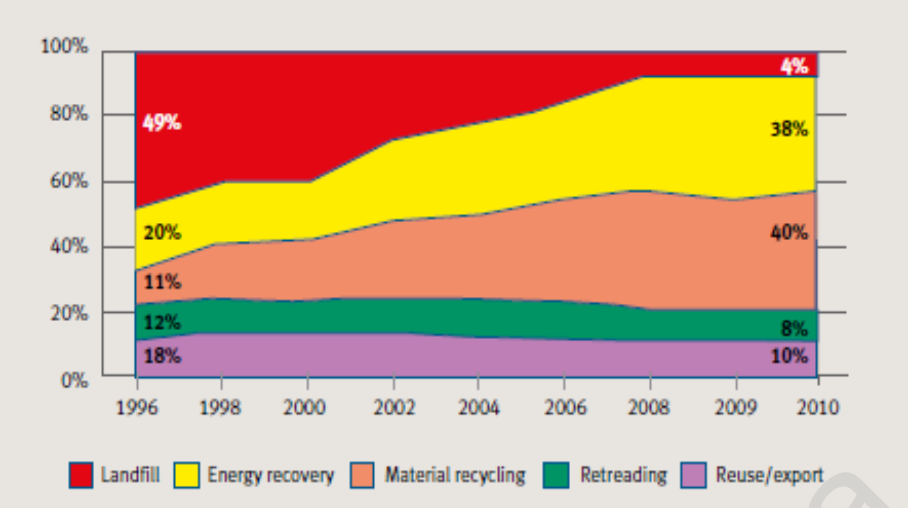

Figure 2.4 Progress in Recovery Routes of Waste Tyres Between 1994 and 2010 (ETRMA, 2011a Retrieved from http://www.etrma.org/uploads/Modules/Documentsmanager/brochure-elt-2011-final.pdf).

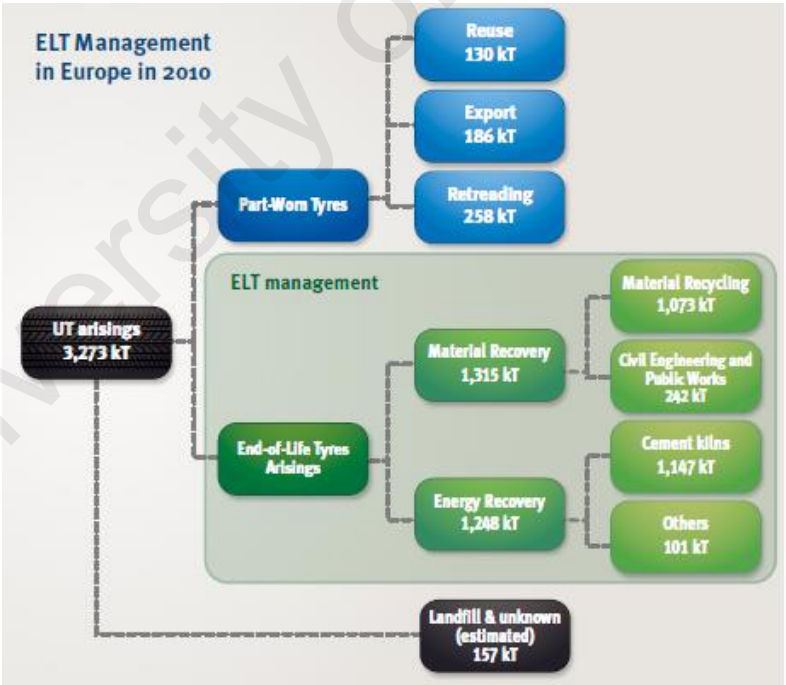

Figure 2.5 Activity of Organizations in the Recovery and Recycling of Tyres (ETRMA, 2011a Retrieved from http://www.etrma.org/uploads/Modules/Documentsmanager/brochure-elt-2011-final.pdf).

Nowadays, these rubberized bitumen materials have spread worldwide and been modified more widely. Rubberized bitumen has been used extensively in Arizona, California, Texas, Florida, South Carolina, Nevada, New Mexico, Mississippi, Oregon and Washington in the USA. It is also used in several countries of Western Europe, Canada and in South Africa. The preference for using rubberized bitumen is due to the high performance (reduced cracking and rutting, increased skid resistance and lower traffic noise). Moreover, using recycled materials could solve environmental problems.

In Malaysia, trials using rubberized bitumen were initiated in the 1950s. The first trial was laid between Kota Bharu and Kuala Krai using 5% rubber powder. Following that, several other trials were laid in the states of Kedah, Perlis, Kelantan, Johor, Negeri Sembilan and Melaka. Unfortunately, none of these trials were monitored closely, and, as such, no details are available. In 1968 a full-scale experiment using natural rubber latex (1.5% and 3%) was carried out at KL-Seremban and KL-Bentong at kilometre 43.45 – 46.6 and 37.01 – 37.50, respectively. However, the trial sections failed after three years due to the rapid increase in traffic (Chew and Ting, 1974). At that point, the Public Works Department concluded that this trial was a failure and any research related to rubber was stopped. Nevertheless, a more intensive research was conducted by the Public Works Department and the Rubber Research Institute of Malaysia (RRIM) in 1987. A number of laboratory assessments and field trials were subsequently conducted under the collaborative study including the Klang trial in 1988, the Rembau trial in 1993, the Sungai Buluh trial in 1996 and the Kuala Lumpur International Airport (KLIA) project in 1998.

2.7.4 Swelling of Crumb Rubber in Bitumen

Crumb rubber acts as a bitumen modifier for which the main purpose of the rubber-bitumen reaction is to increase the viscosity and elasticity of the binder. Therefore, a

high swelling rate of crumb rubber is favourable to obtain a highly viscous rubberized bitumen (Chong et al., 2013).

The interaction between the rubber and bitumen stems from two simultaneous processes: partial digestion of the rubber into the bitumen, and the adsorption of the aromatic oils available in the bitumen with the polymeric chains of the rubber (Lo Presti, D., 2013; Cheovits et al. (1982). The absorption of aromatic oils from the bitumen into the rubber's polymer chains causes the rubber to swell and soften producing a gel-like material. During the reaction, there is a simultaneous reduction in the oily fraction and an increase in the size of the rubber particles with a consequent reduction in the inter-particle distance. According to Heitzman (1992), this reaction implies the formation of gel structures that produce a viscosity increase of up to a factor of 10.

The interaction process is subject to a number of variables, such as type and speed of mechanical mixing, processing conditions, crumb rubber concentration, crumb rubber type, size and specific surface area of the crumb rubber, and the type of base bitumen. These variables affect the chemical interaction, thus offering different physical and engineering properties from the modified binders. The temperature and interaction time used in the processing conditions have a primary importance as well as in any mixing process (wet-mix and dry-mix processes), as rubber swells in a time and temperature dependent manner.

2.7.5 Processing Temperature

Temperature has two effects on the rubber interaction mechanism (swelling): the rate of swelling increases as the temperature increases, while the extent of swelling decreases with increasing temperature (Flory and Rehner, 1943). This phenomenon is in

agreement with Singleton (2000), who conducted swelling tests on crumb rubber particles using flux oil at different temperatures and found that maximum swelling increases almost proportionally with temperature, and that the rate of swelling increases but at a rate faster than the increase in temperature.

The study conducted by Attia et al. (2009) confirmed that temperature controls the rubber interaction mechanism. They found that, at low temperature (160°C), swelling is continual over the entire time period (8 hours). At a blending temperature of 200°C, they noticed that swelling still occurs at the beginning of the process. However, after 20 minutes of blending at 200°C, swelling of the fine material is offset as the swollen rubber particles depolymerise, releasing more components back to the liquid phase of the binder and decreasing viscosity. Moreover, Lalwani et al. (1982) conducted a study by increasing the temperature from 200 to 300°C and found that the binder elasticity is drastically reduced by as much as three times; however, no significant differences occurred due to changing the temperature from 150 to 200°C.

Many researchers conducted the blending of crumb rubber with bitumen at a temperature of 150°C to 200°C (Xie, Z., and Shen, J., 2014; Liu et al., 2014). Green and Tolonen (1977) mentioned that an adequate processing temperature leads to partial depolymerisation/devulcanisation of the rubber network, increasing the amount of components that are incorporated to the bitumen phase (bitumen matrix), and, consequently, reducing both the solid concentration and the rubber particle size. An adequate blending temperature would produce desirable properties of rubberized bitumen, and, thus, generate sufficient performance of the mixture when used as a binder.

A low blending temperature (<150°C) would not produce sufficient chemical reaction between the crumb rubber and the bitumen. As reported by Navarro et al. (2004), the

crumb rubber solubilised in the bitumen phase remains constant and equal to the initial value for processing temperatures between 90°C and 120ºC. This happens because these conditions are not severe enough to break up the chemically cross-linked network.

However, if the mixing temperature is too high (>200°C) together with extensive blending duration (> 2 hours), the swelling will continue to the point where the rubber particles stretch and disperse into the bitumen or so called depolymerisation/ devulcanisation due to long exposure to the high temperature (Heitzman 1992, Chehovits 1993). Oliver (1981) supported that rubber degradation takes place more rapidly at higher blending temperatures as depolymerisation cracks the binder networking into lower molecular weight molecules. Abdelrahman and Carpenter (1998), and Abdelrahman and Carpenter (1999) mentioned that depolymerisation starts very early at high blending temperature and continues up to full destruction of the polymer network if the binder is exposed to a very high temperature for sufficient time (>210ºC). At this stage, the viscosity of the rubberized bitumen decreases while the elasticity continues to modify. In contrast, the settling properties of rubberized bitumen significantly improve when blending is made at 230-260°C for 4-6 hours.

2.7.6 Processing time

The processing time is strongly correlated to the developed properties of rubberized bitumen. According to Lo Presti, D et al. (2012), the processing time develops the properties of rubberized bitumen in two phases: an initial phase or short-term phase that, although it varies with temperature, usually lasts for 30 to 40 minutes, and a second long-term phase that lasts for a few hours. Abdelrahman et al. (1998) mentioned that most of the changes occur in the initial phase, while the properties of rubberized bitumen stabilise in the second phase.

In general, the longer reaction time for digestion of the rubber-modified binder seemed to lead to an increase in the viscosity, which is related to the increase in the rubber mass through binder absorption. Oliver (1981) indicated that an increased digestion time of up to 2 hours over a temperature range of 180°C to 200°C improves the rubberized binder properties. However, various sources have demonstrated that prolonged digestion up to 24 hours causes a reduction in the viscosity and elastic response, suggesting some undesirable rubber degradation.

2.7.7 Incorporating Rubber in the Mixture

The main concern of utilizing crumb rubber is the method and degree of process control required, as the properties of crumb rubber modified binder change with time and temperature (Pavlovich et al., 1979; Chehovits et al., 1982). Time and temperature are the main variables in the bitumen-rubber interaction process that influences the swelling rate by the gel nature of the crumb rubber.

Rubber can be incorporated in the bituminous mixture by means of two processes: the wet process and the dry process. The wet process, which is the only method used in this study, is a technique in which the rubberized binders are produced when fine crumb rubber is mixed with bitumen at elevated temperatures prior to mixing with the aggregate. In the wet process, the crumb rubber acts as a bitumen modifier that is able to increase the binder's viscosity and elasticity. In contrast, in the dry process, the rubber particles, which are generally coarser than those in the wet process, are blended with the aggregate prior to the addition of the bitumen. In the dry process, crumb rubber keeps its physical shape and behaves as a flexible particulate filler in the mixture.

2.7.7.1 Wet Process

The wet process is the method of modifying bitumen with crumb rubber produced from scrap tyres and other components, as required before incorporating the modified binder into the bitumen paving materials. Generally, the wet process results in higher binder content because the binder thickness increases during mixing with the aggregate due to the higher binder viscosity. The concept of adding crumb rubber in bituminous mixture through the wet process can be divided into two broad categories – continuous blend method and terminal blend method.

The first category, the "continuous blend" is described as rubberized bitumen that maintains or exceeds the minimum rotational viscosity threshold of 1500 cPs at 177°C (or 190°C) over the interaction period (Caltrans, 2006). Generally, the rubberized bitumen produced with continuous blend is prepared at a temperature between 160°C to 200°C for duration 30-60 minutes. The benefits offered by the continuous blend include increased viscosity, increased elasticity and resilience; improved durability, improved resistance to surface initiated and fatigue/refelection cracking, improved aging and oxidation resistance, and improved resistance to rutting (Shafabakhsh et al., 2014). Although this may be true, rubberized binders prepared using the wet process also have limitations: high viscosity rubberized bitumen are not suitable for use in dense graded HMA due to inadequate void space in the densely graded aggregate matrix; construction may be more challenging, as temperature requirements are more critical; potential odour, which affects the environmental air quality; requires special storage tanks with augers to solve phase separation during storage; and should be used within hours of production.

In the second category, "terminal blend", the crumb rubber is blended with bitumen at high shear stress (up to 8000 rpm), and maintained at high processing temperature (200-

260°C) for a long mixing duration (>2 hours). It is believed that by blending at very high temperature for a long duration, the crumb rubber depolymerizes and completely dissolves in the bitumen. Therefore, the rubberized bitumen produced is fully digested or better dissolved into the bitumen without leaving visibly discrete particles. This produces a rubberized binder that does not require constant agitation to keep discrete crumb rubber particles uniformly distributed in the hot bitumen. Although the terminal blend seems to solve most of the limitations linked with the wet process, especially the phase separation problem, it may have a negative effect on the development of the performance properties due to crumb rubber depolymerisation. Terminal blends use fine crumb rubber (0.4mm or smaller) and the amount of crumb rubber may vary from 5–20% depending on the application (Willis et al., 2013).

2.7.7.2 Dry Process

The dry process was developed in Sweden in the 1960s (Heitzman, 1991). In this process, the crumb rubber is added to the aggregate before adding the bitumen. The main objective of this process is to use the crumb rubber to replace a percentage of aggregate and modify the grading. In general, coarse crumb rubber (0.4 to 10 mm) is used as a substitute for a small portion of the fine aggregate (typically 1-3 percent by mass of the total aggregate in the mixture).

Previous studies show that the properties of bituminous mixture prepared using the dry process improved through the interaction of the rubber with the bitumen during production (Singleton, 2000; Green and Tolonen, 1977). Therefore, the degree of reaction is affected by the mixing temperature and mixing duration. However, according to Takallou (1988), the reaction between the rubber and bitumen is less important to the properties of the material, as the reaction time is much shorter and the grading size of the crumb rubber is larger with less specific surface area compared to the wet process.

Compared to the wet process, the dry process is a far less popular method due to inconsistent field performance. Field trials have shown the performance of the dry process CRM material used as a surface layer to be inconsistent with its service life varying from two to twenty years. There are several reasons for this: uncontrollable crumb rubber sources, poor workmanship, flexible nature of the rubber particles, the adhesion with bitumen, and the reaction described above. Moreover, as the tyre properties change with age and vary from manufacturer to manufacturer, this variability of scrap tyres makes it even more difficult to control the consistency of the properties of the crumb rubber, and, consequently, the properties of the mixture.

2.8 Trans-Polyoctenamer

Crosslinking agents have recently been introduced into rubberized bitumen as an additive to enhance the compatibility and reaction of crumb rubber to bitumen. Introducing TOR to bitumen as a crosslinking agent can be considered as new. TOR can be utilized effectively for bitumen modification, especially with a combination of crumb rubber to produce thermodynamically stable blends, reduce phase separation when the modified bitumen is stored and reduce tackiness (Burns, 2004).

Trans-polyoctenamer (TOR), which is produced and marketed by Degussa AG with the trademark VESTENAMER®, is a kind of polymer with a double bond structure, of which the main task is to crosslink the sulphur of the asphaltene and the sulphur on the surface of the crumb rubber to form a ring and mesh composed of chain polymers (Liu et al., 2014). TOR is prepared by a structured of cyclooctene, which is synthesized from 1,3-butadiene via 1,5-cyclooctadiene. Cyclooctene is polymerized to polyoctenamer, which produces both linear and cyclic macromolecules. The molecular formula of polyoctenamer is –(C4H7=C4H7)–n and its synthesis is shown in Figure 2.6 (Evonik

DegussaGmbH,http://www.vestenamer.com/sites/dc/Downloadcenter/Evonik/Product/VESTENAMER/en/brochures/VESTENAMER%20Asphalt%20english.pdf.).

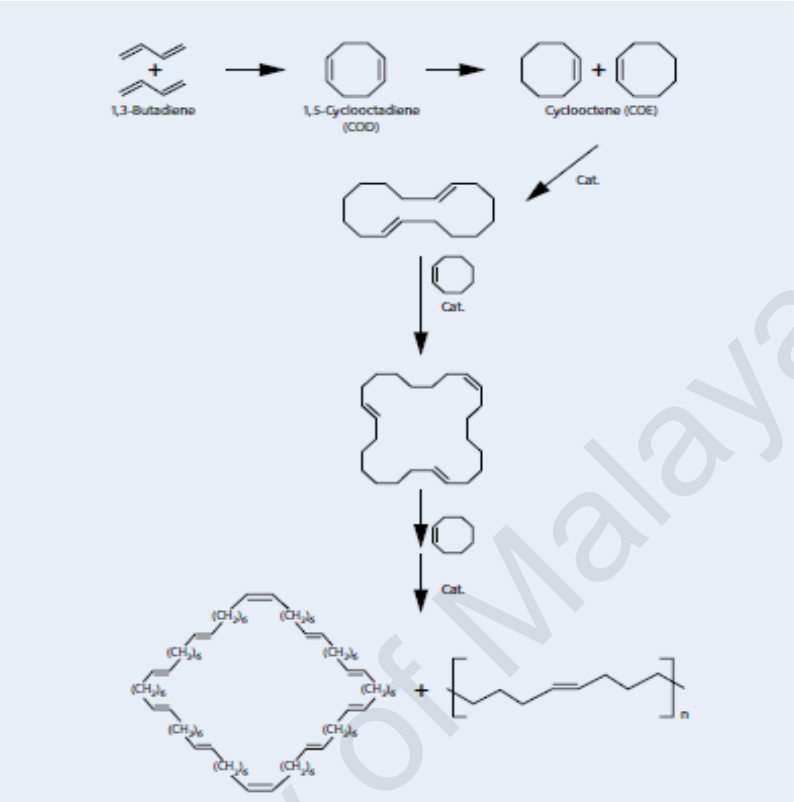

Figure 2.6. Synthesis of Trans-polyoctenamer (Evonik DegussaGmbH, Retrieved from http://www.vestenamer.com/sites/dc/Downloadcenter/Evonik/Product/VESTENAMER/en/brochures/VESTENAMER%20Asphalt%20english.pdf.).

According to Evonik Degussa GmbH, in the brochure entitled High Performance Polymers, the unique and exceptional properties of TOR are characterised by four structural elements: crystallinity, low viscosity above the melting point, high proportion of macrocycles and double bond content. Crystallinity (cis/trans ratio) is controlled by the polymerization conditions. In general, crystallinity increases as the trans-content increases, and, thus, a higher melting point can be obtained. Low viscosity above the melting point is a result of low molecular weight. The high content of macrocycles

permits a considerable reduction in the molecular weight and forms a completely three-dimensional network on crosslinking. TOR contains at least 25% weight of macrocycles with a molecular weight of up to 100,000. These macrocycles offer the high collapse resistance of TOR containing rubber compounds at temperatures above its melting point. TOR contains a double bond at every eighth carbon atom, and vulcanizes with all crosslinking agents commonly used in rubber.

TOR improves the dispersion stability of crumb rubber by facilitating wetting of the crumb rubber surface with the binder and enhancing the interaction between the crumb rubber and bitumen via crosslinking reactions with double bonds, and the sulphur component in bitumen or crumb rubber when mixed at high blending temperature. The crosslinking reactions prevent the sinking of the rubber particles by increasing the viscosity. Moreover, Evonik Degussa GmbH (2015) explained that TOR chemically bonds to the crumb rubber during its blending, and converts the thermoplastic bituminous to a thermoset polymer that can help reduce cracking and rutting.

In that according to Evonik Degussa GmbH, TOR enhances the rutting resistance of bituminous pavements, studies have been conducted recently by many researchers. The studies revealed that TOR increases the high temperature performance of rubberized binders (Plemons, 2013; Xie and Shen, 2014, Solaimanian et al., 2003). For instance, Solaimanian et al. (2003) evaluated the effect of TOR on rubberized bitumen with a virgin bitumen of PG 58-28 and CRM of 14 and 30 meshes. The study reported a one grade increase in the high temperature binder grade for a combination of 5% 14 mesh CRM and 4.5% TOR (by weight of CRM). The high temperature binder grade increased by three grades at 10% 14 mesh CRM. However, the study also reported that 30 mesh CRM did not increase the binder stiffness nearly as much as the 14 mesh CRM. The study conducted by Plemons (2013) using a combination of 0.5% TOR by weight of

bitumen and 10% of crumb rubber (sized 30 and 40 mesh) increased the high temperature grade of PG 67-22 bitumen. However, the use of TOR was not effective in preventing the settlement or separation of the rubber during heated storage.

Moreover, in the study conducted by Min and Jeong (2013), adding different amounts of TOR to air-blown bitumen showed an improvement in the elasticity modulus and temperature susceptibility. Other studies showed that TOR did not adversely affect the low temperature properties, instead, a noticeable improvement was observed through a reduction in the binder stiffness at low temperature as seen from the bending beam rheometer test and dynamic shear rheometer (DSR) test (Solaimanian et al., 2003; Puga., 2013).

Many studies recommended the dosage of TOR as 4.5% by weight of crumb rubber (Burns, 2000; Solaimanian et al., 2003; Bennert, 2004; Puga, 2013). A recent study conducted by Liu et al. (2014) revealed that adding 4.5% of TOR improves the engineering properties of rubberized bitumen. Based on the rheological properties of the modified binder, the study found that TOR decreases the viscosity of CRMB, and increases the workability and compatibility of the mixture. Moreover, fourier transform infrared spectroscopy (FTIR) spectrum analysis showed a complex chemical reaction between TOR and crumb rubber. Furthermore, the scanning electron microscopy (SEM) test analysis showed a more uniform distribution of crumb rubber particles in the bitumen. Based on the differential scanning calorimeter (DSC) test, Liu et al. (2014) observed a good correlation between the rheological property changes of crumb rubber modified bitumen and its internal constituents.

Xie and Shen (2014) investigated the separation properties of rubberized bitumen to which TOR had been added. The study used PG 67-22 and PG 64-22 as the base bitumen, three doses of crumb rubber (8%, 10% and 12% of the weight of binder), and

three doses of TOR (0%, 3% and 6% of the weight of binder) to produce crumb rubber modified bitumen. It was found that the absolute difference taken from the top and bottom of a tube test was improved by 20% less than the control when a dose of 3% TOR was added to the PG 67-22 bitumen. However, a further increase in the dose of the TOR did not decrease the absolute difference in the failure temperature. This study also found that the influence of TOR on the separation of rubberized bitumen is dependent on the type of base binder.

2.9 Concept of Stone Mastic Asphalt (SMA)

Stone mastic asphalt (SMA) has been acknowledged by many researches to provide better rutting resistance of road pavement. SMA is a hot bituminous mixture that is made up of bitumen, stabilizer, mineral filler and less fine aggregate consisting of a mastic binder. Researchers have agreed that this mixture fills the gap in the coarse aggregate skeleton gradation in the formation of the SMA mixture (Jun, Q., and Xiaolei, L, 2008, Ou La and Xiao Jingjing, 2009; Asi, 2006). In like manner, it provides a stable stone-on-stone skeleton that is held together by a rich mixture of binder, filler, and stabilizing additive. As a result, the stability of the pavement increased including the rutting resistance.

According to the National Asphalt Pavement Association (1994), SMA refers to a gap graded aggregate-bituminous hot mixture that maximizes the binder content and coarse aggregate fraction. This mixture is designed to have 3-4% air voids, and relatively high binder content due to the high amount of voids in the mineral aggregate. The mixture is typically prepared with a polymer fibre or modified binder to prevent drainage of the binder. The surface appearance of this mixture is similar to that of an open graded friction course; however, it has low in-place air voids similar to that of a dense graded HMA (Asi, I. M., 2006).

2.9.1 History of SMA

Stone mastic asphalt (SMA) was formulated back in the mid-sixties in Germany. In recognition of its excellent performance, a national standard was set in Germany in 1984. It was a great success and has been used in Europe for more than 20 years (AASHTO, 1991; Brown and Hemant, 1993). In Canada, SMA was introduced in 1991, and, since then, SMA has been employed in the construction of road pavements across its states with significant success. Nowadays, the UK uses SMA to resurface most of the roads that encounter heavy traffic to render surface treatment economical and cost-effective.

Due to the great performance of SMA in Europe, the United States constructed SMA pavements in 1991 through the cooperation of the Federal Highway Administration. According to the European study tour report, SMA in the United States was adopted after the 1990 European bituminous study tour to six European nations. This study tour played a major role in the USA's adoption of SMA as an alternative bituminous mixture. SMA in the United States is known as stone matrix asphalt, which is simply the Americanized version of the SMA in Europe (AASHTO, 1991).

İskender, E. (2013) mentioned that Japan also started to use SMA paving mixtures with great success. Recently, the Ministry of Communications in Saudi Arabia introduced SMA for its road specification. In addition, one test road was constructed in the Eastern Province of Saudi Arabia. In recent years, the SMA with its excellent performance was widely used for the pavement of high-grade highways around the world. For example, in Turkey, the SMA project implementation manifested an important subject within the Eastern Black Sea Region, which has a large landfill area (İskender, E. (2013).

In Malaysia, the concept of Stone Mastic Asphalt (SMA) was introduced to the Malaysian road authorities as early as the 1990s. Since then, numerous studies and several trial projects were initiated for the purpose of studying the durability and stability of SMA (Vasudevan, 2000; Muniady, 2000; Mohamad Razali, 2004). Besides the great performance of SMA, a study conducted by University Putra Malaysia showed that the construction cost of SMA is approximately 10 to 15% cheaper than the conventional mix with an extended pavement life of 1.5 times. This is achieved because of the thickness of the laid SMA surfacing being 30% less than the conventional wearing course layer (Hassim et al., 2005). However this claim contradicts a United States study that reported that the initial cost of SMA is 20% to 25% more than the conventional mix (Yu, J., 2000).

SMA is considered to be a premium mix for use in areas where high-volume traffic conditions exist and frequent maintenance is costly. Yu, J., (2000) reported that the initial cost of SMA is 20% to 26% higher than the conventional mix due to the use of quality materials. Stabilizing additives and high amount of filler are used in the SMA mixtures to stiffen the mastic at higher temperatures and used of high binder contents to ensure the durability and laying characteristics of SMA. Moreover, SMA mixtures are designed to have high aggregate content as compared with dense graded asphalt mixture in order to develop a stone-on-stone structural skeleton for better rut-resistance and durability.

The main costs of pavement construction include the materials, plant, transportation, equipment and labour. Hassim et al., (2005) revealed that the material was determined as the most significant factor in the construction cost of SMA pavement in Malaysia. The materials cost was determined as RN66.60 per square meter (Hassim et al., 2005). As the SMA pavement was constructed using imported fibres to stabilize the mixture;

use of crumb rubber (waste material) may reduce the materials cost. Moreover, the material cost can further be reduced as Malaysia has extensive supply of local crumb rubber at a reasonable price (RM1200/metric ton).

2.9.2 Performance Characteristics of SMA

Many advantages of SMA pavement have been reported by researchers. The unique characteristics of SMA have proven it to be the optimal bituminous pavement, which enables the roads to withstand the heavy vehicle loadings and wear resulting from super wide, studded and single truck tyres (Schimiedlin, 2002). The most important advantages of SMA are its resistance to rutting and its long-term durability (Vaitkus and Paliukaitė, 2013; Coleri, 2012). The durability of SMA should be equal, or greater than dense graded bituminous mixtures and significantly greater than open graded bituminous mixtures. According to the performance evaluation by the National Center for Asphalt Technology (NCAT), SMA is highly resistant to rutting, cracking and other distress compared to conventional HMA mixes (Brown et al., 1997). Similar findings have been observed by many highway authorities in their research reports and case studies. For example, the European asphalt pavement association in 1999, and the US department of transportation in 1998, also reported that the use of SMA on road surfaces could achieve better rut-resistance and durability. Due to their ability to reduce rutting, SMA is usable at intersections where traffic stress is considerably high for which dense grade and open graded aggregates are not a suitable choice.

In tropical regions, including Malaysia, studies on the effects of high temperature variations in terms of rutting potential is highly desirable. Van Thanh, D., and Feng, C. P. (2013) conducted a study on the influence of abnormally high temperatures (60, 65, 70 and 75°C) on the Marshall stability and the dynamic stability of SMA mixtures. The study used three types of fibre (lignin, basalt and polyester) in the preparation of SMA

mixtures. The study showed that the Marshall stability (MS) and dynamic stability (DS) of the three types of fibre SMA mixtures all decreased with increasing temperature. However, the study found that the MS and the DS of the three fibre SMA mixtures at 60-75°C still meet the specification requirement (specification requirement of China: MS≥6 kN and DS ≥3000 cycle/mm. The study concluded that although all three fibre SMA mixtures have very good high temperature stability, the basalt fibre SMA mixture is the best.

SMA has also shown high resistance to plastic deformation, which is a common problem under heavy traffic loads with high tyre pressures (Brown, 1997; Cooley, 2003). Traffic loads cause densification and affect the pavement materials shear strain. Goncalves et al. (2002) mentioned that plastic deformation in bituminous layers is mainly due to an excessively high binder content and low void volume. Moreover, deformation may also be caused by deficiencies in the densification of the layers during construction, or by plastic movement of the bituminous mixture subjected to high temperatures. In SMA mixtures, plastic deformation is minimised by certain mix parameters, such as binder content, aggregate type and gradation, and air void content.

The use of SMA for the surfacing of heavily trafficked roads has become more widespread over the last decade, which is not only due to its excellent resistance to permanent deformation, but also to the comfortable riding characteristics, including relatively low levels of traffic noise compared to dense bituminous concrete. Noise measurements carried out in different European countries have shown significant noise reduction from the use of SMA pavements. As shown by Alauddin and Susan (2010) in a study of sound absorption characteristics of typical pavement, regular superpave, SMA and fine graded mixes were shown to absorb 6.3%, 7.5% and 8.5% of sound, respectively. Moreover the European Asphalt Pavement Association (1998) reported

that SMA pavements with a maximum aggregate size of 11 mm (0/11 mm) or less (0/6 mm) give up to 2 – 3 dB(A) less noise compared with dense bituminous concrete. The noise absorbing characteristics offered by SMA play a significant role in long distance travelling by creating a smooth and quiet trip for the driver and passengers.

Another advantage of SMA is that the manufacturing plant for producing and compacting the SMA mixture, uses the same tools and machinery as for HMA. As with any HMA production process, close communication and cooperation between the agency and contractors is necessary to minimize SMA production problems. It is important to follow every phase of the manufacturing process. Moreover, all specifications and requirements, such as mix design, plant production, paving, compaction and quality assurance should be strictly followed in order to maximize the SMA performance.

In the case of pavements suffering from cracking problems, SMA is an optimal choice to be utilised as an overlay to reduce serious reflection cracking, which may result from the underlying cracked pavements due to the flexible mastic. A case study conducted by Brown (1997), Burlie et al. (2000), and Chen et al. (2009) confirmed that SMA mixtures appear to be more resistant to cracking than dense mixtures. Moreover, Burlie et al. (2000) mentioned that the life cycle performance and cost effectiveness of SMA could be improved through the mitigation of reflective cracking due to the excellent flexibility and fatigue endurance with the rich mastic component.

2.10 Summary

From the literature, it is found that the rutting mechanism of bituminous mixtures is significantly influenced by traffic loading and temperature. Previous studies have shown that an increase in stress levels and temperature lead to an increase in the rutting

parameters. However, studies have shown that the rutting of bituminous mixtures can be reduced by incorporating crumb rubber. Many factors should be considered in the process of using crumb rubber as a modifier; for instance, the processing temperature, the processing time and the blending methods. Moreover, current studies have been performed by incorporating chemical additives with crumb rubber in order to further increase the performance of rubberized bitumen. For instance, a crosslinking agent, namely, trans-polyoctenamer (TOR) has been shown to improve the properties of rubberized bitumen (Ng Puga, K. L. N., & Williams, R. C. ,2016).

The literature also showed that SMA is widely used as road pavement due to its excellent performance, especially its resistance to rutting. In the laboratory, many test methods can be used to assess the rutting resistance of bituminous mixtures including the dynamic creep test performed using a universal testing machine. The literature also revealed that the rutting parameters can be predicted using various models including the Zhou three-stage model.

2.11 Research Gap

Extensive literature has been studied by the author. The author found that crumb rubber is a type of waste material that can be obtained from waste tyres. Many studies mentioned that crumb rubber improves the properties of bituminous materials including its rutting resistance. However, the effects of crumb rubber on the rutting resistance of the bituminous mixtures in different environmental conditions, especially at extreme temperatures (>40°C) and high stress levels, has still not been studied extensively. It has been reported that low stress levels (e.g. 100 kPa) cannot properly manifest the rutting resistance of modified bituminous mixtures. Therefore, this study was conducted to fill the gap, i.e. using different test temperatures (40°C, 50°C and 60°C) and higher stress

levels (200 kPa and 400 kPa) to gain a better understanding about the rutting characteristics of SMA mixtures.

Moreover, this study used a crosslinking agent, namely, trans-polyoctenamer (TOR), in an attempt to improve the chemical reaction between the crumb rubber and bitumen. Researchers claimed that TOR, which is a mixture of linear and microcyclic polymers, chemically bonds the crumb rubber to the bitumen. Researchers believe that incorporating TOR with crumb rubber in bitumen might convert the thermoplastic bitumen to a thermoset polymer, which reduces rutting. Few studies have been conducted by incorporating TOR with crumb rubber for bitumen modification. Consequently, the use of crumb rubber modified bitumen reinforced with TOR in bituminous mixtures has hardly been studied, especially its effects on the rutting resistance of bituminous mixtures. This study was performed to fill this gap, i.e. to evaluate the effects of TOR with crumb rubber on the rutting resistance of SMA mixtures.

In addition, the literature shows that there have been limited studies on the effects of binder blending methods on the properties of bituminous mixtures. Therefore this study was conducted to fill other gaps, i.e. to study the effects of rubberized bitumen prepared with terminal blend and the continuous blend method on its relation with the rutting resistance of the SMA mixtures. It is believed that different blending parameters would significantly modify the rheology of the binder and thus affect the rutting resistance.

Throughout this study, Stone Mastic Asphalt (SMA) with aggregate nominal size 20 mm (SMA 20), as specified by the Malaysian Public Works Department, was utilized. The literature revealed that SMA is a kind of gap graded bituminous mixture that has many advantages including its resistance to rutting compared to dense graded bituminous mixture and open graded bituminous mixture. However, the performance of

SMA 20 to resist rutting has still not been researched extensively. Therefore, the next research gap to be filled is to use the local aggregate gradation (SMA 20) together with modified bitumen to resist rutting.

There are many performance models available to characterise the permanent deformation and further estimate the future service of the pavements. Many researchers found that the Zhou three-stage model seems to outweigh other models. Therefore, this study used the Zhou three-stage model to examine and predict the creep behaviour of the SMA 20 mixtures. Moreover, the model was chosen because no study using the Zhou three-stage model to examine the creep behaviour of SMA 20 mixtures was found.

CHAPTER 3: METHODOLOGY

3.1 Introduction

This chapter explains the methodology that has been used to achieve the research objectives. Figure 3.1 and Figure 3.2 show the methodology flow chart for the whole process utilised in the preparation and testing of the binder and mixture, respectively. This chapter also explains the materials, preparation of samples, experimental procedures, test apparatus, creep model and statistical methods used in the study.

In this study, all the experimental works were conducted at the Highway and Transportation Laboratory, University of Malaya, Kuala Lumpur, Malaysia. The experimental works are in accordance with international standards: Malaysian Standard Specification for Road Works (JKR), Road Engineering Association of Malaysia (REAM), British Standard (BS), American Society for Testing and Materials (ASTM), American Association of State Highway and Transportation Officials (AASHTO) and Australian Standard (AS).

In the study, the laboratory produced binders were given identification names (ID) to differentiate them. Table 3.1 presents the binder ID with the matrix for the eight types of binder that were developed and evaluated in this study. In the identification nomenclature, the ID is as follows: C stands for continuous blend, T for terminal blend, R for rubber content and T for TOR. For example, C4R is crumb rubber modified binder (CRMB) prepared via continuous blend contains 4% crumb rubber, whereas C4RT is crumb rubber modified binder with TOR (CRMB-TOR) prepared with 4% crumb rubber and 4.5% TOR. CRMB prepared with terminal blend is designated as T20R. The control sample is designated as 0R, which was prepared with bitumen 80/100 penetration.

Similar designations were used in the Marshall Specimens prepared from the respective binders throughout this dissertation, as tabulated in Table 3.1. In addition, the group of mixtures were changed from CRMB to CRMM and CRMB-TOR to CRMM-TOR in order to differentiate between the binder (B) and the mixture (M).

3.2 Materials

The SMA mixtures tested in this study were made with a bitumen 80/100 penetration, crumb rubber for preparation of CRMB, TOR for preparation of CRMB-TOR, and mineral aggregate. The aggregate, crumb rubber, TOR and bitumen sources remained constant for this study.

3.2.1 Aggregate

The aggregate was supplied from Kajang Rock Quarry in Kajang, Malaysia. Table 3.2 shows the properties of the aggregate utilized in this study.

3.2.2 Bitumen

Bitumen grade 80/100 penetration obtained from the vacuum distillation residue derived from crude oil is widely used in Malaysian road construction. In this study, bitumen 80/100 was obtained from the Asphalt Technology Sdn. Bhd. located at Port Klang, Malaysia. Table 3.3 shows the specification of the bitumen 80/100 penetration used in this study.

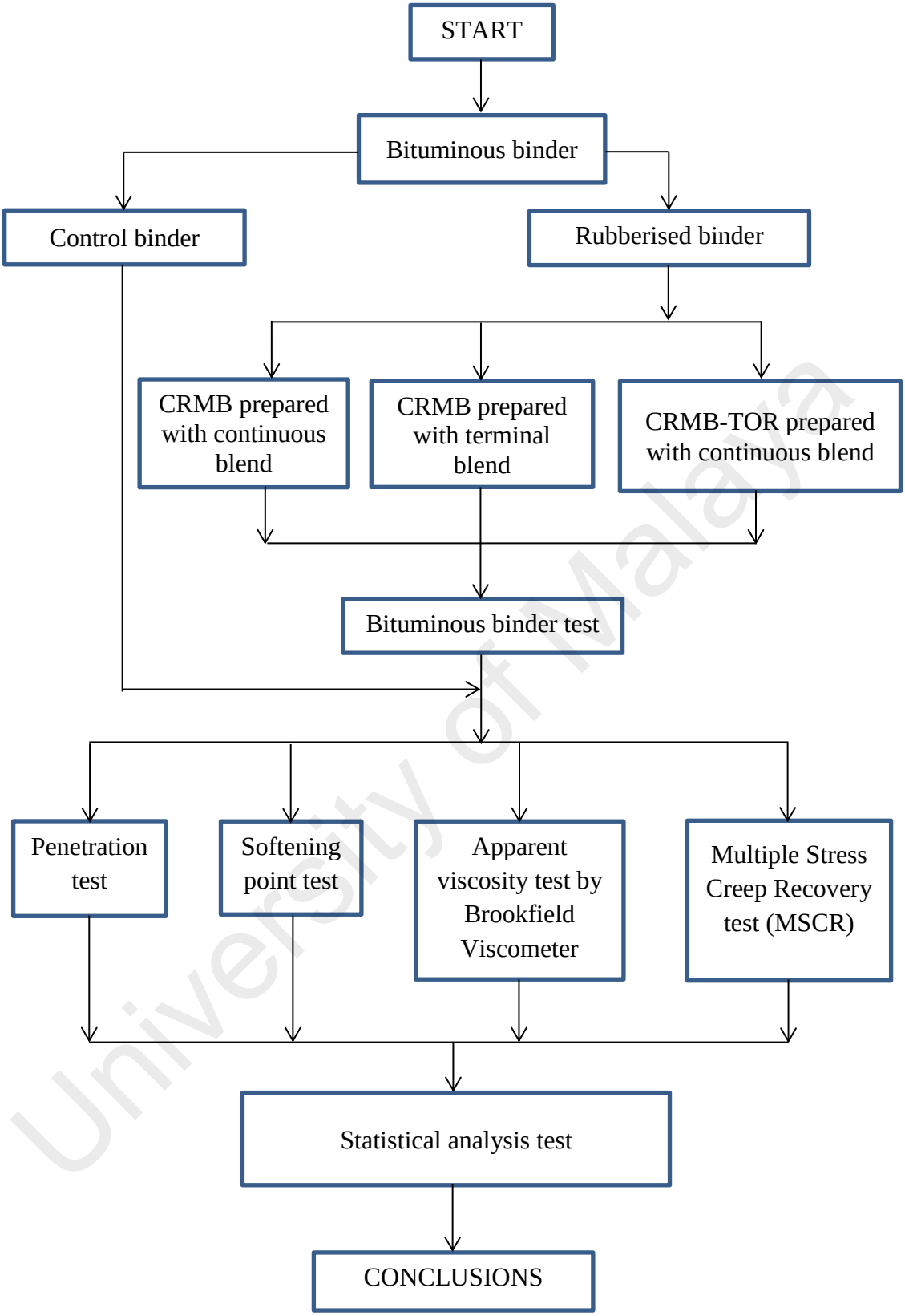

Figure 3.1 Methodology Flow Chart for Binder

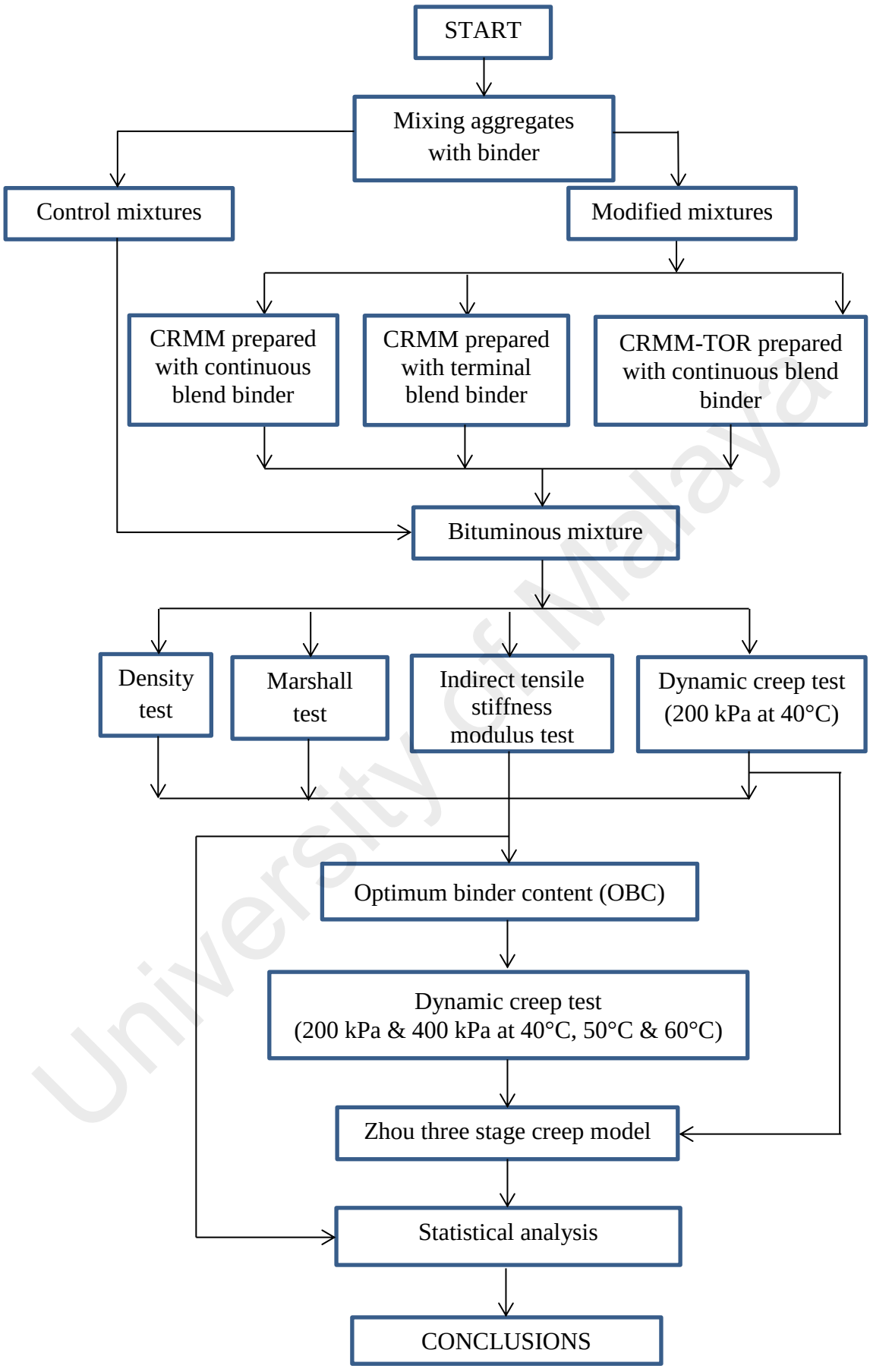

Figure 3.2 Methodology Flow Chart for Bituminous Mixture

Table 3.1 Matrix of Binders Developed

Base Bitumen 80/100 Penetration	Rubber Content, %	Trans-polyoctenamer (TOR), %		Mixing type		Binder group		
Binder ID		**0**	**4.5**	**Continuous blend**	**Terminal blend**	**Control**	**CRMB[a]**	**CRMB-TOR[b]**
0R	0	✓				✓		
C4R	4	✓		✓			✓	
C8R	8	✓		✓			✓	
C12R	12	✓		✓			✓	
C4RT	4		✓	✓				✓
C8RT	8		✓	✓				✓
C12RT	12		✓	✓				✓
T20R	20	✓			✓		✓	

[a] Crumb rubber modified binder

[b] Crumb rubber modified binder added with Transpolyoctenamer

3.2.3 Crumb Rubber

Crumb rubber sized 0.4 mm (40#) obtained through the ambient grinding process was used to produce rubberized binders for this study (see Figure 3.3). The specification of the crumb rubber is presented in Table 3.4. To ensure that the consistency of the crumb rubber was maintained throughout the study, only one batch of crumb rubber was used in this study.

3.2.4 Trans-Polyoctenamer

Trans-polyoctenamer (TOR) with trademark Vestenamer® 8012 (Figure 3.4) bought from Evonik Degussa GmbH, Germany was chosen as the crosslink dispersant agent. The specification of Tran-polyoctenamer is shown in Table 3.5.

Table 3.2 Properties of Crushed Granite Aggregate used in this Study

Property	Unit	Test Method	Value
Coarse aggregate			
L.A. Abrasion	%	ASTM: C131	19.45
Flakiness index	%	BS EN 933-3	2.72
Elongation index	%	BS 812-105.2	11.26
Aggregate crushing value	%	BS 812-110	19.10
Bulk specific gravity	–	ASTM: C127	2.60
Absorption	%	ASTM: C127	0.72
Fine aggregate			
Bulk specific gravity	–	ASTM: C128	2.63
Absorption	%	ASTM: C128	0.4
Soundness loss	%	ASTM: C88	4.1

Table 3.3 Specification of Bitumen 80/100 Penetration used in this Study

Property	Unit	Test Method	Value	
			Min	Max
Penetration at 25°C	0.1 mm	ASTM D5	80	100
Softening Point (Ring & Ball)	ºC	ASTM D36	45	52
Flash Point (Cleveland Open Cup)	ºC	ASTM D92	225	-
Relative Density at 25ºC	g/cm³	ASTM D71	1.00	1.05
Ductility at 25°C	cm	ASTM D113	100	-
Loss on heating, wt.	%.	ASTM D6	-	0.5
Solubility in trichloroethylene, wt., min.	%	ASTM D2042	99	-
Drop in penetration after heating, max.	%	ASTM D5	-	20
Application temperatures, mixing at	ºC	-	140	165

Table 3.4 Specification of Crumb Rubber used in this Study

Property	Unit	Test Method	Value
Acetone Extract	%	ISO 1407	10 ± 3
Ash Content	%	ISO	8 ± 3
Carbon Black	%	ISO 1408	30 ± 5
Rubber Hydrocarbon	%	RHC	52 ± 5
Passing	%	ASTM D5644	>90
Heat Loss	%	ASTM D1509	<1
Metal Content	%	ASTM D56),	<1
Fiber Content	%	ASTM D5603	<3

Table 3.5 Specification of Trans-polyoctenamer used in this Study

Property		Test method	Unit	Value
Molecular weight M_w	GPC	DIN 55672-1	-	90,000
Glass transition temperature	Tg	ISO 11357	^oC	-65
Crystallinity	23^oC	ISO 11357	%	30
Melting point	DSC	ISO 11357	^oC	54
	2nd heating			
Apparent density	23^oC	ISO 60	g/l	560
Density	23^oC	ISO 1183	g/cm^3	0.91
Tensile test		ISO 527-1/-2		
Stress at yield			MPa	7.5
Strain at yield			%	25
Strain at break			%	400
Tensile impact strength		ISO 8256		
	23^oC		kJ/m^2	165
	0^oC		kJ/m^2	190
	-20^oC		kJ/m^2	240

Figure 3.3 Rubber Crumb used in this Study

Figure 3.4 Trans-polyoctenamer used in this Study

3.3 Preparation of Modified Binder

Bitumen 80/100 penetration was used as the control bitumen. The crumb rubber modified binder (CRMB) was prepared using crumb rubber sized 0.4mm (40#) by means of two blending methods; namely, continuous blend and terminal blend. In the

continuous blend method, different percentages of crumb rubber content, namely, 4, 8 and 12% were utilized to produce different concentrations of CRMB. The crumb rubber modified binder with TOR (CRMB-TOR) was prepared by adding 4.5% TOR to each CRMB blend. Both modified bitumens (CRMB and CRMB-TOR) were prepared using a propeller mixer at a speed of 200 rpm for 45 minutes and the mixing temperature was maintained at 180^{o}C.

To achieve the terminal blend binder, CRMB prepared with 20% rubber content was blended at 200^{o}C for 2 hours using a high speed shear mixer (10000 rpm). For all types of CRMB and CRMB-TOR, the amount of crumb rubber was calculated by the weight of the bitumen, while the amount of trans-polyoctonemer (TOR) was calculated by the weight of the crumb rubber.

The prepared CRMB and CRMB-TOR were then tested for the physical and rheological properties. The physical properties were evaluated based on the softening point test (ring-and-ball apparatus) and the penetration test. The rheological properties of the modified binder were analysed based on the apparent viscosity test conducted by brookfield rotational viscometer and the multiple stress creep recovery test (MSCR) performed by dynamic shear rheometer (DSR).

3.4 Preparation of specimen

In this study, aggregate gradation SMA 20 in accordance with the Malaysian Public Works Department was used in the preparation of all the specimens (JKR/SPJ/2008-S4). The aggregate particle size distribution is presented in Table 3.6 and Figure 3.5. The SMA mixtures were prepared with 1100g of aggregate including 2% Portland cement. According to the Standard Specification for Road Works of the Malaysian Public Works Department (JKR/SPJ/2008-S4), a mineral filler should be added as part

of the combined aggregate gradation. Limestone dust, hydrated lime or ordinary Portland cement should be used as a filler. If cement is used, the amount should not exceed 2% by weight of the combined aggregate.

The SMA mixtures were prepared in accordance with the Marshall procedure (ASTM D6926-10). The preparation started with heating the aggregate and portland cement in the oven for one hour at 160°C. The aggregate and portland cement were then transferred to the pan and heated at a higher temperature of 180°C. The binder was added to the aggregate and mixed at 180°C until all the aggregate was fully coated with the binder. The amount of binder was 5, 6 and 7% by weight of the specimen. In order to produce a homogeneous binder, the binder was agitated vigorously before the binder was added to the aggregate. The mixture was then transferred to the Marshall mould and was spaded 15 times around the parameter and 10 times over the interior. The mixture was compacted by applying 50 blows to both sides with the Marshall compactor when the temperature of the mix reached 165°C. Fifty blows were used, which resulted in a significant increase in density (Xue et al., 2009). The temperatures chosen to mix and compact are consistent with field practice when rubberized bitumen is being produced (Puga, 2013). Moreover, Lee et al. (2008) mentioned that a suitable compaction temperature for rubberized bitumen is between 154°C and 173°C. After compaction, the specimen was cured for 24 hours in the mould at room temperature. The control specimens were prepared using similar procedures; however, the mixing temperature was fixed at 160°C and the compaction temperature at 145°C. Each specimen was 100±5mm in diameter and 65±5mm in height. Specimens were then tested for bulk specific gravity (ASTM D2726), indirect tensile stiffness modulus test (AASHTO TP31), Marshall stability and flow (ASTM D2041), and dynamic creep test (AS 2891.12.1-1995).

The optimum binder content (OBC) was then determined in accordance with the Marshall mix design. For the determination of OBC, four graphs, namely, stability, flow, voids in mix (VIM) and voids in mineral aggregate (VMA) were plotted versus the percentage of binder for each bituminous mixture. The OBC was calculated based on the Malaysian SMA Mix requirements (JKR/SPJ/2008-S4): stability (min. 6200N), flow (2-4 mm), VIM (3-5%) and VMA (min. 17%). The same designations were selected for the bituminous mixture specimens prepared from the respective binders.

Table 3.6: SMA 20 Aggregate Gradation

Sieve size (mm)	% Passing	Spec. Range % Passing
19	100	100
12.5	90	85-95
9.5	70	65-75
4.75	24	20-28
2.36	20	16-24
0.6	14	12-16
0.3	13.5	12-15
0.075	9	8-10

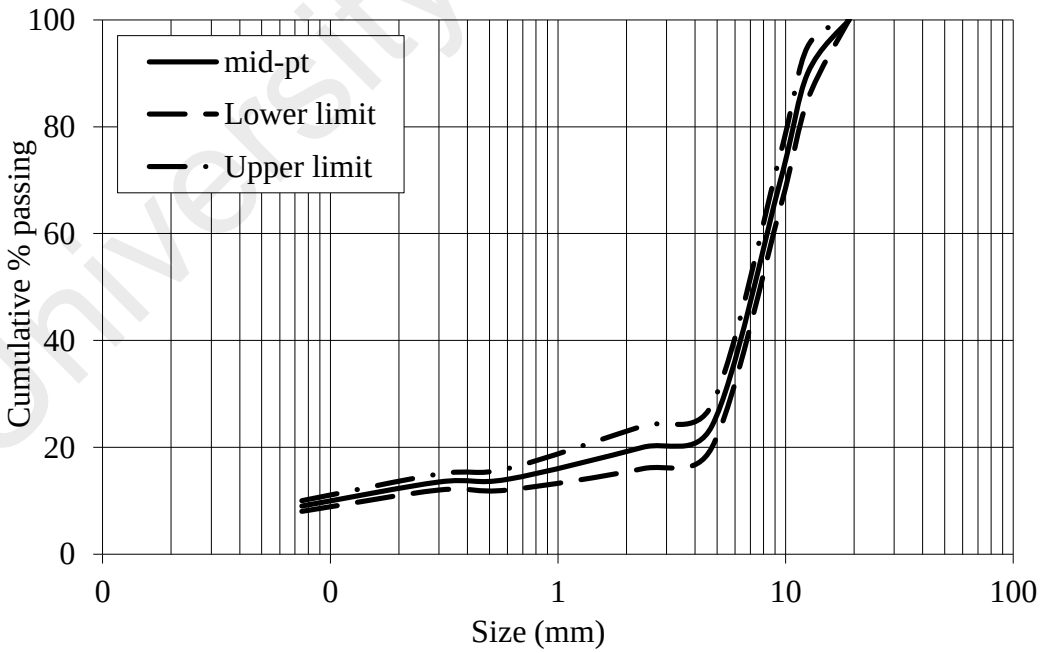

Figure 3.5 SMA 20 Aggregate Gradation

3.5 Physical properties test of binders

3.5.1 Penetration Test

The penetration test was carried out according to ASTM D5. Sufficient bitumen was heated and poured in the penetration cup and conditioned at 25°C for 24 hours prior to testing. The test was conducted at a specified temperature of 25°C; a water bath was used to maintain the test temperature. A 1 mm diameter needle was loaded with a weight of 100 g and allowed to penetrate freely for 5 s into a bitumen sample in which the penetration value illustrated the consistency of the bitumen. This test was significant for classifying the bitumen grade based on the penetration range.

3.5.2 Softening Point Test

The softening point (ring and ball) test was conducted in accordance with ASTM D36. A ring holder assembly filled with binder was placed in a water bath along with two steel balls which were allowed to condition to a starting temperature of 5±1°C for 15 minutes. After the conditioning period, the steel balls were placed on top of the binder in the ring. The test was conducted by heating the two horizontal discs of binder immersed in a water bath at a controlled rate (5°C/min) until the binder softened to the point that the balls dropped and touched the bottom plate of the assembly. The softening point value was recorded as the temperature at which the binder softens enough to allow each steel ball to fall and touch the plate. The temperature of the two specimens was recorded and should not vary by more than 1.2°C.

3.6 Rheological Properties Tests of Binders

3.6.1 Apparent Viscosity by Rotational (Brookfield type) Viscometer

The rotational (brookfield type) viscometer shown in Fig. 3.6 was used to measure the apparent viscosity of the binder in accordance with ASTM D2196-10. In this test, a sufficient amount of binder was heated in an oven so that it was sufficiently fluid to pour into the sample chamber. The sample chamber containing 8–10 ml binder was then positioned in the thermos container. The desired temperature was then stabilized for about 20 minutes before the spindle was lowered into the chamber and the test started. In this study, the test was conducted at various temperatures, namely, 95, 115, 135, 155, 165, 175 and 195°C at a fixed speed of 20 rpm. Generally, for each test temperature, the viscosity value was recorded after 20 minutes.

Figure 3.6 Brookfield Rotational Viscometer

3.6.2 Multiple Stress Creep Recovery (MSCR) Test

Vehicles do not travel at the same speed and do not apply equivalent loads on the pavement structure. In addition, the pavement temperature would vary throughout the year. Therefore, performing the MSCR test at different creep and recovery times with different test temperatures is an attempt to better simulate the actual loading and unloading conditions that can be observed on the road.

The multiple stress creep recovery (MSCR) was measured using a dynamic shear rheometer (see Figure 3.7) under controlled strain conditions. The plate used for MSCR was 25 mm in diameter and in order to improve the repeatability of testing the gap between the parallel plates was selected at 2 mm (M. Attia and M. Abdelrahman, 2009; Bahia and Davies,1994, 1995).

The test was conducted at 1 s creep loading with 9 s recovery over the multiple stress levels of 25, 50, 100, 200, 400, 800, 1600, 3200, 6400, 12,800 and 25,600 Pa, applying 10 cycles at each stress level (Zoorob et al., 2012). In this study, the test was performed at 40°C, 50°C and 60°C. Figure 3.8 shows the typical MSCR test loading results.

The creep parameters, namely, non-recoverable compliance (J_{nr}), percent recoveries (R) and percent differences in non-recoverable compliance ($J_{nr,\ diff}$) were then calculated and analysed. Higher R values and lower J_{nr} values are favourable to the resistance of the binder to rutting.

The non-recoverable compliance (J_{nr}) was calculated by dividing the average non-recovered strain for the 10 creep and recovery cycles with the applied stress for those cycles. The J_{nr} equation is shown in Equation 3.1:

$$J_{nr}\ (Pa^{-1}, kPa^{-1}) = \frac{\varepsilon_{R-}\varepsilon_0}{\sigma(Pa,kPa)} \qquad (3.1)$$

The percent recoveries, R, were calculated by means of the ratio of the percent recovery of the binder at 1/9 s to the one at 2/18 s. Equation 3.2 was used for calculation of the percent recoveries, R:

$$R(\%) = \frac{[(\varepsilon_c - \varepsilon_0) - (\varepsilon_R - \varepsilon_0)]}{\varepsilon_c - \varepsilon_0} x\ 100 \qquad (3.2)$$

The percent differences in the non-recoverable compliance ($J_{nr,\ diff}$) present the stress sensitivity of the binders. For instance, the $J_{nr,\ diff}$ value of the binder when the stress level is increased from 0.1 to 3.2 kPa can be calculated using Equation 3.3. According to Anderson et al. (2010) and D'Angelo J (2010), the $J_{nr,\ diff}$ value can be used to evaluate the susceptibility of the binder to rutting when unexpected heavy traffic loadings are applied on the pavement structure or unusually high temperatures are observed in the field.

$$J_{nr,diff}(\%) = \frac{J_{nr}3200 - J_{nr}100}{J_{nr}100} x100 \qquad (3.3)$$

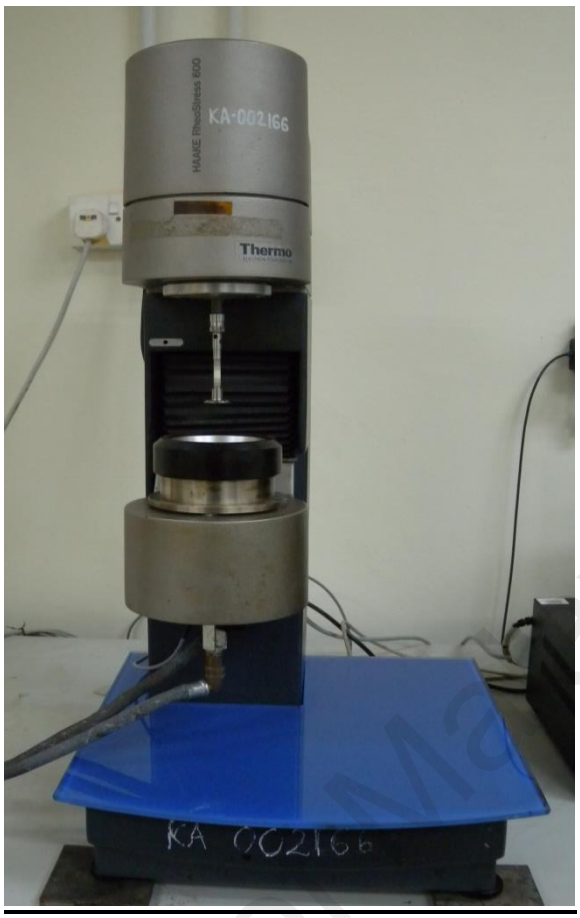

Figure 3.7 Dynamic Shear Rheometer

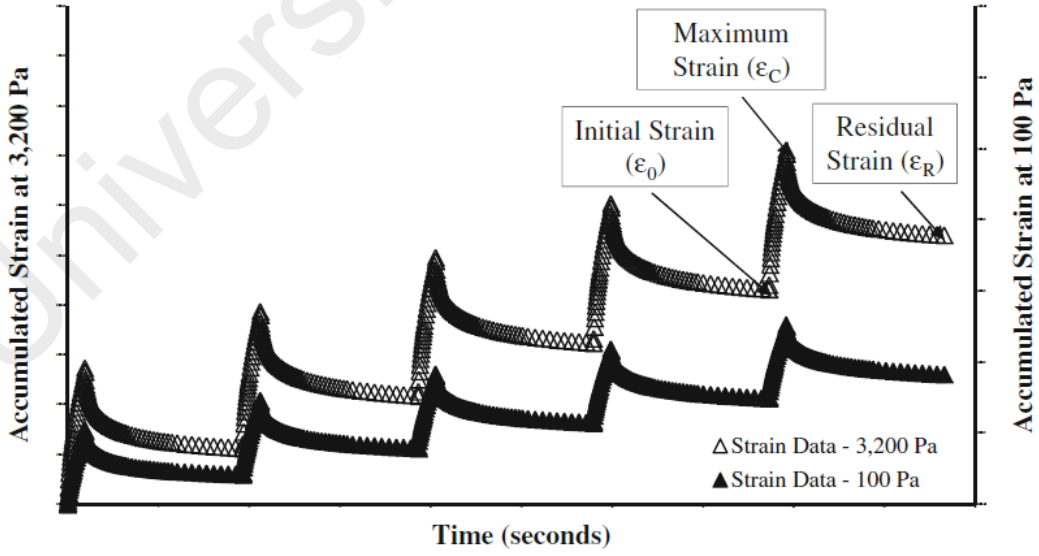

Figure 3.8 An Example of MSCR Test Loading Results at a Stress Level of 100 Pa and 3200 Pa (Domingos et al., 2014)

3.7 Marshall Specimen Tests

The Marshall specimens, prepared as mentioned in section 3.4, were then tested for bulk specific gravity, Marshall stability and flow, stiffness modulus and dynamic creep test (200 kPa at 40°C). The results for each test were analysed to study the effects of the rubber content, TOR and blending type on the properties of the Marshall specimens. The results obtained from the bulk specific gravity, and Marshall stability and flow, were further analysed to determine the optimum binder content value (OBC). The specimens prepared with OBC were tested indirect tensile stiffness modulus and dynamic creep in dry condition (200 kPa and 400 kPa at 40°C, 50°C and 60°C).

3.7.1 Bulk Specific Gravity

The bulk specific gravity test was performed according to ASTM D2726. The bulk specific gravity is determined by weighing the sample in air, in water and in saturated surface dry. By having these three values, Equation 3.4 was used for calculating the bulk specific gravity of the mixture:

$$BSG = \frac{A}{B-C} \qquad (3.4)$$

Where:

BSG = Bulk specific gravity of compacted mixture

A = Weight of dry specimen in air

B = Weight of saturated surface dry specimen

C = Weight of specimen in water

3.7.2 Marshall Stability and Flow

The Marshall stability and flow test was conducted according to ASTM D6927-15. The Marshall stability is the maximum load applied at a constant strain (2 in. per minute) that causes failure, while the Marshall flow value is expressed as the vertical deformation happens at the failure point of the specimen. In order to conduct the test, the Marshall specimen was placed in a water bath at a temperature of 60°C for 30 min before commencing the test. Then, after removing the specimen from the water bath, they were put in the Marshall apparatus and tested immediately. The values were calculated automatically using the Marshall apparatus.

3.7.3 Indirect Tensile Stiffness Modulus (ITSM)

The indirect tensile stiffness modulus (ITSM) test was conducted to determine the stiffness of the specimens in accordance with AASHTO TP31. The test was performed using the universal testing machine (UTM) (see Figure 3.9). In this test, a cylindrical specimen is subjected to a load pulse across its vertical diametral axis and the resultant deformation along the horizontal diametral axis is measured by two linear variable differential transducers (LVDTs). The test was conducted at 25°C with a 1000 N load applied. The test was conducted twice for each specimen by rotating 90°C as the test is a non-destructive test. The stiffness modulus is then calculated as follows (Equation 3.5):

$$S_m = \frac{P \times (v + 0.273)}{\Delta h \times t} \qquad (3.5)$$

Where:

S_m = stiffness modulus, MPa

P = peak vertical load, N

Δh = peak horizontal deformation, mm

t = specimen thickness, mm

v = Poisson's ratio (assumed to be 0.35)

3.7.4 Dynamic Creep Test

The dynamic creep test was performed using the universal testing machine (UTM) (see Figure 3.9) in accordance with AS 2891.12.1-1995. The test was conducted on a standard Marshall specimen (in general, the specimen has a height and diameter of 63.5 and 101.5, respectively). Many studies show that the standard Marshall specimen has been used widely for evaluating the permanent deformation and rutting susceptibility of bituminous mixes using the dynamic creep test (Mehrara and Khodaii, 2011; Tapkin et al., 2013; Tapkin and Keskin, 2013; Moghaddam et al., 2014).

To minimize the end effects, the specimens were trimmed at the top and bottom with a diamond saw to a final thickness of 50 mm. Both sides of each specimen were coated with a thin layer of silicone grease containing graphite flakes in order to obtain smooth faces. This is to eliminate the influence of unevenness of specimen face, which would affect the test results. The dynamic creep test was performed on specimens in dry condition.

The dynamic creep test was started by conditioning the specimen in the temperature controlled cabinet for 2 hours to ensure that the equilibrium temperature was reached. The specimen was then placed between the platens. The assembled platens and specimen was aligned concentrically with the loading axis of the testing machine. The displacement measuring device was then attached to the platens. The vertical deformation was then measured using the LVDTs. In this study, the loading parameters

consisted of a haversine wave shape with two stress levels of 200 kPa and 400 kPa, and three test temperatures of 40°C, 50°C and 60°C were selected. The load was applied for 0.5 s followed by a rest period of 1.5 s. The specimen was terminated after 1800 load cycles or until the accumulated strain reached 100,000 µs. The accumulated strain was calculated using Equation 3.6:

$$\varepsilon = h/H_0 \qquad (3.6)$$

Where

ε = accumulated strain

h = axial deformation, mm

H_0 = initial specimen height, mm

Figure 3.9 Universal Testing Machine

3.8 Creep Model: Zhou's Three-Stage Model

In this study, the Zhou three-stage model was used for a better understanding about the permanent deformation behaviour of the mixtures. Regression analysis, as explained by Zhou et al. (2005), was properly followed to determine the mathematical functions as well as the transition points between each stage and to model each stage.

Zhou's three-stage models are comparable to the field performance. Equation 3.7 – Equation 3.9 show the model equation:

Primary stage: $\varepsilon_p = aN^b \ , \quad N < N_{PS}$ (3.7)

Secondary stage: $\varepsilon_p = \varepsilon_{PS} + c\ (N - N_{PS}),$ and $\varepsilon_{PS} = a\ N_{PS}^b,\ N_{PS} \leq\ N \leq N_{ST}$

(3.8)

Tertiary stage: $\varepsilon_p = \varepsilon_{ST} + d\left(e^{f(N-N_{ST})} - 1\right),\ and\ \varepsilon_{ST} = \varepsilon_{PS} + c(N_{ST} - N_{PS}),\quad N \geq N_{ST}$

(3.9)

3.9 Statistical Analysis

In this study, four percentages of rubber content (0%, 4%, 8% and 12%), three percentages of binder content (5%, 6% and 7%), two percentages of TOR (0% and 4.5%) and two types of blending process (continuous blend and terminal blend) were investigated. Moreover, the effects of temperature and stress levels on the rutting resistance of the mixtures were also considered. Therefore, after studying the individual effects of the independent variables (rubber content, binder content, TOR and blending type) on the properties of the binder and mixture, it is necessary to statistically compare and evaluate the significant effect of each variable involved. In addition, the collective effects due to any combination of the independent variables need to be identified.

Multiple linear regression was considered for such purpose. However, one assumption of the statistical analysis is that the sample population follows a normal distribution. Statistical analysis was performed using statistical software SPSS 18.0.

3.9.1 Multiple Linear Regression

There is more than one factor (rubber content, TOR, binder content, blending type, stress level and temperature) that affects the properties of the binders and mixtures investigated in this study. Therefore, multiple linear regression analysis was employed to compare the significant effects as well as to predict and explain the properties of the binders and mixtures based on different factors. The output of regression analysis is an equation that represents the best prediction for the properties of the binders and mixtures based on the value of a few factors. Moreover, the coefficient of determination (R^2) was used to investigate the contribution of the factors on the variance of the measured properties.

Multiple linear regression with stepwise method was conducted with the assumption that the linearity, normality and homoscedasticity were not violated. It is a method of regressing multiple factors while simultaneously removing those that are not important. The regression was executed at the significance level, $\alpha = .05$ (5%) or confidence level 95%.

3.10 Summary

This chapter consists of several sections: the first section of this chapter discusses the physical properties of the materials used. The second section explains the preparation of the samples and the related test. The third section describes the creep predicted model and statistical analysis used in this study.

The materials used in this study are aggregate, bitumen, crumb rubber and TOR the properties of which are tabulated in Tables 3.2 – 3.5, respectively. In this study, rubberized bitumen was first prepared for use as a binder in preparation of the bituminous mixtures.

The crumb rubber with nominal size of 0.4 mm (40 mesh) was used in the preparation of rubberized binder. Two types of mixing blend, namely, continuous blend and terminal blend were utilised in the preparation of the rubberized binder. Different percentages of rubber content (4%, 8% and 12%) were incorporated into the bitumen 80/100 penetration in preparation of the rubberized binder produced with continuous blend. The amount of rubber content was limited to 12% since a further increase in the rubber content could decrease the performance of the rubberized mixtures (Nuha et al., 2013a; 2013b; 2014). However, for preparation of the rubberized binder with terminal blend, 20% rubber content was used (Fontes et al., 2010).

In order to enhance the compatibility and reaction of the crumb rubber to the bitumen, TOR was used as a crosslink dispersant, which, along with the crumb rubber, was expected to improve the binder performance. The recommended dosage of 4.5% by weight of crumb rubber (Burns, 2000; Solaimanian et al., 2003; Bennert, 2004; Puga, 2013) was added to different percentages of crumb rubber (4%, 8% and 12%) using the continuous blend method.

Aggregate gradation, SMA 20 was utilised in preparation of the bituminous mixtures as suggested by the Road Engineering Association of Malaysia (REAM). In this study, rubberized bitumen and rubberized bitumen reinforced with TOR were used in the preparation of the bituminous mixtures with different percentages of binder content (5%-7%). The effects of binder content, rubber content, TOR and binder blending method in properties of SMA mixtures were evaluated and compared in terms of voids

in the mixture (VIM), voids in mineral aggregate (VMA), indirect tensile stiffness modulus (ITSM) value, stability and flow, and dynamic creep test for the initial stage.

In the second stage of the study, the effects of temperature and stress level on the rutting resistance of the CRMM and CRMM-TOR were analysed. The rutting resistance was then compared with the control specimen. Based on the properties of the mixtures evaluated in the initial stage, control (0R), CB12R, CB12RT and TB20R were selected for the subsequent tests at optimum binder contents. The dynamic creep test was performed for all designated mixtures (0R, CB12R, CB12RT and TB20R) at different stress levels (200 kPa and 400 kPa) and temperatures (40°C, 50°C, 60°C). For each test, three duplicate specimens were prepared and tested.

The predicted creep model, namely, the Zhou three-stage model was proposed in this study. Moreover, statistical analysis was conducted using multiple linear regression (stepwise method) at a confidence level of 95% in order to develop the empirical relationship models as well to determine the significant factors. In this research, the factors that might influence the research objectives are crumb rubber, TOR, binder blending methods, binder content, temperature and stress level.

CHAPTER 4: RESULTS AND DISCUSSION

4.0 Introduction

This chapter presents and discusses the results obtained from the testing that was carried out according to the experimental plans presented in Chapter 3. In addition, this chapter deals with the results of the statistical analysis (multiple linear regression) performed using statistical package for the social sciences (SPSS) software. Multiple linear regression was performed using the stepwise method at the significance level, $\alpha = .05$ (5%) or confidence level of 95%. In this study, all results were plotted and discussed using the average results of the three replicates.

4.1 Analysis and Discussion of Physical Binder Tests

The effects of rubber content, TOR and binder blending methods on the conventional physical properties of modified binder are presented in Table 4.1 and Figures 4.1 (a) – 4.3(d). The physical properties, including softening point value, penetration value and apparent viscosity value, were tested in accordance with ASTM D 36, ASTM D 5 and ASTM D4402-87, respectively.

Table 4.1 Physical Properties of Binders

Binder	Penetration (0.1 mm)	Softening point (°C)	Viscosity at 135°C (mPa.s)	Viscosity at 175°C (mPa.s)
0R	95.00	44.25	375.25	43.75
C4R	75.17	45.50	487.00	100.10
C4RT	77.23	45.00	515.43	104.33
C8R	71.00	46.75	575.25	190.20
C8RT	68.71	49.00	664.24	218.36
C12R	68.43	50.00	897.06	294.00
C12RT	61.75	51.50	930.69	402.07
T20R	65.67	53.88	1277.00	287.75

4.1.1 Penetration Value

The penetration test was conducted to estimate the high temperature performance of binder based on stiffness. It is an empirical test that is fast and inexpensive, and covers the typical service temperature of bituminous pavement.

The results of the penetration test for control, crumb rubber modified binder (CRMB) prepared with different blending methods (continuous blend and terminal blend) and crumb rubber modified binder reinforced with TOR (CRMB-TOR) are presented in Figures 4.1(a) – 4.1(b). The results show that the penetration point of CRMB decreases as the rubber content increases, but at decreasing rates. For instance, the increase from 0% to 4% rubber content shows a significant decrease of about 20.87%; a further increase in rubber content from 4% to 8% and 8% to 12% show a decrease of about 5.55% and 3.62%, respectively. The decrease in penetration value of CRMB is due to the addition of crumb rubber (CR) to the binder, which makes the binder stiffer. The results are consistent with the findings of previous studies (S. A. D. Neto et al., 2006; S. Liu et al., 2009; R. A. Al-Mansob et al., 2014).

Generally, the penetration value of CRMB reinforced with TOR (CRMB-TOR) decreases as the amount of crumb rubber added into the base bitumen increases. For instance, the penetration value decreases 11.03% and 10.13% as TOR is added from 4% to 8% and from 8% to 12% of rubber crumb, respectively. Moreover, the results indicate that adding TOR to CRMB decreases the penetration value faster compared to CRMB without TOR (CRMB). For example, at similar rubber content (4% to 8% and 8% to 12% rubber crumb) the penetration value of CRMB only decreases 5.55% and 3.62% while the penetration value of CRMB-TOR decreases 11.03% and 10.13%, respectively. This finding is better illustrated by the slope of the curve in Figure 4.1 b. The calculated slope value of CRMB-TOR is higher (-1.9351) than that of CRMB

(-0.8423). Therefore, it is confirmed that TOR contributes to a faster decrease in the penetration value, or, in other words, adding TOR to CRMB produces a thicker modified bitumen, thus increasing the difficulty of the penetration needle to penetrate the modified bitumen. In addition, from Figure 4.1b, it seems that CRMB and CRMB-TOR are crossing at 5.9% rubber content. Based on the penetration value, the author assumes that CRMB and CRMB-TOR will present similar physical properties at 5.9% rubber content.

It is interesting to note that CRMB-TOR prepared with 4% CR increases the penetration value about 2.67% (see Figure 4.1b). This indicates that adding TOR to low concentrations of CRMB softens the modified bitumen. However, adding TOR to higher rubber content (8% and 12% CR) results in thicker bitumen, as shown by the decrease in the penetration value. For instance, the penetration value drops 3.23% and 9.76% as TOR is added to 8% and 12% rubber crumb, respectively. This implies that the penetration of CRMB would be improved further by TOR at high percentages of rubber content. A similar pattern was observed by H. Liu *et al.* (2014) when adding TOR to high percentages of rubber content (15%, 20% and 25%), which showed an obvious dropping trend in the penetration value. From the results, it can be concluded that the amount of rubber content is crucial and should be selected properly to achieve sufficient properties of CRMB-TOR, as TOR seems to reduce the penetration value at low rubber content (4% CR) and would increase the penetration value at higher rubber content (more than 8% CR).

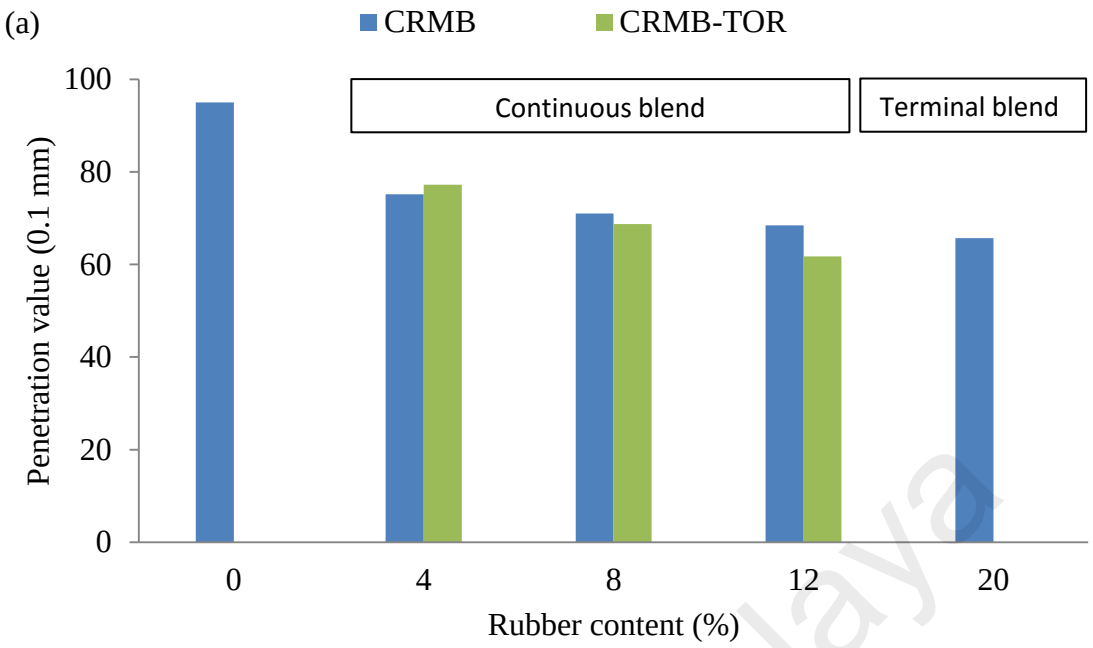

Figure 4.1a: Penetration Value versus Rubber Content

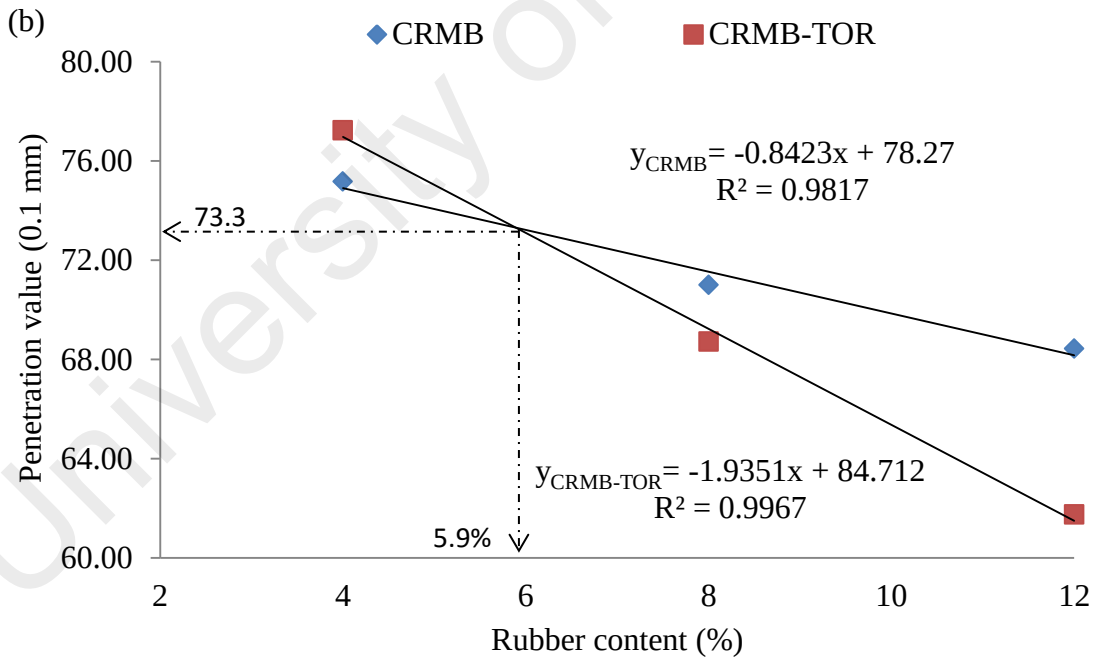

Figure 4.1b: Relationship between Penetration Value and Rubber Content

The effects of binder blending methods on the penetration value are presented in Figure 4.1a. The achieved results display that CRMB prepared with terminal blend (T20R) shows the lowest penetration value. This indicates that T20R is stiffer compared to CRMB prepared with the continuous blend. The main reason is that T20R was prepared with a higher rubber content (20%) than the continuous blend binder (4%-12%). However, it is good to note that T20R decreases the penetration value at a slower rate compared to the continuous blend binder. For instance, T20R decreases the penetration value at 0.328 mm/rubber percent (6.567mm/20%), while the penetration value of the continuous blend binder prepared with 12% rubber content (C12R) decreases at 0.57 mm/rubber percent (6.843mm/12%). The different penetration rates might be due to dissimilar reaction levels observed in both blending type. In the terminal blend binder, the author believes that it involves chemical and thermal interactions while only a chemical reaction occurred in the continuous blend binder. The chemical reaction contains the absorption of light fraction from the base bitumen by the rubber particles thus increasing the stiffness of the rubberized binder. While the thermal reaction involves some kind of softening of the rubber particles due to the devulcanization involved in the preparation of the terminal blend binder. The high mixing temperature (210°C) with long mixing duration (2 hours) imposed in the terminal blend binder causes devulcanization (crumb rubber is completely dispersed in the binder) of the rubber crumb, which explains the lower rate of stiffness compared to that of the continuous blend binder.

4.1.1.1 Multiple Linear Regression Analysis on Penetration Value

Stepwise regression was conducted to determine which factors (rubber content, TOR and binder blending method) were the predictors of the penetration values (Appendix A, Tables A.1a – A.1d). The regression results indicate an overall model of two factors

(rubber content and TOR content) that significantly predict penetration values, R^2 = .703, R^2_{adj} = .696, F (2, 81) = 95.825, p<.05. This model accounted for 70.3% of variance in the penetration values. The rubber content recorded a higher beta value (beta = -.818, p =.000 < .05), followed by TOR (beta = -.316, p =.000 < .05). The regression model, which can be used to estimate the penetration value based on significant factors, is as follows (Equation 4.1):

$$Penetration\ value = -.818\ (Rubber\ content) - .316\ (TOR) \qquad (4.1)$$

A summary of the regression model is presented in Table 4.2. In addition, the bivariate and partial correlation coefficients between each factor and the penetration value are presented in Table 4.3.

Table 4.2 Model Summary: Penetration Value

Step	R	R^2	R^2_{adj}	ΔR^2	F_{chg}	p	df_1	df_2
Rubber content, %	.778	.605	.600	.605	125.428	<0.05	1	82
Transpolyoctenamer, %	.838	.703	.696	.098	26.784	<.05	1	81

Table 4.3 Coefficients for Final Model: Penetration Value

Step	B	β	t	Bivariate r	Partial r
Rubber content, %	-1.242	-.818	-13.400	-.778	-.812
Transpolyoctenamer, %	-1.185	-.316	-5.175	-.211	-.313

4.1.2 Softening Point Value

Generally, the pattern of the softening point results obtained is consistent with the penetration results, as explained in Section 4.1.1. The results of the softening point tests presented in Figures 4.2(a) – 4.2(b) show an increase in the softening point with the increase in rubber content. The higher softening point indicates that the binder is less susceptible to temperature changes, thus enhancing the ability of the binder to resist flow at higher temperature. The main reason for the crumb rubber increasing the

softening point is the ability of crumb rubber to swell and absorb the aromatic oils from the bitumen; this results in an increase in the asphaltenes to resins ratio, which enhances the stiffened property of CRMB.

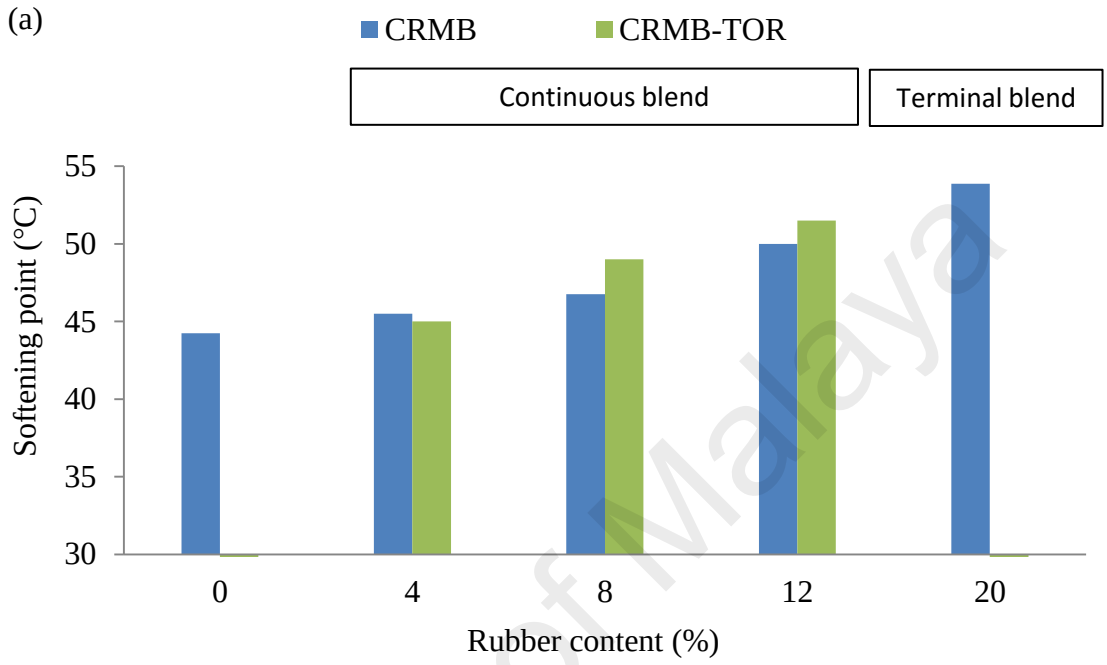

Figure 4.2a: Softening Point Value versus Rubber Content

A general trend was found in Figure 4.2a in that the addition of TOR resulted in an increase in the softening point, thus indicating an increase in the hardness or stiffness of CRMB. Moreover, the effect of TOR on the hardness of the bitumen can also be seen from the slope of the linear graph shown in Figure 4.2b. CRMB-TOR indicates a steeper slope (0.8125) than CRMB (0.5625). This indicates that adding TOR into CRMB gives a better and steadier situation, which can improve the physical properties of CRMB (Liu et al., 2014). This implies that adding TOR to CRMB accelerates the chemical reaction, which improves the rheological properties of the rubberized binder. Therefore, it can be concluded that TOR has an advantage in increasing the softening point value, which is beneficial to high temperature performance and means superior rutting resistance.

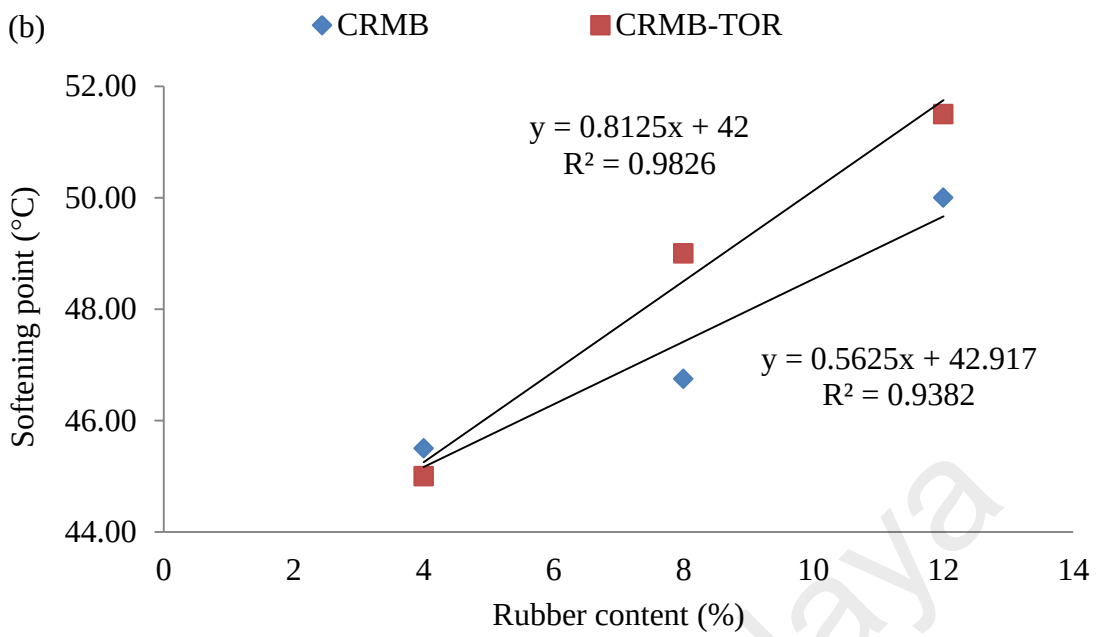

Figure 4.2b: Relationship between Softening Point Value and Rubber Content

The obtained results also indicate that the benefit of TOR is more apparent at higher rubber content. As seen in Figure 4.2a, the addition of TOR to a small percentage of CR (4%) shows a slight decrease in the softening point value from 45.5°C to 45°C, a decrease of about 1.09%. Nevertheless, adding TOR at higher rubber contents (8% and 12%) shows an increase in the softening point value. For instance, adding TOR increased the softening point of C8R from 46.75°C to 49°C (4.59%). This finding is consistent with the penetration value, as explained in section 4.1.1.

Many studies mentioned that bitumen with a higher softening point observes better performance at high pavement temperatures, and, hence, is more resistant to rutting. Epoxidized natural rubber was reported to increase the softening point as well as the rutting resistance of the bitumen (R. A. Al-Mansob et al., 2014). Furthermore, ethylene vinyl acetate (EVA) and ethylene vinyl acetate grafted maleic anhydride (EVA-g-MAH) copolymers increase the softening point of the bitumen, and this modified bitumen was found to be more resistant to rutting (W.-q. Luo and J.-c. Chen, 2011). In addition,

Fontes et al. (2010) observed that the rubberized binder with the highest softening point produced bituminous rubberized mixtures with better resistance to permanent deformation. As can be understood from the previous studies, a higher softening point means better rutting resistance. Hence, it could be stated that CRMB and CRMB - TOR modification improved the rutting property of the bitumen, and, thus, the modification will make it more resistant to rutting, and, therefore, suitable for warmer climates like Malaysia.

The effects of binder blending methods on the hardness of CRMB were worth comparing between T20R and C12R. Similar to the penetration result, T20R shows the highest softening point value, and, therefore, the hardest bitumen due to the high rubber content (see Figure 4.2a). Since the rubber content used in the preparation of both CRMBs is different (T20R was prepared with 20%CR, while 12%CR was used in preparation of C12R), it is more reliable to compare the rate of softening point values. The result indicates that T20R shows slower softening point rates (2.694) compared to C12R (4.17). The harsh preparation of T20R with high speed blending (10,000 rpm) mixed at high temperature (210°C) and long mixing duration (2 hours) seems the main reason for the depolymerisation that reduces the softening rates. It is believed that depolymerisation releases rubber components back to the liquid phase causing a decrease in the hardness.

4.1.2.1 Multiple Linear Regression Analysis on Softening Point Value

Statistical software SPSS 16.0 was performed to analyse the effects of factors (rubber content, TOR and blending type) on the softening point value (Appendix A, Tables A.2a – A.2d). The analysis is performed at the significance level, $\alpha = .05$ (5%) or confidence level of 95%.

Multiple linear regression using the stepwise method was used to assess the ability of factors to predict the softening point value. Tables 4.4 and 4.5 show the summary of analysis. The factors explain 86.7% of the variance in the softening point value, R^2=.867, R^2_{adj}=.859, $F(2,33)=107.260$, $p<.05$. Regression analysis shows that the rubber content and blending type were statistically significant, with the rubber content recording a higher beta value (beta = 1.196, p =.000 < .05), followed by blending type (beta = -.303, p =.000 < .05). The regression equation, which can be used to estimate the softening point value based on the factors, is as follows (Equation 4.2):

Softening point value = 1.196 (Rubber content) - .303 (Blending type) (4.2)

Table 4.4 Model Summary: Softening Point Value

Step	R	R^2	R^2_{adj}	ΔR^2	F_{chg}	p	df_1	df_2
Rubber content, %	.922a	.850	.845	.850	192.270	<.05	1	34
Blending types	.931b	.867	.859	.017	4.193	<.05	1	33

Table 4.5 Coefficients for Final Model: Softening Point Value

Step	B	β	t	Bivariate r	Partial r
Rubber content, %	.673	1.196	8.074	.922	.815
Blending types	-1.978	-.303	-2.048	.777	-.336

4.1.3 Apparent Viscosity Value

The effects of crumb rubber, TOR and binder blending method on the viscous properties of modified bitumen at a wide range of temperatures (between 95°C and 195°C) are presented in Figures 4.3(a) – 3(d). The effects of temperature on the viscosity for the control, CRMB and CRMB-TOR are depicted in Figure 4.3a. The results indicate that the increase in temperature always leads to a decline in viscosity. This could be due to the bitumen becoming less viscous at high temperature; hence, the

attractive forces among the bitumen molecules could overcome the resistance to flow more effectively.

From Figure 4.3a, it seems that the reduction in the viscosity is greater at the initial stage of the temperature increment, and that subsequent increases in the temperature during the latter part had less influence on reducing the viscosity, as was observed for the control, CRMB (C4R, C8R and C12R) and CRMB-TOR (C4RT, C8RT and C12RT). The available results show that the viscosity decreases rapidly between a temperature of 90°C and 165°C. At higher temperatures (above 165°C), the viscosity tends to level off (asymptote) as the temperature rises. This indicates that the binders almost present Newtonian behaviour at temperatures above 165°C, as it exhibits near zero slopes. From the above results, it can be concluded that the viscosities of both the control and modified bitumen (CRMB and CRMB-TOR) were decreased exponentially as a function of temperature due to the Newtonian property of the bitumen.

The effects of rubber content, TOR and blending type are shown more clearly in Figures 4.3(b) – 4.3(d). The obtained results show that the increase in rubber concentration yielded a significant increase in viscosity, which may lead to better rutting resistance (Xiao, Amirkhanian, Juang, 2007). The resulting viscosity increases due to the absorption of the bitumen's aromatic oil causes the swelling of the rubber particles. The swollen rubber increases the difficulty to flow since swollen rubber particles occupy more space than the rubber particles that are not swollen. Therefore, the higher the rubber content within the binder, the higher would be the density of the rubber particles within a unit volume of binder. Subsequently, this increases the viscosity of the binder.

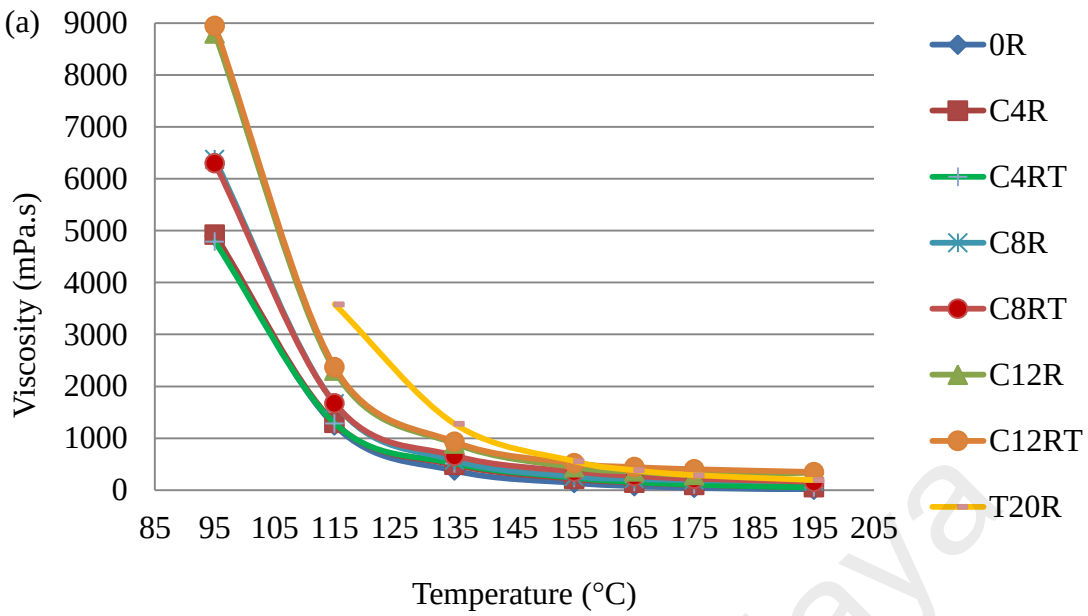

Figure 4.3a: Viscous Properties of Binders at Different Test Temperatures

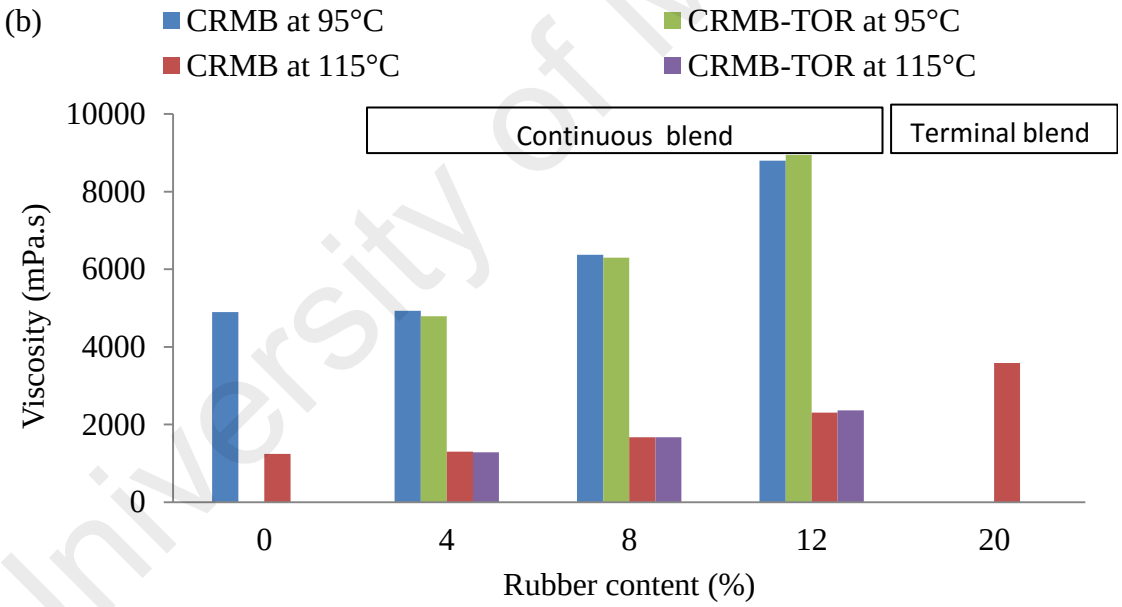

Figure 4.3b: Viscous Properties of Binders at 95°C and 115°C

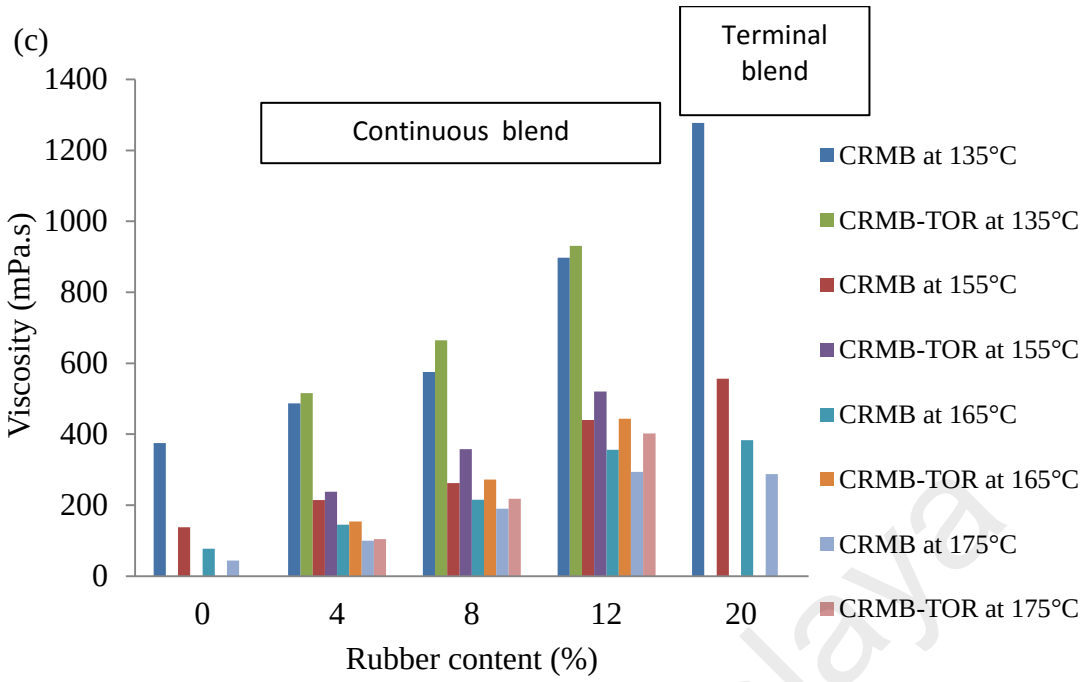

Figure 4.3c: Viscous Properties of Binders at 135°C, 155°C, 165°C and 175°C

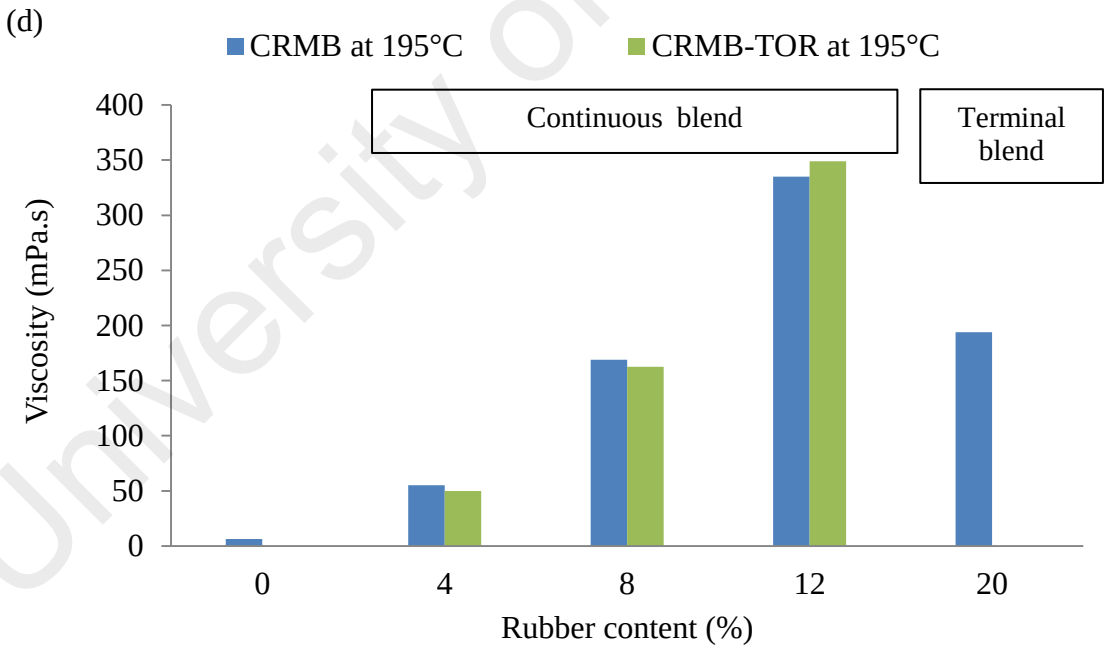

Figure 4.3d: Viscous Properties of Binders at 195°C

As seen in Figure 4.3b, both the control and C4R show similar viscosity values at low temperature (95°C and 115°C). Increasing the temperature to 135°C shows an apparent increase in viscosity as the control has a viscosity value of 375.25mPa.s while C4R

shows 487mPa.s, an increase of about 22.95% (Figure 4.3c). In this study, the effects of rubber content are more significant at 195°C, the highest test temperature (Figure 4.3d). For instance, in the case of C4R, when the temperature rises to 195°C, the viscosity value increases to 55mPa.s, which is 8.8 times higher in comparison with the control (6.25mPa.s). The achieved results explain the behaviour of the crumb rubber being stiffer than the bitumen at high temperature, while, at low temperature, the bitumen is stiffer and the crumb rubber properties do not change significantly. Therefore, the main effects of crumb rubber on the bitumen's viscosity can be seen at higher temperatures. The above reasons explain why the viscosity of modified bitumen remains high compared to the control; hence, confirming a previous study that found that rubberized bitumen is less susceptible to temperature changes (Mashaan et al., 2013; Asim et al., 2013).

Figures 4.3(b) – 4.3(d) show that the viscosity of rubberized bitumen is significantly affected by TOR at all test temperatures. The obtained results show inconsistent trends (dropping and rising) as TOR is added to different concentrations of rubberized bitumen. For example, at low test temperatures (95°C and 115°C) adding TOR to a low CR concentration (4% and 8% CR) indicates a decrease in the viscosity value; however, incorporating TOR with a high rubber content (12%CR) seems to increase the viscosity, as illustrated in Figure 4.3b. A similar trend is observed in Figure 4.3d, which was tested at extreme temperature (195°C); when the CR concentration varied from 4% to 8%, the viscosity presented a dropping tendency, however, when the CR increased to 12%, the viscosity of CRMB showed a rising trend. This finding is in agreement with the penetration value and softening point value, as discussed above (Section 4.11 and 4.12), in which adding TOR to a low crumb rubber concentration causes it to soften the rubberized binder, while adding TOR to a high concentration of crumb rubber leads to an increase in the binder hardness.

Therefore, it can be concluded that in order to achieve the desired viscosity of CRMB, a proper CR concentration should be properly selected, especially when low temperature and extreme temperature were applied. Moreover, in comparing with CRMB, the viscosity values of CRMB-TOR present an upward trend when the test was conducted between 135°C to 175°C, as illustrated in Figure 4.3c, which indicates that TOR has a significant influence on increasing the viscosity value as the temperature increases. That is to say, TOR plays a positive role in enhancing the resistance to deformation.

The effects of binder blending method were found to be significant. As can be seen in Figure 4.3b, the terminal blend binder (T20R) did not display any viscosity value at temperature 95°C, however, increasing the temperature to 115°C shows a lower value compared to the continuous blend binder (C12R). The high rubber content in T20R is the main reason that produces thicker CRMB. Due to the high rubber content (20%CR), the T20R becomes too viscous thus providing greater energy between the rubber particles compared to the shear stress provided by the brookfield viscometer (1 N/mm^2). However, as the temperature increases from 135°C to 175°C, T20R was found to be significant since it presents the highest viscosity. This phenomenon allows utilization of the terminal blend method in the modification of bitumen more effectively. Nevertheless, increasing the temperature to 195°C shows a significant dropping trend for T20R. As shown in Figure 4.3d, the viscosity value of T20R drops almost 2 times compared to C12R. The mixing parameters used in the terminal blend causes the crumb rubber to soften; moreover, the extremely high test temperature conducted in the viscosity test (195°C) leads to depolymerisation/devulcanisation of the rubber network releasing rubber components to the liquid phase thus causing a decrease in the viscosity value. From the obtained results, it can be concluded that the benefits offered by the terminal blend binder were greatly diminished at extreme temperature (195°C) and become more evident at moderate to high temperatures (95°C-175°C), which allows

utilization of the terminal blend method in the modification of rubberized bitumen more effectively. Thus, the terminal blend method was found to be useful in tropical regions by means of increasing the viscosity of rubberized bitumen at environmental temperatures; however, caution should be taken as the terminal blend method produces rubberized bitumen, which is more susceptible at extreme temperature.

4.1.3.1 Multiple Linear Regression Analysis on the Apparent Viscosity Value

Table 4.6 and Table 4.7 show the multiple linear regression analysis using the stepwise method to assess the ability of factors (rubber content, TOR and binder blending method) to predict the viscosity value (Appendix A, Tables A. 3a – A.3d). The regression was conducted at the viscosity value obtained at 175°C. The regression analysis shows that the factors explain 84.0% of the variance in viscosity value, R^2=.84, R^2_{adj}=.831, $F(3,58)=101.331$, p<.05, as shown in Table 4.5. In the final model, the rubber content, TOR and blending type were statistically significant, with the rubber content recording a higher beta value (beta = 1.245, p =.000 < .05), followed by blending type (beta = -.583, p =.000 < .05) then TOR (beta= .336, p= .000<.05) (see Table 4.6). The regression equation that can be used to estimate the viscosity value based on the factors, is shown in Equation 4.3:

$$\textit{Viscosity value} = 1.245\,(\textit{Rubber content}) - .583\,(\textit{Blending type}) + .336\,(\textit{TOR}) \qquad (4.3)$$

Table 4.6 Model Summary: Viscosity Value

Step	R	R^2	R^2_{adj}	ΔR^2	F_{chg}	p	df_1	df_2
Rubber content, %	.778a	.605	.598	.605	91.918	.000	1	60
Blending types	.853b	.728	.719	.123	26.734	.000	1	59
Tran-spolyoctenamer content, %	.916c	.840	.831	.112	40.388	.000	1	58

Table 4.7 Coefficients for Final Model: Viscosity Value

Step	*B*	*β*	*t*	*Bivariate r*	*Partial r*
Rubber content, %	31.863	1.245	15.328	.778	.896
Blending types	-196.627	-.583	-7.197	.362	-.687
Transpolyoctenamer, %	18.189	.336	6.355	.245	.641

4.2. Temperature Susceptibility

The penetration index (PI) and activation energy (E_a) are frequently used to approximate the expected temperature susceptibility for bitumen. The higher the PI value of bitumen, the lower is its temperature susceptibility. In contrast, the lowest E_a value indicates that it is less susceptible to temperature changes.

4.3 Penetration Index

The penetration index (PI), which was developed by Pfeiffer and Van Doormaal (The Shell Bitumen Handbook, 2003), is frequently used to approximate the expected temperature susceptibility for bitumen. PI can be used as a basic performance index that reflects the consistency of bitumen towards temperature change.

The PI was calculated using the results obtained from the penetration and softening point test according to the proposed equation in the Shell Bitumen Handbook. The PI was calculated using Equation 4.4:

$$PI = \frac{1952 - 500 \log pen - 20SP}{50 \log pen - SP - 120} \qquad (4.4)$$

As reported by Bahia et al. (1994), and Yildirim (2007), increased viscosity and softening point as well as an improved penetration index means superior rutting resistance of the road pavement at high temperature, intensive crack resistance at low temperature and fatigue resistance.

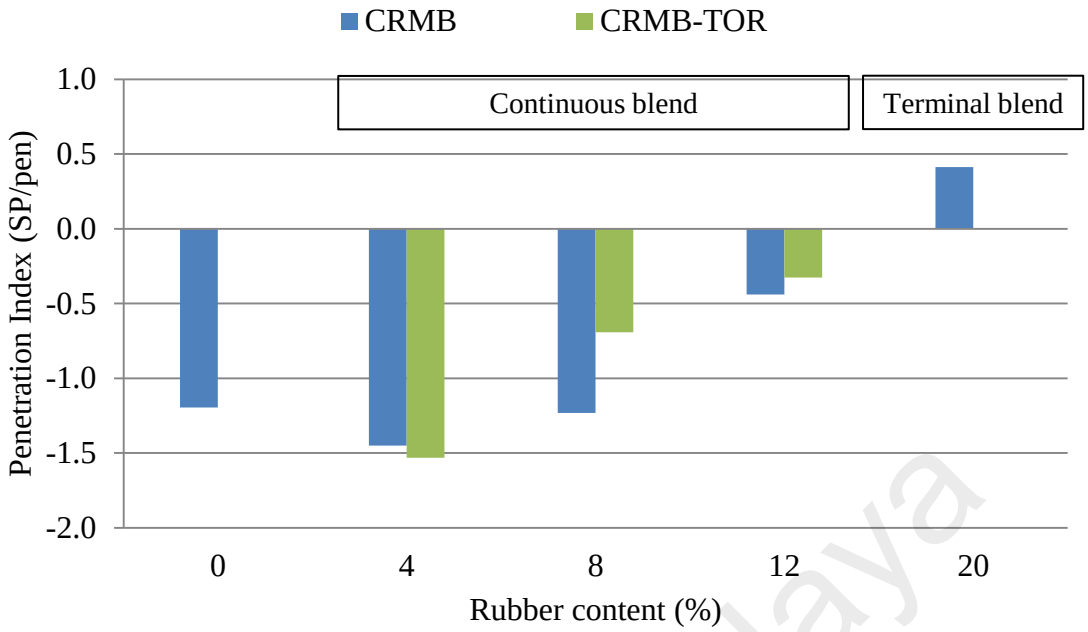

Figure 4.4 Penetration Index

As illustrated in Figure 4.4, the PI value of CRMB increases with the increase in rubber content. Moreover, it is noted that incorporating TOR to a higher rubber content (8% and 12% CR) increases the PI value. The increase in the penetration index shows better temperature-susceptibility performance. In contrast, the addition of TOR to low rubber content (4% CR) decreases the PI value. In addition, the achieved results show that the highest PI value was shown by the terminal blend binder (T20R), which means that the temperature-susceptibility performance is the best.

4.4 Activation Energy

The activation energy is defined as the minimum amount of energy required to activate a normal stable molecule to a state in which it can undergo a chemical reaction, thus converting it to a reactive molecule. In this study, the viscosity values at different test temperatures obtained using the brookfield viscometer were utilised in calculating the activation energy by applying the Arrhenius equation.

4.4.1 Arrhenius Equation

The Arrhenius equation is a formula for the temperature dependence of the reaction rates. The equation specifies a minimum amount of energy called the activation energy, E_a for reactants to transform into products. Equation 4.5 is the Arrhenius equation:

$$\eta = A\, e^{-E/RT} \qquad (4.5)$$

Where η = viscosity values of CRMB at temperature T; A = constant (frequency factor); and E = activation energy; R = perfect gas constant (8.314 J.K $^{-1}$ mol $^{-1}$); and T = absolute temperature (°K)

Figure 4.5 shows an Arrhenius plot calculated from the viscosity values. It shows the plots of viscosity on a logarithmic scale versus the reciprocal of the temperature expressed on an absolute scale. The plot shows that the viscosity of CRMB obeys the Arrhenius equation. It can be seen that increasing the temperature results in an increase in the rate of reaction.

4.4.2 Activation Energy Analysis

The activation energy, E_a, was calculated by applying the Arrhenius equation. It was determined by multiplying the slope of the line (Figure 4.5) by the universal gas constant, R. The activation energy was determined to elucidate the nature of the flow process. Moreover, the activation energy for the binders can be used to rank their temperature susceptibility in a quantitative manner. Low activation energy indicates that the binder is less sensitive to temperature change, while high activation energy shows more sensitivity to temperature change.

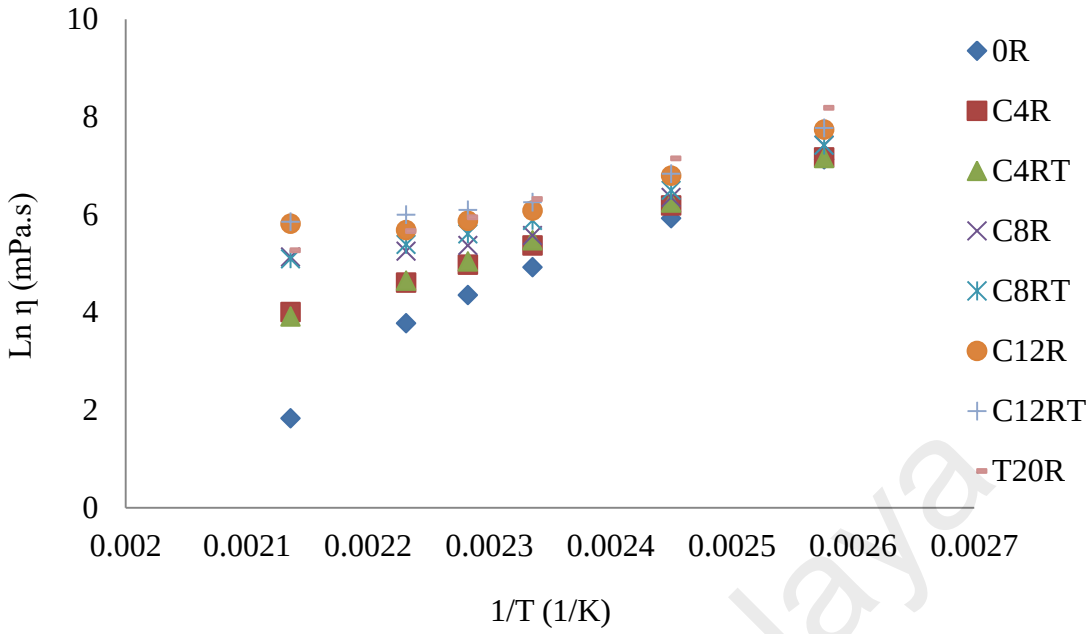

Figure 4.5 Arrhenius Representations for Binders

As can be seen in Figure 4.6, the results show that crumb rubber decreases the activation energy. It seems that crumb rubber activates the reaction between the rubber particles and the bitumen; it increases the energy between them thus dropping the energy needed for CRMB to change to another form. Moreover, Figure 4.6 shows that the addition of TOR to different concentrations of CRMB shows different trends. For instance, adding TOR to low rubber content (4%) increases the activation energy; increasing the rubber content to 8% indicates a similar value between CRMB and CRMB-TOR; while a high rubber content (12%) shows a decrease in activation energy. This indicates that adding TOR to different rubber concentrations influences the interaction between the binder and the rubber particles. In addition, there may be a critical rubber concentration that changes the nature of the interaction among the rubber particles, binder and TOR. Furthermore, different types of blending influence the activation energy. As seen in Figure 4.6, if compared with C12R (continuous blend binder prepared with 12% rubber), the terminal blend binder (T20R) increases the activation energy. It may be that the method used in the terminal blend binder causes a

decline in the reaction between the rubber particles and the bitumen, which leads to an increase in the activation energy for the binder to form another product. From the results, it can be concluded that the rubber contents, TOR and type of binder blend influences the interaction between the rubber particles and the bitumen thus affecting the activation energy.

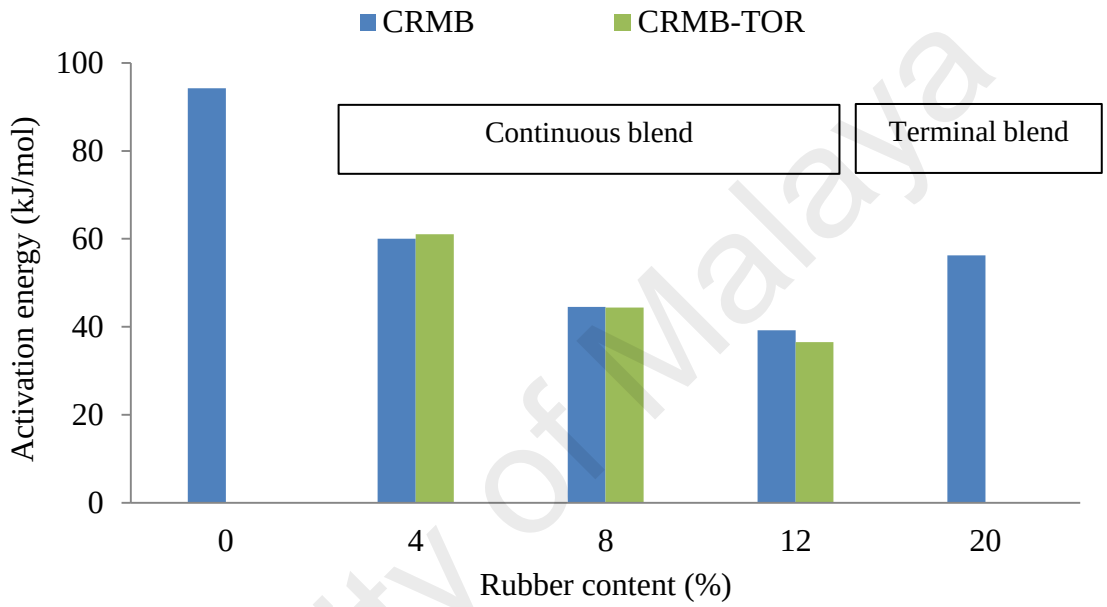

Figure 4.6 Effects of Rubber Crumb and TOR on the Activation Energy of Binders

4.5 Multiple Stress Creep and Recovery (MSCR) Test Results

Multiple stress creep and recovery (MSCR) test were performed to evaluate the high temperature performance of CRMB and CRMB-TOR. The high temperature performance of the binder is related to the rutting resistance of the bituminous pavement.

Many studies mentioned that the non-recoverable creep compliance (J_{nr}) obtained from the MSCR test shows a better correlation with the rutting measurements for bituminous mixtures (D'Angelo, J. 2008,2010; D'Angelo et al., 2007; Dreessen et al., 2009). For

this reason, the MSCR test has been widely used to evaluate the high temperature performance of mixtures in order to better understand real pavement conditions (Yang, X., and You, Z., 2015; Nuñez et al., 2014; DuBois et al., 2014; Domingos et al., 2014, Blazejowski, K. and Dolzycki, B., 2014).

From the MSCR test, the non-recoverable creep compliance (J_{nr}) and percent recovery (% R), which reflects the rutting potential index and elasticity of the binder, respectively, (Yang, X., and You, Z., 2015) were calculated and analysed. A low J_{nr} and high *% R* indicate that the high temperature performance of binders is improved. In this part of the investigation, all the binders were tested in the unaged state at 40°C, 50°C and 60°C.

4.5.1 Effects of Shear Stress on Non-Recoverable Creep Compliance (J_{nr})

Figure 4.7 shows a plot of the J_{nr} versus the applied stress for all the binders at the test temperature of 40°C. All the binders show consistent compliance at stress levels between 25 Pa and 6400 Pa. However, when the stress level was raised to 12,800 Pa, the J_{nr} for all binders except 0R, C12R, C12RT and T20R, increased significantly and differences in the bitumen response (inflection point) were evident. This indicates that at severe stress levels (>6,000 Pa), the binders show a wider spectrum of behaviour, as indicated by the apparent difference of J_{nr}. Therefore, by using the higher levels of stress in the MSCR test, the response of the binder captures the stiffening effects.

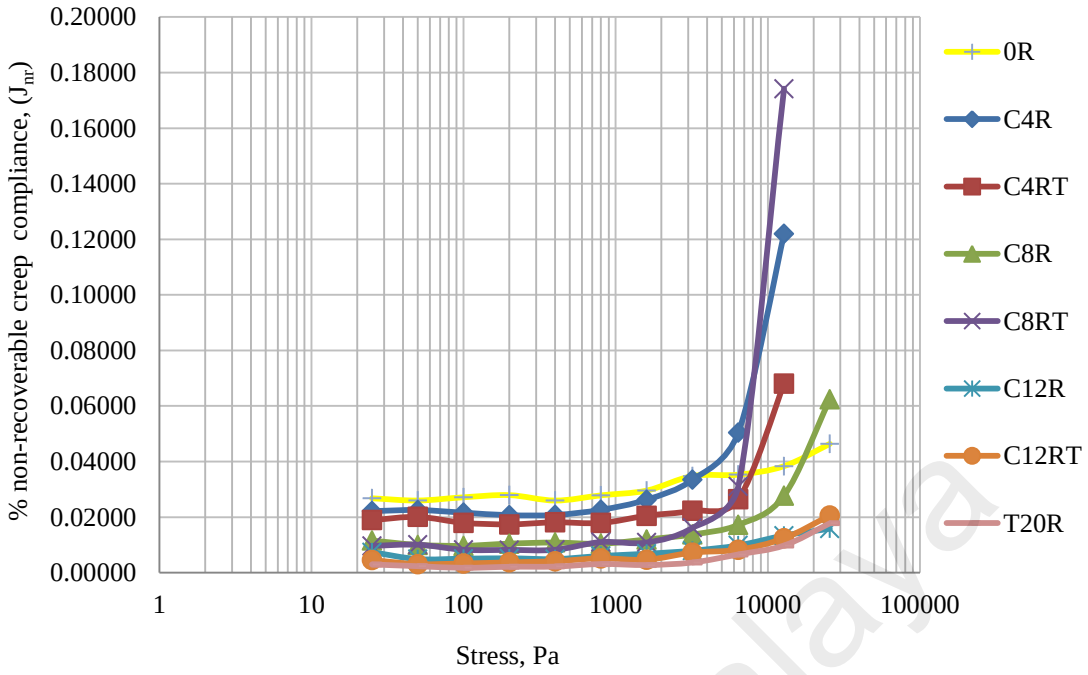

Figure 4.7 Comparisons of J_{nr} Values for Binders at 40°C

Moreover, binders that show a significant increase in J_{nr} as the stress level increases to 12,800 Pa, indicate that such binders are highly prone to rutting when unusual traffic loadings are applied to the pavement surface. This pattern is consistent with the shear thinning behaviour of bitumen, i.e. at low shear rates until a critical shear rate, the molecular order parameter is roughly constant and non-zero; however, as the shear rate increases above the critical value, the molecular order parameter begins to increase with the shear rate (Lemarchand et al., 2015). Nevertheless, 0R, 12R, 12RT and T20R violated this pattern, i.e. they observed consistent J_{nr} at all stress levels. It is possible to say that these effects on the J_{nr} values are, to some extent, related to the presence of the crumb rubber and TOR together with the type of blending in the binder formulation. In other words, the recoverable strain of the binder is affected by the stiffness of the base binder, the volume of the crumb rubber and TOR, and the extent of the chemical reaction in the binder. All of these effects should be identified by the MSCR test, which

improves the ability to relate the binder properties to the mixture performance (rutting resistance).

The use of different stress levels in the MSCR test is to perform the MSCR test with many stress levels (from low to severe) to capture the nonlinear response of the binder and relate that response to rutting in the bituminous mixtures. From Figure 4.7, it can be seen that in order to study the behaviour of the binders in the non-linear range, stress levels higher than 6,000 Pa seem to be needed for crumb rubber modified binder. It can be seen that at a stress level of 12800 Pa, the binder resistance to deformation starts to decrease, as shown by a sharp increase in J_{nr}. This sharp change in non-recoverable creep compliance can be an indicator that the binder is in the nonlinear region.

Another objective to use the different stress levels in the MSCR test is to better simulate the actual traffic conditions that can be observed in the field, as we know that the vehicles do not travel at the same speed and do not apply equivalent loads on the pavement structure. As has been noted in Figure 4.7, the results support the concern of many highway authorities that overloaded vehicles can rapidly accelerate the rutting potential.

Moreover, the test can also be used to rank the binders based on the stress levels. For instance, T20R is the most resistant to deformation followed by 12RT then 12R, as an increase in the stress levels has a relatively minor effect on the J_{nr} value. From the MSCR results, the rank of the binder from most resistant to deformation, to the worst at stress levels below 6,000 Pa is as follows: T20R, 12RT, 12R, 8RT, 8R, C4RT, C4R and 0R. However, increasing the stress level to 12,800 Pa affects the ranking of the binders (T20R is still the best followed by C12RT and C12R at all stress levels). This indicates that a high rubber concentration offers better rutting resistance. Moreover, it can also be mentioned that crumb rubber and TOR are sensitive to the severe stress level as the

ranking of the binder was different, as observed by the intermediate (<6,000 Pa) and high (>6,000 Pa) stress level. This higher nonlinearity in this CRMB and CRMB-TOR binder might lead to poor performance at high stress levels in the pavement; therefore, stress sensitivity should be taken into account in selecting the amount of crumb rubber in the modification of CRMB and CRMB-TOR.

4.5.1.1 Multiple Linear Regression Analysis on Non-Recoverable Creep Compliance

Table 4.8 and Table 4.9 show the multiple linear regression analysis using the stepwise method to assess the ability of the factors (rubber content, TOR and binder blending method) to predict non-recoverable creep compliance (Appendix A, Tables A.4a – A.4d). The factors can explain 90.3% of the variance in J_{nr}, $F(3,20)=62.417$, $p<.05$. In the final model, all the factors were statistically significant, with the rubber content recording a higher beta value (beta = -1.178, p =.000 < .05), followed by blending type (beta= .304, p= .000<.05) then TOR (beta = -.291, p =.000 < .05) (see Table 4.8). Equation 4.6 is the regression equation that can be used to estimate J_{nr}:

Non-recoverable creep compliance = -1.178 (Rubber content) +.304 (Blending type) -.291 (TOR) (4.6)

Table 4.8 Model Summary: Non-Recoverable Compliance

Step	R	R^2	R^2_{adj}	ΔR^2	F_{chg}	p	df_1	df_2
Rubber content (%)	.897a	.805	.796	.805	90.961	.000	1	22
Transpolyoctenamer (%)	.938b	.880	.868	.075	13.042	.002	1	21
Binder blending types	.951c	.903	.889	.024	4.900	.039	1	20

Table 4.9 Coefficients for Final Model: Non-Recoverable Compliance

Step	*B*	*β*	*t*	*Bivariate r*	*Partial r*
Rubber content (%)	-.002	-1.178	-8.563	-.897	-.886
Transpolyoctenamer (%)	-.001	-.291	-4.157	-.213	-.681
Binder blending types	.005	.304	2.214	-.710	.444

4.5.2 MSCR Test Results at 100 Pa and 3200 Pa

The MSCR test procedure was specified as in ASTM D7405 (ASTM, 2008). The standard specifies the test conditions: 1-s creep time, 9-s recovery time and 10 creep-recovery cycles at stress levels 100 Pa and 3200Pa. Therefore, it is necessary to discuss the MSCR results at 100 Pa and 3200 Pa.

4.5.2.1 Actual Strain Curve

Figures 4.8 (a) – 4.8 (b) show the actual strain for all the binders at a shear stress of 100 Pa and 3200 Pa, respectively. Both figures depict the data results at a 1 s creep loading with 9 s recovery phase at test temperature 40°C. During loading, the results show that the actual strain level went up. However, the strain decreases in the recovery phase. The overall test results display a reflection of the visco-elastic-plastic property of the binders (Yang, X., and You, Z., 2015).

Comparing Figure 4.8(a) with Figure 4.8(b), the strain was recovered immediately at low stress level (100 Pa); whereas at the high stress level (3200 Pa) the strain was recovered gradually. This was as expected, as the strain recovered faster at the low stress level (100 Pa) compared to the higher stress level (3200 Pa). At the low stress level, the sample was creeping less than that of the sample creeping at the high stress level; thus, when stress is removed during the recovery phase the strain at low stress

level (100 Pa) recovered faster than that at the high stress level (3200 Pa). Analysis of the percent recovery (Figure 4.10) justifies the above explanation.

Moreover, it was as expected that the maximum strain level of the sample creeping at 3200 Pa was much higher than that of the samples creeping at 100 Pa. Taking the control binder (0R), for instance, the maximum strain levels were 2.71% and 106.1% at 100 Pa and 3200 Pa, respectively; an increase of about 39 times (see Figure 4.8). This indicates that with an increase in the creep level, the maximum strain level also increases. This finding is similar to other research studies (Yang, X., and You, Z., 2015).

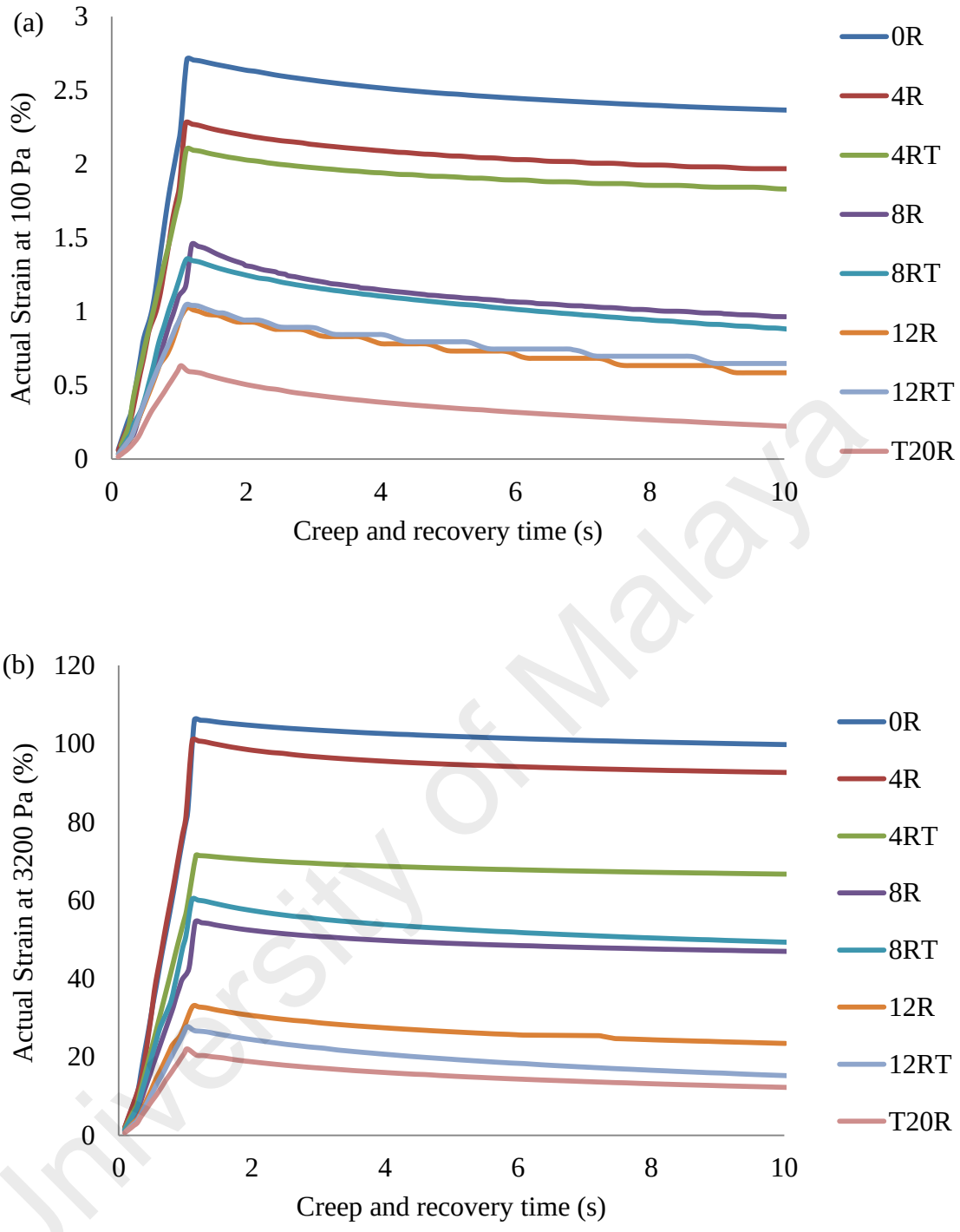

Figure 4.8 Actual Strains of the Binders at 40°C: (a) 100 Pa and (b) 3200 Pa

4.5.2.2 Non-Recoverable Compliance (J_{nr}) and percent Recovery (%R)

Figure 4.9 and Figure 4.10 show the non-recoverable compliance (J_{nr}) and percent recovery (% R), respectively. Both figures were plotted based on the MSCR results at 100 Pa and 3200 Pa. The results indicate that a higher creep loading level (3200 Pa)

resulted in a higher non-recoverable compliance and lower percent recovery. This was mainly due to the higher permanent deformation and lower percent recovery when the creep loading level increases. Take control sample (0R), for instance, the increase in the stress level from 100 Pa to 3200 Pa caused the J_{nr} to increase 1.28 times (from 0.027% to 0.035%) and the *% R* to decrease 2.51 times (12.920% to 5.151%).

Moreover, a comparison of Figure 4.9 with Figure 4.10 shows the close relationship between the non-recoverable compliance and the percent recovery: high non-recoverable compliance pairs with low percent recovery. This finding is in agreement with Adorjányi, K., and Füleki, P. (2011), who found good correlation (R^2 = 0.934-0.941) between non-recoverable compliance and recoverable strain for polymer modified bitumen. This indicates that the binder elasticity has an enormous effect on binder rut resistance behaviour. It was expected that the binder with higher elasticity shows less non-recoverable deformation. As the elasticity of the binder is increasing, the binder can recover a greater amount of deformation, which will result in less permanent deformation. Therefore, a binder with higher elasticity is more viscous-elastic, and, thus, shows a lower non-recoverable compliance value (J_{nr}) and more rut resistance.

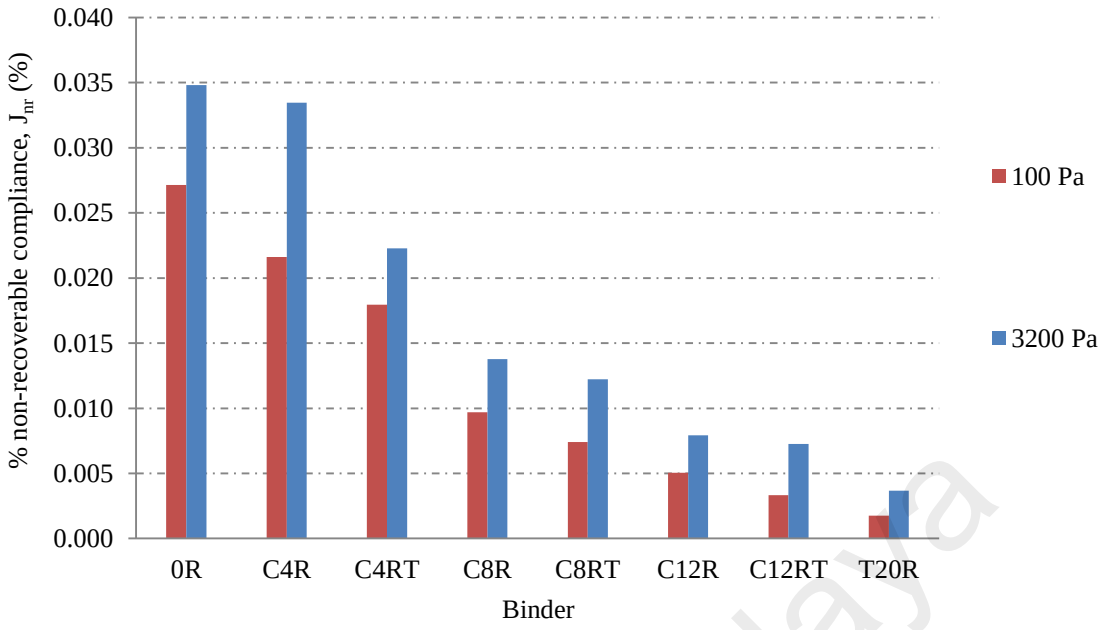

Figure 4.9 Non-Recoverable Compliance of Binders at 100 Pa and 3200 Pa

In terms of the effect of crumb rubber on the MSCR test results, it was observed that all of the CRMB binders had a lower J_{nr} compared to the control binder (0R) (see Figure 4.9). Moreover, adding TOR to CRMB (CRMB-TOR) seems to further decrease the J_{nr} compared with CRMB binders. For instance at a creep loading of 100 Pa, the J_{nr} of 4R, 8R and 12R were 20.37%, 64.30% and 81.38% lower than that of the control binder, respectively. For the crumb rubber binder with TOR (CRMB-TOR) the J_{nr} for 4RT, 8RT and 12RT decreased 33.88%, 69.6% and 87.70% compared to the control binder, respectively. Overall, an increase in the rubber content causes the J_{nr} to show a decreasing trend.

Moreover, adding TOR to the crumb rubber binder seems to decrease the J_{nr} more significantly compared to the control binder. A similar pattern was observed for both stress levels (100 Pa and 3200 Pa). It is possible to attribute these results to the chemical reaction among the base binder, crumb rubber and TOR. Therefore, it can be concluded that the crumb rubber and TOR improve the high temperature stability of the modified

binders and that it would be expected that these binders would offer better rutting resistance in the field.

In terms of the percent recovery (%R), the addition of crumb rubber and TOR led to an increase in the elastic response (Figure 4.10). This indicates that the presence of crumb rubber and TOR was responsible for the reduction in the amount of unrecovered strain of the binder at typical high pavement temperature (40°C).

In addition, T20R is shown to be the best binder, as shown by the lowest J_{nr} and highest %R compared to the control and continuous blend binder. This indicates that the terminal blend process produces a binder with better rutting resistance. These observations suggest that T20R would offer high temperature performance and therefore produce mixtures with high resistance to rutting when used as a binder.

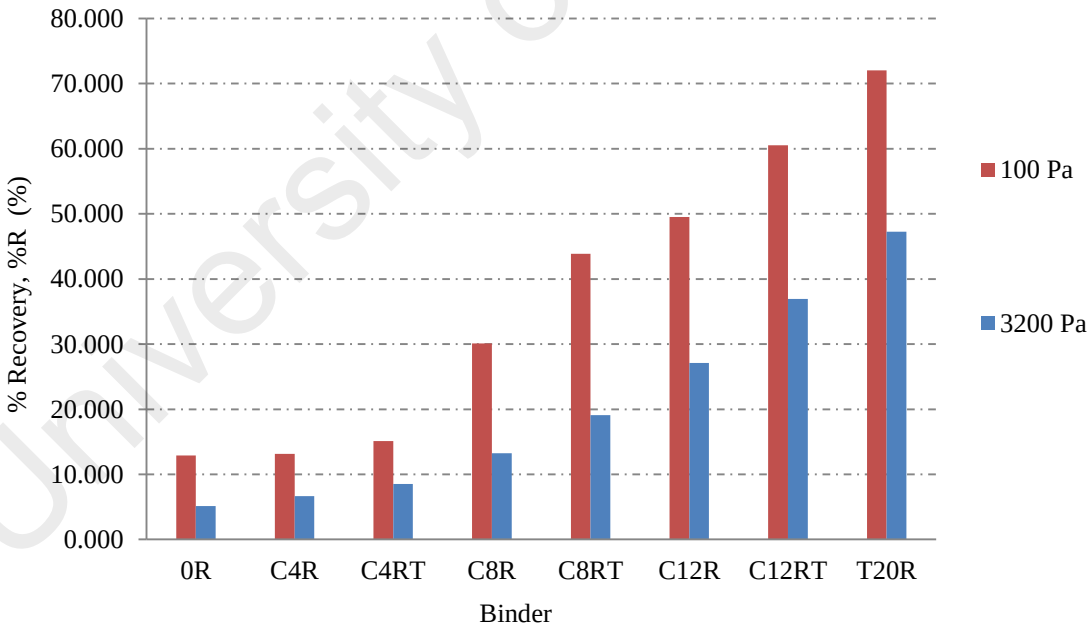

Figure 4.10 percent Recovery of Binders at 100 Pa and 3200 Pa

4.5.3 Effects of Temperature on MSCR Test Results

Figures 4.11(a) – 4.11(b) show the J_{nr} of the binders (0R, C12R, C12RT and T20R) at different temperatures (40°C, 50°C and 60°C) for stress levels of 100 Pa and 3200 Pa, respectively. The results show that the presence of crumb rubber and TOR decreased the J_{nr} values, especially at higher temperatures and stress levels. Since the non-recoverable compliance is an indicator of the susceptibility of the binder to rutting, it can be said that the C12RT and C12R are less prone to the accumulation of unrecovered strain under the creep and recovery loading than the control sample (0R). At low temperature (40°C) the J_{nr} values are almost similar for all binders. This can be explained by the observation of very low strain levels in the binders at 40°C (see Figure 4.9). However, the effects of crumb rubber and TOR become more visible as the temperature increases to 60°C. By considering the properties of the binder only, it can be inferred that the bituminous mixtures prepared with the base bitumen, the crumb rubber modified binder (CRMB) and the crumb rubber modified binder with TOR (CRMB-TOR) would have quite similar rutting performance at a pavement temperature of 40°C. Similarly, this rutting performance would reflect key differences among the three bituminous mixtures if the high pavement temperatures were equal to 50°C and 60°C.

Moreover, as illustrated in Figures 4.11(a) – 4.11(b), at each temperature, the lowest J_{nr} was obtained by T20R, followed by 12RT then 12R and 0R at both stress levels: 100 Pa and 3200 Pa. By considering only the rheological properties of the binder, this indicates that the lowest rutting levels may be obtained when the crumb rubber modified bitumen prepared with terminal blend process (T20R) is used in the bituminous mixture. Similarly, the addition of crumb rubber stabilized with TOR (CRMM-TOR) should enhance the pavement performance at the upper range of service temperatures where rutting is the more dominant distress mode.

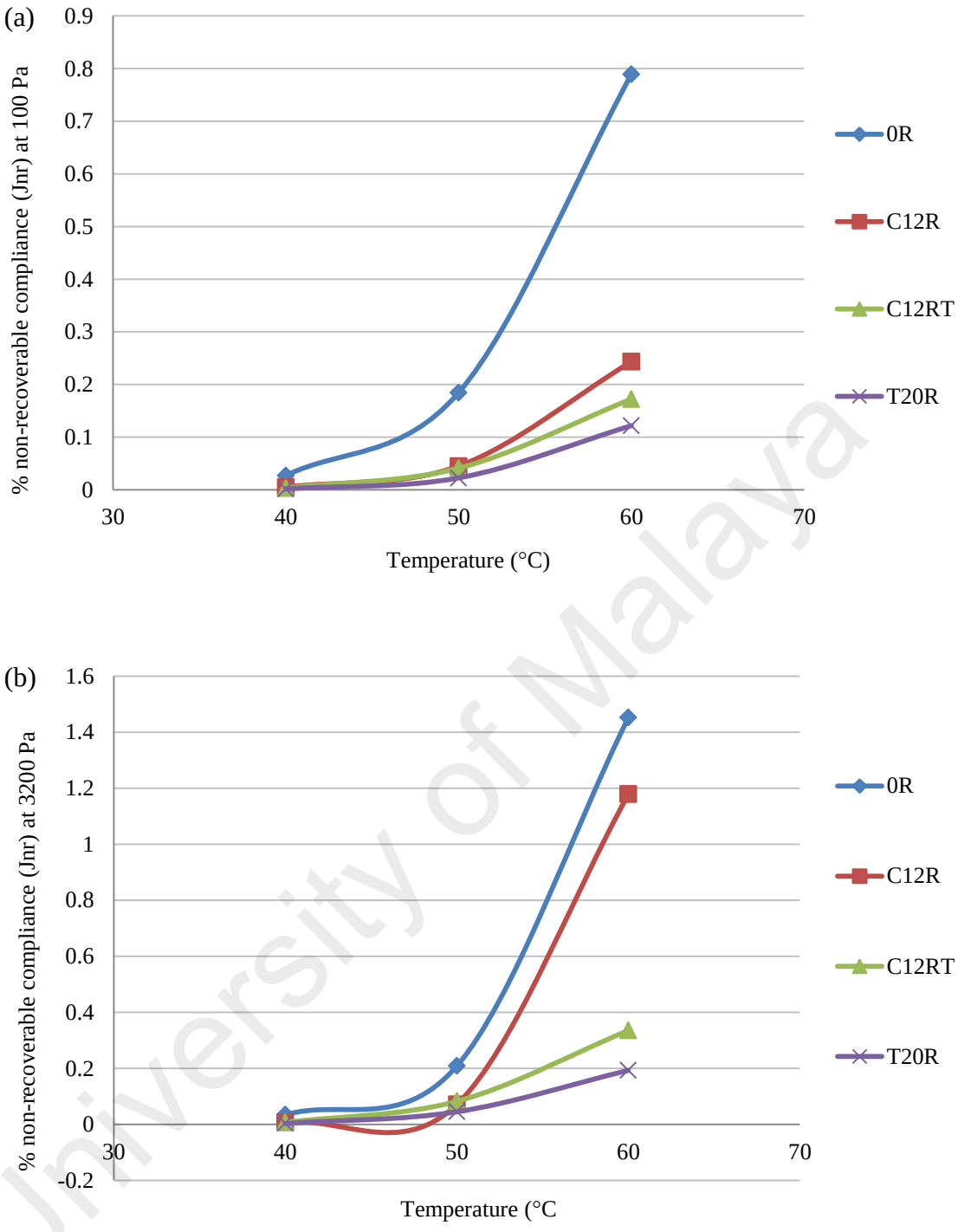

Figure 4.11 Percent Non-Recoverable Compliance versus Temperature at (a) 100 Pa (b) 3200 Pa

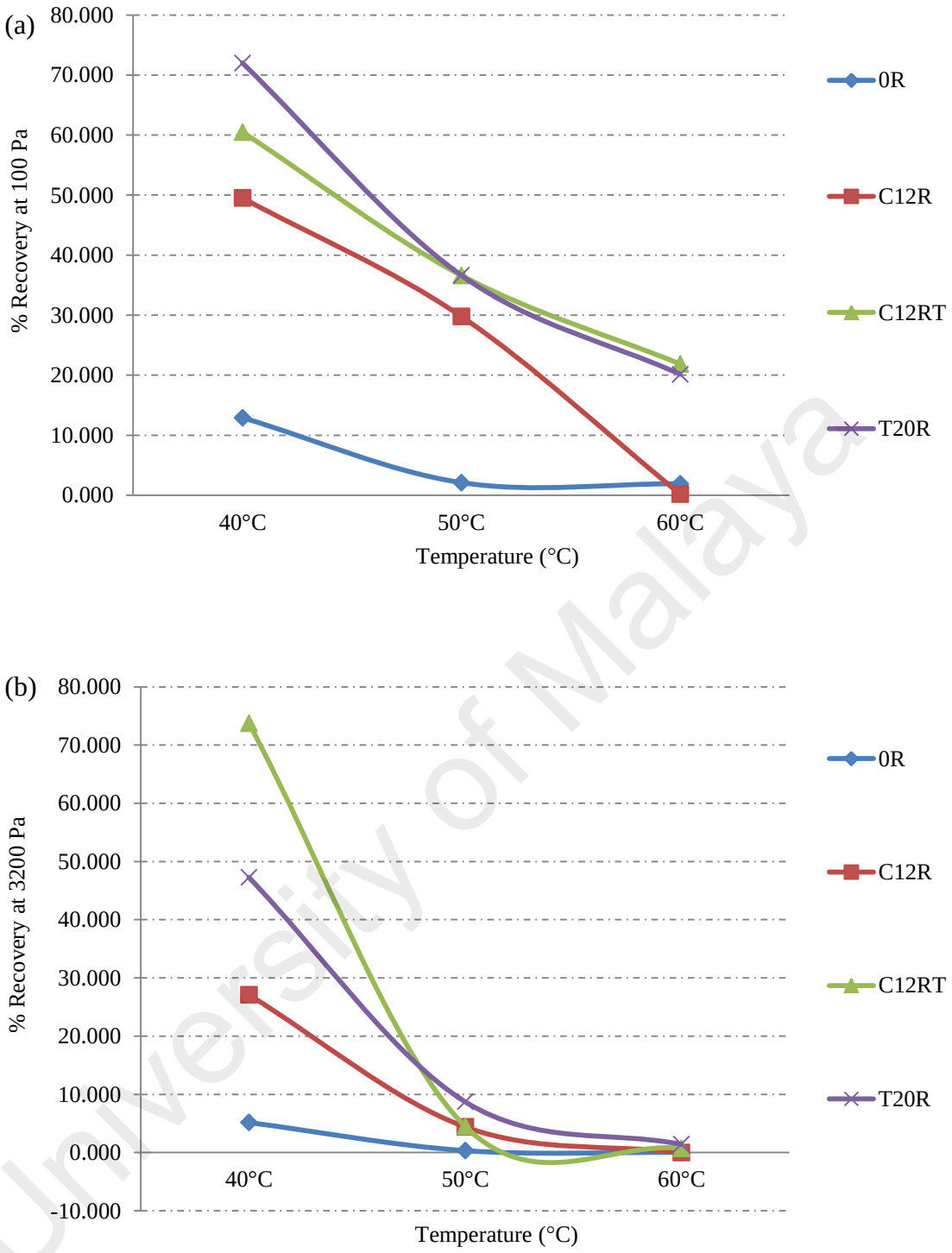

Figure 4.12: Percent Recovery versus Temperature at (a) 100 Pa (b) 3200 Pa

Figures 4.12(a) – 4.12(b) show the effects of temperature on the percent recovery of the binders at stress levels of 100 Pa and 3200 Pa respectively. As expected, the percent recovery decreases as the temperature increases for all binders. However, it is interesting to note that the percent recovery for all binders is close to zero (lower than

1%) under the highest test temperature (60°C) at stress level 3600 Pa. Stated another way, the effects of crumb rubber, TOR and blending type on its percent recovery are not easily recognized when the test conditions are more severe. This means that there is no significant recovery at high temperatures and high stress levels for all binders. Moreover, the %R value for binders tested at low stress (100 Pa) is always higher than that at high stress level (3200 Pa).

The above observations suggest that the stiffness and viscoelastic behaviour of the binder presented by percent recovery and non-recoverable compliance, respectively were strongly dependent on the applied stress as well as on the temperature. Thus, the suggestion should be made that the MSCR test should be done at temperatures determined upon the actual pavement temperature. Although crumb rubber increases the stiffness of the binder, the stress sensitivity of the binder will be greater than a neat binder. This is due to the actual lower stiffness of the base binder controlling the rubber particle interaction at higher stress. As the percentage of crumb rubber is increased to the optimum amount, the particle interaction becomes greater, increasing the apparent stiffness of the binder and reducing the stress sensitivity at any particular stiffness (experienced by 12RT and 12R). In addition, it should be mentioned that the stress sensitivity also varies with temperature. The J_{nr} and %R are very different when measured at 40°C, 50°C and 60°C. When the temperature increases, the region of insensitivity to the stress level will shrink. Therefore, this is a critical factor that indicates the necessity of estimating the stress sensitivity at actual pavement temperatures.

4.6 Summary of Multiple Linear Regression Model: Binders

The effects of factors (rubber content, TOR and blending type) on the properties of the binder are shown in the regression model. Table 4.10 summarizes the regression model

developed from the stepwise multiple linear regression (explained in section 4.1-4.5). It seems that the properties of the binders were significantly affected by most of the factors with high reliability value (R^2 =0.703 to 0.903). The highest reliability value was obtained by non-recoverable compliance (J_{nr}) with R^2 = 0.903. For this reason, J_{nr}, which presents a binder's rutting properties, is chosen for the comparison of the rutting potential of the mixtures. This will be discussed further in Sections 4.9.2.6 and 4.9.4.

Table 4.10 Summary of the Multiple Linear Regression Model for Penetration Value, Softening Point Value, Viscosity Value at 175°C and Non-Recoverable Compliance at 40°C (J_{nr})

Multiple Linear Regression model (Stepwise method)	**Model summary,R^2**
Penetration value = -.818 (Rubber content) - .316 (Transpolyoctenamer)	0.703
Softening point value = 1.196 (Rubber content) - .303 (Blending types)	0.867
Viscosity value at 175°C = 1.245 (Rubber content) - .583 (Blending types) + .336 (Transpolyoctenamer)	0.840
Non-recoverable creep compliance, J_{nr} = -1.178 (Rubber content) +.304 (Blending types) -.291 (Transpolyoctenamer)	0.903

4.7 Volumetric Test Results and Discussion

The volumetric test was conducted on the Marshall specimens. The volumetric parameters, namely, voids in mix (VIM) and voids in the mineral aggregate (VMA) were determined in accordance with ASTM D2041 and D3203. CRMB and CRMB-TOR, as discussed in the previous section, were used as binders. Stone mastic asphalt (SMA) gradation in accordance with Malaysia specification (JKR/SPJ/2008-S4) was utilized in the preparation of all specimens.

4.7.1 Voids in Mix (VIM)

Figures 4.13(a) – 4.13(b) illustrate the relationship between the VIM and binder content for all mixtures. The Malaysian Public Works Department specifies the VIM for SMA mixtures within 3-5% (JKR/SPJ/2008-S4).

As illustrated in Figure 4.13(a), it is observed that the air voids of the mixture are negatively correlated with the binder content (VIM decreases as the binder content increases). A similar pattern was observed for both CRMM (C4R, C8R and C12R) and CRMM-TOR (C4RT, C8RT and C12RT). This result is expected and consistent with previous research studies (Lavin, 2003).

It is important to mention that the VIM for CRMM-TOR is slightly lower compared with CRMM at any percentage of crumb rubber. Taking 4% rubber concentration at 7% binder content, for example, the VIM value for CRMM is 3.06%, while for CRMM-TOR it is 2.92%. This finding confirms the previous study conducted by Solaiman et al. (2003). They found a 20% decrease in VIM as the crumb rubber stabilized with TOR was used as a binder compared with the rubberized binder without TOR in preparation of 19.0 mm maximum nominal size Superpave mix.

Figure 4.13(b) illustrates the relationship between the VIM and rubber content for modified mixtures. Generally, the obtained results show that increasing the rubber content in the mixture results in increases in the air voids as a consequence of the ability of rubber particles to swell and absorb the binder, and, subsequently, leave voids between the aggregate. This finding was also expected and consistent with previous studies (Airey et al., 2003)

A similar pattern was observed for CRMM-TOR. For instance, at 7% binder content, the VIM value for CRMM-TOR prepared with 8% crumb rubber indicates 3.47%, while

the VIM value for CRMM-TOR prepared with a higher crumb rubber (12%) is 4.06%. It seems that the increase in VIM in the CRMM-TOR as the rubber concentration increases could be the result of the crumb rubber concentration rather than TOR. In other words, the crumb rubber concentration is a major factor influencing the VIM value followed by TOR. The difference in VIM between CRMM and CRMM-TOR is very close, which leads the author to believe that the difference is due to the rubber concentration rather than TOR.

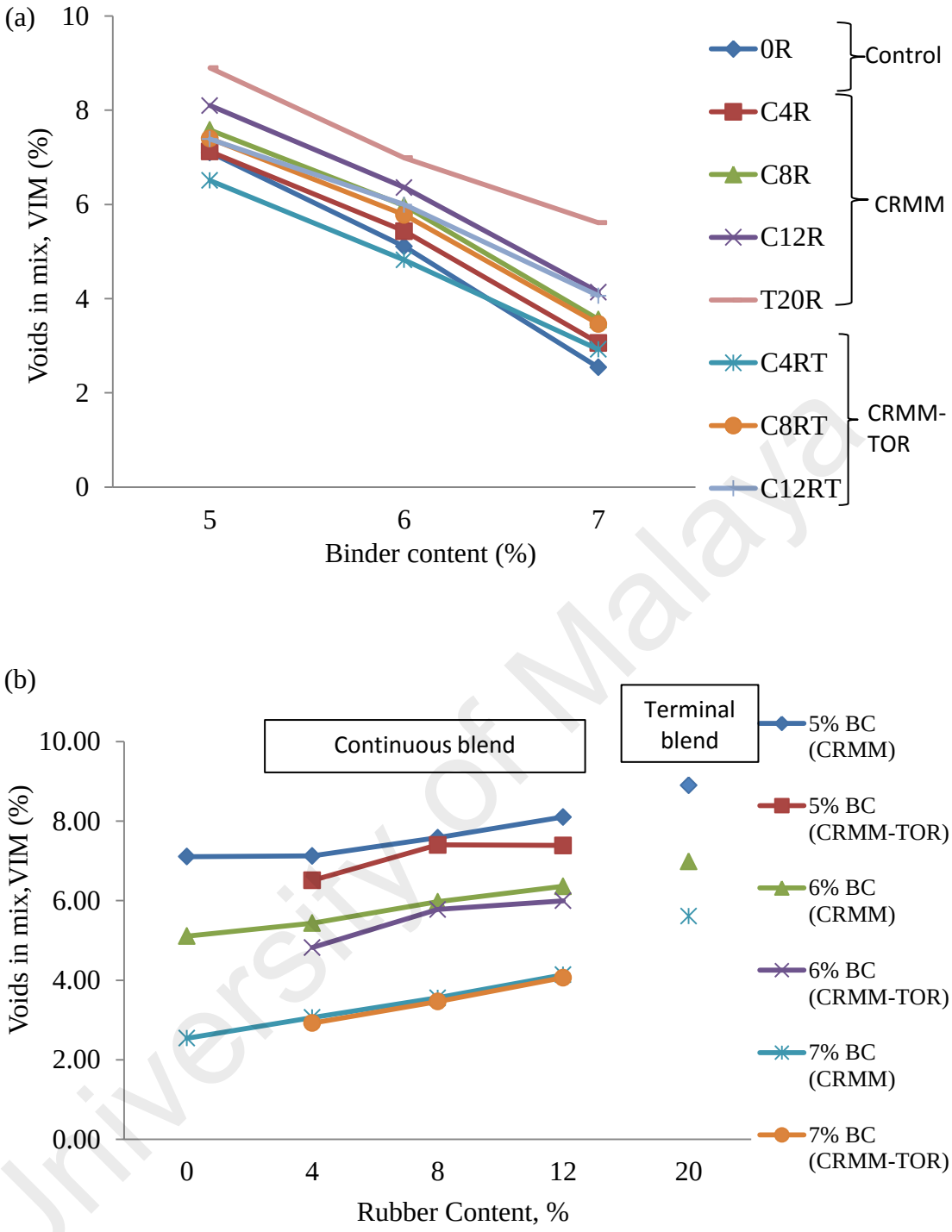

Figure 4.13 VIM Value Versus: (a) Binder Content (b) Rubber Content

The type of binder blending shows that the VIM obtained by mixtures prepared with the terminal blend binder is higher than that for the continuous blend binder. This can be explained by the high rubber content in the terminal blend binder (20%) compared to

the continuous blend (4%-12%). High rubber content results in greater absorption of bitumen, thus leading to an increase in voids in the mixture.

As the obtained results show, the rubber content and TOR affect the VIM values, hence it is essential to carefully design the amount of crumb rubber in order to produce a mixture with sufficient air voids. As a matter of fact, satisfactory air voids help improve pavement performance as adequate air voids allow satisfactory densification due to traffic loads at the beginning of the pavement service. However, excessive air voids can result in cracking, which is due to the insufficient binder coating the aggregate, while low air voids can result in more rutting as well as binder bleeding.

4.7.1.1 Multiple Linear Regression Analysis on VIM

Table 4.11 and Table 4.12 show the multiple linear regression analysis using the stepwise method to assess the ability of factors (rubber content, trans-polyoctenamer content, binder blending method, binder content) to predict VIM. The factors explain 93.2% of the VIM , R^2 = .932, R^2_{adj}= .931, $F(3, 216) = 214.918$, $p<.05$. In the final model, the binder content, rubber content and TOR were statistically significant, with the binder content recording a higher beta value (beta = -.891, p =.000 < .05), followed by rubber content (beta = 0.355, p =.000 < .05) then TOR (beta= -.098, p= .001<.05). The regression equation, which can be used to estimate VIM based on the factors, is written in Equation 4.7:

$$VIM = -.891\,(\text{binder content}) + .355\,(\text{rubber content}) - .098\,(\text{TOR}) \quad (4.7)$$

The Multiple Linear Regression analysis results can be referred to in Appendix A, Tables A. 5a – A.5d. A summary of the regression model is presented in Table 4.11. In addition, the bivariate and partial correlation coefficients between each factor and the VIM are presented in Table 4.12.

Table 4.11 Model Summary: VIM Value

Step	R	R^2	R^2_{adj}	ΔR^2	F_{chg}	p	df_1	df_2
Binder content (%)	.897a	.804	.803	.804	893.099	.000	1	218
Rubber content (%)	.960b	.922	.921	.118	330.280	.000	1	217
Transpolyoctenamer (%)	.965c	.932	.931	.009	29.648	.000	1	216

Table 4.12 Coefficients for Final Model: VIM Value

Step	B	β	t	*Bivariate r*	*Partial r*
Binder content (%)	-1.975	-.891	-50.023	-.897	-.959
Rubber content (%)	.116	.355	19.812	.346	.803
Transpolyoctenamer (%)	-.080	-.098	-5.445	-.101	-.347

4.7.2 Voids in Mineral Aggregate (VMA)

The voids in the mineral aggregate (VMA) are described as the volume of inter granular void space between the aggregate particles of a compacted paving mixture. Generally, the VMA allows space for enough binder to make a durable mixture and enough room for the air voids to ensure a stable mixture. Mirzahosseini et al. (2011) mentioned that in order to resist permanent deformation, bituminous mixtures should have a low percentage of VMA.

The Malaysian Public Works Department specifies that the VMA for SMA mixtures should be more than 17% (JKR/SPJ/2008-S4). VMA is an important property in hot mix asphalt (HMA) and is known to affect a pavement's resistance to rutting. The intention of specifying a minimum value for VMA in the mixture design is to ensure that the binder content is sufficient to provide the durability needed under traffic loading. Inadequate binder content causes the aggregate particles to not bind properly; this allows the water to pass through the thin binder films, which leads to stripping. In contrast, excessive binder content results in an increase in rutting and bleeding.

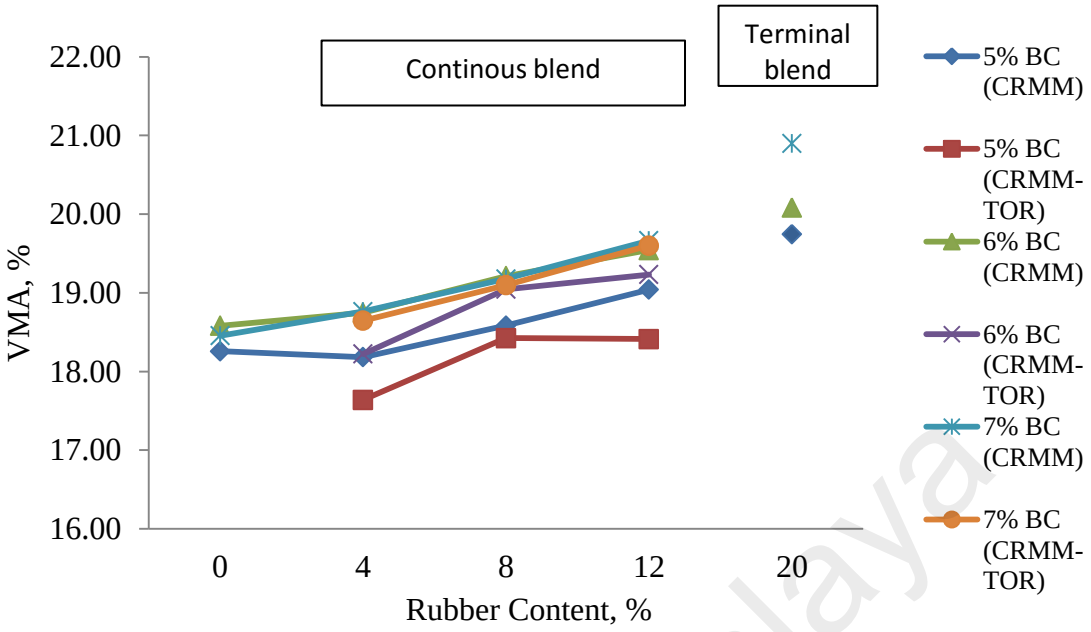

Figure 4.14 VMA Value versus Rubber Content

The obtained VMA results are illustrated in Figure 4.14. It can be seen that the addition of crumb rubber increases the VMA of the mixtures and that this increase is generally more apparent as the rubber content increases. This result is consistent with other research (Xiao et al., 2009).

With respect to the control mixture, when the rubber content increased from 0% to 12%, the VMA increased about 4.10%, 4.91% and 6.15% for the binder contents of 5%, 6% and 7%, respectively. Moreover, in the relationship between VMA and CRMM stabilized with TOR (CRMM-TOR), a similar trend was observed: VMA increases when the rubber content increases. On the other hand, adding TOR to any rubber content (CRMM-TOR) lowers the VMA values compared with CRMM. For instance, in the case of 5% binder content, CRMM-TOR at 4% rubber content shows a lower VIM content (17.64%) compared to CRMM (18.18%).

Additionally, the type of binder blend indicates that the VMA values obtained by the terminal blend binder are higher than those for the continuous blend binder. As can be

seen in Figure 4.14, at binder contents of 5%, 6% and 7%, the VMA values for the terminal blend are 19.75%, 20.08% and 20.90%, respectively, while the VMA values for the continuous blend (in the case of 12% CR) show 19.04%, 19.54% and 19.66%, respectively.

The obtained results show that all the VMA values are within the required specification (min. 17%), which supports the use of crumb rubber and TOR in SMA mixtures. Different blending types in the preparation of rubberized binders also results in acceptable VMA values. Therefore, it can be concluded that all the specimens pass the VMA specification.

4.7.2.1 Multiple Linear Regression on VMA

The multiple linear regression analysis results on VMA can be referred to in Appendix A, Tables A. 6a – A.6d. The summary is listed in Tables 4.13 – 4.14. The regression analysis was conducted to determine which factors (rubber content, TOR, binder blending method, binder content) were the predictors of the VMA values. The regression results indicate an overall model of all the factors (rubber content, binder content, TOR and blending type) that significantly predicts the VMA value, R^2=.692, R^2_{adj}=.686, $F(4,215)=120.665$, $p<.05$. This model accounted for 69.2% of variance in VMA.

Equation 4.8 is the regression model based on the beta weight for predicting the VMA value:

$$VMA = .894\,(\text{rubber content}) + .378\,(\text{binder content}) - .210\,(\text{TOR}) - .201\,(\text{blending type}) \quad (4.8)$$

Table 4.13 Model Summary: VMA Value

Step	R	R^2	R^2_{adj}	ΔR^2	F_{chg}	p	df_1	df_2
Rubber content (%)	.700a	.490	.487	.490	209.202	.000	1	218
Binder content (%)	.792b	.627	.624	.138	80.183	.000	1	217
Transpolyoctenamer (%)	.825c	.681	.677	.054	36.339	.000	1	216
Blending types	.832d	.692	.686	.011	7.521	.007	1	215

Table 4.14 Coefficients for Final Model: VMA Value

Step	B	β	t	*Bivariate r*	*Partial r*
Rubber content (%)	.116	.894	12.371	.700	.645
Binder content (%)	.332	.378	9.954	.370	.562
Transpolyoctenamer (%)	-.069	-.210	-5.383	-.137	-.345
Blending types	-.286	-.201	-2.742	.508	-.184

4.8 Marshall Stability and Flow of Bituminous Mix Test Results

The Marshall Stability and Flow of Bituminous Mix test was conducted in accordance with ASTM D6927 – 15. It is used for laboratory mix design and for the evaluation of the characteristics of bituminous mixtures. The Marshall stability and flow are the bituminous mixture characteristics obtained from the test.

4.8.1 Marshall Stability

Marshall stability is an important property of bituminous mixtures as it can be used as a measure of the bituminous mixture's susceptibility to rutting under traffic. Figure 4.15(a) represents the plot of the Marshall stability versus binder contents for each CRMM and CRMM-TOR. Overall, all the samples showed a similar trend, an increase in stability as the bitumen content increased up to an optimum value. However, the further addition of bitumen resulted in a decrease in the stability values.

The diagram shows that the stability increases as the rubber content increases. All the mixtures provide stability greater than the minimum value of 6.2kN (JKR/SPJ/2008-S4). The Marshall stability values for CRMM and CRMM-TOR were generally higher in comparison to the control. Therefore, the addition of crumb rubber and TOR plays a key role in increasing the stability of the mixture. The increase in stability by adding rubberized bitumen to the hot mix bitumen is attributed to the better adhesion developed between the rubber particles and the bitumen in the mix. It can be considered that the adhesive bond strength controls the failure mechanism in the Marshall stability test. This serves to enhance the interlocking between aggregates to sustain the imposed load, which results in the increased stability value of the mixtures.

The results reveal that the amount of rubber content is significant to ensure acceptable stability of the mixtures, as excessive rubber content results in a decrease in the stability value. As indicated in Figure 4.15(b), the terminal blend binder prepared with 20% crumb rubber results in a lower stability value. A high rubber content (20%) in the preparation of the terminal blend binder contributes to a decrease in the stability value of the mixtures. This is related to the high amount of rubber particles that fill the space to be occupied by the binder, thus decreasing the interlocking offered by the binder and aggregate particles. The test results indicate that the mixtures containing 12% crumb rubber for both CRMM and CRMM-TOR prepared with continuous blend binder show a higher stability than the other mixtures, indicating their higher rutting resistance.

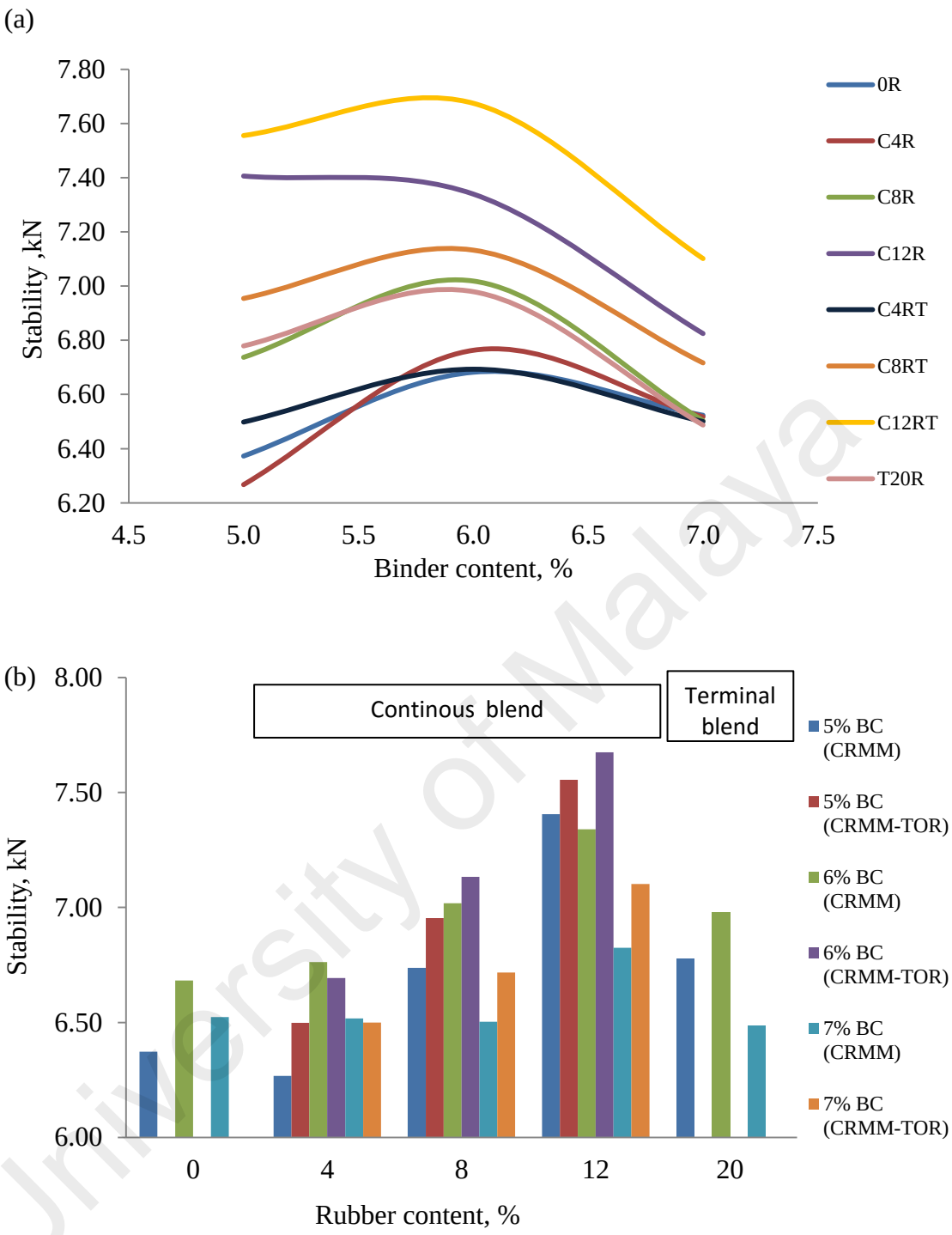

Figure 4.15 Marshall Stability at Different (a) Binder Content, (b) Rubber Content

From Figure 4.15(b), it is evident that the presence of TOR in the rubberized SMA mixtures effectively improves the stability values, which will result in an improvement of the mixture toughness. This indicates that the CRMM-TOR mixtures result in higher rutting resistance than the CRMM and control mixture. It is noted that mixtures gave the

maximum stability at 12% rubber content and that CRMM-TOR shows the highest stability value (7.67 kN). This indicates that CRMM-TOR prepared with 12% CR (C12RT) would present higher rutting resistance and better performance compared to the other mixtures. The percentage increase in stability for C12RT with respect to the control mixture is about 12.91% and about 9% compared to CRMM without TOR (C12R). This result could be attributed to the crumb rubber and TOR adhesion and networking effects in the stabilized mixtures. The plasticizing effect of TOR was regarded as the primary factor contributing to the CRMM-TOR reinforcement. As TOR was blended with crumb rubber in hot bitumen, TOR vulcanizes, which creates a chemical bond between the crumb rubber and the bitumen to produce a uniform, low-tack, rubberized bitumen composite. The ability of TOR to cross-link the crumb rubber to the bitumen creates a rubberized matrix in the mixtures that promotes higher stability.

According to the test results, it was found that CRMM and CRMM-TOR modification significantly increases the stability. Consequently, it can be concluded that the crumb rubber and TOR had a positive effect on the durability of the bituminous mixtures. Hence, it is understood from the Marshall test results that CRMM and CRMM-TOR modification would be worthwhile for the bituminous mixtures to resist rutting.

Figure 4.16 shows the relationship between Marshall stability and VIM. It is known that the air voids content affects the stability of the mixture. Previous studies revealed that mixtures with a lower air void showed the highest stability and vice versa (Sousa et al., 1991). However, this study found a different trend. As shown in Figure 4.10, the stability increases with an increase in VIM. Thus, from the above relationship, it can be concluded that the correlation between the Marshall stability and the VIM for CRMM and CRMM-TOR is different to the general trend shown by conventional mixtures.

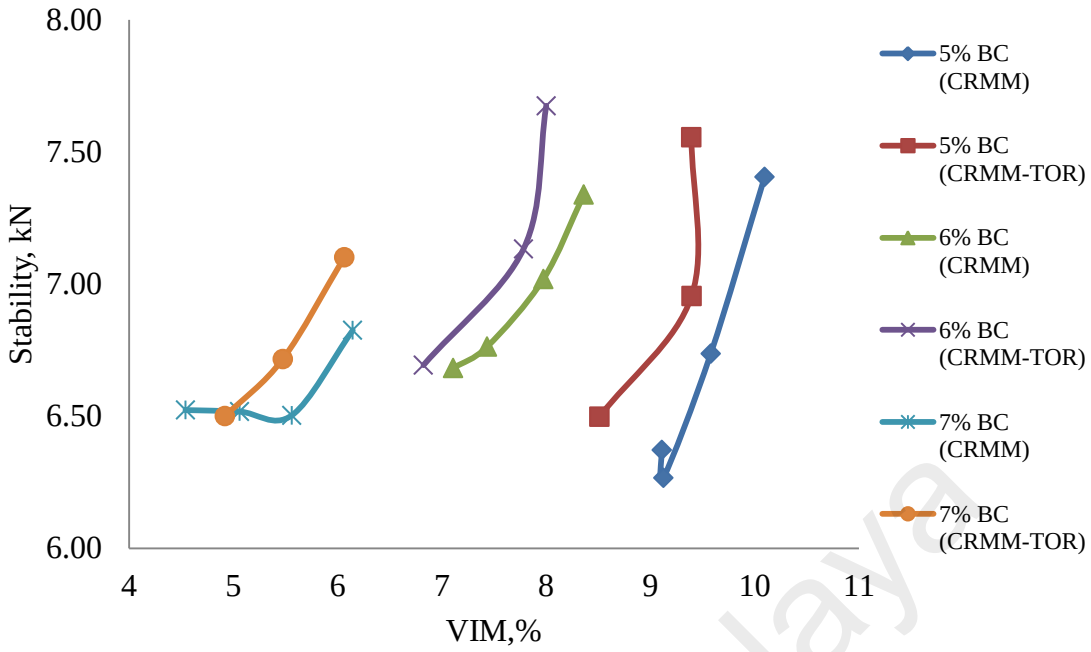

Figure 4.16 Marshall Stability versus VIM

4.8.1.1 Multiple Linear Regression Analysis on Marshall Stability

The regression analysis was conducted to determine which factors (rubber content, TOR, binder blending method, binder content) were the predictors of the stability values.

The multiple linear regression analysis results on Marshall stability can be referred to in Appendix A, Tables A. 7a – A.7d. Tables 4.15 – 4.16 show the summary of multiple linear regression analysis on the stability value. Table 4.15 indicates that three factors contribute 25.5% of the stability value, R^2= .255, R^2_{adj}=.235, $F(3,112)=12.760$, $p<.05$. As shown in Table 4.16, three factors were statistically significant, with blending type recording a higher beta value (beta=-.752) followed by TOR (beta=-.367) and rubber content (beta=.429). The regression model can be written as below (Equation 4.9):

$$Stability = -.752\ (blending\ type) -.367\ (TOR) +.429\ (rubber\ content) \quad (4.9)$$

Table 4.15 Model Summary: Stability Value

Step	R	R^2	R^2_{adj}	ΔR^2	F_{chg}	p	df_1	df_2
Blending types	.327a	.107	.099	.107	13.626	.000	1	114
Transpolyoctenamer (%)	.464b	.215	.201	.109	15.628	.000	1	113
Rubber content (%)	.505c	.255	.235	.039	5.928	.016	1	112

Table 4.16 Coefficients for Final Model: Stability Value

Step	B	β	t	*Bivariate r*	*Partial r*
Blending types	-1.068	-.752	-4.235	-.327	-.372
Transpolyoctenamer (%)	.137	.367	4.399	.285	.384
Rubber content (%)	.056	.429	2.435	-.223	.224

4.8.2 Marshall Flow

Flow is a measure of deformation (elastic plus plastic) of the bituminous mix determined during the Marshall stability test (ASTM D6927). Flow reflects the ability of bituminous pavement to adjust to gradual settlements and movements in the subgrade without cracking. Flow determines the reversible behaviour of the wearing course under traffic loads and affects the plastic and elastic properties of bituminous concrete (Hinislıoglu and Agar, 2004; Kuloglu, 1999). The Malaysian Public Works Department specifies a flow value of between 2 and 4 mm (JKR/SPJ/2008-S4).

Figure 4.17a shows the flow value versus the binder content for rubberized mixtures. As expected, for all mixes, the 5% binder content results in the lowest flow while the 7% binder content shows the highest. In other words, the figure illustrates that the Marshall flow increases following any increase in the bitumen content. This result is consistent with many previous studies (Ahmadinia et al., 2011; Nuha et al., 2013).

Low flow values indicate a mixture that may have insufficient bituminous binder, which may lead to durability problems with the pavement. On the other hand, high binder content increases the flow value because excessive binder in the mixture reduces aggregate interlocking because the aggregate is floating within the mixture, and, thus, results in a high flow value. According to Lavin (2003), high flow values indicate a mixture that has plastic behaviour that leads to the potential for rutting under loading.

For SMA rubberized mixtures prepared with continuous blend binder, Figure 4.17 (b) shows a dropping trend of flow value as the crumb rubber increases. Given that, the reaction between the crumb rubber and the bitumen increases the stiffness of the rubberized binder, and, consequently, the mixture. As a result, the mixes become less flexible and the resistance to deformation increases resulting in a low flow value. Moreover, flow values for most mixtures prepared with 4% (C4R and C4RT), 8% (C8R and C8RT) and 12% crumb rubber (C12R and C12RT) are located within the required specification range of 2 to 4 mm (JKR/SPJ/2008-S4) while none of the mixtures with 20% rubber content were within the range.

The flow value of the SMA mixtures increases after adding 20%CR, as shown in Figure 4.17b. This may be due to the decrease in the stone-to-stone contact of SMA mixtures at higher rubber content. This indicates that there is an optimum amount of rubber content that produces sufficient stiffness to decrease the flow value, and that further addition of rubber content contributes to the formation of a stiffer mixture, which results in an increase in the flow value.

In the case of the relationship between the crumb rubber and TOR in flow value, Figure 4.17(b) shows that adding TOR to 4% rubber content increases the flow value of the mixtures prepared at any binder content. However, further increases in rubber content (8% and 12% CR) show a decrease in flow value. This indicates that TOR is more

effective at a high rubber content, which will result in an improvement in the resistance to permanent deformation.

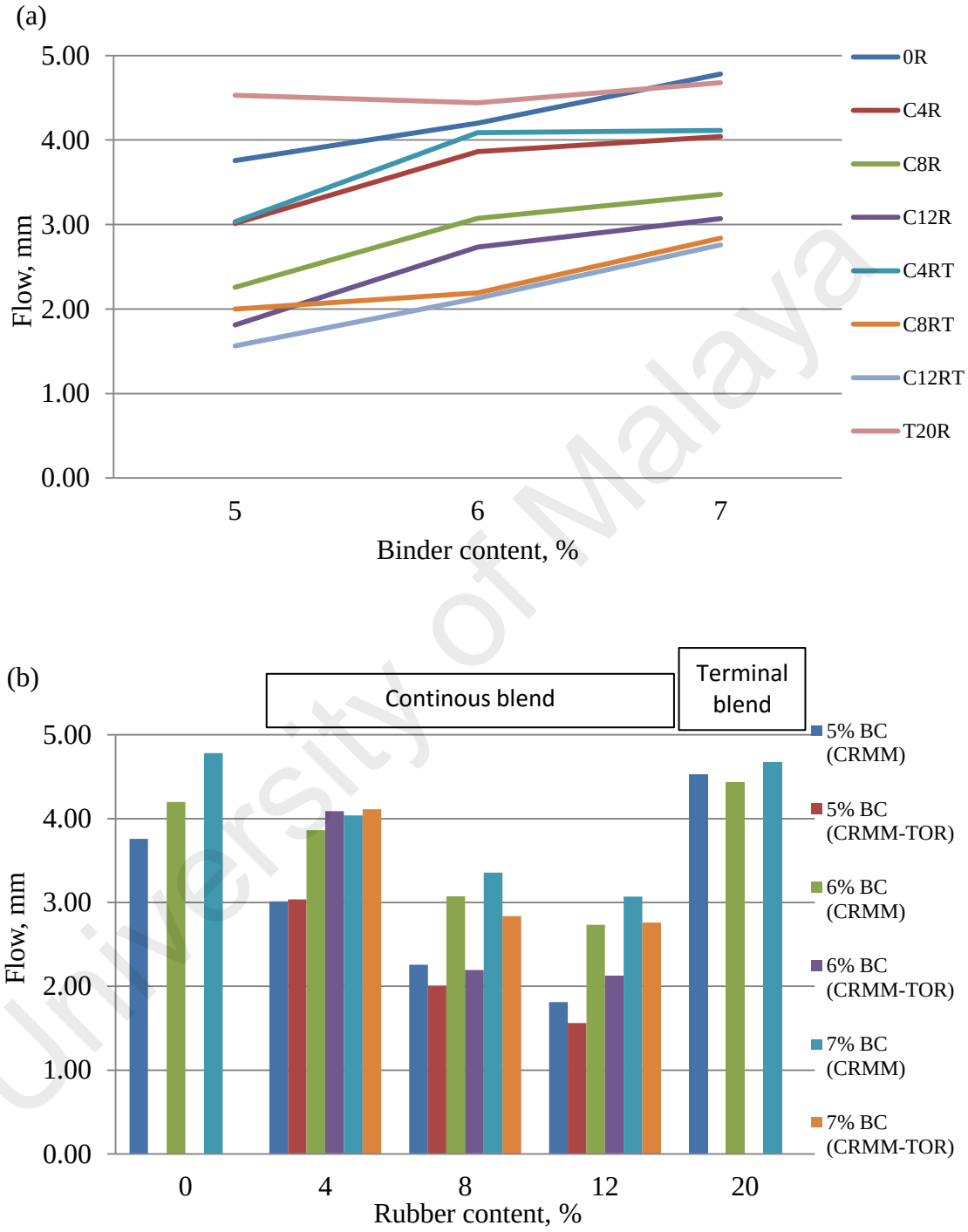

Figure 4.17 Marshall Flow Value versus (a) Binder Content, (b) Rubber Content

4.8.2.1 Multiple Linear Regression Analysis on Marshall Flow

Tables 4.17 – 4.18 show the summary of multiple linear regression analysis on the flow value. Full analyses are shown in Appendix A, Tables A.8a – A.8d. All factors (rubber content, TOR, binder blending method, binder content) were used as independent variables in the analysis.

The analysis shows that all factors significantly contribute to the flow value, R^2 = .471, R^2_{adj}=.451, $F(4,111) = 24.661$, $p<.05$. The model accounted for 44.3% of variance in flow value.

Equation 4.10 shows the regression model based on the β value:

$$\textit{Flow value} = -.744\,(\textit{Binder content}) + .388\,(\textit{TOR}) - .352\,(\textit{Rubber content}) + .357\,(\textit{Blending type}) \quad (4.10)$$

Table 4.17 Model Summary: Flow Value

Step	R	R^2	R^2_{adj}	ΔR^2	F_{chg}	p	df_1	df_2
Binder content (%)	.439a	.193	.186	.193	27.243	.000	1	114
Transpolyoctenamer (%)	.586b	.343	.332	.150	25.864	.000	1	113
Rubber content (%)	.666c	.444	.429	.100	20.208	.000	1	112
Blending types	.686d	.471	.451	.027	5.646	.019	1	111

Table 4.18 Coefficients for Final Model: Flow Value

Step	B	β	t	Bivariate r	Partial r
Binder content (%)	-.123	-.744	-4.983	-.439	-.428
Transpolyoctenamer (%)	.483	.388	5.614	.388	.470
Rubber content (%)	-.166	-.352	-4.986	-.330	-.428
Blending types	.640	.357	2.376	-.344	.220

4.8.3 Marshall Quotient

The Marshall quotient (MQ), calculated as the ratio of stability to flow value, can be used as an indicator to reflect the creep deformation resistance of the mixture. It is used to give an indication of the mixture's stiffness and resistance to permanent deformation including rutting of the bituminous mixture (Haddadi, Ghorbel, and Laradi, 2008; Hinislıoglu and Agar, 2004). The high MQ value indicates a mixture with high stiffness that has a greater ability to spread the applied load and resist rutting deformation (Alavi, Ameri et al., 2010).

Figure 4.18 shows the MQ value versus the rubber content for all mixtures prepared with a different binder content. The figure indicates a consistent finding with the Marshall Stability and Marshall Flow. It is found that MQ increases with the increase in rubber content up to 12% CR; a further increase in rubber content (20% CR) seems to decrease the MQ value. Although adding TOR to 4% CR decreases the MQ value, adding TOR to a higher rubber content (8% and 12% CR) increases the value. Therefore, it can be concluded that crumb rubber and TOR provide better resistance to permanent deformation due to their high MQ and indicate that it can be used in pavements where a stiff bituminous mixture is required to reduce rutting potential.

It is found that CRMM-TOR prepared with 12% CR (C12RT) shows the highest MQ, therefore, it can be concluded that the C12RT has higher stiffness and better resistance against serious deformation as a result of heavy loading.

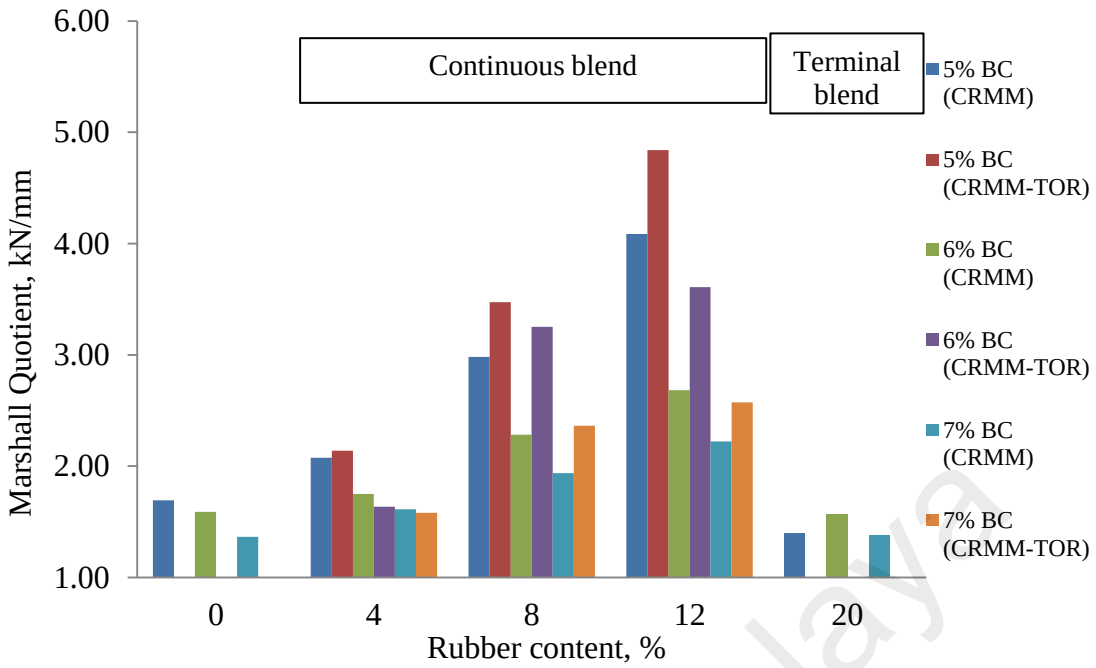

Figure 4.18 Marshall Quotient Value versus Rubber Content

4.9 Performance Test Results

In this study, two performance tests – Indirect tensile stiffness modulus test and dynamic creep test – were performed.

4.9.1 Indirect Tensile Stiffness Modulus (ITSM) Results

The stiffness-modulus test of bituminous mixtures measured in indirect-tensile mode is the most popular form of the stress-strain measurement methods (Kök et al., 2012). It is used to evaluate the elastic properties of the mixtures.

The relationship between the binder content and stiffness modulus of mixtures is presented in Figures 4.19(a) – 4.19(b). It is clearly shown that as the binder content increases, the stiffness modulus of the specimens increase up to a maximum, then decrease as the binder content continues to increase, as shown in Figure 4.19 (a). This is in conformity with the findings of this study (Xiao et al., 2009). According to Hamzah and Teoh (2008), a high binder content causes excessive binder content to replace the

aggregate portion and bulk the mixture. It also causes greater recoverable strain within mixes and reduces the stiffness modulus.

Figure 4.19(b) shows the relationship between the stiffness modulus and the rubber content. It is clearly shown by the mixtures prepared with the continuous blend binder that, as the rubber content increases, the stiffness modulus of the mixtures increases. This observation is explained by the rubber particles, which are great in elastic recovery; this reflects in the stiffness modulus value. This impact is proportional to the amount of rubber incorporated. Moreover, the finding also indicates that the mix behaves in a stiffer manner. In general, the higher the stiffness, the mixture becomes stronger and the better its resistance to rutting.

However, a further increase in rubber content from 12% to 20% CR shows a decrease in the stiffness modulus. It is important to note that mixtures prepared with 20% CR were produced using terminal blend binder. Thus, the decrease in the stiffness modulus value might be due to the behaviour of the terminal blend binder, which lost its elastic properties.

Figure 4.19(b) shows that incorporating TOR in CRMB increases the stiffness modulus value of the mixtures. It is evident that the stiffness modulus of CRMM-TOR is higher compared to the CRMM at any percentage of rubber content. The obtained results indicate that adding TOR to 12%CR results in the highest increment when compared to the stiffness modulus of other percentages of rubber content (4% and 12%CR). The obtained results indicate that the stiffness modulus of CRMM-TOR prepared with 4%, 8% and 12% CR are higher between 2.33% and 3.0%, 1.30% and 1.92%, and 2.36% and 12.18%, respectively, when compared to the stiffness modulus of CRMM. This indicates that incorporating TOR with higher rubber content appears to provide higher stiffness to the bituminous mixture.

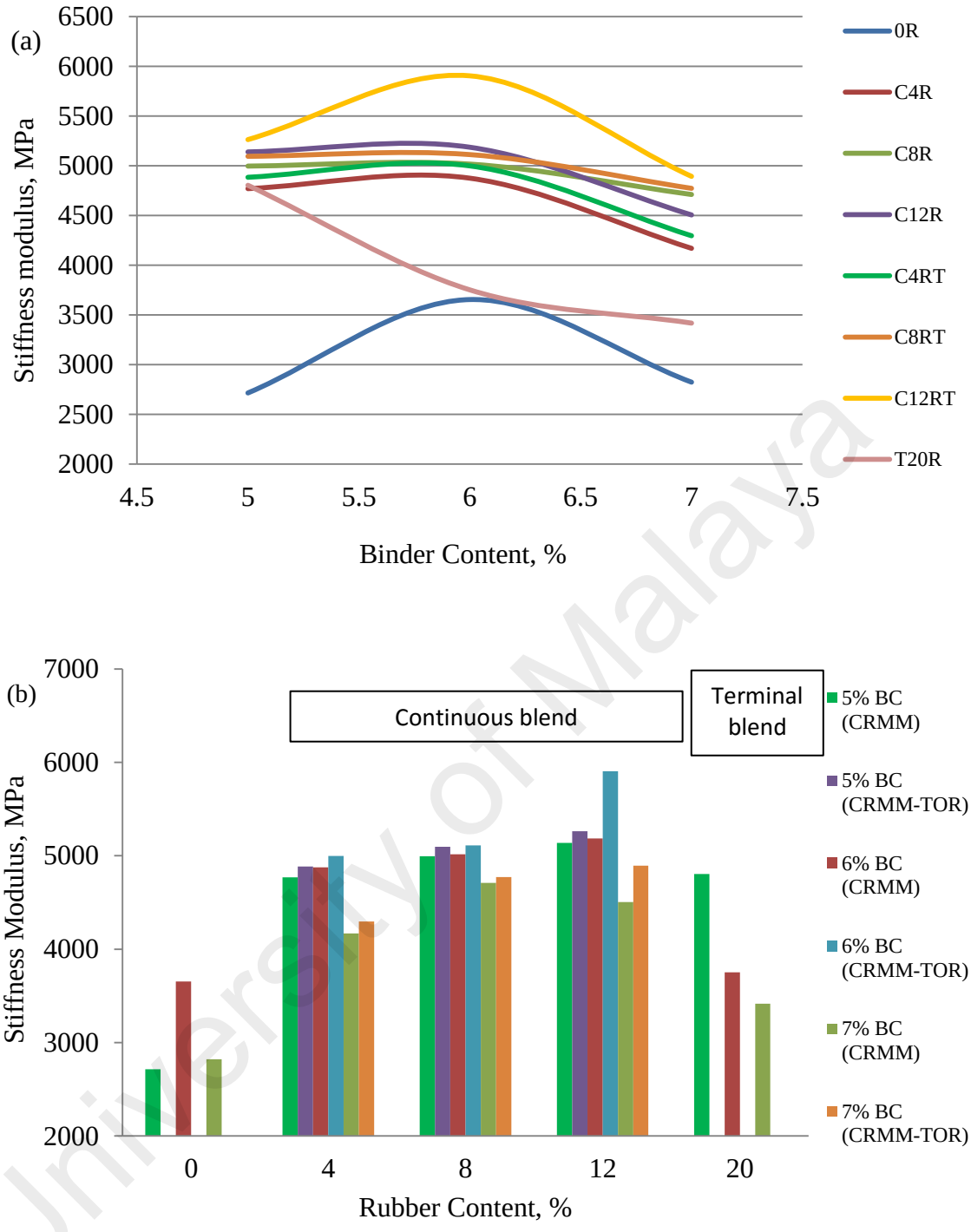

Figure 4.19 Stiffness Modulus Value versus: (a) Binder Content, (b) Rubber Content

4.9.1.1 Multiple Linear Regression on ITSM Value

Tables 4.19 – 4.20 show the summary of multiple linear regression results for the ITSM values. Appendix A, Tables A.9a – A.9d show the results of the analysis.

From all factors (rubber content, TOR, binder blending method and binder content), the stepwise multiple linear regression analysis shows that three factors (TOR, binder content and blending type) contribute significantly to the stiffness modulus value (see Table 4.19). The model indicates that these three factors contribute 36.3% of stiffness modulus value, R^2= .363, R^2_{adj}=.356, F(3,256)=50.558, p<.05.

Based on β value in Table 4.20, the regression model can be written as in Equation 4.11:

Stiffness modulus value = .454(tranpolyoctenamer) -.290(Binder content) +.275 (Blending type) (4.11)

Table 4.19 Model Summary: Indirect Tensile Stiffness Modulus

Step	R	R^2	R^2_{adj}	ΔR^2	F_{chg}	p	df_1	df_2
Transpolyoctenamer (%)	.452a	.204	.201	.204	68.867	.000	1	268
Binder content (%)	.536b	.287	.282	.083	31.047	.000	1	267
Blending type	.603c	.363	.356	.076	31.674	.000	1	266

Table 4.20 Coefficients for Final Model: Indirect Tensile Stiffness Modulus

Step	B	β	t	Bivariate r	Partial r
Transpolyoctenamer (%)	158.851	.454	9.287	.452	.495
Binder content (%)	-270.279	-.290	-5.935	-.287	-.342
Blending type	428.900	.275	5.628	.270	.326

4.9.2 Dynamic Creep Test at 200 kPa, 40°C

The dynamic creep test was performed using the universal testing machine (UTM) at 40°C. A 200 kPa stress was applied for 0.5 s followed by a rest period of 1.5 s for a total of 1800 cycles. The dynamic creep results were analysed based on the creep curve

and ultimate strain. To further analyse the results, Zhou's three-stage model was applied.

4.9.2.1 Dynamic Creep Curve at 200 kPa, 40°C

The creep curves of all specimens were plotted as the accumulated permanent strains versus the loading cycles. All the creep curves were plotted using the average results of the three replicates. This means that the accumulated permanent strains of the three replicate specimens were averaged for each single loading cycle, and then the averaged data points were used to plot the creep curves.

Figure 4.20 shows the dynamic creep curve for all mixtures at test temperature 40°C with 200 kPa stress level. As expected, the cumulative permanent strain increases with an increase in the load cycle. In general, applying 200 kPa for 1800 cycles at the test temperature of 40°C makes the mixtures enter the secondary stage of the creep curve.

The obtained results also indicate that the cumulative permanent strain for the control mixture is higher compared to that of the rubberized mixtures. For instance, the highest creep curve is shown by 0R6B, while the rubberized mixtures are between the control and CRMM-TOR, as shown in Figure 4.20. Moreover, 0R7B is the only mixture that enters the tertiary stage of the creep curve. As a higher accumulated strain indicates lower rutting resistance, it can be concluded from the creep curve that rubberized mixtures show better rutting resistance compared to the control mixture.

The creep curves for the control and CRMM mixtures increase up to 60,000 μs and 45,000 μs, respectively. Nevertheless, this value is much lower for the CRMM-TOR, which is about 30,000 μs. This impact is proportional to 1.5 times and 2 times lower compared to the control and CRMM, respectively. These observations suggest that the addition of TOR improves the behaviour of the specimens by increasing the life of the

samples under repeated creep testing (increased rutting resistance). This is an important step in the generation of high performance bituminous paving products.

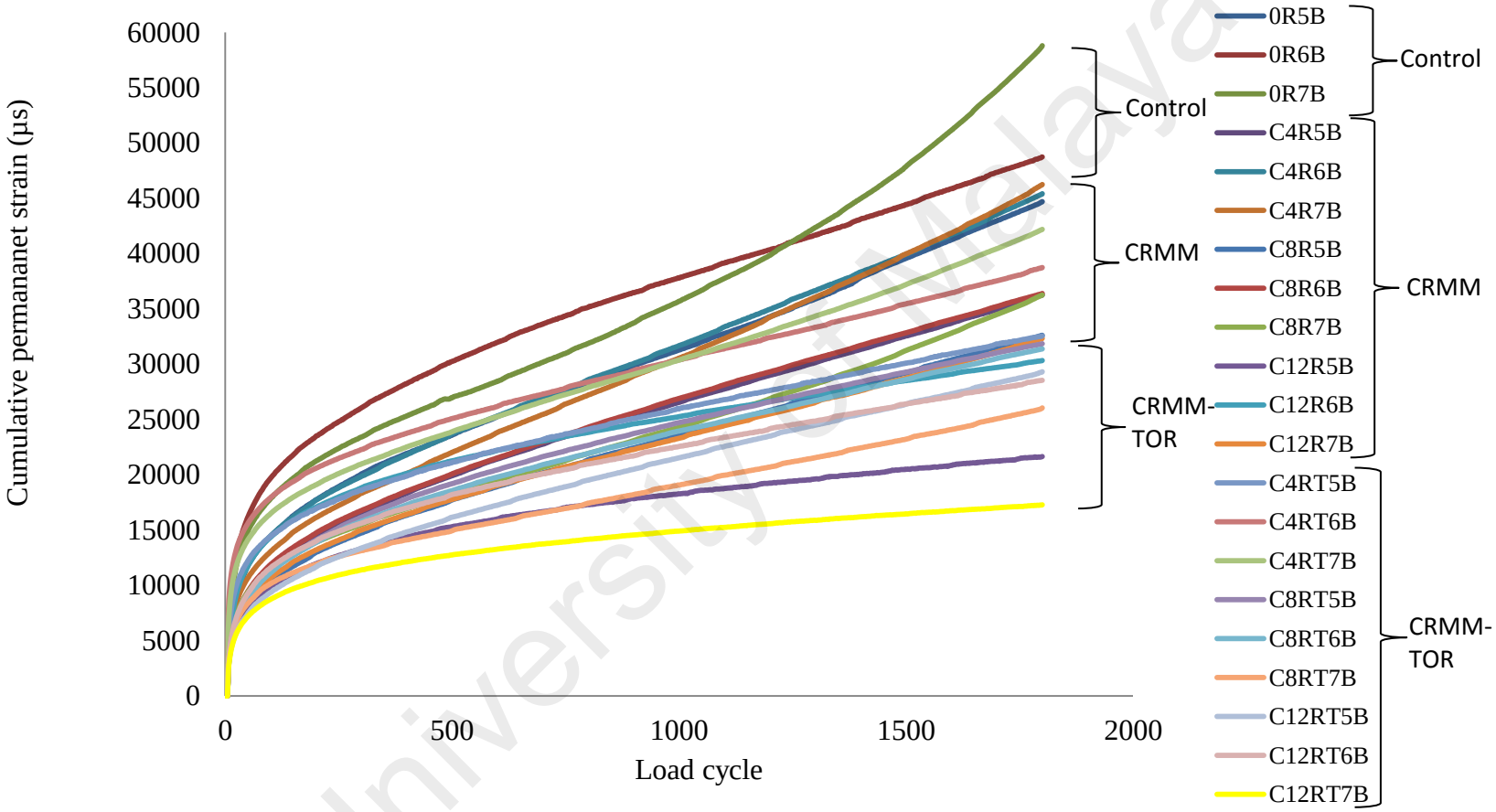

Figure 4.20 Cumulative Permanent Strains versus Load Cycle for Mixtures

4.9.2.2 Ultimate Strain at 200 kPa, 40°C

The results of the ultimate strain after 1800 load cycles are illustrated in Figures 4.21 – 4.22. Table 4.21 shows comparisons of the ultimate strain between CRMM and CRMM-TOR. Figure 4.21 indicates that the ultimate strain decreases with an increase in rubber content. This result is expected.

In all cases, incorporating TOR seems to decrease the ultimate strain as the rubber content increases (Figure 4.21). This pattern is similar to ultimate strain, as shown by the effects of crumb rubber. However, the obtained results indicate that incorporating TOR is able to further decrease the ultimate strain of the mixtures. Moreover, the effect of TOR in decreasing the ultimate strain is influenced by the binder content, as shown in Figure 4.22 and Table 4.21. For instance, at high binder content (7%), adding TOR decreases the ultimate strain by 1.10, 1.39 and 1.87 times, as TOR is added to 4%, 8% and 12% rubber content, respectively. The above figure indicates that the rate of reduction increases with an increase in the rubber content. This is similar for mixtures prepared with 6% binder content, i.e. the ultimate strain reduces with the addition of TOR. However, at 6% binder content, the rate of reduction decreases with an increase of rubber content, i.e. 1.17, 1.16 and 1.06 times, as TOR is added to 4%, 8% and 12% rubber content. Although at a low binder content (5%), adding TOR to 4% and 8% rubber content decreases the ultimate strain, a further increase to 12% rubber content seems to increase the ultimate strain value by about 0.74 times. From the above explanation, it is concluded that the binder content is very important in the preparation of all mixtures, especially CRMM-TOR, as the results proved that insufficient binder content increases the ultimate strain of CRMM-TOR compared with CRMM (ultimate strain C12RT5B > C12R5B), and, thus, decreases the rutting resistance.

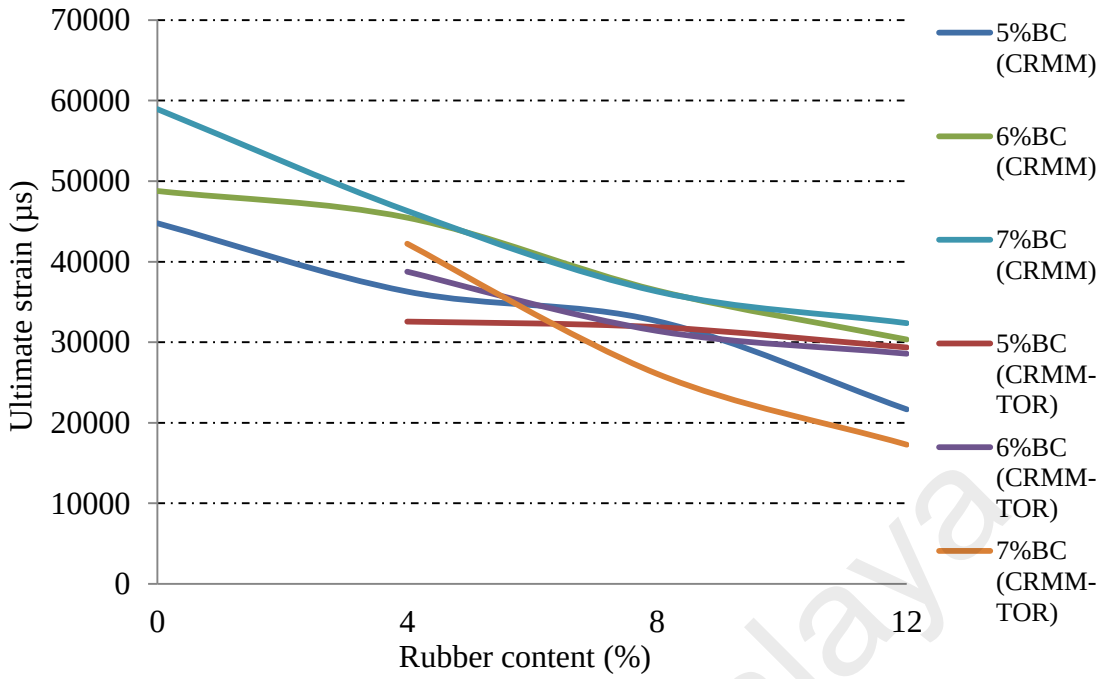

Figure 4.21: Ultimate Strain versus Rubber Content

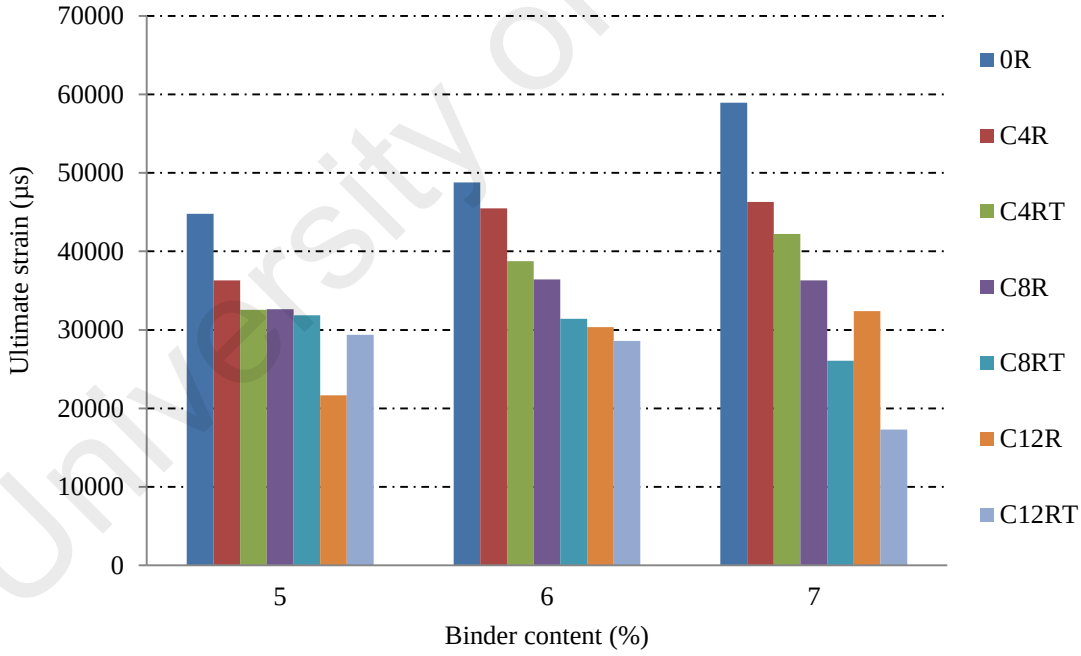

Figure 4.22: Ultimate Strain versus Binder Content

Table 4.21 Difference in Ultimate Strain between CRMM and CRMM-TOR

CRMM	Ultimate strain of CRMM, µs	CRMM-TOR	Ultimate strain of CRMM-TOR, µs	Improve or decline on ultimate strain (Ultimate strain of CRMM / Ultimate strain of CRMM-TOR), times
C4R5B	36291.39	C4RT5B	32566.04	+1.11
C8R5B	32628.21	C8RT5B	31876.26	+1.02
C12R5B	21666.67	C12RT5B	29355.47	-0.74
C4R6B	45471.7	C4RT6B	38762.89	+1.17
C8R6B	36427.53	C8RT6B	31411.66	+1.16
C12R6B	30338.73	C12RT6B	28577.08	+1.06
C4R7B	46309.28	C4RT7B	42234.46	+1.10
C8R7B	36309.34	C8RT7B	26086.96	+1.39
C12R7B	32370.94	C12RT7B	17281.71	+1.87

+ Improve
- Decline

4.9.2.3 Zhou's Three-Stage Model at 200 kPa, 40°C : End Point at First Stage at 200 kPa, 40°C

In this study, a mathematical model, termed Zhou's three-stage model, was used to further analyse the permanent deformation of bituminous mixtures. Zhou's model proposes a different mathematical model for the primary, secondary and tertiary stages with a simple algorithm for estimating the end point of each stage. Moreover, other permanent deformation parameters, such as the end point of the first stage, slope of the secondary stage, and Flow Number (FN) can also be determined. Regression analysis was utilized for modelling each stage in order to find the parameters as well as the end points between each stage. The mathematical models, the end points and other parameters for each stage are presented in Table 4.22.

Furthermore, the mathematical model can be used to calculate the strain value. As shown in Table 4.22, the strain values calculated from the model are similar to the measured strain values obtained from the experiment.

The end point for the first stage calculated in accordance with Zhou's model is displayed in Figure 4.23. As seen from the figure, a different pattern is observed for all binder contents. For this reason, the end point for the first stage is not suitable to explain the effects of the rubber content and TOR in respect of the rutting resistance of rubberized mixtures. Moreover, these findings suggest that the rubber content and TOR do not have a significant effect on the end point for the first stage.

The end point for the first stage indicates the initial axial strain of the mixtures, which is equivalent to permanent deformation in the densification stage. On the condition that all the mixtures display different patterns for the end point for the first stage with respect to rubber content, it is difficult to conclude the effects of the crumb rubber and TOR on the densification behaviour of CRMM and CRMM-TOR (see Figure 4.23).

The effect of the binder content on the end point for the first stage can be seen in Figure 4.24. Generally, all the mixtures showed a similar trend; an increase in the end point for the first stage as the bitumen content increased up to an optimum value. However, the further addition of bitumen resulted in a decrease in the end point for the first stage values.

Table 4.22 Zhou's Three-Stage Models and Boundary Points at 200 kPa Stress and 40°C Temperature.

Sample	Primary stage				Secondary stage				Tertiary stage
	Model	End point	Measured strain,μs	Predicted strain,μs	Model	End point	Measured strain,μs	Predicted strain,μs	Model
0R5B	$\varepsilon_P = 3719.8N^{0.2967}$	N = 489	23358.10	23452.00	ε_P = 23358.10+16.048 (N-489)	a	a	a	a
0R6B	$\varepsilon_p=5300.7N^{0.2814}$	N = 625	32440.97	32520.00	ε_p=32440.97+13.538(N-625)	a	a	a	a
0R7B	$\varepsilon_P = 4408.7N^{0.308}$	N = 151	20674.52	19860.00	ε_P = 20674.52+17.621 (N-151)	N = 747	33837.41	31176.64	ε_p=33837.41 + 1534.4 (e $^{0.0032(N-747)}$ - 1)
C4R5B	$\varepsilon_p=2095.4N^{0.3639}$	N = 705	22788.88	22897.50	ε_p=22788.88+12.054(N-705)	a	a	a	a
C4R6B	$\varepsilon_p=3139.4N^{0.3333}$	N = 189	18016.09	17490.57	ε_p=18016.09+16.688(N-189)	a	a	a	a
C4R7B	$\varepsilon_p=3139.8N^{0.3117}$	N = 555	22505.99	23072.16	ε_p=22505.99+18.423(N-555)	a	a	a	a
C4RT5B	$\varepsilon_p=4600.5N^{0.2467}$	N = 829	24144.18	24415.09	ε_p=24144.18+8.3221(N-829)	a	a	a	a
C4RT6B	$\varepsilon_p=6908.3N^{0.2078}$	N = 701	26959.47	27340.21	ε_p=26959.47+10.187(N-701)	a	a	a	a
C4RT7B	$\varepsilon_p=5799.9N^{0.2268}$	N = 427	22908.76	22944.94	ε_p=22908.76+13.638(N-427)	a	a	a	a
C8R5B	$\varepsilon_p=2386.4N^{0.3218}$	N = 575	18441.84	18675.21	ε_p=18441.84+11.348(N-575)	a	a	a	a
C8R6B	$\varepsilon_p=2597.8N^{0.3295}$	N = 629	21715.06	21979.06	ε_p=21715.06+12.176(N-629)	a	a	a	a
C8R7B	$\varepsilon_p=2897.5N^{0.2967}$	N = 575	19090.48	19182.89	ε_p=19090.48+13.703(N-575)	a	a	a	a
C8RT5B	$\varepsilon_p=2432.6N^{0.3334}$	N = 805	22639.30	22772.42	ε_p=22639.30+9.1082(N-805)	a	a	a	a
C8RT6B	$\varepsilon_p=2444.6N^{0.3279}$	N = 759	21509.93	21547.61	ε_p=21509.93+9.449(N-759)	a	a	a	a
C8RT7B	$\varepsilon_p=2796.5N^{0.2778}$	N = 263	13148.57	12795.03	ε_p=13148.57+8.4058(N-263)	a	a	a	a
C12R5B	$\varepsilon_p=2477.7N^{0.2957}$	N = 607	16483.05	16176.47	ε_p=16483.05+4.6235(N-607)	a	a	a	a
C12R6B	$\varepsilon_p=3869.2N^{0.2789}$	N = 499	21883.73	21284.71	ε_p=21883.74+6.784(N-499)	a	a	a	a
C12R7B	$\varepsilon_p=2476N^{0.3175}$	N = 577	18639.06	18795.41	ε_p=18639.06+10.927(N-577)	a	a	a	a
C12RT5B	$\varepsilon_p=2059.8N^{0.3303}$	N = 567	16723.75	16953.13	ε_p=16723.75+9.8936(N-567)	a	a	a	a
C12RT6B	$\varepsilon_p=2878N^{0.2977}$	N = 911	21884.64	21897.23	ε_p=21884.64+7.4625(N-911)	a	a	a	a
C12RT7B	$\varepsilon_p=2591.3N^{0.2588}$	N = 679	14008.95	13672.20	ε_p=14008.95+3.1683(N-679)	a	a	a	a

[a] Not found at the end of 1800 cycles

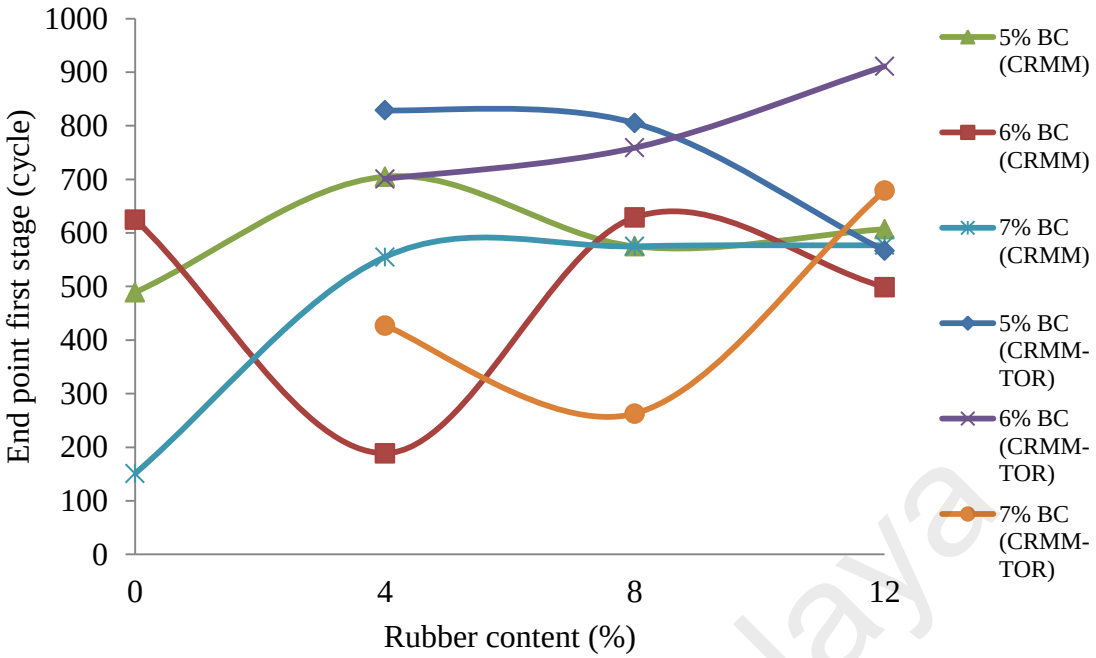

Figure 4.23: End Point of First Stage for Mixtures

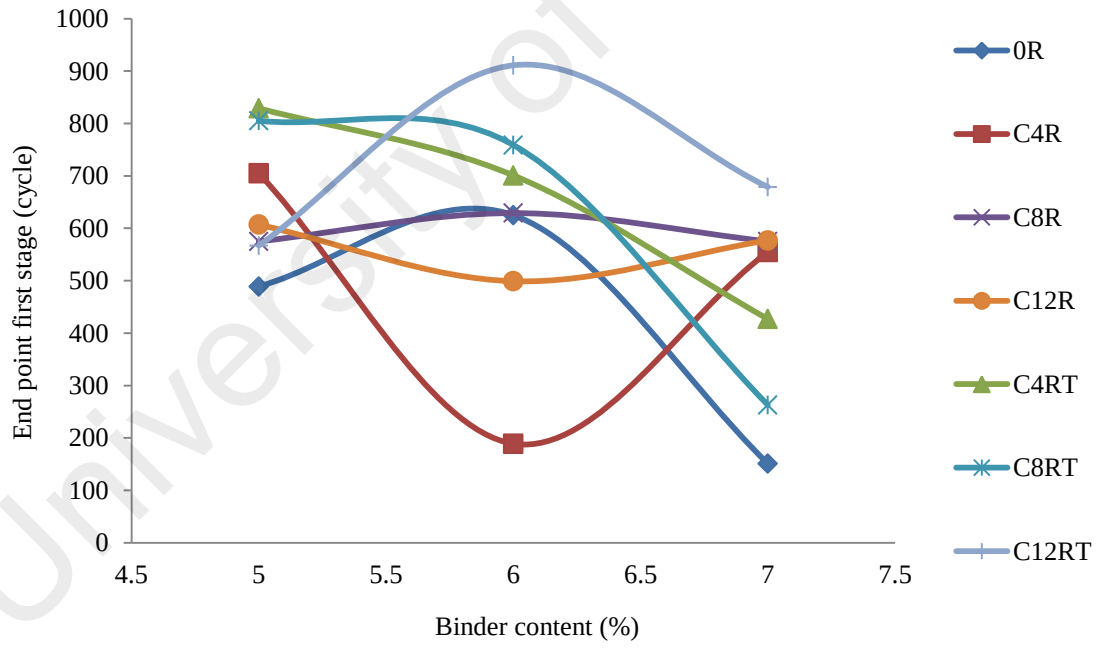

Figure 4.24: End Point of First Stage versus Binder Content

4.9.2.4 Zhou's Three-Stage Model at 200 kPa, 40°C : Slope of Secondary Stage at 200 kPa, 40°C

The slope of the secondary stage is calculated from the regression line of the typical repeated load creep curve that excludes the primary stage and tertiary stage. Therefore, it perfectly reflects the rate of deformation affected by the load cycling. For constant stress loading conditions, the creep strain rate is approximately constant during the secondary creep phase. Hence, the slope of the secondary stage is another permanent deformation characteristic that shows the developing rate of deformation (He and Wong, 2007; He and Wong, 2008).

The slope of the secondary stage for all mixtures is given in Figures 4.25 – 4.26. Figure 4.25 shows the effects of the rubber content and TOR with the slope of the secondary stage value, while Figure 4.26 presents the relationship between the slope of the secondary stage and the binder contents.

Figure 4.25 shows that the slope of the secondary stage for rubberized mixtures reduces as the rubber content increases. Moreover, adding TOR affects the slope of the secondary stage showing a decrease of 24%-245% versus the rubberized mixtures without TOR (CRMM), as clearly shown by the rubber content of 4% and 8%. However, a significant decrease is shown by mixtures prepared with 12% rubber and 7% binder content, i.e. C12R7B showed 10.93 micro strain/cycle of slope and C12RT7B attained 3.16 micro strain/cycle of slope (decrease 245%). This is a very significant improvement.

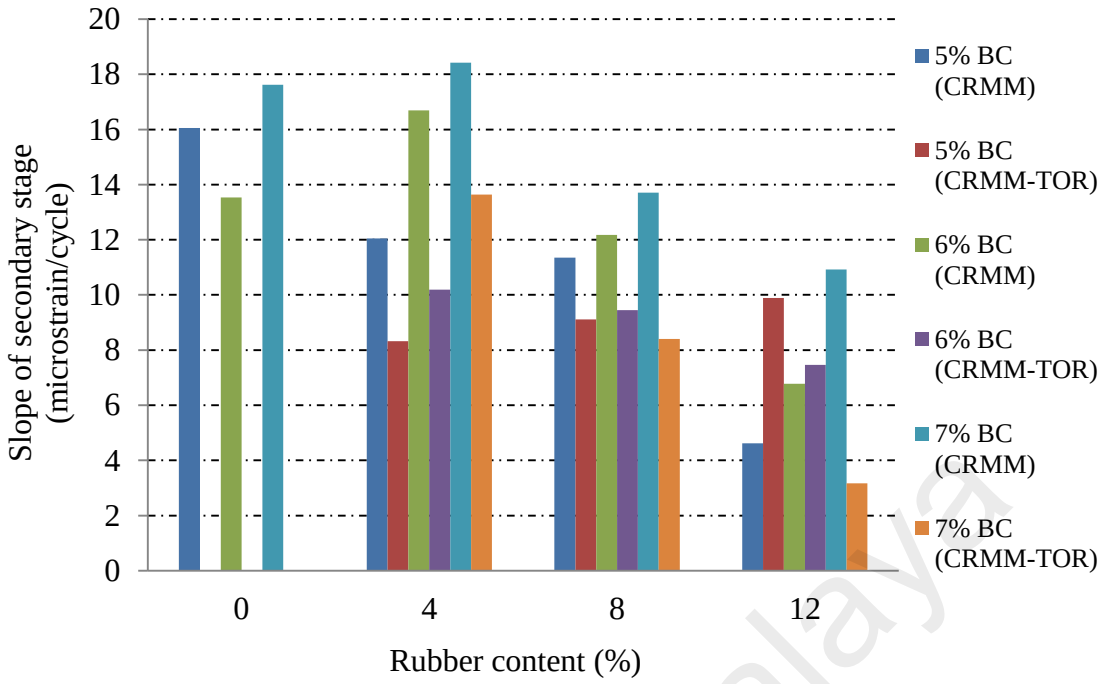

Figure 4.25: Slope of Secondary Stage versus Rubber Content

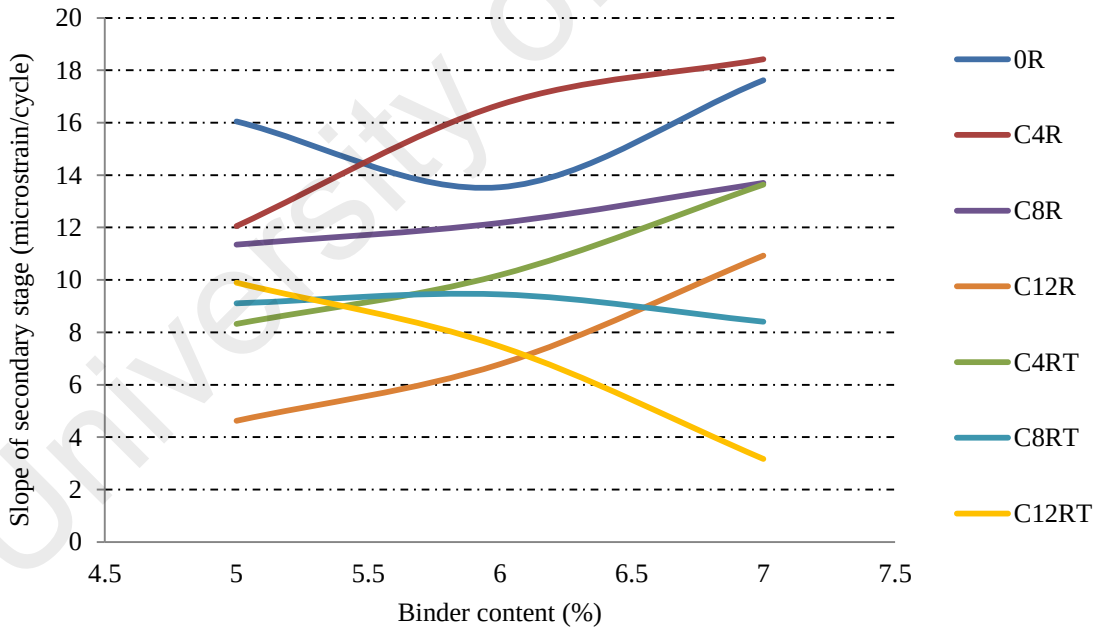

Figure 4.26: Slope of Secondary Stage versus Binder Content

4.9.2.5 Multiple Linear Regression on Ultimate Strain at 200 kPa, 40°C

Statistical analysis was performed using SPSS software to analyse the relationships between permanent deformation of the mixtures and the factors. Multiple linear regression using the stepwise method was employed to determine the significant level as well the regression model.

To determine permanent deformation of the mixtures, the ultimate strain and slope of the secondary stage were selected as the dependent variables, while the factors (rubber content, binder content and TOR) were selected as independent variables. The confidence interval of 95% ($\alpha = 0.05$) was used in the analysis.

The summary of Multiple Linear Regression on ultimate strain at 200 kPa, 40°C is tabulated in Tables 4.23 – 4.24. Complete analysis can be referred to in Appendix A, Tables A.10a – A.10d. The factors explain 81.2% of the variance in ultimate strain. The analysis indicates that all factors (rubber content, binder content and TOR) have a significant effect on the slope of the secondary stage when the *P* value is less than 0.05. The highest beta value was achieved by rubber content (beta = -.792, p =.000 < .05), followed by TOR (beta = -.259, p =.000 < .05) then the binder content (beta = .168, p =.003 < .05).

The regression equation, which can be used to predict the ultimate strain based on the factors, is as follows (Equation 4.12):

$$\textit{Ultimate strain at 200 kPa and 40°C} = -.792\,(\textit{Rubber content}) - .259\,(\textit{TOR}) + .168\,(\textit{Binder content}) \quad (4.12)$$

Table 4.23 Model Summary: Ultimate Strain at 200 kPa, 40°C

Step	R	R^2	R^2_{adj}	ΔR^2	F_{chg}	p	df_1	df_2
Rubber content (%)	.850a	.722	.718	.722	166.594	.000	1	64
Transpolyoctenamer (%)	.886b	.784	.777	.062	18.026	.000	1	63
Binder content (%)	.901c	.812	.803	.028	9.308	.003	1	62

Table 4.24 Coefficients for Final Model: Ultimate Strain at 200 kPa, 40°C

Step	B	β	t	*Bivariate r*	*Partial r*
Rubber content (%)	-1827.634	-.792	-13.986	-.850	-.871
Transpolyoctenamer (%)	-1101.452	-.259	-4.566	-.444	-.502
Binder content (%)	1978.809	.168	3.051	.144	.361

4.9.2.6 Multiple Linear Regression on the Slope of the Secondary Stage at 200 kPa, 40°C

The result of the multiple linear regression is tabulated in Tables 4.25 – 4.26. The factors can explain 68.7% of the variance in ultimate strain, R^2=.687, R^2_{adj}=.672, $F(3,62)=45.423$, $p<.05$. Analysis of the results indicates that all the factors (rubber content, TOR, and binder content) have a significant effect on the slope of the secondary stage when the *P* value is less than 0.05. The highest beta value was achieved by the rubber content (beta = -.671, p =.000 < .05), followed by TOR (beta = -.317, p =.000 < .05) then the binder content (beta = .211, p =.004 < .05).

The regression equation, which can be used to predict the ultimate strain based on factors is as follows (Equation 4.13):

Slope of secondary stage at 200 kPa and 40°C = -.671 (Rubber content) - .317 (TOR) + .211 (Binder content) (4.13)

Table 4.25 Model Summary: Slope of Secondary Stage at 200 kPa, 40°C

Step	R	R^2	R^2_{adj}	ΔR^2	F_{chg}	p	df_1	df_2
Rubber content (%)	.742a	.550	.543	.550	78.278	.000	1	64
Transpolyoctenamer (%)	.802b	.643	.631	.093	16.330	.000	1	63
Binder content (%)	.829c	.687	.672	.045	8.827	.004	1	62

Table 4.26 Coefficients for Final Model: Slope of Secondary Stage at 200 kPa, 40°C

Step	B	β	t	*Bivariate r*	*Partial r*
Rubber content (%)	-.644	-.671	-9.178	-.742	-.759
Transpolyoctenamer (%)	-.562	-.317	-4.333	-.472	-.482
Binder content (%)	1.035	.211	2.971	.189	.353

4.9.2.7 Comparison of Creep Parameter and MSCR

In order to study the effects of the binder on the rutting resistance of the mixtures, it is worth correlating the rutting susceptibility of the binder with the rutting potential of the mixtures. With this intention, the non-recoverable compliance (J_{nr}) of the binder (CRMB and CRMB-TOR) was correlated with the creep parameter of the mixtures (CRMM and CRMM-TOR); namely, ultimate strain. J_{nr} was determined from the multiple stress creep and recovery (MSCR) test of the binders while the ultimate strain was obtained from the dynamic creep test of the mixtures.

Figure 4.27 shows a plot of the ultimate strain versus non-recoverable compliance (J_{nr}). The ultimate strain of the mixtures and J_{nr} of the binders was tested at stress levels of 200 kPa and 100 Pa, respectively. Both binders and mixtures were tested at 40°C.

A comparison between the rutting performance evaluated with the dynamic creep test and the J_{nr} obtained from the MSCR test shows a very strong correlation (R^2 = 0.9593). This indicates that the MSCR test, particularly when conducted at a single test temperature, was capable of characterising and ranking the high temperature

performance of all the bitumen types (80/100 penetration bitumen, CRMB and CRMB-TOR) used in this study. Moreover, the MSCR test results are highly correlated with the ultimate strain values obtained using the dynamic creep test, thus the MSCR test can be used to predict the rutting performance of the mixtures. Furthermore, a strong correlation would be expected between the mix performance in the field and the binder performance tested using the MSCR test. The previous research conducted by D'Angelo et al. (2007) showed that a comparison between the rutting performance of the mix in the field and the J_{nr} had a strong correlation with a R^2 value over 0.8.

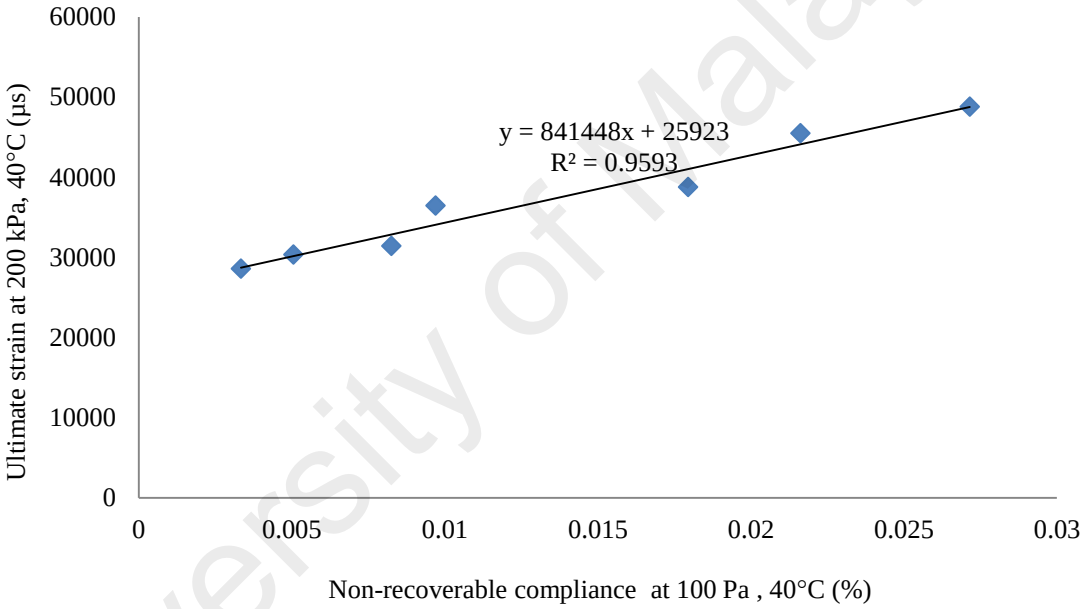

Figure 4.27 Ultimate Strain at 200 kPa, 40°C versus Non-Recoverable Compliance (J_{nr})

4.9.3 Results of Dynamic Creep Test at Different Test Conditions

This section discusses the effects of different temperatures (40°C, 50°C and 60°C) and stress levels (200 kPa and 400 kPa) on the control mixture, CRMM and CRMM-TOR. In order to analyse the effects of the blending type, T20R (prepared with terminal blend binder) and C12R (prepared with continuous blend binder) were selected. Moreover,

C12RT was selected to represent mixtures reinforced with TOR and the test results, which were then compared with C12R, were used to evaluate the effects of TOR. The selection of the combination of the above mixtures was based on the MSCR test and dynamic creep test (at 200kPa, 40°C), as both tests results show that C12R, C12RT and T20R might offer better rutting resistance.

Furthermore, the control mixture (0R) was chosen so that the performance of all selected mixtures (T20R, C12R, C12RT) could be compared with the control. All the mixtures were prepared at optimum binder content (OBC), as shown in Table 4.27. The OBC was determined in accordance with the Standard Specification for Road Works, Section 4: Flexible Pavement published by the Malaysian Public Works Department (JKR/SPJ/2008-S4), which also complies with the Marshall mix design procedure (ASTM D6927-15). According to the specification, four graphs, namely, stability, flow, voids in mix (VIM) and voids in mineral aggregate (VMA), were plotted versus the percentage of binder for each bituminous mixture. OBCs were calculated based on the SMA Mix requirements (JKR/SPJ/2008-S4): stability (min. 6200N), flow (2-4 mm), VIM (3-5%) and VMA (min. 17%). The properties of the mixtures are shown in Table 4.27.

Table 4.27 Properties of the Mixtures

Mixture ID	Binder blending type	Sample indication	Rubber content (%)	TOR content (%)	VIM (%)	VMA (%)	Bulk density	OBC (%)
0R	N/A	Control	0	0	5.42	18.55	2.312	5.78
T20R	Terminal blend (TB)	CRMM	20	0	5.75	20.76	2.272	6.86
C12R	Continuous blend (CB)	CRMM	12	0	5.21	19.65	2.297	6.50
C12RT	Continuous blend (CB)	CRMM-TOR	12	4.5	4.57	19.55	2.304	6.75

**N/A* Not applicable (base bitumen 80/100 penetration was used as a binder)

4.9.3.1 Dynamic Creep Curve for Different Test Conditions

After testing, the dynamic creep curves of all the specimens were obtained. These data are depicted in Figures 4.28(a) – 4.28(f). Higher accumulated axial strain values indicate that the mixes have lower rutting resistance potential. It is apparent that specimens prepared with rubberized bitumen show a lower cumulative permanent strain compared to the control specimen. This is because crumb rubber that has partially digested into the bitumen absorbs the aromatic oils from the bitumen into the rubber's polymer chains. This implies the formation of a gel-like material, which results in the higher viscosity and elasticity of the bitumen. Such interactions improve the binder networking and allow a greater film thickness surrounding the aggregate in the mixture. This will reinforce the aggregate bonding of the mixtures thus resulting in higher strength. Furthermore, the crumb rubber that is not digested in the bitumen will maintain its integrity, interweave together, and form a three-directional network when distributed uniformly in the mixture. This spatial reinforcing network could reinforce the mixtures and resist damage propagation.

Moreover, incorporating TOR as a cross-link dispersant agent in the preparation of the rubberized binder indicates a significant enhancement in the behaviour of the mixture, as shown by C12RT for all test conditions (Figures 4.28(a) – 4.28(f)). This implies that the TOR improves the rheological properties of the rubberized binder by activating the crumb rubber and bitumen to form a chemical reaction. The reaction permits crosslinking with the sulphur associated with the asphaltenes and maltenes in the bitumen to create a macropolymer network. Finally, a uniform, low tack, rubber-like composite is produced, which is capable of improving the rutting resistance of the mixtures (Yadollahi and Sabbagh Mollahosseini, 2011).

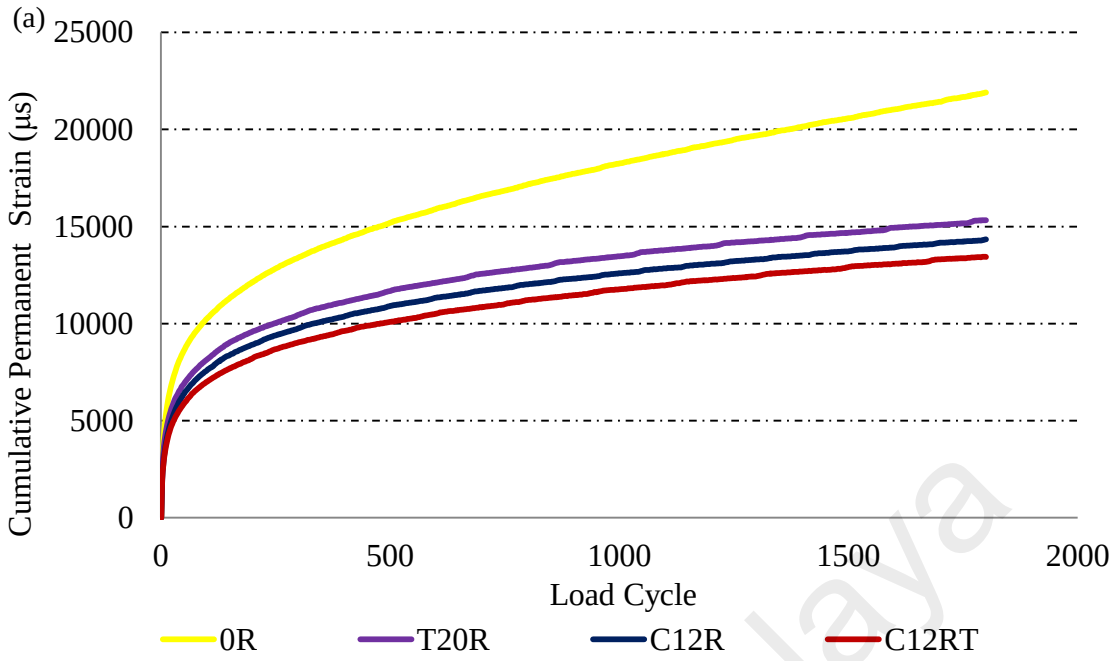

Figure 4.28(a): Cumulative Permanent Strain versus Load Cycle for Mictures at 200 kPa and 40°C

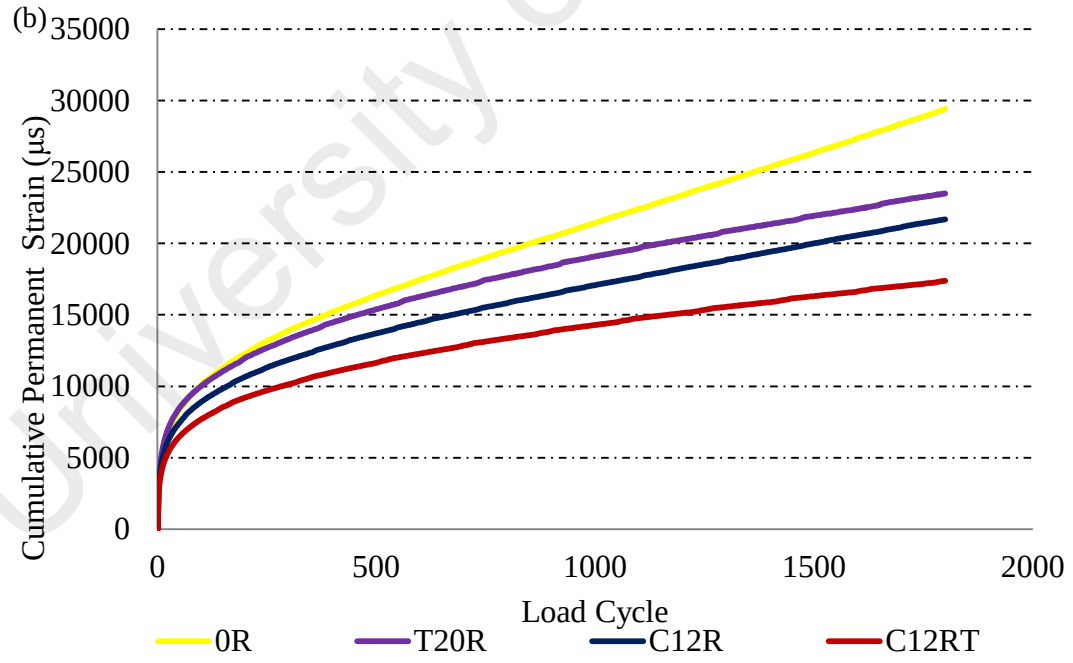

Figure 4.28(b): Cumulative Permanent Strain versus Load Cycle at 200 kPa and 50°C

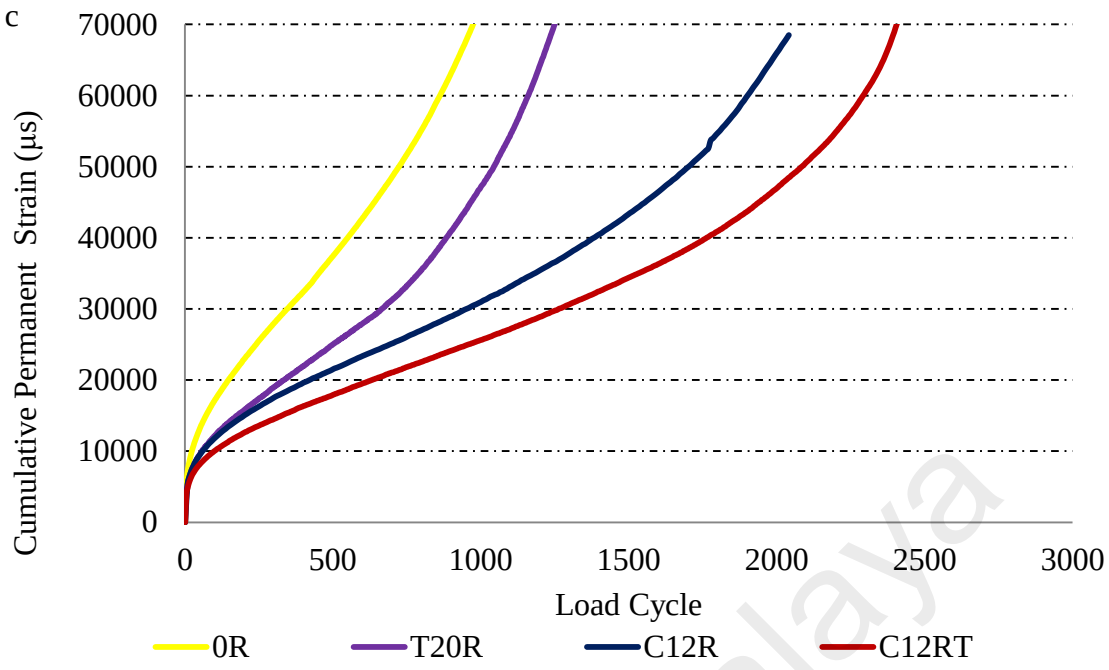

Figure 4.28(c) : Cumulative Permanent Strain versus Load Cycle at 200 kPa and 60°C

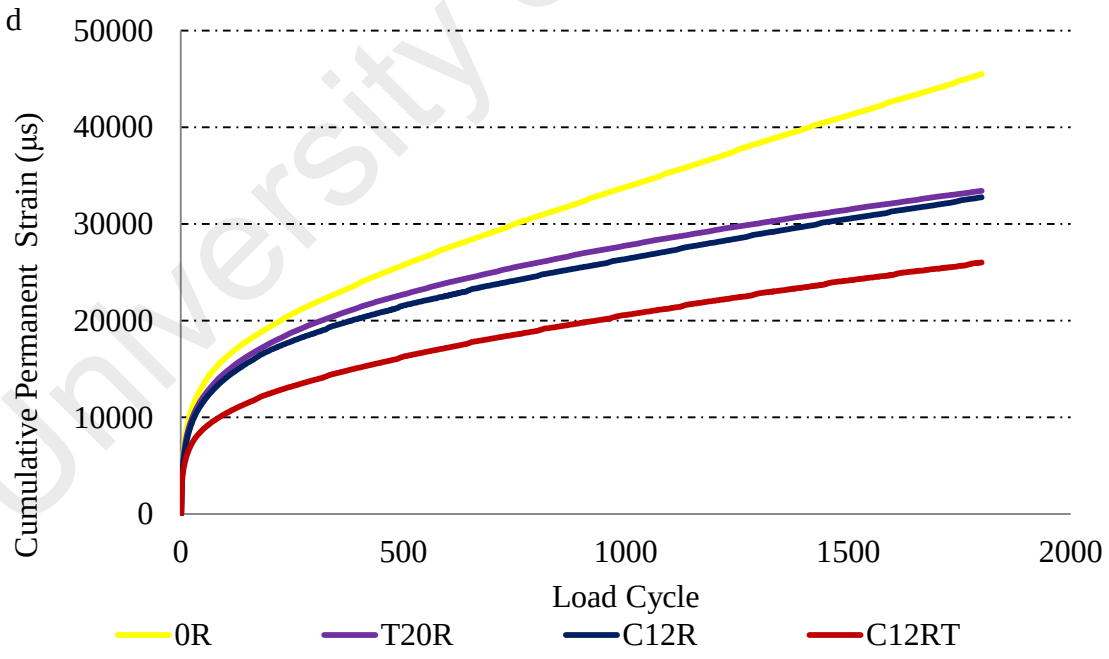

Figure 4.28(d): Cumulative Permanent Strain versus Load Cycle at 400 kPa and 40°C

e

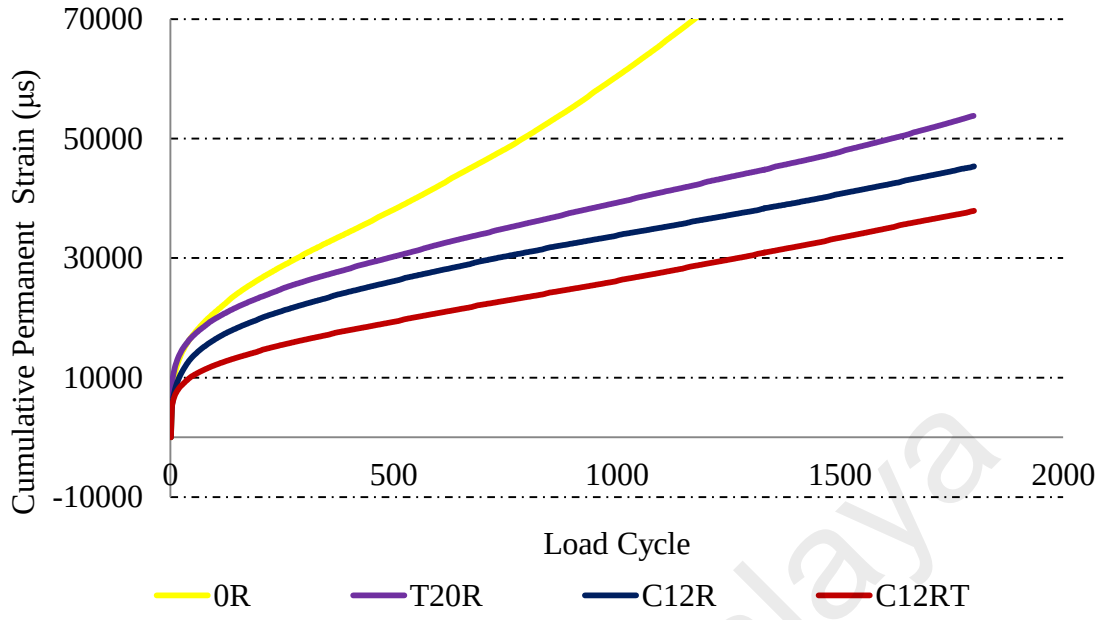

Figure 4.28(e): Cumulative Permanent Strain versus Load Cycle at 400 kPa and 50°C

f

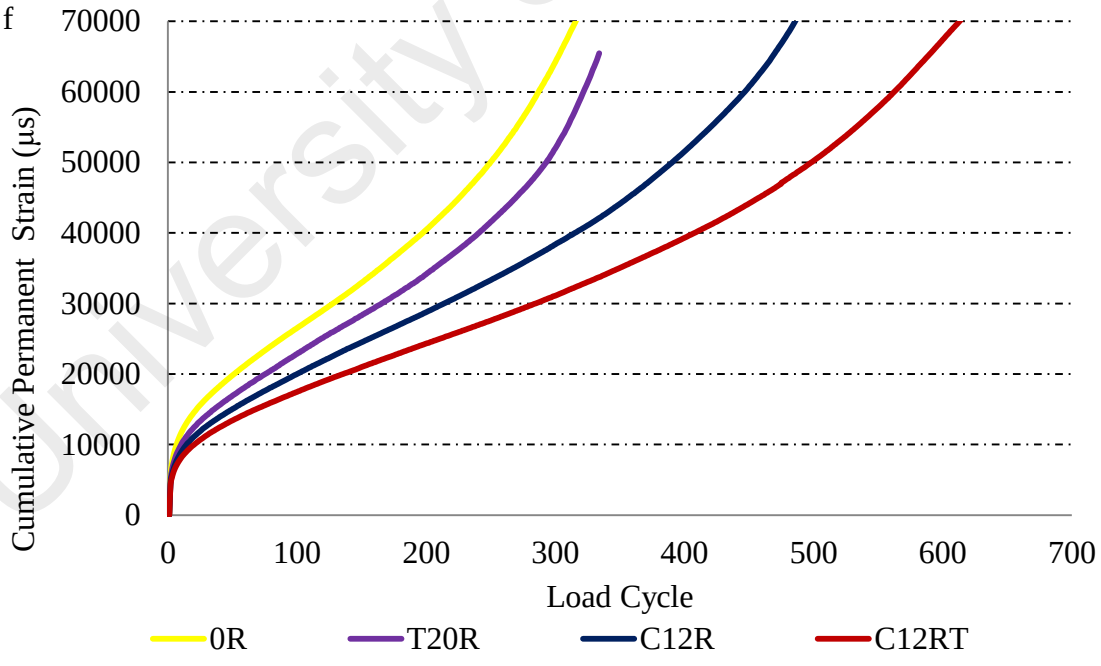

Figure 4.28(f): Cumulative Permanent Strain versus Load Cycle at 400 kPa and 60°C

The obtained results indicate that mixtures prepared with a continuous blend binder (C12RT and C12R) present the best rutting resistance followed by the terminal blend (T20R) and control (0R). The terminal blend mixture was prepared with a high viscous binder; nevertheless, it shows less rutting resistance compared to the continuous blend mixtures. This can be explained by the processing conditions used in the terminal blend binder. The high mixing temperature (210°C) and high shear stress (10,000 rpm) together with the long mixing duration (2 hours) used in the preparation of the terminal blend binder leads to depolymerisation/devulcanisation of the rubber network. Depolymerisation starts releasing rubber components back to the liquid phase causing a decrease in the stiffness, and a further increase in the mixing temperature and mixing duration leads to the failure stage in which the rubberized binder loses its elastic properties (Hicks et al., 2010; Presti, 2013).

4.9.3.2 Effects of Temperature and Stress Level on Dynamic Creep Curve

Figures 4.29(a) – 4.29(b) show the creep curve for all the mixtures tested at stress levels 200 kPa and 400 kPa, respectively. The test temperatures were 40°C, 50°C and 60°C. It can be seen that there are significant differences among these curves. At test temperatures 40°C and 50°C at both stress levels 200kPa and 400kPa, the results show that each dynamic creep curve consists of two parts, namely, primary stage and secondary stage. In this test condition, the tertiary stage of the specimen did not occur except for the control mixture tested at the 400 kPa stress level and 50°C. A further increase in temperature from 50°C to 60°C causes higher cumulative permanent strain. As illustrated in Figure 4.29(a) and Figure 4.29(b), all the mixtures enter the tertiary stage as the temperature increases to 60°C. All the mixtures reach 70,000 μs after applying a number of load cycles in which the LVDTs go out of range. At both stress

levels (200 kPa and 400 kpa), the control mixture (0R) enters the tertiary stage earlier followed by T20R, C12R and C12RT.

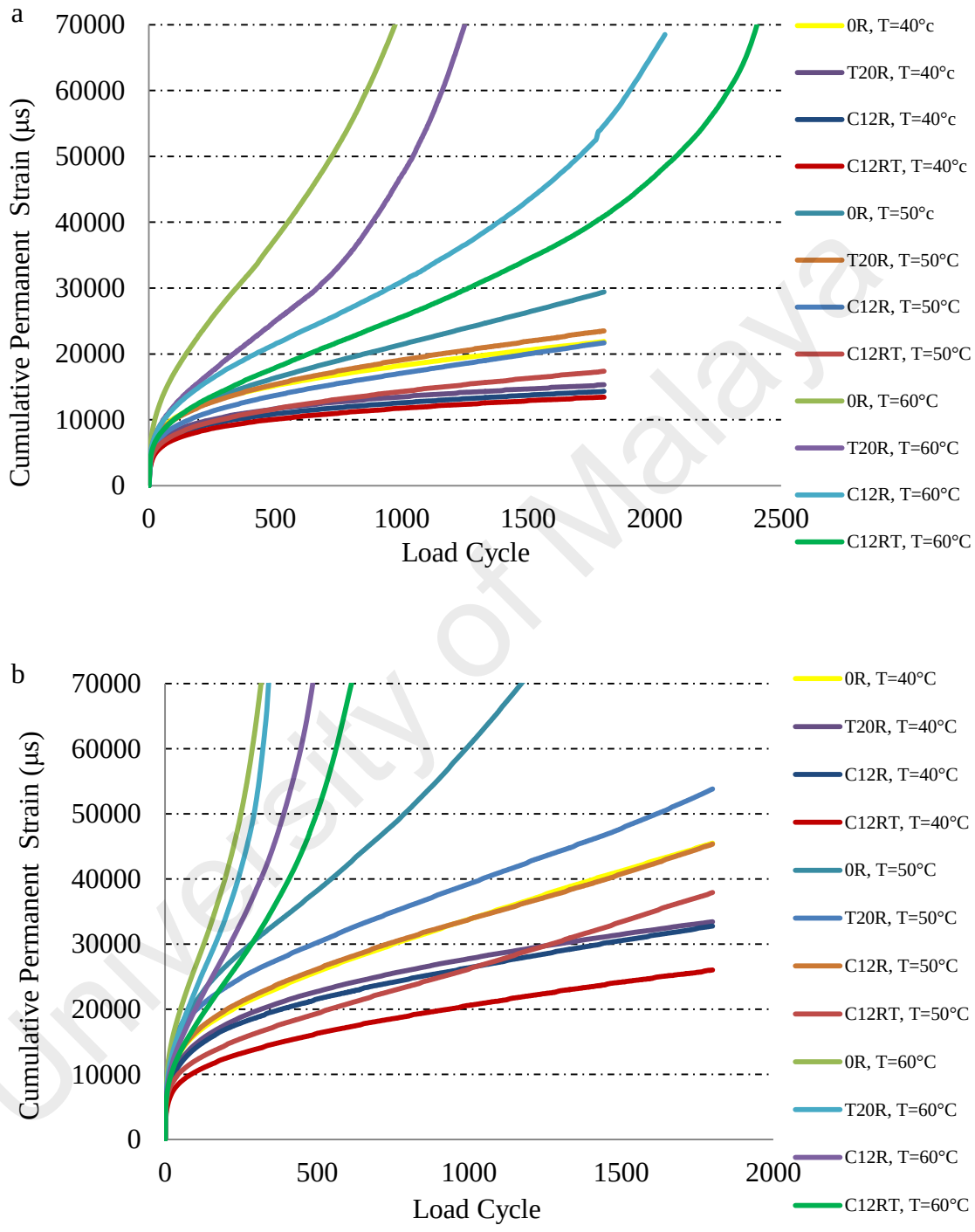

Figure 4.29 Creep Curve at Different Temperatures at (a) 200 kPa (b) 400 kPa

The test results also determine that the strain values increase by an increment in stress level (from 200 kPa to 400 kPa) for all test temperatures. For instance, the increase in

stress level from 200 kPa to 400 kPa at 50°C, results in the control mixture entering the tertiary stage. Moreover, at 60°C, the increase in stress level from 200 kPa to 400 kPa indicates that all the mixtures reach the tertiary stage faster. Furthermore, the number of cycles that the LVDTs go out of range is shorter at 400 kPa compared to the 200 kPa stress level. For instance, at 200 kPa and 60°C temperature, the number of cycles that the LVDTs go out of range is 973, 1249, 2041 and 2401 cycles for 0R, T20R, C12R and C12RT, respectively. A further increase in stress level from 200 kPa to 400 kPa at 60°C temperature shows that the number of cycles that makes the LVDT go out of range reduces by around one-third to one-fourth, i.e. 313, 339, 482 and 613 cycles for 0R, T20R, C12R and C12RT, respectively.

4.9.3.3 Ultimate Strain for Different Test Conditions

The results of the ultimate strain after 1800 load cycles at test temperatures 40°C and 50°C are illustrated in Figure 4.30. The ultimate strain value at 60°C was not plotted because the LVDTs go out of range for all mixtures, and, therefore, the maximum ultimate strain (100,000 μs) was observed.

It is important to note that the ultimate strain increases at higher temperature. For instance, at 200 kPa stress, in the case of the control mixture when the temperature increases from 40°C to 50°C, the strain value increases from 21901.06 μs to 29418.91 μs, which is 1.34 times higher in comparison with 40°C. However, the dependency of the ultimate strain on the temperature in the CRMM is considerably lower than that of the control mixture, especially the specimen with the addition of TOR. For example, at stress levels 200 kPa and 400 kPa, an increase of 10°C (from 40°C to 50°C) causes the ultimate strain for 0R to increase 1.34 and 2.20 times, while C12RT rises at a lower rate compared to the control mixture, that is, 1.29 and 1.46 times, respectively.

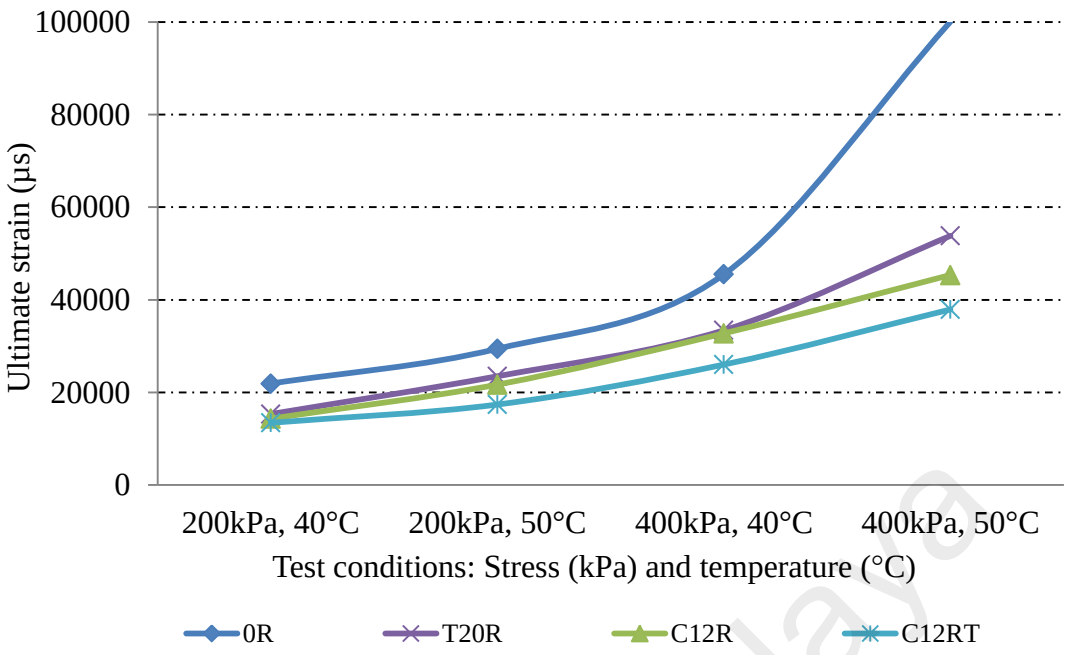

Figure 4.30: Ultimate Strains at Different Stress Levels and Temperature.

A similar trend was observed by increasing the stress level in which the ultimate strain increases by an increment in stress (from 200 kPa to 400 kPa) for both 40°C and 50°C temperatures. In the control mixture, the rate of increment is more than for CRMM and CRMM-TOR. The results show that the ultimate strain increased 3.40, 2.29, 2.09, and 2.18 times for 0R, T20R, C12R and C12RT, respectively, as the stress increased from 200 kPa to 400 kPa at 50°C. This shows that the control mixture deform more than three times while CRMM and CRMM-TOR show a better deformation rate as the stress increases.

It is worth mentioning that CRMM and CRMM-TOR show an insignificant difference in the ultimate strain compared to the control mixture at test conditions 200 kPa, 40°C and 200 kPa, 50°C. However, the difference becomes apparent at test condition 400 kPa, 40°C. A further increase in temperature (from 40°C to 50°C) at 400 kPa stress level shows a drastic increase in the ultimate strain of the control mixture. This indicates that an increase of 10°C from 40°C to 50°C at 400 kPa caused an extreme growth in the

ultimate strain of the control mixture so that these samples faced a total destruction at 100,000 μs. In contrast, in the CRMM and CRMM-TOR mixtures, the ultimate strain is much lower, which is 53815.11 μs, 45359.73 μs and 37915.94μs for T20R, C12R and C12RT, respectively, which is equivalent to 1.89, 2.20 and 2.64 times less compared to 0R. From the above explanations, the dependency of permanent deformation on the temperature and stress level in the CRMM and CRMM-TOR mixtures is considerably lower than that for the control mixture.

Moreover, the T20R, C12R and C12RT show comparable performance at low test conditions (200 kPa, 40°C), as they plotted almost a similar point. However, the difference becomes more apparent as the test condition increases, especially at the highest test condition (400kPa, 50°C). From the above observations, the efficiency of crumb rubber, TOR and blending type were clearly observed at the highest test condition.

4.9.3.4 Zhou's Three-Stage Model at Different Test Conditions: Effects of Temperature and Stress Levels

In this study, Zhou's three-stage model was used for a better understanding of the permanent deformation behaviour of the mixtures. Regression analysis, as explained by Zhou et al. (2004), was utilized to determine the mathematical functions as well as transition points between each stage and use it for modelling each stage. The results are presented in Tables 4.28 – 4.29. The achieved results show that all mixtures obey the Zhou model as they reached the primary stage and secondary stage. Moreover, some mixtures attained the tertiary stage when tested at high test conditions (200 kpa, 60°C and 400 kpa, 60°C). Zhou's Three-Stage Model at Different Test Conditions: Flow Number (FN) at Different Test Conditions

Zhou's model confirms the importance of the temperature and stress level on the permanent deformation of the bituminous mixtures. As seen in Tables 4.28 – 4.29, none of the mixtures went through the tertiary stage at low temperatures (40°C and 50°C). However, with an increase of 10°C, from 50°C to 60°C, it seems that all the stages are presented. Zhou's models also determined that an increase in stress levels lead to an increase in permanent deformation, as shown by the control mixture tested at 50°C temperature for stress levels of 200 kPa and 400 kPa. The attained result shows that the control mixture tested at 50°C and 200 kPa stress level enters the secondary stage at 479 cycles and did not reach its tertiary stage until the end of the test. A further increase in stress level (from 200 kPa to 400 kPa) demonstrates that the control mixture enters the secondary stage at a lower cycle (169 cycles) and reaches its tertiary stage at 829 load cycles.

4.9.3.5 Zhou's Three-Stage Model at Different Test Conditions: Predicted Strain versus Measured Strain

The mathematical model at each stage predicts precisely the strain value for the control, CRMM and CRMM-TOR. For instance, in the case of the control mixture at 200 kPa and temperature of 60°C, the models predict the strain 21429.6 με and 50260.5 με for the end point primary and end point secondary stages, respectively, which are comparable values to the measured strain, i.e. 21786.8 με and 51394.7 με for similar end points. In general, for all mixtures, the predicted strain values calculated from the model are similar to the measured strain values obtained from the dynamic creep test, as can be seen in Tables 4.28 – 4.29.

Table 4.28 Zhou's Three-Stage Models and Boundary Points at 200 kPa stress.

		Primary stage				Secondary stage				Tertiary stage
Test temperature	**Sample**	**Model**	**End point**	**Measured strain, *με***	**Predicted strain, *με***	**Model**	**End point**	**Measured strain, *με***	**Predicted strain, *με***	**Model**
40°C	0R	$\varepsilon_p = 2979.3N^{0.2628}$	N=1173	19100.08	19086.48	$\varepsilon_p = 19086.48 + 4.422\ (N-1173)$	[a]	[a]	[a]	[a]
	T20R	$\varepsilon_p = 2712.8N^{0.2343}$	N=1063	13708.17	13884.64	$\varepsilon_p = 13884.64 + 2.173\ (N-1063)$	[a]	[a]	[a]	[a]
	C12R	$\varepsilon_p = 2331.3N^{0.2486}$	N=865	12222.56	12523.92	$\varepsilon_p = 12523.92 + 2.235\ (N-865)$	[a]	[a]	[a]	[a]
	C12RT	$\varepsilon_p = 2169.4N^{0.248}$	N=831	11294.98	11492.13	$\varepsilon_p = 11492.13 + 2.223\ (N-831)$	[a]	[a]	[a]	[a]
50°C	0R	$\varepsilon_p = 2513.8N^{0.3004}$	N=479	16116.79	16051.05	$\varepsilon_p = 16051.05 + 9.904\ (N-479)$	[a]	[a]	[a]	[a]
	T20R	$\varepsilon_p = 2828.6N^{0.2729}$	N=735	17265.137	17130.95	$\varepsilon_p = 17130.95 + 5.733\ (N-735)$	[a]	[a]	[a]	[a]
	C12R	$\varepsilon_p = 2505.7N^{0.2737}$	N=701	15183.12	15059.21	$\varepsilon_p = 15059.21 + 5.886\ (N-701)$	[a]	[a]	[a]	[a]
	C12RT	$\varepsilon_p = 2227.5N^{0.2673}$	N=901	13865.05	13728.26	$\varepsilon_p = 13728.26 + 3.865\ (N-901)$	[a]	[a]	[a]	[a]
60°C	0R	$\varepsilon_p = 3033.3N^{0.3769}$	N=179	21786.87	21429.68	$\varepsilon_p = 21429.68 + 50.938\ (N-179)$	N=745	51394.74	50260.59	$\varepsilon_p = 50260.6 + 2159.8\ (e^{0.0086\ (N-745)}-1)$
	T20R	$\varepsilon_p = 2479.8N^{0.3449}$	N=109	12573.35	12502.16	$\varepsilon_p = 12506.19 + 31.592\ (N-109)$	N=813	36121.42	34746.96	$\varepsilon_p = 34747.0 + 2749.6\ (e^{0.0055\ (N-813)}-1)$
	C12R	$\varepsilon_p = 2582.3N^{0.3321}$	N=281	17038.48	16796.63	$\varepsilon_p = 16796.63 + 20.296\ (N-281)$	N=1417	40954.44	39852.89	$\varepsilon_p = 39852.9 + 1474.2\ (e^{0.0054\ (N-1417)}-1)$
	C12RT	$\varepsilon_p = 2392.1N^{0.3133}$	N=297	14427.23	14239.47	$\varepsilon_p = 14239.47 + 16.825\ (N-297)$	N=1785	40528.14	39275.07	$\varepsilon_p = 39275.1 + 1387.8\ (e^{0.0054\ (N-1785)}-1)$

[a] Not found at the end of 1800 cycles

Table 4.29 Zhou's Three-Stage Models and Boundary Points at 400 kPa stress.

Test temperature	Sample	Primary stage Model	Primary stage End point	Primary stage Measured strain, μs	Primary stage Predicted strain, μs	Secondary stage Model	Secondary stage End point	Secondary stage Measured strain, μs	Secondary stage Predicted strain, μs	Tertiary stage Model
40°C	0R	$\varepsilon_p = 4088N^{0.2949}$	N=469	25185.27	25074.93	$\varepsilon_p = 25074.93 + 15.1\ (N-469)$	[a]	[a]	[a]	[a]
	T20R	$\varepsilon_p = 3889.3N^{0.2845}$	N=1035	28045.16	28029.93	$\varepsilon_p = 28029.93 + 6.995\ (N-1035)$	[a]	[a]	[a]	[a]
	C12R	$\varepsilon_p = 3740.9N^{0.2823}$	N=979	26216.27	26138.10	$\varepsilon_p = 26138.10 + 7.977\ (N-979)$	[a]	[a]	[a]	[a]
	C12RT	$\varepsilon_p = 2891.4N^{0.277}$	N=647	17659.15	17367.15	$\varepsilon_p = 17367.15 + 7.19\ (N-647)$	[a]	[a]	[a]	[a]
50°C	0R	$\varepsilon_p = 5146.9N^{0.307}$	N=169	25046.38	24860.33	$\varepsilon_p = 24860.33 + 39.439\ (N-169)$	N=829	51849.49		$\varepsilon_p = 50890.1 + 2789.6\ (e^{0.0046\ (N-829)}-1)$
	T20R	$\varepsilon_p = 6176.7N^{0.2523}$	N=369	27549.523	27442.09	$\varepsilon_p = 27442.09 + 17.677\ (N-369)$	[a]	[a]	[a]	[a]
	C12R	$\varepsilon_p = 4100.3N^{0.2983}$	N=599	27859.29	27626.26	$\varepsilon_p = 27626.26 + 14.184\ (N-599)$	[a]	[a]	[a]	[a]
	C12RT	$\varepsilon_p = 3923.8N^{0.2462}$	N=269	15792.31	15556.50	$\varepsilon_p = 15556.5 + 14.162\ (N-269)$	[a]	[a]	[a]	[a]
60°C	0R	$\varepsilon_p = 5014.9N^{0.3525}$	N=60	21252.78	21235.41	$\varepsilon_p = 21235.41 + 135.17\ (N-60)$	N=206	41464.50	40970.23	$\varepsilon_p = 40970.2 + 2401.6\ (e^{0.0215\ (N-206)}-1)$
	T20R	$\varepsilon_p = 4351.6N^{0.3484}$	N=65	18767.02	18632.36	$\varepsilon_p = 18632.36 + 117.42\ (N-65)$	N=245	40711.57	39767.96	$\varepsilon_p = 39768.0 + 1333.2\ (e^{0.0355\ (N-245)}-1)$
	C12R	$\varepsilon_p = 3909.8N^{0.3461}$	N=74	17532.57	17267.38	$\varepsilon_p = 17341.86 + 93.494\ (N-74)$	N=353	44529.37	43426.686	$\varepsilon_p = 43426.7 + 2097.8\ (e^{0.0186\ (N-353)}-1)$
	C12RT	$\varepsilon_p = 3693.4N^{0.3309}$	N=75	15547.31	15412.89	$\varepsilon_p = 15412.89 + 72.695\ (N-75)$	N=439	43009.84	41873.87	$\varepsilon_p = 41873.9 + 2049.6\ (e^{0.0148\ (N-439)}-1)$

[a] Not found at the end of 1800 cycles

4.9.3.6 Zhou's Three-Stage Model at Different Test Conditions: End Point at First Stage at Different Test Conditions

The end point for the first stage is known as the transition point from the first stage to the second stage for all mixtures. It indicates the initial axial strain of the mixtures, which reflects the permanent deformation in the densification stage. The higher the end point for the first stage, the larger the initial permanent deformation.

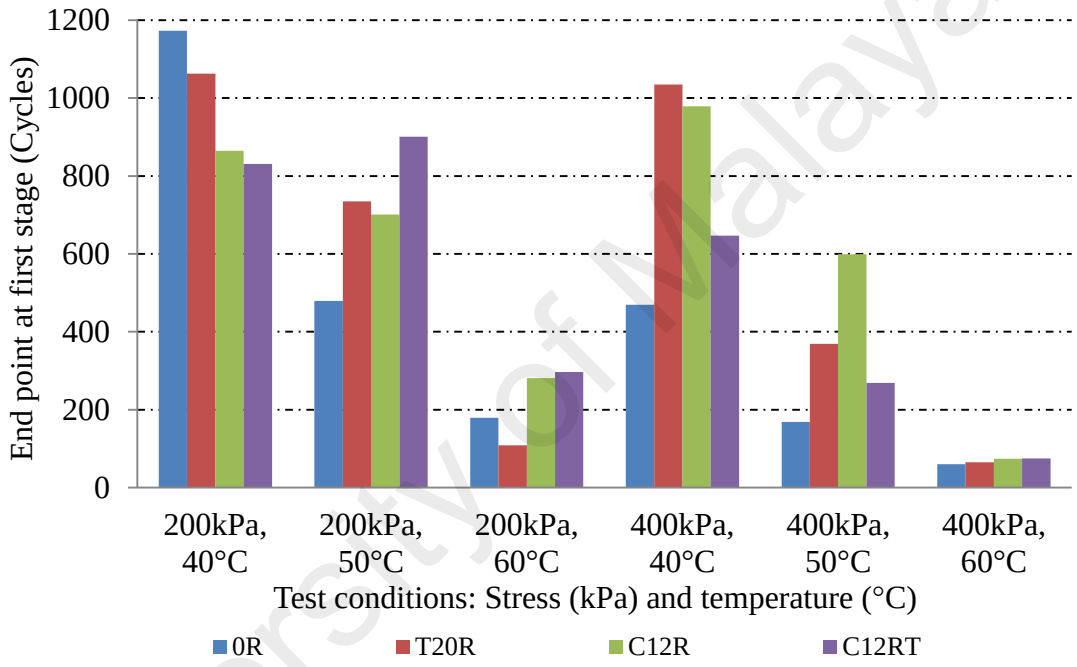

Figure 4.31: End Point at First Stage for Different Test Conditions

Figure 4.31 presents the end point at the first stage of the creep curve for all mixtures for different test conditions. As seen from the figure, different patterns are observed for each test condition. Therefore, it is difficult to conclude the effect of rubber, TOR and blending type on the rutting resistance based on the end point for the first stage. These observations suggest that initial permanent deformation cannot be used to evaluate the rutting resistance of rubberized mixtures.

As expected, the end point for the first stage decreases as the stress level and temperature increase. As the first stage presents the compactive behaviour and the second stage presents the shear flow (plastic) behaviour of the mixture (Gokhale et al., 2005), it means that the specimen changes to plastic behaviour faster as the stress level and temperature increase. At 40°C, for instance, increasing the stress level from 200 kPa to 400 kPa leads the control mixture to enter the second stage from 1173 cycles to 469 cycles, which is 2.5 times faster.

4.9.3.7 Zhou's Three-Stage Model at Different Test Conditions: Slope of Secondary Stage at Different Test Conditions

Figure 4.32 shows the slope of the secondary stage for the control, CRMM and CRMM-TOR under different stress levels and temperatures. Similar to the ultimate strain results, Figure 4.32 shows that modifying the bituminous mixtures with crumb rubber and TOR decreases the temperature and stress susceptibility of the mixtures. In other words, the dependency of the permanent deformation on the temperature and stress in CRMM and CRMM-TOR is considerably lower than that of the control mixture.

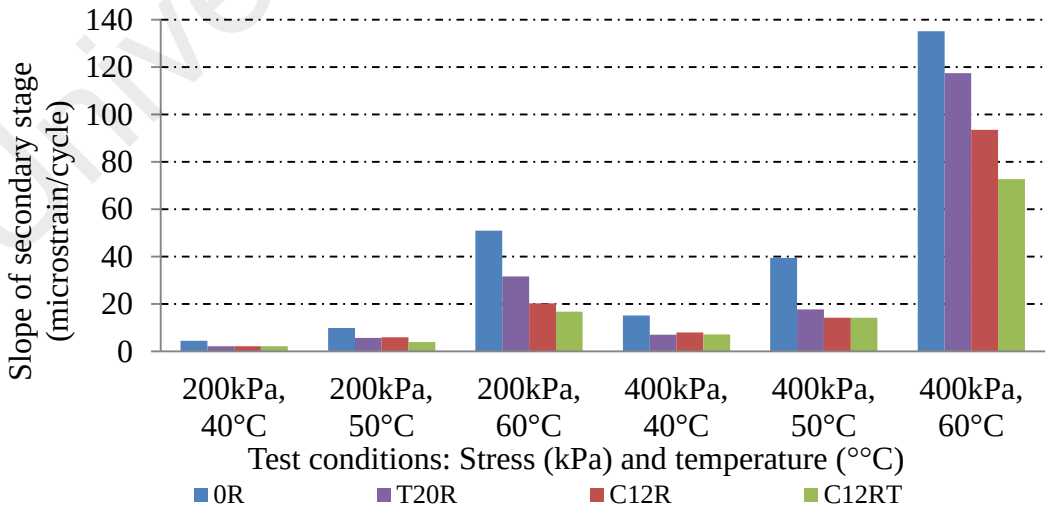

Figure 4.32: Slope of Secondary Stage for Different Stress Levels and Temperatures

At both temperatures (40°C and 50°C) for both stress levels (200 kPa and 400 kPa), Figure 4.32 illustrates that the slope of the control mixture is the highest, while T20R, C12R and C12RT show comparable slope value. However, at high temperature (60°C) at both 200 kPa and 400 kPa stress levels, the effect of the rubberized mixtures is more apparent with the highest slope being shown by the control, followed by T20R, C12R and C12RT. This indicates that the effects of crumb rubber, TOR and binder blending methods are more apparent at high temperatures. For instance, at 50°C and 200 kPa stress level, the slope obtained for CRMM and CRMM-TOR is similar, i.e. 5.733, 5.886 and 3.865 for T20R, C12R and C12RT. However, an increase of 10°C from 50°C to 60°C at the same stress level leads to a significant difference, i.e. 31.593, 20.296 and 16.825 for T20R, C12R and C12RT, respectively (increased about 3.4 – 5.5 times). In addition, the effects of crumb rubber, TOR and blending type can be clearly seen at test conditions 200 kPa, 60°C, and 400 kPa, 60°C, as both test conditions show the highest difference among the mixtures.

For all test conditions, CRMM and CRMM-TOR show a lower slope compared to the control mixture. For example, at 60°C and 200 kPa stress level, the slope obtained for C12RT, C12R, T20R and the Control is 16.825, 20.296, 31.592 and 50.938, respectively, which indicates that the slope gradients for C12RT, C12R and T20R are 3.03, 2.51 and 1.61 times lower compared to the control.

4.9.3.8 Zhou's Three-Stage Model at Different Test Conditions: Flow Number (FN) at Different Test Conditions

The Flow number (FN) is also recognized as the end point of the secondary stage. It is a transition point between the secondary stage and the tertiary stage. Figure 4.33 shows the FN value at 60°C for both stress levels 200 kPa and 400 kPa. The FN value for other test conditions (200 kPa, 40°C; 200 kPa, 50°C; 400 kPa, 40°C and 400 kPa, 50°C) was

not observed. This is due to the short loading cycles (1800); the tertiary stage was not achieved, thus the FN value could not be determined.

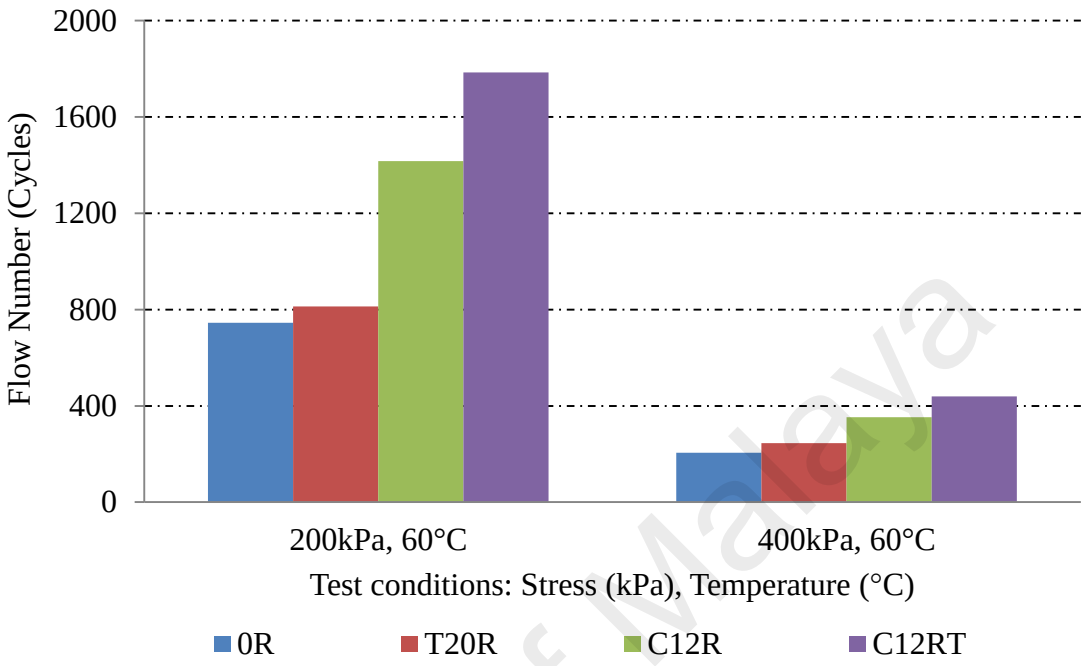

Figure 4.33 Flow Number (FN) for Different Stress Levels at 60°C

As can be seen in Figure 4.33, the FN increases considerably when utilizing rubberized bitumen in the mixture. This figure illustrates that CRMM and CRMM-TOR show a longer stage (total primary and secondary stages) compared to the control mixture before entering the tertiary stage. For instance, T20R, C12R and C12RT show 1.09, 1.90 and 2.40 times longer compared to the control. Again, the FN value shows that the stress levels affect the resistance to permanent deformation as all mixtures enter the tertiary stage faster at 400 kPa compared to 200 kPa.

4.9.3.9 Relationship between Ultimate Strain and Slope of Secondary Stage for Different Test Conditions

In order to confirm the significance of Zhou's three-stage model, the ultimate strain value as the typical dynamic creep parameter was compared with the slope of the secondary stage obtained through Zhou's three-stage model.

The relationship between the ultimate strain and slope of the secondary stage is shown in Figure 4.34. The relationship coefficient of the fitted curve, R^2, is 0.9806. This indicates that there is a good correlation between these two parameters. Therefore, it is confirmed that the parameters obtained via Zhou's three-stage model are significant for analysing the permanent deformation of rubberized mixtures.

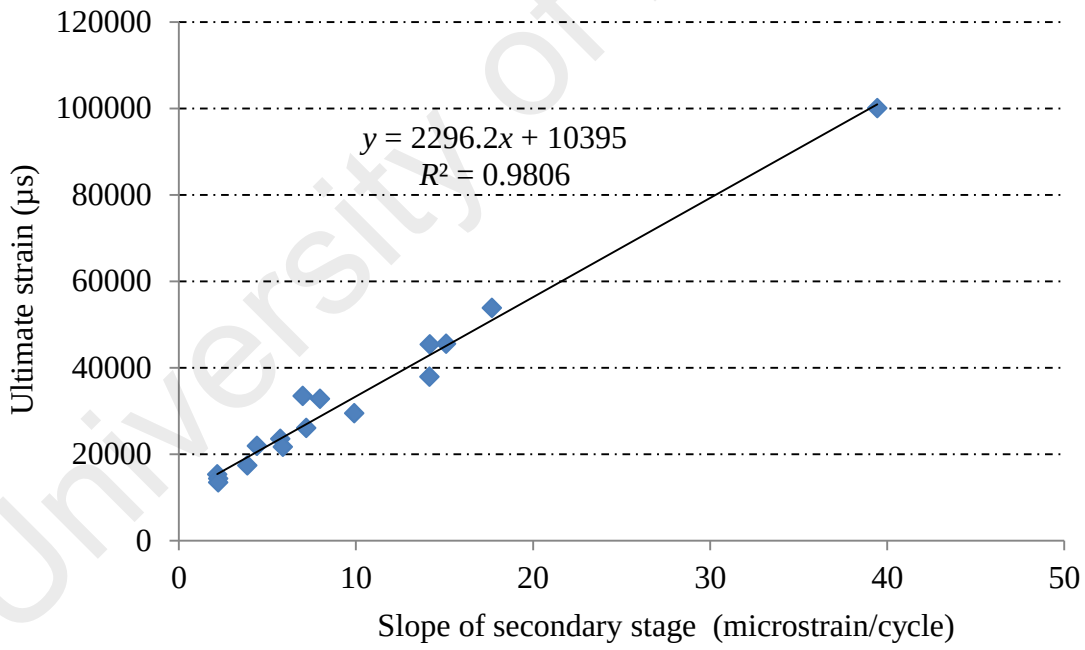

Figure 4.34: Ultimate Strain versus Slope of Secondary Stage

Moreover, the relationship illustrates that the ultimate strain increases with an increase in the slope. Therefore, if the slope of the secondary stage of the mix is enhanced, then its susceptibility to permanent deformation will increase as a consequence. Thus, the

ultimate strain and slope of the secondary stage are considered to be useful parameters for evaluating the permanent deformation susceptibility of the mixtures.

4.9.3.10 Multiple Linear Regression on the Slope of the Secondary Stage at Different Temperatures and Stress Levels

To present permanent deformation of the mixtures, the slope of the secondary stage was selected as the dependent variable, while the factors (stress, temperature, TOR, binder blending type, binder content and rubber content) were selected as the independent variables (Appendix A, Tables A.12a – A.12d). The confidence interval of 95% (α = 0.05) was used in the analysis.

The summary of multiple linear regression is tabulated in Tables 4.30 – 4.31. The factors can explain 67.4% of the variance in the Slope of the secondary stage, R^2=.674, R^2_{adj}=.661, $F(3,73)=50.386$, p<.05.

Table 4.30 indicates that the temperature, stress and binder content have a significant effect on the slope of the secondary stage when the *P* value is less than 0.05. As shown in Table 4.31, the highest beta value was achieved by the temperature (beta = .689, *p* =.000 < .05), followed by stress (beta = .428, *p* =.000 < .05) then the binder content (beta = -.191, *p* =.006 < .05).

The regression equation that can be used to predict the Slope of the secondary stage based on the factors is as follows (Equation 4.14):

Slope of secondary stage at different temperatures and stress levels = .689 (Temperature) +.428 (Stress) -.191(Binder content) (4.14)

Table 4.30 Model Summary: Slope of secondary stage at different temperatures and stress levels

Step	R	R^2	R^2_{adj}	ΔR^2	F_{chg}	p	df_1	df_2
Temperature,°C	.684a	.468	.461	.468	66.080	.000	1	75
Stress, kPa	.799b	.638	.628	.170	34.682	.000	1	74
Binder Content, %	.821c	.674	.661	.036	8.138	.006	1	73

Table 4.31 Coefficients for Final Model: Slope of secondary stage at different temperatures and stress levels

Step	B	β	t	*Bivariate r*	*Partial r*
Temperature,°C	3.070	.689	10.307	.684	.770
Stress, kPa	.157	.428	6.387	.411	.599
Binder Content, %	-16.144	-.191	-2.853	-.141	-.317

4.9.4 Comparison of Multiple Stress Creep Recovery (MSCR) Test Results and Dynamic Creep Test Results

Many studies support the idea that the analysis of the creep-recovery behaviour of binders is a key feature to accurately predict the response of the bituminous mixtures, as well as when it is applied in a real pavement. The MSCR test not only satisfies the above measurements but also significantly contributes to the prediction of the resistance of the bituminous mixture to rutting at different loadings and/or temperatures. The test has recently been recognized by many research studies.

Bernier et al. (2012), in their study of rutting susceptibility of polymer-modified bituminous mixtures using asphalt pavement analyzer (APA), found no correlation between the APA results and any of the MSCR parameters. On the other hand,

Blazejowski, K. and Dolzycki, B. (2014) found a high correlation between the MSCR and the wheel-tracking slope for different types of bituminous mixture (R^2>0.7). Since different relationships have been observed, it is necessary to study the correlation of the MSCR results with the dynamic creep test results for the binders used in this study (CRMB and CRMB-TOR). With this in mind, this section analyses a comparison between MSCR the test results and the dynamic creep test results.

Figures 4.35(a) – 4.35(f) show the comparison between the non-recoverable compliance (J_{nr}) of the binders with the slope of the secondary stage of the mixtures. A comparison is made to study the relationship of the binder's rutting resistance with the mixture's rutting resistance. The low J_{nr} (obtained from MSCR test) and slope of the secondary stage (acquired from dynamic creep test) indicate better rutting resistance for binders and mixtures, respectively.

The obtained results show that, at low temperatures (40°C), the J_{nr} for all binders (0R, C12R, C12RT and T20R) correlate well with the slope of the secondary stage for mixtures (see Figure 4.35(a) and 4.35(d)). Stated another way, the ranking of binders from best to worst are similar to those for the slope of the secondary stage for mixtures: T20R> C12RT> C12R> 0R. As the temperature increases from 40°C to 50°C and 60°C, the binder's ranking is still the same; in contrast, the mixture ranking is changed. As seen in Figures 4.35(b), 4.35(c), 4.35(e) and 4.35(f), at 50°C and 60°C, the C12RT and C12R outperform the T20R; thus, the mixture ranking from best to worst changed: C12RT > C12R > T20R > 0R. Table 4.32 summarizes the ranking for all binders and mixtures based on the J_{nr} and slope of the secondary stage, respectively, as illustrated in Figures 4.35(a) – 4.35(f).

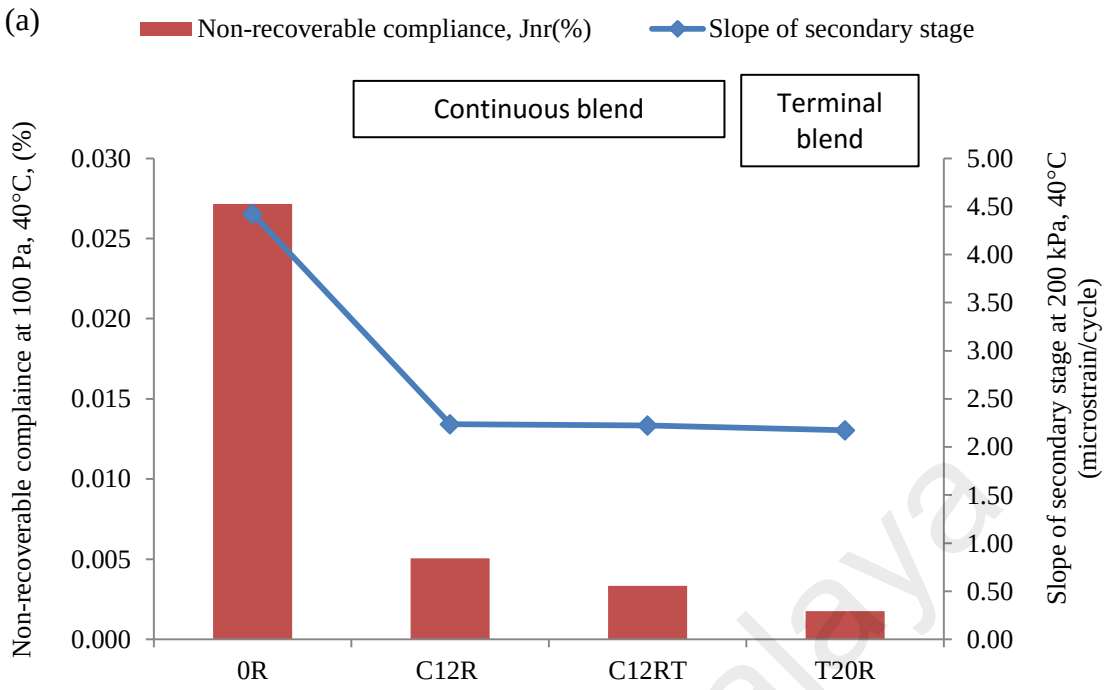

Figure 4.35(a) Non-recoverable compliance at 100 Pa, 40°C vs. Slope of secondary stage at 200 kPa, 40°C

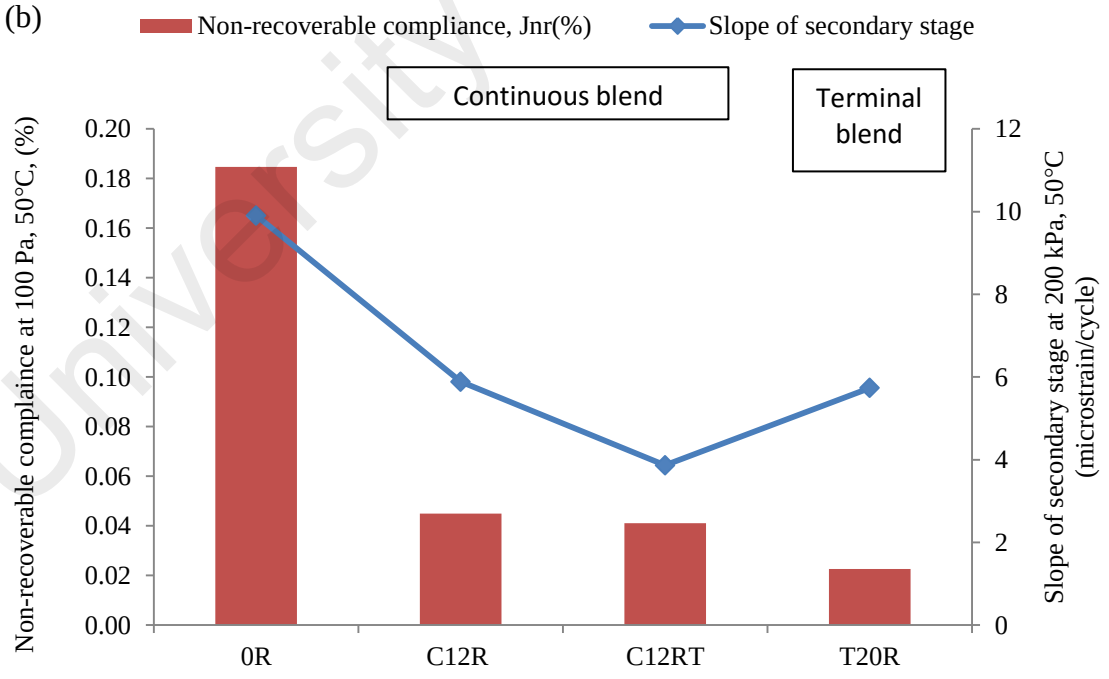

Figure 4.35(b) Non-recoverable compliance at 100 Pa, 50°C vs. Slope of secondary stage at 200 kPa, 50°C

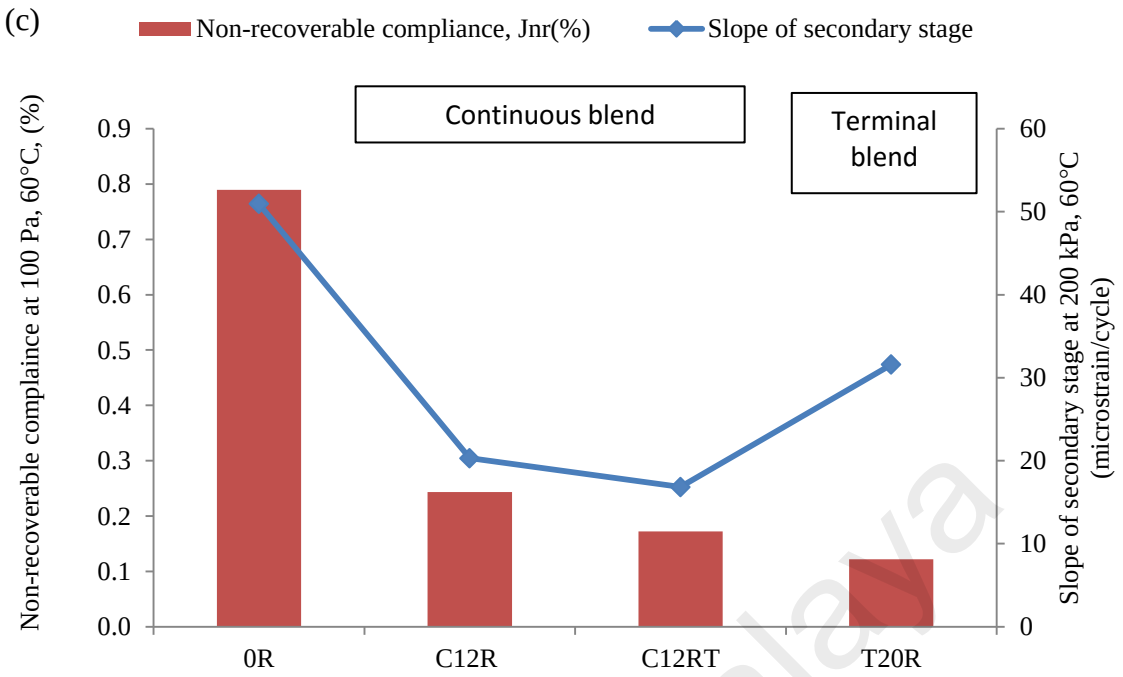

Figure 4.35(c) Non-recoverable compliance at 100 Pa, 60°C vs. Slope of secondary stage at 200 kPa, 60°C

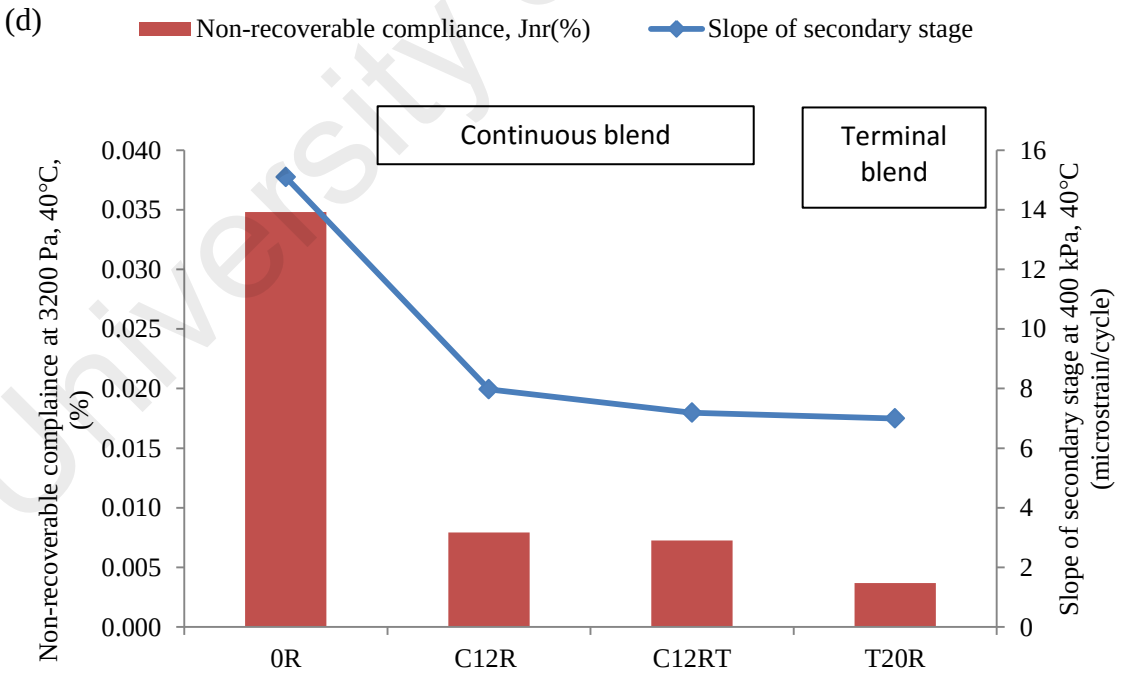

Figure 4.35(d) Non-recoverable compliance at 3200 Pa, 40°C vs. Slope of secondary stage at 400 kPa, 40°C

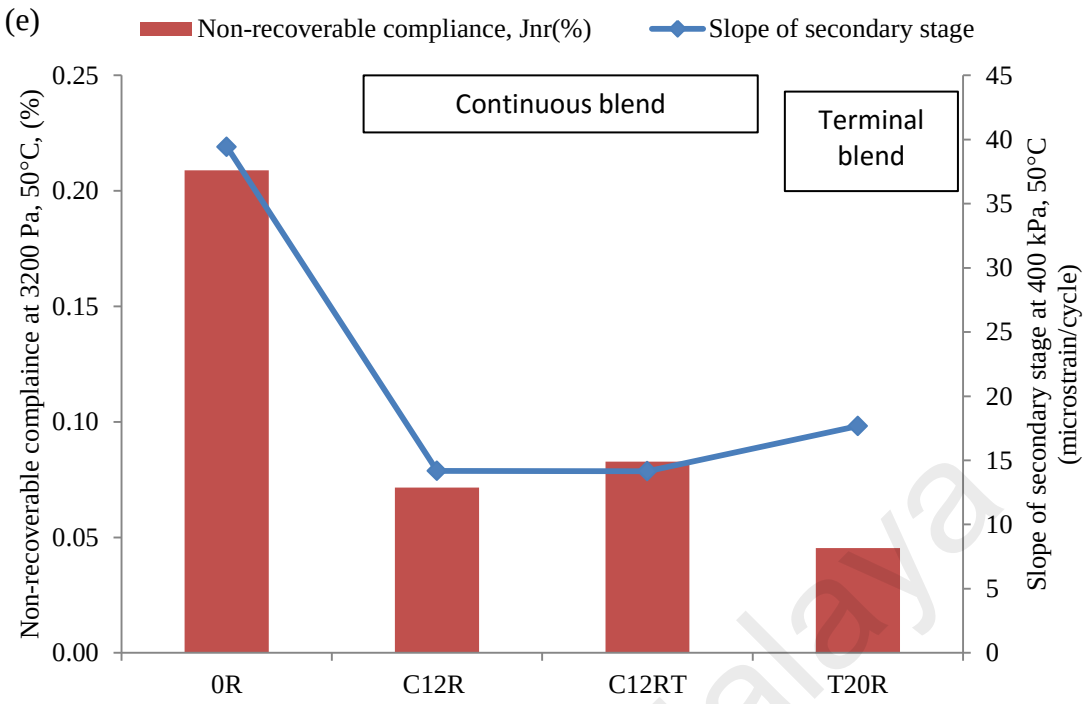

Figure 4.35(e) Non-recoverable compliance at 3200 Pa, 50°C vs. Slope of secondary stage at 400 kPa, 50°C

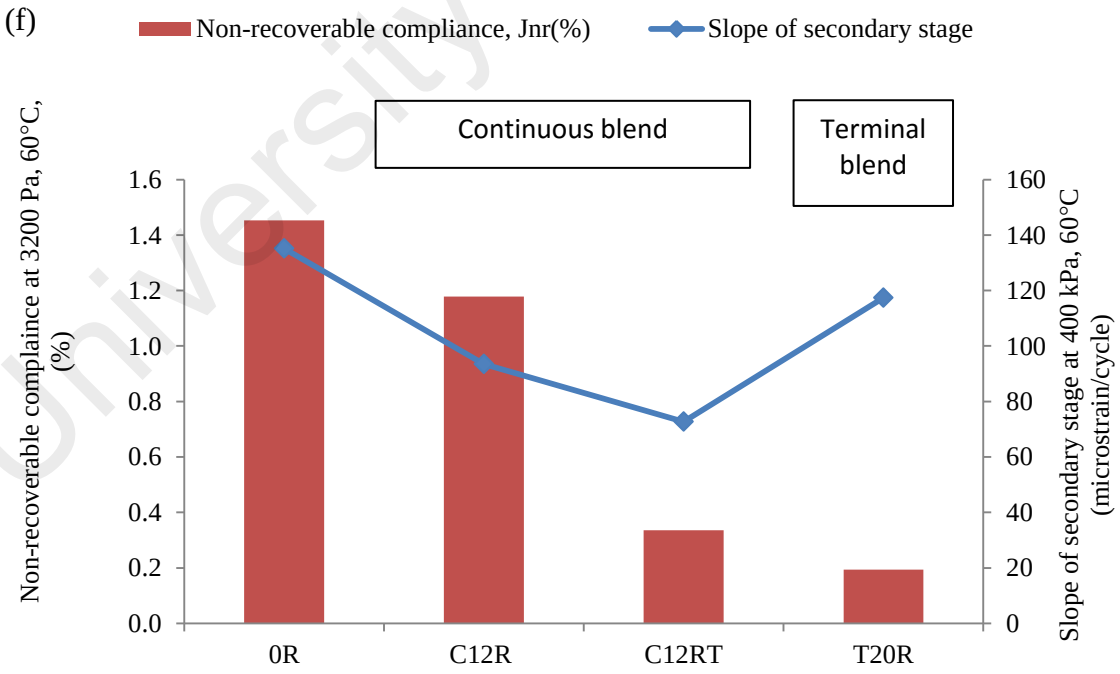

Figure 4.35(f) Non-recoverable compliance at 3200 Pa, 60°C vs. Slope of secondary stage at 400 kPa, 60°C

Under these circumstances, it can be concluded that the T20R mixture is susceptible to high temperature. Despite the fact that the T20R binder had the lowest J_{nr} values at all test temperatures (40°C-60°C), at temperatures higher than 40°C, the T20R mixture changed from being the most resistant to rutting at temperature 40°C to the worst in comparison with the other rubberized mixtures (C12R and C12RT). This can be observed clearly in Figure 4.35(c). In terms of binder, the figure illustrates that the J_{nr} for T20R is lower compared to that for C12RT. This indicates that the T20R binder has better rutting resistance compared to the C12RT binder (J_{nr} value 0.1219% and 0.1724% for T20R and C12RT, respectively). This observation suggests that the rutting resistance for the T20R binder improves 29.29% in comparison to the C12RT binder. However, in terms of the mixture, the slope of the secondary stage obtained by the T20R mixture is higher in comparison to the C12RT mixture (Slope of secondary stage 31.592 and 16.825 micro strain/cycle for T20R and C12RT, respectively). This impact is proportional to a decrease in the rutting resistance of T20R compared to C12RT (decrease 46.74%). These observations suggest that the creep-recovery behaviour of T20R cannot be used to predict the response of the T20R bituminous mixture, as well as the rutting resistance.

Moreover, this interesting finding gives rise to doubt about the use of the MSCR test to predict the rutting performance of the mixtures prepared with different binders blending type at high test temperatures. At low temperatures (40°C), the MSCR test can be used to predict the rutting resistance of mixtures as comparable performance was observed for all binders and mixtures. At high temperatures (50°C and 60°C), the MSCR test shows a high correlation between the control and the continuous blend binder (C12R and C12RT) with the respective mixtures; however, the test is not able to offer good correlation when it comes to the terminal blend binder.

A comparative study conducted by Blazejowski, K. and Dolzycki, B. (2014) shows similar experience to that of the author. They found that the modified binders with styrene-butadiene-styrene (SBS) were unsatisfactory from the MSCR test results; in contrast, in the wheel-tracking test they did not show this behaviour. They also mentioned that some binders performed well in the MSCR test; however, converse results were shown by the mixtures in the wheel-tracking test. These findings suggest that the results of the binders alone are not sufficient to evaluate the impact of the binder used for bituminous mixture properties, especially when modified binders are considered.

In addition, in the research conducted by Blazejowski, K. and Dolzycki, B. (2014) they found that evaluation of the binder tests alone was not sufficient for assessment of specific types of bituminous mixtures, especially Stone Mastic Asphalt (SMA), as their study revealed that SMA observed the worst R^2 determination coefficients between the binder test results and the wheel-tracking test results.

Table 4.32 Summary of ranking for all binders and mixtures based on the J_{nr} and slope of the secondary stage from Figures 4.35(a) – 4.35(f)

Figure	**J_{nr} at stress level and temperature**	**Slope of secondary stage at stress level and temperature**	**Ranking of binder based on J_{nr} (best to worst)**	**Ranking of mixture based on slope of secondary stage (best to worst)**
Figure 4.35(a)	100 Pa, 40°C	200 kPa, 40°C	T20R>C12RT>C12R>0R	T20R>C12RT>C12R>0R
Figure 4.35(b)	100 Pa, 50°C	200 kPa, 50°C	T20R>C12RT>C12R>0R	C12RT>T20R>C12R>0R
Figure 4.35(c)	100 Pa, 60°C	200 kPa, 60°C	T20R>C12RT>C12R>0R	C12RT>C12R>T20R>0R
Figure 4.35(d)	3200 Pa, 40°C	400 kPa, 40°C	T20R>C12RT>C12R>0R	T20R>C12RT>C12R>0R
Figure 4.35(e)	3200 Pa, 50°C	400 kPa, 50°C	T20R>C12RT>C12R>0R	C12RT>C12R>T20R>0R
Figure 4.35(f)	3200 Pa, 60°C	400 kPa, 60°C	T20R>C12RT>C12R>0R	C12RT>C12R>T20R>0R

4.10 Summary of Multiple Linear Regression Model: Mixtures

Table 4.33 summarizes the regression model for mixtures determined from statistical analysis "Multiple Linear Regression". Details of the analysis are explained in Sections 4.7-4.9. The model was developed with respect to the laboratory experiments: Marshall stability and flow test, indirect tensile stiffness modulus test and dynamic creep test. The table shows that most of the factors (rubber content, binder content, TOR, blending type, temperature and stress level) affect the properties of the mixture. The highest reliability coefficient, R^2 is shown by the ultimate strain at 200 kPa, 40°C (R^2 = .812), while the lowest R^2 is attained by the stability value (.255).

Table 4.33: Summary of Multiple Linear Regression Model for Mixtures

Multiple Linear Regression model	R^2
Stability = -.752 (blending types) -.367 (Trans-polyoctenamer) +.429 (rubber content)	.255
Flow value = -.744(Rubber content) + .388 (Binder content) - .352(Trans-polyoctenamer) +.357 (Blending type)	.443
Stiffness modulus value = .454(Trans-polyoctenamer) -.290 (Binder content) +.275 (Blending type)	.363
Ultimate strain at 200 kPa, 40°C = -.792 (Rubber content) - .259 (Trans-polyoctenamer) + .168 (Binder content)	.812
Slope of secondary stage at 200 kPa, 40°C = -.671 (Rubber content) - .317 (Trans-polyoctenamer) + .211 (Binder content)	.687
Slope of secondary stage at different temperature and stress levels = .689 (Temperature) +.428 (Stress) -.191(Binder content)	.674

4.11 Summary

The study reveals that crumb rubber, TOR and binder blending methods affect the physical and rheological properties of the binder. The stability, flow and stiffness of the SMA 20 mixtures are also affected by the addition of crumb rubber and TOR. From the results, it seems that most of the factors (stress level, temperature, TOR, binder blending method, binder content and rubber content) affect the rutting resistance of SMA 20 mixtures, as shown by the dynamic creep test results. The finding was supported using the Zhou three-stage model. Detailed conclusions can be found in Chapter 5.

CHAPTER FIVE: CONCLUSION AND RECOMMENDATIONS

5.1 Introduction

This chapter presents the findings of the study carried out on SMA 20 mixtures prepared with different percentages of crumb rubber and TOR as crosslinking agent. Moreover, the effects of the binder blending methods on the rutting resistance of the SMA 20 mixtures are also presented.

The effects of variables (rubber content, TOR, blending method, binder content) on the rutting resistance were studied using the dynamic creep test together with other conventional tests (Marshall stability and flow of asphalt concrete test and Indirect tensile stiffness modulus test). In order to investigate the effect of the environmental conditions, the dynamic creep test was conducted at different temperatures and stress levels.

The statistical analysis was conducted using mutiple linear regression analysis (stepwise method) to evaluate the effects of the variables on the rutting resistance of the SMA 20 mixtures, and, consequently, to develop the empirical relationship model. Moreover, the creep behaviour (rutting) of the specimens was further examined and predicted using the Zhou three-stage creep model.

This study also evaluates the physical and rheological properties of the binders used in preparation of SMA 20 mixtures. From the experimental works and statistical analysis, the study managed to develop a relationship between the binder properties and the mixture's permanent deformation behaviour in the form of a model.

5.2 Conclusion

Based on the analysis of the test results and modelling efforts undertaken in this research work, many conclusions have been drawn; these include:

1. Objective number 1: To investigate the effects of crumb rubber (CR), Trans-polyoctenamer (TOR) and binder blending methods on the physical and rheological properties of bitumen binders.

The physical and rheological properties of CRMB-TOR were compared with crumb rubber modified binder without TOR (CRMB) and control bitumen (bitumen 80/100 penetration). The conventional physical properties of CRMB and CRMB-TOR were observed through the penetration test and softening point. The results demonstrated that the properties of CRMB-TOR had a quite significant difference from CRMB; the softening point and penetration value of CRMB-TOR improved significantly, which was beneficial to high temperature performance.

Furthermore, the rheological properties of CRMB and CRMB-TOR were evaluated using the Brookfield viscosity test and multiple stress creep and recovery test. Both tests were performed to evaluate the high temperature performance of CRMB and CRMB-TOR. The results from the Brookfield viscosity test indicated that TOR had a significant influence on increasing the viscosity value as the temperature increased. That is to say, the TOR played a positive role in enhancing the resistance to deformation. From the MSCR test, the addition of CR to the base binder (bitumen 80/100 penetration) reduced the non-recoverable creep compliance (Jnr) and increased the percent recovery. Furthermore, the rheology of CRMB was significantly affected by the addition of TOR. This indicated that the TOR improved the high temperature stability of CRMB. Therefore, it can be concluded that the bituminous mixtures prepared with CRMB-TOR

would be less susceptible to the appearance of rutting compared with the mixtures prepared with CRMB without TOR.

Another conclusion to note is that the reaction of TOR with crumb rubber was significantly affected by the amount of crumb rubber. The results obtained showed that adding TOR to low concentrations of CRMB resulted in a low softening point and viscosity values, and increased the penetration value. This indicated that adding TOR to low concentrations (4% CR) of CRMB softened the CRMB-TOR. However, adding TOR to a higher rubber content (8% and 12%) resulted in stiffer CRMB-TOR. This implied that the physical properties of CRMB would be improved further by TOR at high percentages of rubber content. On the other hand, the rheology of CRMB-TOR was improved by adding TOR to all percentages of crumb rubber, as shown by the low non-recoverable compliance (Jnr) and high the percent recovery (% R). This indicated that adding TOR to all amounts of crumb rubber (4%-12%) improved the high temperature performance of CRMB-TOR, and that it would be expected that CRMB-TOR would offer better rutting resistance in the mixture.

In addition, binder blending methods (terminal and continuous blend) appeared to influence the physical and rheology of the binder due to the dissimilar reaction levels observed in both blending methods. The study observed that CRMB prepared using the terminal blend method improved the binder's stiffness at a slower rate compared to the continuous blend binder. Moreover, from the multiple stress creep and recovery result it seemed that the terminal blend binder observed the best rutting resistance and elasticity, as shown by the low Jnr and high % R, respectively.

2. Objective number 2: To investigate the effects of crumb rubber (CR), Trans-polyoctenamer (TOR) and binder blending methods to the stability, flow and stiffness characteristics of SMA 20 mixtures.

The characteristics of the SMA 20 mixtures prepared with CRMB and CRMB-TOR were evaluated using the Marshall Stability, and Flow of Asphalt Concrete and Indirect Tensile Modulus Test. The statistical analysis (Multiple linear regression with stepwise method) performed to determine the influence of the crumb rubber, TOR and binder blending methods on the stability, flow and stiffness of the SMA 20 mixtures revealed a significant difference at $p < 0.05$. The test results determined that the stability, flow and stiffness of the crumb rubber modified mixture reinforced with Trans-polyoctenamer (CRMM-TOR) were better compared to the crumb rubber modified mixture without Trans-polyoctenamer (CRMM). This indicated that favourable properties of SMA 20 mixtures can be achieved by adding TOR.

The SMA 20 mixtures prepared with a terminal blend binder seemed to have a lower stability and stiffness value, and a higher flow value compared with the SMA 20 mixtures prepared with the continuous blend binder. This finding is interesting because the terminal blend binder showed better physical and rheological properties compared with the continuous blend binder and might offer better characteristics and performance for the SMA 20 mixture when used as the binder. However, the test results showed an adverse pattern, i.e. SMA 20 mixtures prepared with terminal blend binder showed lower characteristics compared with the SMA 20 mixture prepared with a continuous blend binder. The harsh blending condition (crumb rubber was blended with bitumen at 210°C for 2 hours with 10, 000 rpm) employed in the preparation of the terminal blend binder might be the reason for the above results. In the terminal blend, the crumb

rubber started to depolymerize releasing the rubber components back to the liquid phase thereby causing a decrease in the stiffness and elastic properties of the binder, and, consequently, affecting the stability of the mixture.

3. Objective number 3: To evaluate the influence of crumb rubber (CR), Trans-polyoctenamer (TOR), binder blending methods, stress levels and temperatures on the rutting parameters of SMA 20 mixtures using the dynamic creep test. Next, the empirical relationship model was developed based on multiple linear regression analysis (Stepwise method).

From the results, it seems that most of the factors (crumb rubber (CR), TOR, binder blending method, binder content, stress level and temperature) affect the rutting resistance of SMA 20 mixtures, as shown by the dynamic creep test results. The regression model was developed based on multiple linear regression (stepwise method) analysis. Table 4.35, as presented in Chapter 4, shows a summary of the empirical relationship model developed using multiple linear regression. From the table, a good relationship between the dynamic creep test results (ultimate strain and slope of secondary stage) with the engaged factors has been determined (R^2=0.674-0.812). The analysis determined that all the factors significantly affect the rutting resistance of SMA 20 mixtures.

In addition, the results from the dynamic creep test at higher stress levels and temperatures indicate that the permanent deformation resistance of the control, crumb rubber modified mixtures (CRMM) and crumb rubber modified mixtures reinforced with TOR (CRMM-TOR) decreased. However, both CRMM and CRMM-TOR are less susceptible to temperature compared to the control mixture.

4. Objective number 4: To develop the creep model based on the Zhou three-stage model. Moreover, the creep parameters obtained by the dynamic creep test results (dynamic creep curve and ultimate strain) were compared with the Zhou three-stage model (slope at secondary stage and flow number).

The creep behaviour of SMA 20 mixtures was further examined using the Zhou-three-stage model. The model is presented in Tables 4.22, 4.28 and 4.29. The study observed that the predicted strain values from the Zhou model are similar to the measured strain values obtained from the dynamic creep test. This indicates that the creep curve observes the Zhou model trend. Moreover, Zhou's model confirmed that most of the factors (crumb rubber (CR), Trans-polyoctenamer (TOR), binder blending method, binder content, stress level and temperature) significantly influence the permanent deformation.

The study found that the methods for analysing permanent deformation from the dynamic creep test results (dynamic creep curve and ultimate strain) and Zhou three-stage model creep parameters (slope at secondary stage and flow number) are consistent. However, the end point for the first stage determined via the Zhou model did not display proper evaluation of the densification behaviour (first stage) of rubberized SMA 20 mixtures; thus it is not suitable for use for predicting rutting resistance.

5. Objective number 5: To develop a relationship between the binder rheology (CRMB and CRMB-TOR) and rutting resistance of SMA 20 mixtures.

The results show different patterns in the relationship between the binder rheology with the rutting resistance of the SMA 20 mixtures. The results reveal that the rutting resistance of SMA 20 prepared with a continuous blend binder can be predicted from

the rheology of the binders. This conclusion was made based on the relationship between the non-recoverable compliance (J_{nr}) of the binder determined from the multiple stress creep and the recovery (MSCR) test with the ultimate strain of the mixtures obtained from the dynamic creep test and slope of secondary stage attained from the Zhou model. The relationship shows that a continuous blend binder with better rheology (low J_{nr}) produces a mixture with higher rutting resistance (see Figure 4.27). The results show the ultimate strain increases as the non-recoverable compliance increases. It indicates positive correlation with a linear equation of y = 841448x + 25923 with R^2 value of 0.9593.

On the other hand, in the case of mixtures prepared with the terminal blend binder, they showed a different pattern. The terminal blend binder shows the best rheology (lowest J_{nr}), as determined by the MSCR test results; however, when using as a binder in the mixture, the mixture produced does not show equivalent quality as the binder especially when tested at high temperature (refer Figure 4.35). Moreover, the study found that mixtures prepared with a terminal blend binder are among the worst mixtures, as shown by the dynamic creep parameters, stability, flow and stiffness value. From this study, it can be concluded that permanent deformation of the modified SMA 20 mixtures prepared with terminal blend binder cannot be predicted solely on the rheology of the binders. Therefore, tests on the mixtures are significant to evaluate the rutting resistance of the mixtures.

From the above phenomenon, another conclusion can be derived, i.e. the physical and rheological properties of the CRMB and CRMB-TOR are not an important factor regarding a mixture's rutting resistance. This is because the terminal blend mixtures were prepared with high viscous rubberized bitumen compared with the continuous blend mixtures. However, the bituminous mixture evaluations seem to indicate that the

continuous blend mixtures present the best rutting resistance compared to the terminal blend mixtures.

It is important to realize that the preliminary evaluation of the rutting resistance of bituminous mixtures could be done using the binder test results (in case of SMA 20 mixtures prepared with continuous blend binder). Although this may be true, it is essential to remember that the rutting resistance of bituminous mixtures also depends on many factors including the type of aggregate mixture. Hence, the final evaluation should be made using bituminous mixture rutting resistance tests, as it would offer better assessment of the full-scale behaviour.

5.3 Recommendations for Future Study

Based on the study, the following recommendations have been suggested;

1. The effects of TOR on the performance of mixtures can be expanded upon by using different percentages of TOR.
2. The chemical reaction between TOR, crumb rubber and bitumen should be studied for a better understanding concerning their effects on the rutting resistance of the mixtures.
3. A comprehensive experimental study may be conducted on the moisture sensitivity. For instance dynamic creep test in wet conditions coupled with the Indirect Tensile Strength Test in dry and wet conditions can be proposed.
4. Full scale accelerated testing should be carried out to investigate the performance of these mixtures in the field under local environmental conditions.

5.4 Proposed Construction Guidelines of the SMA20 Rubberized Pavement

Based on the laboratory works, this study determined that incorporating crumb rubber modified bitumen (CRMB) and crumb rubber modified bitumen reinforced with trans-polyoctenamer (CRMB-TOR) improves the stability, flow, stiffness and rutting resistance of the SMA 20 mixture. The findings would not mean anything if it is kept in the author's knowledge without translating into the practice. These precious findings are important for highway authorities, researchers and practitioners to be implemented in the construction of SMA 20 in Malaysian roads.

In order for the SMA20 rubberized pavement to perform as expected, the proper production and construction practices must be implemented as explained below:

1. Binder Production

In the blending plant, the bitumen and crumb rubber are blended to produce homogeneous rubberized bitumen. The blending time and temperature should be properly controlled as these two parameters significantly contribute to the rheology of the rubberized bitumen. The produced rubberized bitumen should transport to the operational plant using a truck equipped with an auger to maintain uniformity of the rubberized bitumen.

It is important to have an operational plant that capable to produce a fully coated rubberized SMA mixture. If there is a delay in the delivery of the rubberized bitumen by more than four hours, the operation plant should able to reheat the binder slowly prior to the use of temperature as specified in the design procedure. The binder must be thoroughly mixed and the viscosity of the rubberized asphalt must be verified within the limits. If the viscosity is out of the range, the rubberized binder must be adjusted to produce the desired viscosity by adding additional bitumen and/or crumb rubber.

2. Hot Mix Production

The rubberized bitumen and the aggregates are mixed at the production plant. The operation facilities for the rubberized mixture are similar with the conventional mixture, with the exception that the mix is produced at higher temperature. The blending equipment (or agitated nurse trucks) is hooked up to both the drum (filled with the rubberized binder) and batch plants to supply the rubberized binder for the job. However, caution on the production rates should be identified. For instance, high binder content as required by the SMA mixture may result in decreasing the plant operation. Moreover, production of the mixture's plant is highly dependent on the production capacity of the binder's plant.

It is important to ensure that the crumb rubber is uniformly distributed in the bitumen prior to mix with the aggregate. Therefore agitated tank is required to continuously blend the rubberized binder. Moreover, larger pipes and supply lines with high capacity pumps are used to allow smooth flow of the rubberized bitumen.

The mixing temperature of the mixture is very critical. The rubberized bitumen and aggregates need to be mixed at a higher temperature than conventional mixes. The temperature of the mixture should be tested periodically to ensure it is within the specifications. Blue smoke is an indicator of overheating. On the other hand, a stiff mix as it is dumped into the transport truck may be an indication the temperature is too low.

3. Hot Mix Transport and Placement

The transportation of the SMA rubberized mixture can be accomplished in any truck typically used for the conventional hot mix. Release agents for the truck beds should be either soapy water or silicone emulsions. Under no circumstances should solvent based release agents (e.g., diesel) be used. Except for extremely short hauls, it is necessary to

cover the trucks with canvas to prevent mixture to not cool below the placement and compaction temperatures.

During the transporting, the inspector should look for any signs which reflect to potential problem such as blue smoke, stiff appearance, slumped mix, dull appearance and rising steam; as mentioned signs are indicating of overheated mix, cool mix, excess binder or moisture, not enough binder and excess moisture; respectively.

The handling and placement of the SMA rubberized mixture must be accomplished in such a way to minimize segregation, crusts, lumps, or migration of the rubberized binder. It may be necessary to cover the hauling units with tarps and/or placed the material directly into the paver to minimize heat loss. The materials must be delivered at a rate that allows the paver to operate continuously. It is important to check the temperature of the mixture regularly to prevent problems in laying and compaction. Mixture should be paved only when the surface temperature and weather conditions are optimum.

Compaction of the SMA rubberized mixture can be performed using vibratory or static steel-wheel rollers. For a successful job, compaction must be accomplished at a temperature as specified in the design. Cautions must be taken as a lift thickness, pavement surface temperature, ambient temperature, and wind contribute to the time available for compaction.

Sufficient time should be allowed for the pavement to fully cured before open to the traffic to prevent the surface materials might be picked up by the traffic. This can be corrected by applying a light application of sand. If necessary, excess sand may need to be removed by a pick-up broom.

REFERENCES

AASHTO TP31. Standard test method for determining the stiffness modulus of bituminous mixtures by indirect tension. *American Association of State Highway and Transportation officials*, 2000 edition; interim edition 4/2001

AASHTO, FHWA, NAPA, SHRP, AI, and TRB. Report on the 1990 European asphalt study tour. Washington, DC: *American Association of State Highway and Transportation officials*; 1991.

Abdelrahman, M.A. and Carpenter, S.H., (1998) "Controlling low temperature properties of asphalt rubber binders" *2nd transportation specialty conference*, Canadian Society of Civil Engineering, Halifax, Nova Scotia, Canada,

Abdelrahman, M.A. and Carpenter, S.H., (1999) "The mechanism of the interaction of asphalt cement with crumb rubber modifier (CRM)". *Transportation Research Record*, 1661, 106–113, USA

Adorjányi, K., & Füleki, P. (2011). Performance evaluation of bitumens at high temperature with multiple stress creep recovery test. *Hungarian Journal of Industry and Chemistry*, 39(2), 195-199.

Ahari, A., Forough, S., Khodaii, A., and Nejad, F (2014) .Modeling the Primary and Secondary Regions of Creep Curves for SBS-Modified Asphalt Mixtures under Dry and Wet Conditions. (2014). *Journal of Materials in Civil Engineering*, 26(5), 904-911. doi: doi:10.1061/(ASCE)MT.1943-5533.0000857

Ahmadinia, E., Zargar, M., Karim, M. R., Abdelaziz, M., & Ahmadinia, E. (2012). Performance evaluation of utilization of waste Polyethylene Terephthalate (PET) in stone mastic asphalt. *Construction and Building Materials*, 36(0), 984-989. doi: http://dx.doi.org/10.1016/j.conbuildmat.2012.06.015

Ahmadinia, E., Zargar, M., Karim, M. R., Abdelaziz, M., & Shafigh, P. (2011). Using waste plastic bottles as additive for stone mastic asphalt. [doi: 10.1016/j.matdes.2011.06.016]. *Materials & Design*, 32(10), 4844-4849.

Airey, G. D., Rahman, M. M., & Collop, A. C. (2003). Absorption of bitumen into crumb rubber using the basket drainage method. *International Journal of Pavement Engineering*, 4(2), 105-119.

Alataş, T., Yılmaz, M., Kök, B. V., & Koral, A. f. (2012). Comparison of permanent deformation and fatigue resistance of hot mix asphalts prepared with the same performance grade binders. [doi: 10.1016/j.conbuildmat.2011.12.021]. *Construction and Building Materials*, 30(0), 66-72.

Alavi, A. H., Ameri, M., Gandomi, A. H., & Mirzahosseini, M. R. (2010). Formulation of flow number of asphalt mixes using a hybrid computational method. *Construction and Building Materials.* doi:10.1016/j.conbuildmat.2010.09.01.

Al-Mansob, R. A., Ismail, A., Alduri, A. N., Azhari, C. H., Karim, M. R., & Yusoff, N. I. M. (2014). Physical and rheological properties of epoxidized natural rubber modified bitumens. *Construction and Building Materials*, 63(0), 242-248.

Ameri, M., Mansourian, A., & Sheikhmotevali, A. H. (2013). Laboratory evaluation of ethylene vinyl acetate modified bitumens and mixtures based upon performance related parameters. *Construction and Building Materials*, 40(0), 438-447.

Anderson M, D'Angelo J, Walker D (2010) MSCR: a bettertool for characterizing high temperature performance properties. Asphalt—*The Magazine of the Asphalt Institute*, Lexington. Retrieved from http://www.irfnews.org/wp-content/uploads/IRF-Examiner-Vol4-Winter2014.pdf

Arabani, M., & Azarhoosh, A. R. (2012). The effect of recycled concrete aggregate and steel slag on the dynamic properties of asphalt mixtures. *Construction and Building Materials*, 35(0), 1-7.

AS 2891.12.1-1995 Methods of sampling and testing asphalt - *Determination of the permanent compressive strain characteristics of asphalt - Dynamic creep test*

Asim Hassan Ali, Nuha S. Mashaan, and Mohamed Rehan Karim, "Investigations of Physical and Rheological Properties of Aged Rubberised Bitumen," *Advances in Materials Science and Engineering*, vol. 2013, Article ID 239036, 7 pages, 2013. doi:10.1155/2013/239036

ASTM D 2041 Standard Test Method for Theoretical Maximum Specific Gravity and Density of Bituminous Paving Mixtures, *Annual book of ASTM standards*, vol. 04.04, Easton, MD, USA; 2000.

ASTM D1559. Standard test method for marshal test. *Annual book of ASTM standards*, vol. 04.03. West Conshohocken: American Society for Testing and Materials; 2002.

ASTM D2726, Standard Test Method for Bulk Specific Gravity and Density of Non-Absorptive Compacted Bituminous Mixtures, *Annual book of ASTM standards*, vol. 04.04, Easton, MD, USA; 2000.

ASTM D36 Standard Test Method for Softening Point of Bitumen (Ring-and-Ball Apparatus), *Annual book of ASTM standards*, vol. 04.04, Easton, MD, USA; 2000.

ASTM D36-06. Test method for softening point of bitumen (ring-and-ball apparatus), *Annual book of ASTM standards*, vol. 04.04, Easton, MD, USA; 2000.

ASTM D4402-87. Test method for viscosity determinations of unfilled asphalts using the Brookfield thermosel apparatus, *Annual book of ASTM standards*, Vol. 04.04, Easton, MD, USA; 2000.

ASTM D5 Standard Test Method for Penetration of Bituminous Materials, *Annual book of ASTM standards* vol. 04.04, Easton, MD, USA; 2000.

ASTM D5-97. Standard Test method for penetration of bituminous materials,. *Annual book of ASTM standards* vol. 04.03, Easton, MD, USA; 2000.

ASTM D6926 - 10 Standard Practice for Preparation of Bituminous Specimens Using Marshall Apparatus, *Annual book of ASTM standards*, vol. 04.04, Easton, MD, USA; 2000.

ASTM D6927 - 15 Standard Test Method for Marshall Stability and Flow of Asphalt Mixtures, *Annual book of ASTM standards*, vol. 04.04, Easton, MD, USA; 2000.

ASTM D6931. Standard test method for indirect tensile (IDT) strength of bituminous mixtures; 2012, *Annual book of ASTM standards*, vol. 04.04, Easton, MD, USA; 2000.

ASTM D7405. Standard test method for Multiple Sress Creep and Recovery (MSCR) of asphalt binder using a dynamic shear rheometer. PA (US): *American Society for Testing and Materials;* 2008.

ATJ 5/85, "Manual for the structural design of flexible pavement," *Jabatan Kerja Raya Malaysia*, 2013

Attia, M., & Abdelrahman, M. (2009). Enhancing the performance of crumb rubber-modified binders through varying the interaction conditions. *International Journal of Pavement Engineering*, 10(6), 423-434.

B.J. Burns, Fall Technical Meeting and Rubber Mini Expo 04, *American Chemical Society*, Rubber Division, 166th, Columbus, OH, United States, 2004,131 (October 5–8).

Baghaee Moghaddam, T., Karim, M. R., & Syammaun, T. (2012). Dynamic properties of stone mastic asphalt mixtures containing waste plastic bottles. [doi: 10.1016/j.conbuildmat.2012.02.054]. *Construction and Building Materials*, 34(0), 236-242.

Baghaee Moghaddam, T., Soltani, M., & Karim, M. R. (2014). Evaluation of permanent deformation characteristics of unmodified and Polyethylene Terephthalate modified asphalt mixtures using dynamic creep test. *Materials & Design*, 53(0), 317-324.

Baghaee Moghaddam, T., Soltani, M., & Karim, M. R. (2014). Experimental characterization of rutting performance of Polyethylene Terephthalate modified asphalt mixtures under static and dynamic loads. *Construction and Building Materials*, 65(0), 487-494. doi: http://dx.doi.org/10.1016/j.conbuildmat.2014.05.006

Bahia, H., & Davies, R. (1994). Effect of crumb rubber modifiers on performance related properties of asphalt binders. *Journal of the Association of Asphalt Paving Technologists*, 63, 414–439.

Bahia, H., & Davies, R. (1995). Factors controlling the effects of crumb rubber on critical properties of asphalt binders. *Journal of the Association of Asphalt Paving Technologists*, 64, 130–162.

Bai, F., Yang, X., & Zeng, G. (2016). A stochastic viscoelastic–viscoplastic constitutive model and its application to crumb rubber modified asphalt mixtures. Materials & Design, 89, 802-809.

Bernier, A., Zofka, A., & Yut, I. (2012). Laboratory evaluation of rutting susceptibility of polymer-modified asphalt mixtures containing recycled pavements. *Construction and Building Materials,* 31(0), 58-66.

Blazejowski, K. and Dolzycki, B. (2014) Relationships between Asphalt Mix Rutting Resistance and MSCR Test Results. *Design, Analysis, and Asphalt Material Characterization for Road and Airfield Pavements*: pp. 202-209.doi: 10.1061/9780784478462.025

Bonaquist, R., Churilla, C., Freund, D., "Effect o f Load, Tire Pressure, and Type of Flexible Pavement Response," *Public Roads,* Vol. 52, No. 1, June 1988, pp. 1-7.

Brown ER, Rajib BM, Haddock John E, Bukowski John. Performance of stone matrix asphalt (SMA) mixtures in the United States, *NCAT report* no. 97-1, Auburn University, AL; January 1997.

Brown, E. R., & Manglorkar, H. (1993). Evaluation of laboratory properties of SMA mixtures. *National Center for Asphalt Technology*, Report, (93-5), 159.

Brown, E.R. and Cross, S. (1989) A study of in-place rutting of asphalt pavements. *J. Asphalt Paving Techn.*, Association of Asphalt Paving Technologists, 58, 1–30.

Burlie, R., Uzarowski, L., & Emery, J. (2000). Use of stone mastic asphalt to mitigate reflective cracking. In E. H. Mohamed (Ed.), *Fourth International RILEM Conference on Reflective Cracking in Pavements-Research in Practice* (pp. 279-288). RILEM Publications SARL.

Burns, B. (2000). Rubber-modified asphalt paving binder. EP 0994161 A2, filed Oct 131999, and issued Apr 19, 2000.

Caltrans. Asphalt Rubber Usage Guide. s.l.: State of California Department ofTransportation, *Materials Engineering and Testing Services*; 2006.

Chehovits, J., 1993. Binder design procedures. Session 9.0, crumb rubber modifier workshop notes, Federal Highway Administration, Office of Technology Applications.

Chehovits, J., Dunning, R., and Morris, G., 1982. Characteristic of asphalt–rubber by the sliding plate microviscometer. *Journal of the Association of Asphalt Paving Technologists*,51, 241.

Chen, D. H., Won, M., Scullion, T., & Bilyeu, J. (2009). Minimizing Reflective Cracking With Applications of the Rolling Dynamic Deflectometer and Overlay Tester. *In National Conference on Preservation, Repair, and Rehabilitation of Concrete Pavements*.

Chen, D., Bilyeu, J., Scullion, T., Lin, Deng-Feng, and Zhou, Fujie (2002) Forensic evaluation of the premature failures of the SPS-1 sections, *Journal of Performance of Constructed Facility, ASCE*.

Cheovits JG, Dunning RL, Morris GR. Characteristics of asphalt-rubber by the slide plate microviscometer. *Association of Asphalt Paving Technologists*. vol.51. 1982. p. 240–61.

Chew S.H. and Thing W.H. NR in Malaysia roads. *Rubber in Engineering Conference*, Kuala Lumpur. 1974

Chong, P., Xun, P., Xing, M., & Chen, S. (2013). Investigation of asphalt binder containing various crumb rubbers and asphalts. *Construction and Building Materials*, 40(0), 632-641. doi: http://dx.doi.org/10.1016/j.conbuildmat.2012.11.063

Coleri, E., Harvey, J. T., Yang, K., & Boone, J. M. (2012). A micromechanical approach to investigate asphalt concrete rutting mechanisms. [doi: 10.1016/j.conbuildmat.2011.11.041]. *Construction and Building Materials*, 30(0), 36-49.

Coleri, E., Tsai, B.W., and Monismith, C.L. (2008). Pavement Rutting PerformancePrediction by Integrated Weibull Approach. In Transportation Research Record:Journal of the Transportation Research Board, No. 2087, *Transportation Research Board of the National Academies*, Washington, D.C., pp. 120–130.

D'Angelo J (2010) The multiple stress creep recovery (MSCR) procedure. Federal Highway Administration, Washington. http://onlinepubs.trb.org/onlinepubs/circulars/ec147.pdf

D'Angelo, J. (2008). "Multi-stress creep and recovery test method a new specification." *The Association of Modified Asphalt Producers*, St. Louis, MO.

D'Angelo, J., Kluttz, R., Dongré, R., Stephens, K., and Zanzotto, L. (2007). "Revision of the superpave high temperature binder specification: the multiple stress creep recovery test." *J. Assoc. Asphalt Paving Technol*., 76, 123–162.

De Zhang Huang. Brief analysis of causes and prevention measures ruttinggeneration of asphalt pavement. *J Fujian Mater* 2012;3(131):31–3.

Dehnad, M. H., Khodaii, A., & Moghadas Nejad, F. (2013). Moisture sensitivity of asphalt mixtures under different load frequencies and temperatures. *Construction and Building Materials*, 48(0), 700-707.

Domingos, M. D. I., & Faxina, A. L. (2014). Creep-recovery behavior of asphalt binders modified with SBS and PPA. Journal of Materials in Civil Engineering, 26(4), 781-783.

Dreessen, S., Planche, J. P., and Gardel, V. (2009). "A new performance related test method for rutting prediction: MSCRT." Advanced testing and characterization

of bituminous materials, A. Loizos, M. Partl, T. Scarpas, and I. L. Al-Qadi, eds., CRC Press, London, 971–980.

DuBois, E., Mehta, D. Y., & Nolan, A. (2014). Correlation between multiple stress creep recovery (MSCR) results and polymer modification of binder. Construction and Building Materials, 65(0), 184-190.

Eisenmann, J., & Hilmer, A. (1987). Influence of Wheel Load and Inflation Pressure on the Rutting Effect at Asphalt-Pavements: Experiments and Theoretical Investigation. *International Conference on the Structural Design*.

ERPA – European Recovered Paper Association (Belgium), 2010. European Declaration on Paper Recycling 2006–2010, Monitoring Report 2009. Retrieved from http://www.erpa.info/european0.html.

ETRMA - European Tyre & Rubber Manufacturers' Association (Belgium), 2010a. AValuable Resource with Growing Potential 2010 edition. Retrieved from http://www.etrma.org/default.asp

ETRMA – European Tyre & Rubber Manufacturers' Association (Belgium), 2010b.Used Tyres Recovery 2010 (table) – UT/Part Worn Tyres/ELT's Europe – VolumesSituation 2010, Retrieved from http://www.etrma.org/default.asp(May 2011).

ETRMA – European Tyre & Rubber Manufacturers' Association (Belgium), 2011. The Annual Report 2010/2011. Retrieved from http://www.etrma.org/ default.asp

ETRMA – European Tyre & Rubber Manufacturers' Association (Belgium), 2011b.End of life tyres , A valuable resource with growing potential. Retrieved from http://www.etrma.org/uploads/Modules/Documentsmanager/brochure-elt-2011-final.pdf

ETRMAstatistics. Retrieved from http://www.etrma.org/pdf/20101220%20Brochure%20ELT_2010_final%20version.pdf>; 2012.

Evonik Degussa GmbH in the brochure. High performance polymers 45764 Marl Germany

EvonikDegussaGmbH. Retrieved from http://www.vestenamer.com/sites/dc/Downloadcenter/Evonik/Product/VESTENAMER/en/brochures/ VESTENAMER%20Asphalt%20english.pdf.

FHWA. The multiple stress creep recovery (MSCR) procedure. Final report to Federal Highway Administration. Report no. FHWA-HIF-11-038; 2011.

Finn, F. N., Monismith, C. L., & Markevich, N. J. (1983). Pavement performance and asphalt concrete mix design. *In Proceedings of the Association of Asphalt Paving Technologists* (Vol. 52, pp. 121-150).

Flory, P.J. and Rehner, J. Jnr. (1943),"Statistical Mechanics of Cross-Linked Polymer Networks, Part I. Rubber Elasticity", *The Journal of Chemical Physics*, Vol 11, No. 11.

Fontes, L. P. T. L., Trichês, G., Pais, J. C., & Pereira, P. A. A., "Evaluating permanent deformation in asphalt rubber mixtures," *Construction and Building Materials*, 24(7), 1193-1200. doi: 10.1016/j.conbuildmat.2009.12.021,2010.

Gillespie, T. D. (1993). Effects of heavy-vehicle characteristics on pavement response and performance (No. 353). *Transportation Research Board*.

Gokhale, S., Choubane, B., Byron, T., & Tia, M. (2005). Rut initiation mechanisms in asphalt mixtures as generated under accelerated pavement testing. Transportation research record: *Journal of the transportation research board*, 136-145.

Goncalves, F. P., Ceratti, J. A., & Bernucci, L. B. (2002). Study of permanent deformations in asphalt concrete layers. *In Proceeding of 4 th European symposium on performance of bituminous and hydraulic materials in pavements*, Bitmat (Vol. 4).

Green, E. L. and Tolonen, W. J. (1977). "The Chemical and Physical Properties of Asphalt-Rubber Mixtures." Report ADOT-RS-14 (162), *Arizona Department of Transportation.*

Haddadi, S., Ghorbel, E., & Laradi, N. (2008). Effects of the manufacturing process on the performances of the bituminous binders modified with EVA. *Construction and Building Materials*, 22(6), 1212–1219.

Hamzah, M. O., & Teoh, C. Y. (2008). Effects Of Temperature On Resilient Modulus Of Dense Asphalt Mixtures Incorporating Steel Slag Subjected To Short Term Oven Ageing.

Hamzah, M. O., Jaya, R. P., Prasetijo, J., & Azizi, K. (2009). Effects of Temperature and Binder Type on the Dynamic Creep of Asphaltic Concrete.Modern *Applied Science*, 3(7), p3.

Han Zidong. Research on temperature field of road structure. D Xi an: Chang an Daxue; 2001.

Hassim, S., Harahap, R., Muniandy, R., Kadir, M., & Mahmud, A. (2005). Cost comparison between stone mastic asphalt and asphalt concrete wearing course. Am J Appl Sci, 2(9), 1350-5.

Hassim, Salihudin, et al. "Cost Comparison between Stone Mastic Asphalt and Asphalt Concrete Wearing Course." *American Journal of Applied Sciences* 2.9 (2005): 1350.

He, G. P., & Wong, W. G. (2007). Laboratory study on permanent deformation of foamed asphalt mix incorporating reclaimed asphalt pavement materials. Construction and Building Materials, 21(8), 1809-1819.

He, G. P., & Wong, W. G. (2008). Effects of moisture on strength and permanent deformation of foamed asphalt mix incorporating RAP materials. Construction and Building Materials, 22(1), 30-40.

Heitzman, M. (1991),"Design and Construction of Asphalt Paving Materials with Crumb Rubber Modifier", *Transportation Research Record* 1339, TRB, Washington, D.C., pp. 1-8.

Heitzman, M., (1992). State of the practice-design and construction of asphalt paving materials with crumb rubber modifier. USA: *Federal Highway Administration*, Report FHWA-SA-92-022.

Hicks, R. G., Cheng, D., & Duffy, T. (2010). Evaluation of rubberized asphalt terminal blends and a preliminary study on warm mix technologies with asphalt rubber-final summary report. Report No. CP2C-2010-104. *California Pavement Preservation Center*, May 2010. Retrieved from http://www.csuchico.edu/cp2c/documents/Report/CIWMB-Draft_Final_report_5-14-10.pdf

Hinislıoglu, S., & Agar, E. (2004). Use of waste high density polyethylene as bitumen modifier in asphalt concrete mix. *Materials Letters*, 58(3–4), 267–271.

İskender, E. (2013). Rutting evaluation of stone mastic asphalt for basalt and basalt–limestone aggregate combinations. *Composites Part B: Engineering*, 54(0), 255-264. doi: http://dx.doi.org/10.1016/j.compositesb.2013.05.019

JATMA – The Japan Automobile Tyre Manufacturers Association NC (Japan), 2010. Tyre Industry of Japan 2010, Retrieved from http://www.jatma.or.jp/ english/media/

JKR/SPJ/2008-S4 Standard Specification for Road Works Section 4: Flexible Pavament, *Public Works Department of Malaysia*

Jun, Q., & Xiaolei, L. (2008). Talking about application of SMA asphalt mixture on the highway. *Shanxi Architecture*, 34(25), 185-186.

Kaloush KE, Witczak MW , "Tertiary flow characteristics of asphalt mixtures," *Association of Asphalt Paving Technologists*, pp. 248-280,2002

Kaloush KE, Witczak MW, Way GB, "Performance evaluation of Arizona asphalt rubber mixtures using advanced dynamic material characterization tests," Department of Civil and Environmental Engineering, College of Engineering and Applied Sciences, *Arizona State University*, July 2002.

Kalyoncuoglu, S. F., & Tigdemir, M. (2011). A model for dynamic creep evaluation of SBS modified HMA mixtures. *Construction and Building Materials*, 25(2), 859-866

Kandhal, P. S., & Cooley, L. A. (2003). Accelerated laboratory rutting tests: Evaluation of the asphalt pavement analyzer (No. 508). *Transportation Research Board*.

Karim, M. R., Ibrahim, N. I., Saifizul, A. A., & Yamanaka, H. (2014). Effectiveness of vehicle weight enforcement in a developing country using weigh-in-motion sorting system considering vehicle by-pass and enforcement capability. *IATSS Research*, 37(2), 124-129.

Khodaii, A., & Mehrara, A. (2009). Evaluation of permanent deformation of unmodified and SBS modified asphalt mixtures using dynamic creep test. *Construction and Building Materials,* 23(7), 2586-2592.

Khodaii, A., Moghadas Nejad, F., Forough, S., and Saleh Ahari, A. (2014).Investigating the Effects of Loading Frequency and Temperature on Moisture Sensitivity of SBS-Modified Asphalt Mixtures. (2014). *Journal of Materials in Civil Engineering*, 26(5), 897-903. doi: doi:10.1061/(ASCE)MT.1943-5533.0000875

Kim, Y. R. (2008). Modeling of asphalt concrete.

Kök, B. V., Yilmaz, M., & Geçkil, A. (2012). Evaluation of low-temperature and elastic properties of crumb rubber–and SBS-modified bitumen and mixtures. *Journal of Materials in Civil Engineering*, 25(2), 257-265.

KPKT (2011). A study on scrap tyres management for peninsular Malaysia. National Solid Waste Mangement Department Ministry of Housing and Local Government.

Kronfuss, F., R. Krzemien, G. Nievelt, and P. Putz. (1984). Verformungsfestigkjeit yon Asphalten Ennitthmg im Kriechtest, Bundesministerium fur Bauten and Technik, Strassenforschung, Heft 240, Wien, Austria.

Kuloglu, N. (1999). Effect of astragalus on characteristics of asphalt concrete. *Journal of Materials in Civil Engineering*, 11(4), 283.

Lavin, P. (2003). Asphalt pavements: A practical guide to design, production and maintenance for engineers and architects. London: Spon.

Lee, S. J., Amirkhanian, S. N., Shatanawi, K., & Thodesen, C. (2008). Influence of compaction temperature on rubberized asphalt mixes and binders. *Canadian Journal of Civil Engineering*, 35(9), 908-917.

Lemarchand, C. A., Bailey, N. P., Todd, B. D., Daivis, P. J., & Hansen, J. S. (2015). Non-Newtonian behavior and molecular structure of Cooee bitumen under shear flow: a non-equilibrium molecular dynamics study. arXiv preprint arXiv:1501.00564.

Li, Q., Ni, F., Gao, L., Yuan, Q., & Xiao, Y. (2014). Evaluating the rutting resistance of asphalt mixtures using an advanced repeated load permanent deformation test under field conditions. *Construction and Building Materials*, 61(0), 241-251. doi: http://dx.doi.org/10.1016/j.conbuildmat.2014.02.052

Liu, H., Chen, Z., Wang, W., Wang, H., & Hao, P. (2014). Investigation of the rheological modification mechanism of crumb rubber modified asphalt (CRMA) containing TOR additive. *Construction and Building Materials*, 67, Part B(0), 225-233.

Liu, S., Cao, W., Fang, J., & Shang, S. (2009). Variance analysis and performance evaluation of different crumb rubber modified (CRM) asphalt. *Construction and Building Materials*, 23(7), 2701-2708.

Lo Presti, D. (2013). Recycled Tyre Rubber Modified Bitumens for road asphalt mixtures: A literature review. *Construction and Building Materials*, 49(0), 863-881. doi: http://dx.doi.org/10.1016/j.conbuildmat.2013.09.007

Lo Presti, D., Airey, G., & Partal, P. (2012). Manufacturing Terminal and Field Bitumen-Tyre Rubber Blends: The Importance of Processing Conditions. *Procedia - Social and Behavioral Sciences*, 53(0), 485-494. doi: http://dx.doi.org/10.1016/j.sbspro.2012.09.899

Luo, W.-q., & Chen, J.-c. (2011). Preparation and properties of bitumen modified by EVA graft copolymer. *Construction and Building Materials*, 25(4), 1830-1835.

Podolsky, J. H., Buss, A., Williams, R. C., & Cochran, E. W. (2016). The rutting and stripping resistance of warm and hot mix asphalt using bio-additives. *Construction and Building Materials*, 112, 128-139.

Solaimanian, M., Anderson, D., & Hunter, D. (2003). Evaluation of VESTENAMER reactive modifier in crumb rubber asphalt. Performance of Asphalt Binder and Asphalt Concrete. Modified by ground tire and VESTENAMER – a laboratory study. 379 Interpace Parkway, P.O. Box 677,Parsippany, NJ 07054-0677: *Degussa Corporation*; September 2003.

Mashaan, N. S., & Karim, M. R. (2013). Investigating the rheological properties of crumb rubber modified bitumen and its correlation with temperature susceptibility. *Materials Research*, 16(1), 116-127.

Meena, S., & Biligiri, K. P. (2016). Binder rheological predictive models to evaluate rutting performance of asphalt mixtures. *Construction and Building Materials*, 111, 556-564.

Mehrara, A., & Khodaii, A.(2011) , "Evaluation of Asphalt Mixtures' Moisture Sensitivity by Dynamic Creep Test," *Journal of Materials in Civil Engineering*, 23(2), 212-219. doi: doi:10.1061/(ASCE)MT.1943-5533.0000146,2011.

Metcalf, J. (1996). Application of Full-Scale Accelerated Pavement Testing. NationalCooperative Highway Program, Synthesis of Highway Practice 235.Brown, E., et al. ~1989!. ''A study of in-place rutting of asphalt pavements.*''J. Asphalt Paving Technol.*, 58, 1–30.

Min, K. E., & Jeong, H. M. (2013). Characterization of air-blown asphalt/trans-polyoctenamer rubber blends. *Journal of Industrial and Engineering Chemistry*, 19(2), 645-649. doi: http://dx.doi.org/10.1016/j.jiec.2012.09.017

Mirzahosseini, M. R., Aghaeifar, A., Alavi, A. H., Gandomi, A. H., & Seyednour, R. (2011). Permanent deformation analysis of asphalt mixtures using soft computing techniques. *Expert Systems with Applications*, 38(5), 6081-6100.

Mohamad Razali, O. and S. Zulakmal, 2004. Innovative pavements in Malaysia. *ISTAC Conf., Ikram*, Malaysia.

Mohammad, L. N. (2006). Performance Tests for Hot Mix Asphalt (HMA) Including Fundamental and Empirical Procedures (No. 1469). *ASTM International*.

Monismith CL, Ogawa N, Freeme CR. Permanent deformation of subgrade soils due to repeated loadings. *Transport Res Rec* 1975;537:1–17.

Muniady, R., S. Ali and O. Husaini, 2000. Laboratory evaluation of cellulose oil palm fiber for stone mastic asphalt mixes. *Intl. J. Pavements*, 1: 13-21.

Navarro F. J., Partal P., Martinez-Boza F., Gallegos C., (2004) "Thermo-rheological behaviour and storage stability of ground tyre rubber-modified bitumens", *Fuel*, Volume 83, Issues 14-15.

Neto, S. A. D., Farias, M. M., Pais, J. C., Pereira, P. A. A., & Sousa, J. B. (2006). Influence of Crumb Rubber and Digestion Time on the Asphalt Rubber Binders. *Road Materials and Pavement Design*, 7(2), 131-148.

Ng Puga, K. L. N. (2013). Rheology and performance evaluation of Polyoctenamer as Asphalt Rubber modifier in Hot Mix Asphalt, *M.Sc. Dissertation*, Iowa State University

Ng Puga, K. L. N., & Williams, R. C. (2016). Low temperature performance of laboratory produced asphalt rubber (AR) mixes containing polyoctenamer. *Construction and Building Materials*, 112, 1046-1053.

Nuha Salim Mashaan, Asim H. Ali, Suhana Koting, and Mohamed Rehan Karim, "Dynamic Properties and Fatigue Life of Stone Mastic Asphalt Mixtures Reinforced with Waste Tyre Rubber," *Advances in Materials Science and Engineering*, vol. 2013, Article ID 319259, 9 pages, 2013. doi:10.1155/2013/319259

Nuha Salim Mashaan, Asim H. Ali, Suhana Koting, and Mohamed Rehan Karim, "Performance Evaluation of Crumb Rubber Modified Stone Mastic Asphalt Pavement in Malaysia," *Advances in Materials Science and Engineering*, vol. 2013, Article ID 304676, 8 pages, 2013. doi:10.1155/2013/304676

Nuha Salim Mashaan, Mohamed Rehan Karim, Mahrez Abdel Aziz, Mohd Rasdan Ibrahim, Herda Yati Katman, and Suhana Koting, "Evaluation of Fatigue Life of CRM-Reinforced SMA and Its Relationship to Dynamic Stiffness," *The Scientific World Journal*, vol. 2014, Article ID 968075, 11 pages, 2014. doi:10.1155/2014/968075

Nuñez, J. Y. M., Domingos, M. D. I., & Faxina, A. L. (2014). Susceptibility of low-density polyethylene and polyphosphoric acid-modified asphalt binders to rutting and fatigue cracking. *Construction and Building Materials*, 73(0), 509-514.

Oliver, J.W.H. (1981) "Modification of Paving Asphalts by Digestion with Scrap Rubber", *Transportation Research Record* 821, TRB.

Ou La, Xiao Jingjing. Design composition of SMA asphalt mixture. *J Anhui Arch* 2009;164(1):103–5.

Paterson, W.D.O., 1987, Road Deterioration and Maintenance Effects: Models for Planning and Management, *World Bank*, Washington, D.C.

Pavlovich, R., Shuler, T., and Rosner, J., 1979. Chemical & physical properties of asphalt-rubber, phase II product specification and test procedures. Arizona: *Arizona Department of Transportation*, FHWA/AZ-79/121.

Pérez, I., Medina, L., & Romana, M. G. (2006). Permanent deformation models for a granular material used in road pavements. *Construction and Building Materials*, 20(9), 790-800.

Plemons, C. D. (2013). Evaluation of the effect of crumb rubber properties on the performance of asphalt binder, *Doctoral dissertation*, Auburn University, Auburn, Alabama

Read, J and Whiteoak, D (2003). "Shell Bitumen Handbook." 5th. Ed. London

RMA – Rubber Manufacturers Association (USA), 2009. Scrap Tire Markets in the United States 9th Biennial Report. Retrieved from http:// www.rma.org/scrap_tires/

Sandra Kumar (2006), Waste Tyre Management in Malaysia, *PhD Thesis*, Universiti Putra Malaysia

Shafabakhsh, G. H., Sadeghnejad, M., & Sajed, Y. (2014). Case study of rutting performance of HMA modified with waste rubber powder. *Case Studies in Construction Materials*, 1(0), 69-76. doi: http://dx.doi.org/10.1016/j.cscm.2014.04.005

Shatanawi, K. M., Biro, S., Geiger, A., & Amirkhanian, S. N. (2012). Effects of furfural activated crumb rubber on the properties of rubberized asphalt. [doi: 10.1016/j.conbuildmat.2011.08.041]. *Construction and Building Materials*, 28(1), 96-103.

Singleton, T.M., Airey, G.D. and Collop, A.C. (2000), "Effect of Rubber-Bitumen Interaction on the Mechanical Durability of Impact Absorbing Asphalt", *Proceedings of the 2nd Eurasphalt and Eurobitume Congress*, Vol. 4, Barcelona, pp. 1053-1060.

Solaimanian, M., Anderson, D., & Hunter, D. (2003). Evaluation of VESTENAMER reactive modifier in crumb rubber asphalt. Performance of Asphalt Binder and Asphalt Concrete. Modified by ground tire and VESTENAMER – a laboratory study. 379 Interpace Parkway, P.O. Box 677,Parsippany, NJ 07054-0677: *Degussa Corporation*; September 2003.

Song Xiaoyan, Du Yuezong. Thermodynamic analysis of the stability of thepolymer modified asphalt. *J Petrol Asphalt* 2004;3:40–5.

Sousa, J. B., Craus, J., & Monismith, C. L. (1991). Summary report on permanent deformation in asphalt concrete. *Strategic highway research program (No. SHRP-A-318).* Berkeley: National Research Council, Institute of Transportation Studies, University of California.

Sousa, J.B., Deacon, J.A., Weissman, S., Harvey, J.T. and Monismith, C.L. (1994) Permanent Deformation Response of Asphalt Aggregate Mixes Report SHRP-A-415, *Strategic Highway Research Program*, National Research Council, Washington, D.C., p 437.

Takallou, H.B. and Hicks, R.G. (1988),"Development of Improved Mix and Construction Guidelines for Rubber-Modified Asphalt Pavement", *Transportation Research Record* 1171, Transportation Research Board, Washington D.C.

Tanco, A. J., 1992, "Permanent Deformation Response of Conventional and ModifiedAsphalt-Aggregate Mixes under Simple and Compound Shear Loading Conditions,"*Ph.D. thesis*, University of California, Berkeley.

Tapkın, S., & Keskin, M. (2013). Rutting analysis of 100 mm diameter polypropylene modified asphalt specimens using gyratory and Marshall compactors. *Materials Research*, 16(2), 546-564.

Tapkin, S., Çevik, A., Uşar, Ü., & Gülşan, E. (2013). Rutting prediction of asphalt mixtures modified by polypropylene fibers via repeated creep testing by utilising genetic programming. *Materials Research*, 16(2), 277-292

Tayebali, A. A., 1990, "Influence of Rheological Properties of Modified Asphalt Binders on the Load-Deformation Characteristics of the Binder-Aggregate Mixtures," *Ph.D. thesis*, University of California, Berkeley

Vaitkus, A., & Paliukaitė, M. (2013). Evaluation of Time Loading Influence on Asphalt Pavement Rutting. *Procedia Engineering*, 57(0), 1205-1212. doi: http://dx.doi.org/10.1016/j.proeng.2013.04.152

Van Thanh, D., & Feng, C. P. (2013). Study on Marshall and Rutting test of SMA at abnormally high temperature. *Construction and Building Materials*, 47(0), 1337-1341. doi: http://dx.doi.org/10.1016/j.conbuildmat.2013.06.032

Vasudevan, J., R. Muniady, O. Husaini and R.S. Radin Omar, 2000. Cellulose oil palm fiber (COPF) in stone mastic asphalt for Malaysian roads. *Proc. 4th Malaysian Road Conf*. Kuala Lumpur: REAAM.

Viljoen, A.W., and K. Meadows. (1981). Creep Test - A Mix Design Tool to Rank Asphalt Mixes in Terms of Their Resistance to Permanent Deformation Under Heavy Traffic, *National Institute for Transport and Road Research*, Pretoria, South Africa, Technical Note TP-36-81.

Waller, H. F. (1993). Use of waste materials in hot-mix asphalt (Vol. 1193). Astm International.

Whiteoak D, Read JM. The shell bitumen handbook. London: *Thomas Telford Services Ltd*.; 2003.

Willis, J. R., Turner, P., Plemmons, C., Rodezno, C., Rosenmayer, T., Daranga, C., et al. (2013). Effect of rubber characteristics on asphalt binder properties. Paper presented at the *Asphalt Paving Technology*: Association of Asphalt Paving Technologists-Proceedings of the Technical Sessions.

Xiao, F., Amirkhanian, S., & Juang, C. H. (2007). Rutting resistance of rubberized asphalt concrete pavements containing reclaimed asphalt pavement mixtures. Journal of Materials in Civil Engineering, 19(6), 475-483.

Xiao, F., Amirkhanian, S. N., Shen, J., & Putman, B. (2009). Influences of crumb rubber size and type on reclaimed asphalt pavement (RAP) mixtures. *Construction and Building Materials*, 23(2), 1028-1034.

Xie, Z., & Shen, J. (2014). Effect of cross-linking agent on the properties of asphalt rubber. *Construction and Building Materials*, 67, Part B(0), 234-238. doi: http://dx.doi.org/10.1016/j.conbuildmat.2014.03.039

Xie, Z., & Shen, J. (2016). Performance properties of rubberized stone matrix asphalt mixtures produced through different processes. *Construction and Building Materials*, 104, 230-234.

Xu, Y., & Sun, L. (2013). Study on Permanent Deformation of Asphalt Mixtures by Single Penetration Repeated Shear Test. Procedia - *Social and Behavioral Sciences*, 96(0), 886-893. doi: http://dx.doi.org/10.1016/j.sbspro.2013.08.101

Xu, O., Xiao, F., Han, S., Amirkhanian, S. N., & Wang, Z. (2016). High temperature rheological properties of crumb rubber modified asphalt binders with various modifiers. *Construction and Building Materials*, 112, 49-58.

Xue, Y., Hou, H., Zhu, S., & Zha, J. (2009). Utilization of municipal solid waste incineration ash in stone mastic asphalt mixture: Pavement performance and environmental impact. *Construction and Building Materials*, 23(2), 989-996.

Yadollahi, G., & Mollahosseini, H. S. (2011). Improving the performance of Crumb Rubber bitumen by means of Poly Phosphoric Acid (PPA) and Vestenamer additives. *Construction and Building Materials*, 25(7), 3108-3116.

Yang, X., & You, Z. (2015). High temperature performance evaluation of bio-oil modified asphalt binders using the DSR and MSCR tests. *Construction and Building Materials*, 76(0), 380-387.

Yildirim, Y. (2007). Polymer modified asphalt binders. *Construction and Building Materials*, 21(1), 66-72.

Yu, J., 2000. Stone Mastic Asphalt pavement technology for the new millennium. *The 4th Malaysian Road Conf.* Kuala Lumpur: REAAM.

Yu Ji (2015). Overloaded trucks damaging public infrastructure and endangering travellers, *The Star Online*. Retrieved from

http://www.thestar.com.my/News/Nation/2015/08/03/Lori-hantu-haunting-dam-roads-Overloaded-trucks-damaging-public-infrastructure-and-endangering-trave/

Zhang Min, Zou Guilian, Hu Jin Long, Wan Taotao, Peng Xiao Lin. Analysisinfluencing factors of rutting resistance of asphalt mixture. *J Sci Technol* Eng2012;12(12):3015–8.

Zhang, J., Alvarez, A. E., Lee, S. I., Torres, A., & Walubita, L. F. (2013). Comparison of flow number, dynamic modulus, and repeated load tests for evaluation of HMA permanent deformation. *Construction and Building Materials*, 44(0), 391-398. doi: http://dx.doi.org/10.1016/j.conbuildmat.2013.03.013

Zhou, F., & Scullion, T. (2002). Discussion: Three Stages of Permanent Deformation Curve and Rutting Model. *International Journal of Pavement Engineering*, 3(4), 251-260. doi: 10.1080/1029843021000083676

Zhou, F., & Scullion, T. (2003). Preliminary field validation of simple performance tests for permanent deformation: case study. *Transportation Research Record:* Journal of the Transportation Research Board, 1832(1), 209-216.

Zhou, F., Chen, D. H., Scullion, T., & Bilyeu, J. (2003). Case study: Evaluation of laboratory test methods to characterize permanent deformation properties of asphalt mixes. *International Journal of Pavement Engineering*, 4(3), 155-164.

Zhou, F., Scullion, T., & Sun, L. (2004). Verification and Modeling of Three-Stage Permanent Deformation Behavior of Asphalt Mixes. *Journal of Transportation Engineering*, 130(4), 486-494. doi: doi:10.1061/(ASCE)0733-947X(2004)130:4(486)

Zhu, T., Ma, T., Huang, X., & Wang, S. (2016). Evaluating the rutting resistance of asphalt mixtures using a simplified triaxial repeated load test. *Construction and Building Materials*, 116, 72-78.

Zoorob, S. E., Castro-Gomes, J. P., Pereira Oliveira, L. A., & O'Connell, J. (2012). Investigating the Multiple Stress Creep Recovery bitumen characterisation test. *Construction and Building Materials*, 30(0), 734-745.

Appendix A: Statistical Test Analysis Results

Table A.1a Stepwise Multiple Linear Regression on Penetration Value (Model Summary)

Model	R	R Square	Adjusted R Square	Std. Error of the Estimate	Change Statistics				
					R Square Change	F Change	df1	df2	Sig. F Change
1	.778[a]	.605	.600	5.21407	.605	125.428	1	82	.000
2	.838[b]	.703	.696	4.54786	.098	26.784	1	81	.000

a. Predictors: (Constant), Rubber content, %
b. Predictors: (Constant), Rubber content, %, Transpolyoctenamer content, %

Table A.1b Stepwise Multiple Linear Regression on Penetration Value (ANOVA)

Model		Sum of Squares	df	Mean Square	F	Sig.
1	Regression	3409.944	1	3409.944	125.428	.000[a]
	Residual	2229.294	82	27.187		
	Total	5639.238	83			
2	Regression	3963.913	2	1981.957	95.825	.000[b]
	Residual	1675.325	81	20.683		
	Total	5639.238	83			

a. Predictors: (Constant), Rubber content, %
b. Predictors: (Constant), Rubber content, %, Transpolyoctenamer content, %
c. Dependent Variable: Penetration value (0.1 mm)

Table A.1c Stepwise Multiple Linear Regression on Penetration Value (Coefficients)

Model		Unstandardized Coefficients		Standardized Coefficients	t	Sig.	Correlations			Collinearity Statistics	
		B	Std. Error	Beta			Zero-order	Partial	Part	Tolerance	VIF
1	(Constant)	82.105	1.085		75.696	.000					
	Rubber content, %	-1.180	.105	-.778	-11.199	.000	-.778	-.778	-.778	1.000	1.000
2	(Constant)	84.678	1.069		79.228	.000					
	Rubber content, %	-1.242	.093	-.818	-13.400	.000	-.778	-.830	-.812	.983	1.017
	Transpolyoctenamer content, %	-1.185	.229	-.316	-5.175	.000	-.211	-.498	-.313	.983	1.017

a. Dependent Variable: Penetration value (0.1 mm)

Table A.1d Stepwise Multiple Linear Regression on Penetration Value (Excluded Variables)

Model		Beta In	t	Sig.	Partial Correlation	Collinearity Statistics		
						Tolerance	VIF	Minimum Tolerance
1	Transpolyoctenamer content, %	-.316[a]	-5.175	.000	-.498	.983	1.017	.983
	Blending types	-.126[a]	-1.077	.285	-.119	.352	2.843	.352
2	Blending types	-.093[b]	-.907	.367	-.101	.350	2.855	.346

a. Predictors in the Model: (Constant), Rubber content, %
b. Predictors in the Model: (Constant), Rubber content, %, Transpolyoctenamer content, %
c. Dependent Variable: Penetration value (0.1 mm)

Table A.2a Stepwise Multiple Linear Regression on Softening Point Value (Model Summary)

Model	R	R Square	Adjusted R Square	Std. Error of the Estimate	Change Statistics				
					R Square Change	F Change	df1	df2	Sig. F Change
1	.922[a]	.850	.845	1.47429	.850	192.270	1	34	.000
2	.931[b]	.867	.859	1.40959	.017	4.193	1	33	.049

a. Predictors: (Constant), Rubber content, %
b. Predictors: (Constant), Rubber content, %, Blending types

Table A.2b Stepwise Multiple Linear Regression on Softening Point Value (ANOVA)

Model		Sum of Squares	df	Mean Square	F	Sig.
1	Regression	417.905	1	417.905	192.270	.000[a]
	Residual	73.900	34	2.174		
	Total	491.806	35			
2	Regression	426.237	2	213.118	107.260	.000[b]
	Residual	65.569	33	1.987		
	Total	491.806	35			

a. Predictors: (Constant), Rubber content, %
b. Predictors: (Constant), Rubber content, %, Blending types
c. Dependent Variable: Softening point value (°C)

Table A.2c Stepwise Multiple Linear Regression on Softening Point Value (Coefficients)

Model		Unstandardized Coefficients		Standardized Coefficients	t	Sig.	Correlations			Collinearity Statistics	
		B	Std. Error	Beta			Zero-order	Partial	Part	Tolerance	VIF
1	(Constant)	43.784	.441		99.299	.000					
	Rubber content, %	.519	.037	.922	13.866	.000	.922	.922	.922	1.000	1.000
2	(Constant)	46.453	1.370		33.919	.000					
	Rubber content, %	.673	.083	1.196	8.074	.000	.922	.815	.513	.184	5.429
	Blending types	-1.978	.966	-.303	-2.048	.049	.777	-.336	-.130	.184	5.429

a. Dependent Variable: Softening point value (°C)

Table A.2d Stepwise Multiple Linear Regression on Softening Point Value (Excluded Variables)

Model		Beta In	t	Sig.	Partial Correlation	Collinearity Statistics		
						Tolerance	VIF	Minimum Tolerance
1	Transpolyoctenamer content, %	.112[a]	1.692	.100	.283	.963	1.038	.963
	Blending types	-.303[a]	-2.048	.049	-.336	.184	5.429	.184
2	Transpolyoctenamer content, %	.123[b]	1.979	.057	.330	.957	1.045	.180

a. Predictors in the Model: (Constant), Rubber content, %
b. Predictors in the Model: (Constant), Rubber content, %, Blending types
c. Dependent Variable: Softening point value (°C)

Table A.3a Stepwise Multiple Linear Regression on Apparent Viscosity (Model Summary)

Model	R	R Square	Adjusted R Square	Std. Error of the Estimate	Change Statistics				
					R Square Change	F Change	df1	df2	Sig. F Change
1	.778[a]	.605	.598	77.40966	.605	91.918	1	60	.000
2	.853[b]	.728	.719	64.75817	.123	26.734	1	59	.000
3	.916[c]	.840	.831	50.14757	.112	40.388	1	58	.000

a. Predictors: (Constant), Rubber content, %
b. Predictors: (Constant), Rubber content, %, Blending types
c. Predictors: (Constant), Rubber content, %, Blending types, Transpolyoctenamer content, %

Table A.3b Stepwise Multiple Linear Regression on Apparent Viscosity (ANOVA)

Model		Sum of Squares	df	Mean Square	F	Sig.
1	Regression	550798.256	1	550798.256	91.918	.000[a]
	Residual	359535.313	60	5992.255		
	Total	910333.569	61			
2	Regression	662909.919	2	331454.960	79.038	.000[b]
	Residual	247423.649	59	4193.621		
	Total	910333.569	61			
3	Regression	764476.377	3	254825.459	101.331	.000[c]
	Residual	145857.192	58	2514.779		
	Total	910333.569	61			

a. Predictors: (Constant), Rubber content, %
b. Predictors: (Constant), Rubber content, %, Blending types
c. Predictors: (Constant), Rubber content, %, Blending types, Transpolyoctenamer content, %
d. Dependent Variable: Viscosity value at 175°C (mPas)

Table A.3c Stepwise Multiple Linear Regression on Apparent Viscosity (Coefficients)

Model		Unstandardized Coefficients		Standardized Coefficients	t	Sig.	Correlations			Collinearity Statistics	
		B	Std. Error	Beta			Zero-order	Partial	Part	Tolerance	VIF
1	(Constant)	59.629	20.941		2.847	.006					
	Rubber content, %	19.910	2.077	.778	9.587	.000	.778	.778	.778	1.000	1.000
2	(Constant)	329.965	55.141		5.984	.000					
	Rubber content, %	30.375	2.667	1.187	11.388	.000	.778	.829	.773	.424	2.357
	Blending types	-181.754	35.152	-.539	-5.170	.000	.362	-.558	-.351	.424	2.357
3	(Constant)	301.582	42.933		7.024	.000					
	Rubber content, %	31.863	2.079	1.245	15.328	.000	.778	.896	.806	.419	2.388
	Blending types	-196.627	27.322	-.583	-7.197	.000	.362	-.687	-.378	.421	2.375
	Transpolyoctenamer content, %	18.189	2.862	.336	6.355	.000	.245	.641	.334	.987	1.013

a. Dependent Variable: Viscosity value at 175°C (mPas)

Table A.3d Stepwise Multiple Linear Regression on Apparent Viscosity (Excluded Variables)

Model		Beta In	t	Sig.	Partial Correlation	Collinearity Statistics		
						Tolerance	VIF	Minimum Tolerance
1	Transpolyoctenamer content, %	.304[a]	4.222	.000	.482	.995	1.005	.995
	Blending types	-.539[a]	-5.170	.000	-.558	.424	2.357	.424
2	Transpolyoctenamer content, %	.336[b]	6.355	.000	.641	.987	1.013	.419

a. Predictors in the Model: (Constant), Rubber content, %
b. Predictors in the Model: (Constant), Rubber content, %, Blending types
c. Dependent Variable: Viscosity value at 175°C (mPas)

Table A.4a Stepwise Multiple Linear Regression on Non-Recoverable Compliance (Model Summary)

Model	R	R Square	Adjusted R Square	Std. Error of the Estimate	Change Statistics				
					R Square Change	F Change	df1	df2	Sig. F Change
1	.897[a]	.805	.796	.0040562	.805	90.961	1	22	.000
2	.938[b]	.880	.868	.0032608	.075	13.042	1	21	.002
3	.951[c]	.903	.889	.0029946	.024	4.900	1	20	.039

a. Predictors: (Constant), Rubber content (%)
b. Predictors: (Constant), Rubber content (%), Transpolyoctenamer content (%)
c. Predictors: (Constant), Rubber content (%), Transpolyoctenamer content (%), Blending types

Table A.4b Stepwise Multiple Linear Regression on Non-Recoverable Compliance (ANOVA)

Model		Sum of Squares	df	Mean Square	F	Sig.
1	Regression	.001	1	.001	90.961	.000[a]
	Residual	.000	22	.000		
	Total	.002	23			
2	Regression	.002	2	.001	76.896	.000[b]
	Residual	.000	21	.000		
	Total	.002	23			
3	Regression	.002	3	.001	62.417	.000[c]
	Residual	.000	20	.000		
	Total	.002	23			

a. Predictors: (Constant), Rubber content (%)
b. Predictors: (Constant), Rubber content (%), Transpolyoctenamer content (%)
c. Predictors: (Constant), Rubber content (%), Transpolyoctenamer content (%), Blending types
d. Dependent Variable: Non-recoverable compliance

Table A.4c Stepwise Multiple Linear Regression on Non-Recoverable Compliance (Coefficients)

Model		Unstandardized Coefficients		Standardized Coefficients	t	Sig.	Correlations			Collinearity Statistics	
		B	Std. Error	Beta			Zero-order	Partial	Part	Tolerance	VIF
1	(Constant)	.023	.001		15.882	.000					
	Rubber content (%)	-.001	.000	-.897	-9.537	.000	-.897	-.897	-.897	1.000	1.000
2	(Constant)	.025	.001		19.315	.000					
	Rubber content (%)	-.001	.000	-.916	-12.078	.000	-.897	-.935	-.914	.996	1.004
	Transpolyoctenamer content (%)	-.001	.000	-.274	-3.611	.002	-.213	-.619	-.273	.996	1.004
3	(Constant)	.018	.003		5.251	.000					
	Rubber content (%)	-.002	.000	-1.178	-8.563	.000	-.897	-.886	-.595	.255	3.924
	Transpolyoctenamer content (%)	-.001	.000	-.291	-4.157	.000	-.213	-.681	-.289	.983	1.017
	Blending types	.005	.002	.304	2.214	.039	-.710	.444	.154	.256	3.907

a. Dependent Variable: Non-recoverable compliance

Table A.4d Stepwise Multiple Linear Regression on Non-Recoverable Compliance (Excluded Variables)

Model		Beta In	t	Sig.	Partial Correlation	Collinearity Statistics		
						Tolerance	VIF	Minimum Tolerance
1	Transpolyoctenamer content (%)	-.274[a]	-3.611	.002	-.619	.996	1.004	.996
	Blending types	.239[a]	1.317	.202	.276	.259	3.857	.259
2	Blending types	.304[b]	2.214	.039	.444	.256	3.907	.255

a. Predictors in the Model: (Constant), Rubber content (%)
b. Predictors in the Model: (Constant), Rubber content (%), Transpolyoctenamer content (%)
c. Dependent Variable: Non-recoverable compliance

Table A.5a Stepwise Multiple Linear Regression on Voids in Mix (Model Summary)

Model	R	R Square	Adjusted R Square	Std. Error of the Estimate	Change Statistics				
					R Square Change	F Change	df1	df2	Sig. F Change
1	.897a	.804	.803	.78924	.804	893.099	1	218	.000
2	.960b	.922	.921	.49812	.118	330.280	1	217	.000
3	.965c	.932	.931	.46817	.009	29.648	1	216	.000

a. Predictors: (Constant), Binder content (%)
b. Predictors: (Constant), Binder content (%), Rubber content (%)
c. Predictors: (Constant), Binder content (%), Rubber content (%), Transpolyoctenamer content (%)

Table A.5b Stepwise Multiple Linear Regression on Voids in Mix (ANOVA)

Model		Sum of Squares	df	Mean Square	F	Sig.
1	Regression	556.306	1	556.306	893.099	.000[a]
	Residual	135.791	218	.623		
	Total	692.097	219			
2	Regression	638.255	2	319.127	1286.186	.000[b]
	Residual	53.842	217	.248		
	Total	692.097	219			
3	Regression	644.753	3	214.918	980.538	.000[c]
	Residual	47.344	216	.219		
	Total	692.097	219			

a. Predictors: (Constant), Binder content (%)
b. Predictors: (Constant), Binder content (%), Rubber content (%)
c. Predictors: (Constant), Binder content (%), Rubber content (%), Transpolyoctenamer content (%)
d. Dependent Variable: Voids in mix (%)

Table A.5c Stepwise Multiple Linear Regression on Voids in Mix (Coefficients)

Model		Unstandardized Coefficients		Standardized Coefficients	t	Sig.	Correlations			Collinearity Statistics	
		B	Std. Error	Beta			Zero-order	Partial	Part	Tolerance	VIF
1	(Constant)	17.483	.403		43.352	.000					
	Binder content (%)	-1.987	.066	-.897	-29.885	.000	-.897	-.897	-.897	1.000	1.000
2	(Constant)	16.643	.259		64.338	.000					
	Binder content (%)	-1.985	.042	-.896	-47.311	.000	-.897	-.955	-.896	1.000	1.000
	Rubber content (%)	.113	.006	.344	18.174	.000	.346	.777	.344	1.000	1.000
3	(Constant)	16.685	.243		68.590	.000					
	Binder content (%)	-1.975	.039	-.891	-50.023	.000	-.897	-.959	-.890	.998	1.002
	Rubber content (%)	.116	.006	.355	19.812	.000	.346	.803	.353	.988	1.012
	Transpolyoctenamer content (%)	-.080	.015	-.098	-5.445	.000	-.101	-.347	-.097	.986	1.014

a. Dependent Variable: Voids in mix (%)

Table A.5d Stepwise Multiple Linear Regression on Voids in Mix (Excluded Variables)

Model		Beta In	t	Sig.	Partial Correlation	Collinearity Statistics		
						Tolerance	VIF	Minimum Tolerance
1	Rubber content (%)	.344[a]	18.174	.000	.777	1.000	1.000	1.000
	Transpolyoctenamer content (%)	-.059[a]	-1.981	.049	-.133	.998	1.002	.998
	Blending types	.264[a]	10.943	.000	.596	1.000	1.000	1.000
2	Transpolyoctenamer content (%)	-.098[b]	-5.445	.000	-.347	.986	1.014	.986
	Blending types	-.101[b]	-2.856	.005	-.191	.279	3.588	.279
3	Blending types	-.064[c]	-1.869	.063	-.126	.266	3.764	.266

a. Predictors in the Model: (Constant), Binder content (%)
b. Predictors in the Model: (Constant), Binder content (%), Rubber content (%)
c. Predictors in the Model: (Constant), Binder content (%), Rubber content (%), Transpolyoctenamer content (%)
d. Dependent Variable: Voids in mix (%)

Table A.6a Stepwise Multiple Linear Regression on Voids in Mineral Aggregates (Model Summary)

Model	R	R Square	Adjusted R Square	Std. Error of the Estimate	Change Statistics				
					R Square Change	F Change	df1	df2	Sig. F Change
1	.700[a]	.490	.487	.50447	.490	209.202	1	218	.000
2	.792[b]	.627	.624	.43206	.138	80.183	1	217	.000
3	.825[c]	.681	.677	.40067	.054	36.339	1	216	.000
4	.832[d]	.692	.686	.39475	.011	7.521	1	215	.007

a. Predictors: (Constant), Rubber content (%)
b. Predictors: (Constant), Rubber content (%), Binder content (%)
c. Predictors: (Constant), Rubber content (%), Binder content (%), Transpolyoctenamer content (%)
d. Predictors: (Constant), Rubber content (%), Binder content (%), Transpolyoctenamer content (%), Blending types

Table A.6b Stepwise Multiple Linear Regression on Voids in Mineral Aggregates (ANOVA)

Model		Sum of Squares	df	Mean Square	F	Sig.
1	Regression	53.239	1	53.239	209.202	.000[a]
	Residual	55.478	218	.254		
	Total	108.717	219			
2	Regression	68.207	2	34.104	182.686	.000[b]
	Residual	40.509	217	.187		
	Total	108.717	219			
3	Regression	74.041	3	24.680	153.738	.000[c]
	Residual	34.676	216	.161		
	Total	108.717	219			
4	Regression	75.213	4	18.803	120.665	.000[d]
	Residual	33.504	215	.156		
	Total	108.717	219			

a. Predictors: (Constant), Rubber content (%)
b. Predictors: (Constant), Rubber content (%), Binder content (%)
c. Predictors: (Constant), Rubber content (%), Binder content (%), Transpolyoctenamer content (%)
d. Predictors: (Constant), Rubber content (%), Binder content (%), Transpolyoctenamer content (%), Blending types
e. Dependent Variable: Voids in mineral aggregate (%)

Table A.6c Stepwise Multiple Linear Regression on Voids in Mineral Aggregates (Coefficients)

Model		Unstandardized Coefficients		Standardized Coefficients	t	Sig.	Correlations			Collinearity Statistics	
		B	Std. Error	Beta			Zero-order	Partial	Part	Tolerance	VIF
1	(Constant)	18.227	.057		317.547	.000					
	Rubber content (%)	.091	.006	.700	14.464	.000	.700	.700	.700	1.000	1.000
2	(Constant)	16.266	.224		72.492	.000					
	Rubber content (%)	.091	.005	.701	16.907	.000	.700	.754	.701	1.000	1.000
	Binder content (%)	.326	.036	.371	8.955	.000	.370	.519	.371	1.000	1.000
3	(Constant)	16.306	.208		78.323	.000					
	Rubber content (%)	.094	.005	.726	18.778	.000	.700	.787	.722	.988	1.012
	Binder content (%)	.335	.034	.382	9.930	.000	.370	.560	.382	.998	1.002
	Transpolyoctenamer content (%)	-.076	.013	-.233	-6.028	.000	-.137	-.379	-.232	.986	1.014
4	(Constant)	16.689	.248		67.247	.000					
	Rubber content (%)	.116	.009	.894	12.371	.000	.700	.645	.468	.274	3.647
	Binder content (%)	.332	.033	.378	9.954	.000	.370	.562	.377	.996	1.004
	Transpolyoctenamer content (%)	-.069	.013	-.210	-5.383	.000	-.137	-.345	-.204	.940	1.064
	Blending types	-.286	.104	-.201	-2.742	.007	.508	-.184	-.104	.266	3.764

a. Dependent Variable: Voids in mineral aggregate (%)

Table A.6d Stepwise Multiple Linear Regression on Voids in Mineral Aggregates (Excluded Variables)

Model		Beta In	t	Sig.	Partial Correlation	Collinearity Statistics		
						Tolerance	VIF	Minimum Tolerance
1	Transpolyoctenamer content (%)	-.215[a]	-4.622	.000	-.299	.988	1.012	.988
	Binder content (%)	.371[a]	8.955	.000	.519	1.000	1.000	1.000
	Blending types	-.308[a]	-3.448	.001	-.228	.279	3.585	.279
2	Transpolyoctenamer content (%)	-.233[b]	-6.028	.000	-.379	.986	1.014	.986
	Blending types	-.287[b]	-3.762	.000	-.248	.279	3.588	.279
3	Blending types	-.201[c]	-2.742	.007	-.184	.266	3.764	.266

a. Predictors in the Model: (Constant), Rubber content (%)
b. Predictors in the Model: (Constant), Rubber content (%), Binder content (%)
c. Predictors in the Model: (Constant), Rubber content (%), Binder content (%), Transpolyoctenamer content (%)
d. Dependent Variable: Voids in mineral aggregate (%)

Table A.7a Stepwise Multiple Linear Regression on Stability (Model Summary)

Model	R	R Square	Adjusted R Square	Std. Error of the Estimate	Change Statistics				
					R Square Change	F Change	df1	df2	Sig. F Change
1	.327[a]	.107	.099	.74088	.107	13.626	1	114	.000
2	.464[b]	.215	.201	.69748	.109	15.628	1	113	.000
3	.505[c]	.255	.235	.68275	.039	5.928	1	112	.016

a. Predictors: (Constant), Blending types
b. Predictors: (Constant), Blending types, Transpolyoctenamer content (%)
c. Predictors: (Constant), Blending types, Transpolyoctenamer content (%), Rubber content (%)

Table A.7b Stepwise Multiple Linear Regression on Stability (ANOVA)

Model		Sum of Squares	df	Mean Square	F	Sig.
1	Regression	7.479	1	7.479	13.626	.000[a]
	Residual	62.575	114	.549		
	Total	70.054	115			
2	Regression	15.082	2	7.541	15.501	.000[b]
	Residual	54.972	113	.486		
	Total	70.054	115			
3	Regression	17.845	3	5.948	12.760	.000[c]
	Residual	52.209	112	.466		
	Total	70.054	115			

a. Predictors: (Constant), Blending types
b. Predictors: (Constant), Blending types, Transpolyoctenamer content (%)
c. Predictors: (Constant), Blending types, Transpolyoctenamer content (%), Rubber content (%)
d. Dependent Variable: Stability

Table A.7c Stepwise Multiple Linear Regression on Stability (Coefficients)

Model		Unstandardized Coefficients		Standardized Coefficients	t	Sig.	Correlations			Collinearity Statistics	
		B	Std. Error	Beta			Zero-order	Partial	Part	Tolerance	VIF
1	(Constant)	7.529	.248		30.350	.000					
	Blending types	-.464	.126	-.327	-3.691	.000	-.327	-.327	-.327	1.000	1.000
2	(Constant)	7.469	.234		31.916	.000					
	Blending types	-.524	.119	-.369	-4.390	.000	-.327	-.382	-.366	.984	1.016
	Transpolyoctenamer content (%)	.124	.031	.332	3.953	.000	.285	.349	.329	.984	1.016
3	(Constant)	8.048	.330		24.364	.000					
	Blending types	-1.068	.252	-.752	-4.235	.000	-.327	-.372	-.345	.211	4.738
	Transpolyoctenamer content (%)	.137	.031	.367	4.399	.000	.285	.384	.359	.954	1.048
	Rubber content (%)	.056	.023	.429	2.435	.016	-.223	.224	.199	.214	4.667

a. Dependent Variable: Stability

Table A.7d Stepwise Multiple Linear Regression on Stability (Excluded Variables)

Model		Beta In	t	Sig.	Partial Correlation	Collinearity Statistics		
						Tolerance	VIF	Minimum Tolerance
1	Rubber content (%)	.295[a]	1.576	.118	.147	.221	4.527	.221
	Transpolyoctenamer content (%)	.332[a]	3.953	.000	.349	.984	1.016	.984
	Binder content (%)	-.044[a]	-.499	.618	-.047	1.000	1.000	1.000
2	Rubber content (%)	.429[b]	2.435	.016	.224	.214	4.667	.211
	Binder content (%)	-.044[b]	-.531	.597	-.050	1.000	1.000	.984
3	Binder content (%)	-.044[c]	-.542	.589	-.051	1.000	1.000	.211

a. Predictors in the Model: (Constant), Blending types
b. Predictors in the Model: (Constant), Blending types, Transpolyoctenamer content (%)
c. Predictors in the Model: (Constant), Blending types, Transpolyoctenamer content (%), Rubber content (%)
d. Dependent Variable: Stability

Table A.8a Stepwise Multiple Linear Regression on Flow (Model Summary)

Model	R	R Square	Adjusted R Square	Std. Error of the Estimate	Change Statistics				
					R Square Change	F Change	df1	df2	Sig. F Change
1	.439[a]	.193	.186	.88927	.193	27.243	1	114	.000
2	.586[b]	.343	.332	.80574	.150	25.864	1	113	.000
3	.666[c]	.444	.429	.74491	.100	20.208	1	112	.000
4	.686[d]	.471	.451	.72992	.027	5.646	1	111	.019

a. Predictors: (Constant), Rubber content (%)
b. Predictors: (Constant), Rubber content (%), Binder content (%)
c. Predictors: (Constant), Rubber content (%), Binder content (%), Transpolyoctenamer content (%)
d. Predictors: (Constant), Rubber content (%), Binder content (%), Transpolyoctenamer content (%), Blending types

Table A.8b Stepwise Multiple Linear Regression on Flow (ANOVA)

Model		Sum of Squares	df	Mean Square	F	Sig.
1	Regression	21.544	1	21.544	27.243	.000[a]
	Residual	90.152	114	.791		
	Total	111.696	115			
2	Regression	38.335	2	19.168	29.524	.000[b]
	Residual	73.361	113	.649		
	Total	111.696	115			
3	Regression	49.548	3	16.516	29.765	.000[c]
	Residual	62.148	112	.555		
	Total	111.696	115			
4	Regression	52.557	4	13.139	24.661	.000[d]
	Residual	59.140	111	.533		
	Total	111.696	115			

a. Predictors: (Constant), Rubber content (%)
b. Predictors: (Constant), Rubber content (%), Binder content (%)
c. Predictors: (Constant), Rubber content (%), Binder content (%), Transpolyoctenamer content (%)
d. Predictors: (Constant), Rubber content (%), Binder content (%), Transpolyoctenamer content (%), Blending types
e. Dependent Variable: Flow

Table A.8c Stepwise Multiple Linear Regression on Flow (Coefficients)

Model		Unstandardized Coefficients		Standardized Coefficients	t	Sig.	Correlations			Collinearity Statistics	
		B	Std. Error	Beta			Zero-order	Partial	Part	Tolerance	VIF
1	(Constant)	3.790	.136		27.971	.000					
	Rubber content (%)	-.073	.014	-.439	-5.219	.000	-.439	-.439	-.439	1.000	1.000
2	(Constant)	.893	.583		1.532	.128					
	Rubber content (%)	-.073	.013	-.439	-5.761	.000	-.439	-.476	-.439	1.000	1.000
	Binder content (%)	.483	.095	.388	5.086	.000	.388	.432	.388	1.000	1.000
3	(Constant)	1.089	.541		2.014	.046					
	Rubber content (%)	-.071	.012	-.429	-6.088	.000	-.439	-.499	-.429	.999	1.001
	Binder content (%)	.483	.088	.388	5.501	.000	.388	.461	.388	1.000	1.000
	Transpolyoctenamer content (%)	-.149	.033	-.317	-4.495	.000	-.330	-.391	-.317	.999	1.001
4	(Constant)	.299	.625		.478	.634					
	Rubber content (%)	-.123	.025	-.744	-4.983	.000	-.439	-.428	-.344	.214	4.667
	Binder content (%)	.483	.086	.388	5.614	.000	.388	.470	.388	1.000	1.000
	Transpolyoctenamer content (%)	-.166	.033	-.352	-4.986	.000	-.330	-.428	-.344	.954	1.048
	Blending types	.640	.270	.357	2.376	.019	-.344	.220	.164	.211	4.738

a. Dependent Variable: Flow

Table A.8d Stepwise Multiple Linear Regression on Flow (Excluded Variables)

Model		Beta In	t	Sig.	Partial Correlation	Collinearity Statistics		
						Tolerance	VIF	Minimum Tolerance
1	Transpolyoctenamer content (%)	-.317[a]	-4.006	.000	-.353	.999	1.001	.999
	Binder content (%)	.388[a]	5.086	.000	.432	1.000	1.000	1.000
	Blending types	.199[a]	1.112	.269	.104	.221	4.527	.221
2	Transpolyoctenamer content (%)	-.317[b]	-4.495	.000	-.391	.999	1.001	.999
	Blending types	.199[b]	1.229	.222	.115	.221	4.527	.221
3	Blending types	.357[c]	2.376	.019	.220	.211	4.738	.211

a. Predictors in the Model: (Constant), Rubber content (%)
b. Predictors in the Model: (Constant), Rubber content (%), Binder content (%)
c. Predictors in the Model: (Constant), Rubber content (%), Binder content (%), Transpolyoctenamer content (%)
d. Dependent Variable: Flow

Table A.9a Stepwise Multiple Linear Regression on Resilient Modulus (Model Summary)

Model		R	R Square	Adjusted R Square	Std. Error of the Estimate	Change Statistics				
						R Square Change	F Change	df1	df2	Sig. F Change
dimension0	1	.452[a]	.204	.201	684.09082	.204	68.867	1	268	.000
	2	.536[b]	.287	.282	648.69235	.083	31.047	1	267	.000
	3	.603[c]	.363	.356	614.36154	.076	31.674	1	266	.000

a. Predictors: (Constant), Transpolyoctenamer (%)
b. Predictors: (Constant), Transpolyoctenamer (%), Binder content (%)
c. Predictors: (Constant), Transpolyoctenamer (%), Binder content (%), Blending type

Table A.9b Stepwise Multiple Linear Regression on Resilient Modulus (ANOVA)

Model		Sum of Squares	df	Mean Square	F	Sig.
1	Regression	3.223E7	1	3.223E7	68.867	.000[a]
	Residual	1.254E8	268	467980.248		
	Total	1.576E8	269			
2	Regression	4.529E7	2	2.265E7	53.818	.000[b]
	Residual	1.124E8	267	420801.764		
	Total	1.576E8	269			
3	Regression	5.725E7	3	1.908E7	50.558	.000[c]
	Residual	1.004E8	266	377440.104		
	Total	1.576E8	269			

a. Predictors: (Constant), Transpolyoctenamer (%)
b. Predictors: (Constant), Transpolyoctenamer (%), Binder content (%)
c. Predictors: (Constant), Transpolyoctenamer (%), Binder content (%), Blending type
d. Dependent Variable: Resilient modulus

Table A.9c Stepwise Multiple Linear Regression on Resilient Modulus (Coefficients)

Model		Unstandardized Coefficients		Standardized Coefficients	t	Sig.	Correlations			Collinearity Statistics	
		B	Std. Error	Beta			Zero-order	Partial	Part	Tolerance	VIF
1	(Constant)	4307.990	52.937		81.380	.000					
	Transpolyoctenamer (%)	158.056	19.046	.452	8.299	.000	.452	.452	.452	1.000	1.000
2	(Constant)	5917.213	293.136		20.186	.000					
	Transpolyoctenamer (%)	158.278	18.061	.453	8.764	.000	.452	.473	.453	1.000	1.000
	Binder content (%)	-267.936	48.086	-.288	-5.572	.000	-.287	-.323	-.288	1.000	1.000
3	(Constant)	5070.914	315.732		16.061	.000					
	Transpolyoctenamer (%)	158.851	17.105	.454	9.287	.000	.452	.495	.454	1.000	1.000
	Binder content (%)	-270.279	45.543	-.290	-5.935	.000	-.287	-.342	-.290	1.000	1.000
	Blending type	428.900	76.209	.275	5.628	.000	.270	.326	.275	1.000	1.000

a. Dependent Variable: Resilient modulus

Table A.9d Stepwise Multiple Linear Regression on Resilient Modulus (Excluded Variables)

Model		Beta In	t	Sig.	Partial Correlation	Collinearity Statistics		
						Tolerance	VIF	Minimum Tolerance
1	Blending type	.273[a]	5.248	.000	.306	1.000	1.000	1.000
	Rubber content (%)	.252[a]	4.799	.000	.282	.996	1.004	.996
	Binder content (%)	-.288[a]	-5.572	.000	-.323	1.000	1.000	1.000
2	Blending type	.275[b]	5.628	.000	.326	1.000	1.000	1.000
	Rubber content (%)	.257[b]	5.204	.000	.304	.996	1.004	.996
3	Rubber content (%)	.078[c]	.815	.416	.050	.264	3.790	.264

a. Predictors in the Model: (Constant), Transpolyoctenamer (%)
b. Predictors in the Model: (Constant), Transpolyoctenamer (%), Binder content (%)
c. Predictors in the Model: (Constant), Transpolyoctenamer (%), Binder content (%), Blending type
d. Dependent Variable: Resilient modulus

Table A.10a Stepwise Multiple Linear Regression on Ultimate Strain at 200 kPa, 40°C (Model Summary)

Model		R	R Square	Adjusted R Square	Std. Error of the Estimate	Change Statistics				
						R Square Change	F Change	df1	df2	Sig. F Change
dimension0	1	.850[a]	.722	.718	5088.42060	.722	166.594	1	64	.000
	2	.886[b]	.784	.777	4522.32543	.062	18.026	1	63	.000
	3	.901[c]	.812	.803	4250.72213	.028	9.308	1	62	.003

a. Predictors: (Constant), Rubber content (%)
b. Predictors: (Constant), Rubber content (%), Transpolyoctenamer (%)
c. Predictors: (Constant), Rubber content (%), Transpolyoctenamer (%), Binder content (%)

Table A.10b Stepwise Multiple Linear Regression on Ultimate Strain at 200 kPa, 40°C (ANOVA)

Model		Sum of Squares	df	Mean Square	F	Sig.
1	Regression	4.313E9	1	4.313E9	166.594	.000[a]
	Residual	1.657E9	64	2.589E7		
	Total	5.971E9	65			
2	Regression	4.682E9	2	2.341E9	114.469	.000[b]
	Residual	1.288E9	63	2.045E7		
	Total	5.971E9	65			
3	Regression	4.850E9	3	1.617E9	89.479	.000[c]
	Residual	1.120E9	62	1.807E7		
	Total	5.971E9	65			

a. Predictors: (Constant), Rubber content (%)
b. Predictors: (Constant), Rubber content (%), Transpolyoctenamer (%)
c. Predictors: (Constant), Rubber content (%), Transpolyoctenamer (%), Binder content (%)
d. Dependent Variable: Ultiate strain (micro second)

Table A.10c Stepwise Multiple Linear Regression on Ultimate Strain at 200 kPa, 40°C (Coefficients)

Model		Unstandardized Coefficients		Standardized Coefficients	t	Sig.	Correlations			Collinearity Statistics	
		B	Std. Error	Beta			Zero-order	Partial	Part	Tolerance	VIF
1	(Constant)	49003.066	1238.117		39.579	.000					
	Rubber content (%)	-1960.775	151.914	-.850	-12.907	.000	-.850	-.850	-.850	1.000	1.000
2	(Constant)	50170.444	1134.207		44.234	.000					
	Rubber content (%)	-1820.414	139.002	-.789	-13.096	.000	-.850	-.855	-.766	.943	1.060
	Transpolyoctenamer (%)	-1089.459	256.605	-.256	-4.246	.000	-.444	-.472	-.248	.943	1.060
3	(Constant)	38342.079	4020.895		9.536	.000					
	Rubber content (%)	-1827.634	130.675	-.792	-13.986	.000	-.850	-.871	-.769	.943	1.060
	Transpolyoctenamer (%)	-1101.452	241.226	-.259	-4.566	.000	-.444	-.502	-.251	.943	1.060
	Binder content (%)	1978.809	648.595	.168	3.051	.003	.144	.361	.168	.999	1.001

a. Dependent Variable: Ultimate strain (micro second)

Table A.10d Stepwise Multiple Linear Regression on Ultimate Strain at 200 kPa, 40°C (Excluded Variables)

Model		Beta In	t	Sig.	Partial Correlation	Collinearity Statistics		
						Tolerance	VIF	Minimum Tolerance
1	Binder content (%)	.164[a]	2.596	.012	.311	.999	1.001	.999
	Transpolyoctenamer (%)	-.256[a]	-4.246	.000	-.472	.943	1.060	.943
2	Binder content (%)	.168[b]	3.051	.003	.361	.999	1.001	.943

a. Predictors in the Model: (Constant), Rubber content (%)
b. Predictors in the Model: (Constant), Rubber content (%), Transpolyoctenamer (%)
c. Dependent Variable: Ultimate strain (micro second)

Table A.11a Stepwise Multiple Linear Regression on Slope of Secondary Stage at 200 kPa, 40°C (Model Summary)

Model	R	R Square	Adjusted R Square	Std. Error of the Estimate	Change Statistics				
					R Square Change	F Change	df1	df2	Sig. F Change
1	.742[a]	.550	.543	2.69591	.550	78.278	1	64	.000
2	.802[b]	.643	.631	2.42146	.093	16.330	1	63	.000
3	.829[c]	.687	.672	2.28375	.045	8.827	1	62	.004

a. Predictors: (Constant), Rubber content (%)
b. Predictors: (Constant), Rubber content (%), Transpolyoctenamer (%)
c. Predictors: (Constant), Rubber content (%), Transpolyoctenamer (%), Binder content (%)

Table A.11bStepwise Multiple Linear Regression on Slope of Secondary Stage at 200 kPa, 40°C (ANOVA)

Model		Sum of Squares	df	Mean Square	F	Sig.
1	Regression	568.919	1	568.919	78.278	.000[a]
	Residual	465.149	64	7.268		
	Total	1034.068	65			
2	Regression	664.668	2	332.334	56.679	.000[b]
	Residual	369.400	63	5.863		
	Total	1034.068	65			
3	Regression	710.706	3	236.902	45.423	.000[c]
	Residual	323.362	62	5.216		
	Total	1034.068	65			

a. Predictors: (Constant), Rubber content (%)
b. Predictors: (Constant), Rubber content (%), Transpolyoctenamer (%)
c. Predictors: (Constant), Rubber content (%), Transpolyoctenamer (%), Binder content (%)
d. Dependent Variable: Slope of secondary stage (microstrain/cycle)

Table A.11c Stepwise Multiple Linear Regression on Slope of Secondary Stage at 200 kPa, 40°C (Coefficients)

Model		Unstandardized Coefficients		Standardized Coefficients	t	Sig.	Correlations			Collinearity Statistics	
		B	Std. Error	Beta			Zero-order	Partial	Part	Tolerance	VIF
1	(Constant)	15.942	.656		24.303	.000					
	Rubber content (%)	-.712	.080	-.742	-8.847	.000	-.742	-.742	-.742	1.000	1.000
2	(Constant)	16.537	.607		27.230	.000					
	Rubber content (%)	-.641	.074	-.667	-8.606	.000	-.742	-.735	-.648	.943	1.060
	Transpolyoctenamer (%)	-.555	.137	-.313	-4.041	.000	-.472	-.454	-.304	.943	1.060
3	(Constant)	10.349	2.160		4.790	.000					
	Rubber content (%)	-.644	.070	-.671	-9.178	.000	-.742	-.759	-.652	.943	1.060
	Transpolyoctenamer (%)	-.562	.130	-.317	-4.333	.000	-.472	-.482	-.308	.943	1.060
	Binder content (%)	1.035	.348	.211	2.971	.004	.189	.353	.211	.999	1.001

a. Dependent Variable: Slope of secondary stage (microstrain/cycle)

Table A.11d Stepwise Multiple Linear Regression on Slope of Secondary Stage at 200 kPa, 40°C (Excluded Variables)

Model		Beta In	t	Sig.	Partial Correlation	Collinearity Statistics		
						Tolerance	VIF	Minimum Tolerance
1	Binder content (%)	.206[a]	2.562	.013	.307	.999	1.001	.999
	Transpolyoctenamer (%)	-.313[a]	-4.041	.000	-.454	.943	1.060	.943
2	Binder content (%)	.211[b]	2.971	.004	.353	.999	1.001	.943

a. Predictors in the Model: (Constant), Rubber content (%)
b. Predictors in the Model: (Constant), Rubber content (%), Transpolyoctenamer (%)
c. Dependent Variable: Slope of secondary stage (microstrain/cycle)

Table A.12a Stepwise Multiple Linear Regression on Slope of Secondary Stage at Different Temperature and Stress Levels (Model Summary)

Model		R	R Square	Adjusted R Square	Std. Error of the Estimate	Change Statistics				
						R Square Change	F Change	df1	df2	Sig. F Change
dimension0	1	.684[a]	.468	.461	27.01508	.468	66.080	1	75	.000
	2	.799[b]	.638	.628	22.44178	.170	34.682	1	74	.000
	3	.821[c]	.674	.661	21.43196	.036	8.138	1	73	.006

a. Predictors: (Constant), Temperature,°C
b. Predictors: (Constant), Temperature,°C, Stress, kPa
c. Predictors: (Constant), Temperature,°C, Stress, kPa, Binder Content, %

Table A.12b Stepwise Multiple Linear Regression on Slope of Secondary Stage at Different Temperature and Stress Levels (ANOVA)

Model		Sum of Squares	df	Mean Square	F	Sig.
1	Regression	48226.242	1	48226.242	66.080	.000[a]
	Residual	54736.087	75	729.814		
	Total	102962.328	76			
2	Regression	65693.462	2	32846.731	65.220	.000[b]
	Residual	37268.867	74	503.633		
	Total	102962.328	76			
3	Regression	69431.333	3	23143.778	50.386	.000[c]
	Residual	33530.995	73	459.329		
	Total	102962.328	76			

a. Predictors: (Constant), Temperature,°C
b. Predictors: (Constant), Temperature,°C, Stress, kPa
c. Predictors: (Constant), Temperature,°C, Stress, kPa, Binder Content, %
d. Dependent Variable: Slope of secondary stage at different stress levels & temperatures

Table A.12c Stepwise Multiple Linear Regression on Slope of Secondary Stage at Different Temperature and Stress Levels (Coefficients)

Model		Unstandardized Coefficients		Standardized Coefficients	t	Sig.	Correlations			Collinearity Statistics	
		B	Std. Error	Beta			Zero-order	Partial	Part	Tolerance	VIF
1	(Constant)	-123.107	18.828		-6.539	.000					
	Temperature,°C	3.051	.375	.684	8.129	.000	.684	.684	.684	1.000	1.000
2	(Constant)	-168.175	17.412		-9.659	.000					
	Temperature,°C	3.053	.312	.685	9.790	.000	.684	.751	.685	1.000	1.000
	Stress, kPa	.151	.026	.412	5.889	.000	.411	.565	.412	1.000	1.000
3	(Constant)	-66.570	39.308		-1.694	.095					
	Temperature,°C	3.070	.298	.689	10.307	.000	.684	.770	.688	1.000	1.000
	Stress, kPa	.157	.025	.428	6.387	.000	.411	.599	.427	.993	1.007
	Binder Content, %	-16.144	5.659	-.191	-2.853	.006	-.141	-.317	-.191	.992	1.008

a. Dependent Variable: Slope of secondary stage at different stress levels & temperatures

Table A.12d Stepwise Multiple Linear Regression on Slope of Secondary Stage at Different Temperature and Stress Levels (Excluded Variables)

Model		Beta In	t	Sig.	Partial Correlation	Collinearity Statistics		
						Tolerance	VIF	Minimum Tolerance
1	Stress, kPa	.412[a]	5.889	.000	.565	1.000	1.000	1.000
	Rubber content, %	-.110[a]	-1.319	.191	-.152	1.000	1.000	1.000
	Transpolyoctenamer, %	-.151[a]	-1.817	.073	-.207	.999	1.001	.999
	Blending types	-.085[a]	-1.006	.317	-.116	1.000	1.000	1.000
	Binder Content, %	-.155[a]	-1.869	.066	-.212	1.000	1.000	1.000
2	Rubber content, %	-.148[b]	-2.167	.034	-.246	.992	1.008	.992
	Transpolyoctenamer, %	-.154[b]	-2.257	.027	-.255	.999	1.001	.999
	Blending types	-.122[b]	-1.766	.082	-.202	.992	1.008	.992
	Binder Content, %	-.191[b]	-2.853	.006	-.317	.992	1.008	.992
3	Rubber content, %	.379[c]	1.716	.090	.198	.089	11.236	.089
	Transpolyoctenamer, %	-.096[c]	-1.332	.187	-.155	.858	1.166	.852
	Blending types	.323[c]	1.987	.051	.228	.162	6.181	.162

a. Predictors in the Model: (Constant), Temperature,°C
b. Predictors in the Model: (Constant), Temperature,°C, Stress, kPa
c. Predictors in the Model: (Constant), Temperature,°C, Stress, kPa, Binder Content, %
d. Dependent Variable: Slope of secondary stage at different stress levels & temperatures

APPENDIX B: PUBLICATIONS / PROCEEDINGS

1. Herda Yati Katman, Mohd Rasdan Ibrahim, Mohamed Rehan Karim, Suhana Koting, and Nuha Salim Mashaan, "Effect of Rubberized Bitumen Blending Methods on Permanent Deformation of SMA Rubberized Asphalt Mixtures," Advances in Materials Science and Engineering, vol. 2016, Article ID 4395063, 14 pages, 2016. doi:10.1155/2016/4395063. (*ISI-Cited Publication*)
2. Herda Yati Katman, Mohd Rasdan Ibrahim, Mohamed Rehan Karim, Suhana Koting, and Nuha Salim Mashaan, "Creep-Recovery behaviour of Crumb Rubber Modified Bitumen (CRMB) Containing Trans-Polyoctenamer," Road Materials and Pavement Design, Under Review. (*ISI-Cited Publication*)
3. Herda Yati Katman, Mohd Rasdan Ibrahim, Mohamed Rehan Karim,, Mohd. Yazip Matori, Strength Properties of Bitumen Emulsion Stabilized Mix Containing High Percentages of Reclaimed Asphalt Pavement, KSCE Journal of Civil Engineering (ISI Indexed Journal), (*ISI-Cited Publication*) Under Review
4. Herda Yati Katman, Mohd Rasdan Ibrahim, Mohamed Rehan Karim, Nuha Salim Mashaan, and Suhana Koting, Evaluation of Permanent Deformation of Unmodified and Rubber-Reinforced SMA Asphalt Mixtures Using Dynamic Creep Test, Advances in Materials Science and Engineering Volume 2015 (2015), Article ID 247149, 11 pages (ISI Indexed Journal), (*ISI-Cited Publication*)
5. Nuha Salim Mashaan, Mohamed Rehan Karim, Mahrez Abdel Aziz, Mohd Rasdan Ibrahim, Herda Yati Katman, and Suhana Koting, Evaluation of Fatigue Life of CRM-Reinforced SMA and Its Relationship to Dynamic Stiffness, The Scientific World Journal Volume 2014 (2014), Article ID 968075, 11 pages (ISI Indexed Journal), (*ISI-Cited Publication*)
6. Mohd Rasdan Ibrahim, Herda Yati Katman, Mohamed Rehan Karim, Suhana Koting, and Nuha S. Mashaan, The Effect of Crumb Rubber Particle Size to the Optimum

Binder Content for Open Graded Friction Course, The Scientific World Journal Volume 2014 (2014), Article ID 240786, 8 pages (ISI Indexed Journal), (*ISI-Cited Publication*)

7. Suhana Koting, Mohamed Rehan Karim, Hilmi Mahmud, Nuha S. Mashaan, Mohd Rasdan Ibrahim, Herdayati Katman, and Nadiah Md Husain, Effects of Using Silica Fume and Polycarboxylate-Type Superplasticizer on Physical Properties of Cementitious Grout Mixtures for Semiflexible Pavement Surfacing, The Scientific World Journal Volume 2014 (2014), Article ID 596364, 7 pages (ISI Indexed Journal), (*ISI-Cited Publication*)
8. Mohd Rasdan Ibrahim, Herda Yati Katman, Mohamed Rehan Karim, Suhana Koting, and Nuha S. Mashaan, A Review on the Effect of Crumb Rubber Addition to the Rheology of Crumb Rubber Modified Bitumen, Advances in Materials Science and Engineering Volume 2013 (2013), Article ID 415246, 8 pages (ISI Indexed Journal), (*ISI-Cited Publication*)
9. Herda Yati Katman, Mohd Rasdan Ibrahim, Mohd. Yazip Matori,Shuhairy Norhisham, Norlela Ismail, Effects of reclaimed asphalt pavement on indirect tensile strength test of conditioned foamed asphalt mix, IOP Conf. Series: Earth and Environmental Science 16 (2013) 012098, 4th International Conference on Energy and Environment 2013 (ICEE 2013), 4 pages.
10. Herda Yati Katman, Mohd Rasdan Ibrahim, Mohd. Yazip Matori,Shuhairy Norhisham, Norlela Ismail, Effects of reclaimed asphalt pavement on indirect tensile strength test of foamed asphalt mix tested in dry condition, IOP Conf. Series: Earth and Environmental Science 16 (2013) 012091, 4th International Conference on Energy and Environment 2013 (ICEE 2013), 4 pages..
11. H.Y Katman, M.R Ibrahim, M.Y Matori, S. Norhisham, N. Ismail, R. Che Omar, Tensile Strength of Reclaimed Asphalt Pavement, International Journal of Civil & Environmental Engineering IJCEE-IJENS (2012) Vol: 12 No: 03,14-19

12. Herda Yati KATMAN1, Mohd Rasdan IBRAHIM2, Mohd. Yazip MATORI3, Shuhairy NORHISHAM1, Norlela ISMAIL1, Rohayu CHE OMAR1, Effect of Foamed Bitumen on Tensile Strength of Reclaimed Asphalt Pavement Mix, 2012, Journal of Engineering Research and Education (JERE) UniMAP.
13. Herda Yati KATMAN a, Mohd Rasdan IBRAHIM b, Mohamed Rehan KARIM c, Abdel Aziz MAHREZ d, Resistance to Disintegration of Rubberized Porous Asphalt, Asian Transport Studies, Volume 1, Issue 4 (2011), 445-455